Lipid droplets under stressful conditions

Armen Khatchadourian

Department of Pharmacology and Therapeutics

McGill University, Montreal

October, 2012

A thesis submitted to McGill University in partial fulfillment of the requirements of the degree of Doctor of Philosophy

Abstract

Lipid droplets (LDs) are phylogenetically conserved and ubiquitous organelles with many cellular functions. In the last two decades, our understanding of LD biology and of their roles in physiological processes has increased dramatically. In addition, increasing evidence suggests that LDs are highly involved in inflammatory processes, and in metabolic disorders such as type 2 diabetes mellitus (T2DM). Despite such advancement, many aspects of LD biology and of their roles in health and disease remain unknown.

The core of LDs is highly enriched with neutral lipids and these can be mobilized to provide metabolic energy. The phospholipid monolayer surrounding the LD core is associated with a wide variety of proteins, including structural and signaling proteins, as well as metabolic enzymes. While LDs may be induced by physiological stimuli such as dietary fatty acids, they can also be formed under stressful conditions, in the absence of such fatty acids. However, exactly how cellular stress leads to LD accumulation remains unclear. Our main objective is to understand the regulation of LD formation under stressful conditions, specifically oxidative stress, inflammation, and metabolic stress.

We first investigated LDs in cells exposed to environmental stressors, namely cytotoxic metallic nanoparticles (e.g cadmium telluride nanocrystals) and reactive oxygen species (hydrogen peroxide). LD formation and expression of perilipin-2, a key structural LD protein, were highly increased in rodent cells exposed to these stress agents. Interestingly, supplementation with antioxidant N-acetyl cysteine or pharmacological inhibition of p38 mitogen activated protein kinase (MAPK) reduced stress-induced LD accumulation, suggesting that oxidative stress and p38 MAPK activation play a role in the induction of LD formation. Stimulation of LD formation by oleic acid, a dietary fatty acid, reduced stressor-induced cell death, suggesting that LDs may exert protective functions against oxidative stress.

Inflammatory leukocytes and macrophages contain a large number of LDs. While this phenomenon has been widely investigated in peripheral immune cells, its explanation remains elusive in immune cells of the central nervous system. We therefore investigated LD dynamics and regulation in microglia, the resident immune cells in the brain. We

found that stimulation of microglia with toll-like receptor 4 (TLR4) agonist, lipopolysaccharides (LPS), increased LD formation and perilipin-2 expression in an Akt and p38 MAPK-dependent manner. Interestingly, LPS-induced LDs extensively colocalized with cytosolic phospholipase A_2-α (cPLA$_2$-α), a key enzyme involved in the synthesis of eicosanoids, which are inflammatory lipid mediators. We also found that treatment with dietary n-3fatty acid, docosahexaenoic acid (DHA), considerably altered LD size and number, reduced association of cPLA$_2$-α with LDs, and attenuated LPS-induced inflammatory signaling in microglia. Collectively, these findings imply that LD formation may contribute to increased eicosanoid synthesis in activated microglia and could be microglial biomarkers of inflammation in the central nervous system.

To gain a better insight into the role of LDs in human pathology, we sought to examine alterations in LD metabolism in pancreatic tissue obtained from T2DM and obese individuals. Immunohistochemical studies revealed increased islet and extra-islet perilipin-2 expression in tissues from lean or obese T2DM donors, but not in non-T2DM obese donors, suggesting that the diabetic status, but not the obesity status, is a requirement for increasing perilipin-2 expression and LD formation. We propose that in islets, and in particular within the β-cells, perilipin-2 reduces lipotoxicity by stabilizing LDs and preventing the leakage of fatty acids from LDs into the cytosol. Gene expression analysis by RT-qPCR confirmed the increase in perilipin-2 expression and revealed significant alterations in several genes related to islet function, metabolism and antioxidant defense. These alterations seem to be consistently associated with obesity and T2DM and imply an adaptive and compensatory response to insulin resistance and metabolic stress.

In sum, our studies show that LDs are an integral part of the adaptive cellular response to oxidative, inflammatory and metabolic stress. Increasing evidence suggests that by serving as a storage depot for misfolded proteins and toxic lipids, LDs play a protective role in stressed cells. However, in stimulated leukocytes and macrophage, they can also contribute to the inflammatory response by participating in pro-inflammatory lipid synthesis (e.g. that of eicosanoids). This suggests that LDs may have cell- and tissue - specific functions ranging from lipid storage (in adipocytes), to cytoprotection (in non-

adipose tissue) and inflammation (in macrophages and leukocytes). Perhaps, the most important challenge in LD research in the upcoming decade will be to determine how the subcellular lipid and protein composition of this organelle affects its function in different cells.

Résumé

Les gouttelettes lipidiques (GL) sont des organites phylogénétiquement conservées et impliquées dans plusieurs fonctions cellulaires. Durant les deux dernières décennies, notre compréhension des rôles biologiques et physiologiques des GL a augmenté de manière draconienne. Plusieurs observations suggèrent fortement que les GL jouent un rôle important dans l'inflammation, ainsi que dans les désordres métaboliques tels que le diabète de type 2 (DT2). Malgré cette avancée, plusieurs aspects de la biologie des GL et de leurs rôles dans des maladies demeurent méconnus.

Le centre des GL est riche en lipides neutres qui peuvent se mobiliser et servir comme source d'énergie. La couche phospholipidique entourant le centre de la GL est associée à plusieurs protéines et enzymes métaboliques. Bien que les GL puissent être induites par des acides gras, elles peuvent aussi l'être dans des conditions de stress. Par contre, les mécanismes de l'accumulation de GL par des conditions de stress ne sont pas encore bien compris. Notre objectif principal est de comprendre la régulation de la formation de GL par le stress oxydatif, l'inflammation et le stress métabolique.

Premièrement, nous avons investigué les GL dans des cellules exposées à des stresseurs tels que des nanocrystaux de tellurure de cadmium et des dérivés réactifs d'oxygène. La formation de GL et l'expression de perilipin-2, qui est une protéine structurelle des GL, ont tous deux augmenté dans les cellules stressées. De plus, une supplémentation en antioxydant (n-acétylcystéine) ou un traitement avec un inhibiteur de p38 MAPK a réduit l'accumulation de GL causée par le stress. Ces observations suggèrent que le stress oxydatif et p38 MAPK jouent un rôle dans l'accumulation de GL dans des cellules stressées. Il était intéressant de noter qu'une stimulation de formation de GL par l'acide oléique, un acid gras mono-insaturé, a protégé les cellules contre les effets nocifs des stresseurs, ce qui suggère que les GL pourraient jouer un rôle protecteur dans des conditions de stress.

Il est bien connu que les leucocytes et macrophages qui sont engagés dans l'inflammation contiennent une grande quantité de GL. Même si ce phénomène a bien été exploré dans les cellules immunitaires périphériques, il reste inexploré dans le système nerveux central

(SNC). Ce faisant, nous avons investigué la dynamique et la régulation des GL dans les microglies, les cellules résidentes immunitaires dans le cerveau. Nous avons trouvé que dans les microglies stimulées avec les lipopolysaccharides (LPS), les GL et l'expression de perilipin-2 ont augmenté d'une manière dépendante de l'activation de l'Akt et p38 MAPK. Dans ces cellules activées, la phospholipase cytosolique A_2-α (PLC A_2-α), une enzyme fonctionnant dans la synthèse d'éicosanoides, des médiateurs lipidiques inflammatoires, colocalisait avec les GL. Nous avons également trouvé que le traitement de microglies avec l'acide docosahexaénoique (ADH) a considérablement changé le nombre et la grandeur de GL, a réduit l'association de GL avec PLC A_2-α et a atténué la signalisation inflammatoire. Ensemble, ces résultats indiquent que la formation de GL pourrait contribuer à la synthèse d'éicosanoides dans les microglies activées et servir de biomarqueurs d'inflammation dans le SNC.

Pour mieux comprendre le rôle des GL dans la pathologie humaine, nous les avons examinées dans des tissues pancréatiques provenant de patients obèses ou diabétiques T2. Nos études immunohistochimiques ont révélé une augmentation de perilipin-2 dans les îlots de Langerhans chez les patients diabétiques obèses ou maigres, mais pas dans ceux de patients non-diabétiques. Ceci suggère que le DT2, mais non l'obésité, est requis pour une augmentation de perilipin-2 dans le pancréas. On propose que dans les îlots, et particulièrement dans les cellules β, perilipin-2 réduit la lipotoxicité en stabilisant les GL ainsi diminuant la fuite d'acides gras de l'intérieur des GL vers le cytosol. L'analyse d'expression de gènes par RT-PCR a confirmé l'augmentation de perilipin-2 observé antérieurement dans les îlots et a également révélé des altérations dans des gènes reliés aux fonctions des îlots, au métabolisme, et aux défenses anti-oxydantes. Ces changements, qui sont souvent associés à l'obésité et au DT2, constituent un mécanisme d'adaptation à la résistance à l'insuline et au stress métabolique.

Pour résumer, nos études démontrent que l'accumulation de GL fait partie intégrante de l'adaptation des cellules au stress. L'évidence suggère que les GL pourraient être considérées comme des dépôts de stockage pour des lipides toxiques, et ainsi jouer un rôle protecteur dans les cellules stressées. Dans les leucocytes et macrophages, elles contribuent à la réponse inflammatoire en participant à la synthèse de lipides pro-

inflammatoires. Ceci suggère que les GL ont des fonctions qui varient d'une cellule à l'autre. Durant la prochaine décennie, le plus grand obstacle dans la recherche sur les GL sera de déterminer comment la composition lipidique ou protéinique de ces organites affecte leurs fonctions biologiques.

Table of Contents

List of Figures

Acknowledgements

I am grateful to my supervisor, **Dusica Maysinger**, for providing me with intellectual guidance through this work and also with financial support. I thank her for sharing with me her enthusiasm and joy for science.

Thanks to my thesis committee members, **Daniel Bernard (thesis advisor), Gregory Miller, Anne McKinney and Vladimir Titorenko,** for giving me direction and precious advice during my progress reports.

I am thankful to my laboratory colleagues, **Noura Al-Hajaj, Sebastien Boridy, Angela Choi, Manasi Jain** and **Kevin Neibert** for the good times we shared. I wish them great success in their future endeavors.

Sincere thanks to our collaborators, **Dr Vladimir Titorenko**, **Dr Maria Petropavlovskaya**, and **Dr Gonzalo Cosa**. I really enjoyed working with you.

I also thank faculty members for everything they have taught me; I have learned so much with you. I am grateful to staff members, **Hélène Duplessis, Chantal Grignon**, **David Kalant** and **Tina Tremblay**; they were always there to help.

I also thank **Dr. Claire Brown** from McGill Life Sciences Complex Imaging Facility for providing invaluable advice and assistance on image analysis..

The greatest thanks go to **my family, friends** and **Mlle Ariane Racine** for being who they are.

List of Abbreviations

4,4-difluoro-1,3,5,7,8-pentamethyl-4-bora-3a,4a-diaza-s-indacene (BODIPY 493/503)

Activator protein-1 (AP-1)

Adipose differentiation-related protein (ADRP)

Bovine serum albumin (BSA)

Cadmium telluride (CdTe)

Carnitine palmitoyltransferase 1A (CPT1A)

C-Jun N-terminal kinase (JNK)

Cytosolic phospholipase A_2 alpha (cPLA_2-α)

Diacylglycerol (DAG)

Differential interference contrast (DIC)

Dihydroethidium (DHE)

Docosahexaenoic acid (DHA)

Endoplasmic reticulum (ER)

Extracellular signal-regulated kinase (ERK)

Fat specific protein 27 (FSP27)

Forkhead box protein O1 (FOXO1)

Free fatty acid (FFA)

Glucokinase (GCK)

Glucose transporter -2 (GLUT-2)

Glutathione peroxidase 1 (GPX1)

Heme oxygenase 1 (HMOX1)

Lipid droplet (LD)

Lipopolysaccharides (LPS)

Mitogen-activated protein kinases (MAPK)

N-acetylcysteine (NAC)

Nitric oxide (NO)

Non-diabetic normal, ND-N

Non-diabetic obese, ND-O

Oleic acid (OA)

Palmitic acid (PA)

Peroxisome proliferator activated protein alpha (PPARα)

Peroxisome proliferator activated protein gamma (PPARγ)

Pheochromocytoma 12 cells (PC12 cells)

Phosphatidylinositol 3-kinase (PI3K)

Reactive oxygen species (ROS)

Sequestosome 1 (SQSTM1)

Toll-like receptor 4 (TLR4)

Triacylglycerol (TAG)

Type 2 diabetes mellitus (T2DM)

Type 2 diabetic normal, T2DN

Type 2 diabetic obese, T2DO

Uncoupling protein 2 (UCP2)

Contributions of Authors

The thesis describes the work of four manuscripts presented in Chapters 2 to 5.
Dr Dusica Maysinger was the principal investigator of all presented works and provided intellectual guidance in all of the manuscripts.

Manuscript 1 (Chapter 2)

Lipid droplets: their role in nanoparticle-induced oxidative stress.

Armen Khatchadourian and Dusica Maysinger.

Published in Molecular Pharmaceutics (American Chemical Society)
VOL. 6, NO.4, 1125-1137 (August, 2009)
Armen Khatchadourian: performed all experiments, acquired and analyzed data, created figures, wrote the first draft of manuscript

Manuscript 2 (Chapter 3)

Dynamics and regulation of lipid droplet formation in lipopolysaccharide (LPS)-stimulated microglia.
Armen Khatchadourian, Bourque SD, Richard VR, Titorenko VI, Maysinger D.
Published in Biochimica et Biophysica Acta (BBA) - Molecular and Cell Biology of Lipids
VOL. 1821, NO.4, 607-617 (April 2012)
Armen Khatchadourian: performed almost all of the experiments, acquired and analyzed data, created figures, wrote the first draft of manuscript
Simon D Bourque: performed mass spectrometric measurements of lipids and contributed to data interpretation.
Vincent R. Richard: performed mass spectrometric measurements of lipids.
Vladimir I. Titorenko: contributed to data interpretation, discussion, and writing of the manuscript.

Manuscript 3 (Chapter 4) (under review, in NeuroMolecular Medicine)

Docosahexaenoic acid (DHA): a modulator of lipid droplet proliferation and a facilitator of their interaction with mitochondria in hyperactive microglia

Dusica Maysinger, Armen Khatchadourian, Vincent R. Richard, Noura Al-Hajaj, Simon D. Bourque, Vladimir I. Titorenko

Armen Khatchadourian: performed about half of all experiments, acquired and analyzed data, created figures, contributed to writing and editing

Vincent R. Richard: mass spectrometry-based analysis of lipids

Noura Al-Hajaj: Performed ELISA assays, transcription factor translocation studies,

Simon D. Bourque: mass spectrometry-based analysis of lipids

Vladimir Titorenko: contributed to the writing of the first draft

Manuscript 4 (Chapter 5) (to be submitted)

Type 2 diabetes and obesity are associated with pancreatic upregulation of perilipin-2 and gene expression alterations

Armen Khatchadourian, Maria Petropavlovskaia, Jason Patapas, Julia Makhlin, Lawrence Rosenberg, Dusica Maysinger

Armen Khatchadourian: performed immunohistochemical staining of donor tissue, created figures, performed statistical analysis, substantial contribution to the writing of the manscript.

Maria Petropavlovskaya: performed RT-qPCR-based analysis of gene expression, substantial contribution to the writing of the manscript.

Jason Patapas: participated in tissue collection.

Julia Makhlin: performed RT-qPCR-based analysis of gene expression

Lawrence Rosengerg: Read the final draft.

CHAPTER 1

Introduction

1.1 Background, rationale and aims of the study

Lipid droplets (LDs), also called lipid bodies, are neutral lipid-rich organelles found in virtually all mammalian cell types and tissues (Murphy, 2001). Traditionally considered to be inert compartments involved in long-term storage of fat (neutral lipids), they are now known to be dynamic and multifunctional organelles with a complex lipidomic and proteomic profile (Bartz et al., 2007; Welte, 2007). In the last decade, a significant number of studies have uncovered the functions of LDs in short-term cellular processes such as signaling, as well as in long-term processes such as energy storage. In model organisms from yeast to mice, LDs play roles in developmental processes, environmental responses, ageing and in pathological events. In particular, LD dysfunction in humans is now known to be implicated in metabolic disorders such as obesity, type 2 diabetes mellitus (T2DM), atherosclerosis and metabolic syndrome (Greenberg et al., 2011; Le Lay & Dugail, 2009).

Studies have shown that environmental stress and other stressors such as exposure to reactive oxygen species (ROS), chemotherapeutic agents, X-ray irradiation, xenobiotics, and hypoxia stimulate LD accumulation in eukaryotic cells. Historically, the accumulation of LDs in disease tissues and under pathological conditions has been known since the second half of the 19th century. The phenomenon was referred to as "fatty degeneration" or "fatty change". By the last decade of the 20th century, LDs were already well-known to be involved in obesity-related disorders and in inflammatory processes. Subsequently, technological advances in molecular biology allowed a much better understanding of the role of LDs in cellular function.

Despite the growing body of evidence implicating LDs in stressed tissue and pathological conditions, their biological purpose and the mechanisms contributing to their formation remain unclear. Given that many pathological conditions are characterized by oxidative stress and inflammation, we speculated that investigating LDs under those conditions and during metabolic stress in human pathology, especially obesity and T2DM, would uncover some of the roles of LDs in pathology generally.

The key questions driving the work were:

1) How is LD formation regulated under stressful conditions and what role does it play?
2) How do LDs contribute to pro-inflammatory signaling in the central nervous system?
3) How do human metabolic disorders, namely obesity and T2DM, affect LD and LD-associated proteins?

The resulting investigations had the following aims:

Aim 1: To elucidate cellular mechanisms regulating LD formation under oxidative stress induced by exogenous stressors.

Aim 2: To -investigate the dynamics of LDs and the cellular mechanisms leading to LD formation in microglia activated by the pro-inflammatory agent, lipopolysaccharides (LPS)

Aim 3: To elucidate the role of LDs in the anti-inflammatory effect of an omega-3 fatty acid, docosahexaneoic acid (DHA).

Aim 4: To study the role of LDs in pancreata and pancreatic islets of human donors with T2DM and obesity.

These investigations were anticipated to elucidate the role of LDs in pathological conditions, and in particular to provide a better understanding of their roles in prominent metabolic disorders such as obesity and T2DM. The findings could also lead to new therapeutic strategies for obesity and T2DM.

1.2 Introduction to lipid droplets

1.2.1 Terminology of lipid droplets

A multitude of different names have been used in the literature to refer to these cytosolic lipid assemblies. Depending on the biological organisms or cell types in which they were studied, LDs have been referred to as oil bodies (plant seeds), lipid particles (yeast), lipid

bodies (animal cells), lipid droplets (animal cells), adiposomes (in mammalian adipocytes), lipid vacuoles (animals cells), oleosomes (oil seeds) (Murphy, 2001). Currently, the most common term to describe these cytosolic lipid inclusions is “lipid droplets”, although “lipid body” is also frequently used by different groups.

1.2.2 Lipid droplets: from plants to mammals

Most eukaryotic and prokaryotes are able to accumulate cytosolic lipidic inclusions that are surrounded by a phopholipid monolayer and a variety of proteins. In eukaryotes, the core of these spheroidal structures is composed primarily of neutral lipid esters, such as triacylglycerols (TAG) and cholesteryl esters. The lipidic inclusions, or LDs, play essential roles in cell survival as they act as carbon (energy) storage sites, which can be mobilized during lack of nutrients (Murphy, 2001).

LDs are phylogenetically conserved organelles present in plants, microalgae, fungi and animals. In plants, seed LDs are organelles for long-term neutral lipid storage and provide a source of carbon and energy for seed germination and seedling growth (Murphy, 2001; Tzen et al., 1993). LDs in yeast serve as carbon/energy storage sites and provide lipids for membrane synthesis thereby supporting cellular growth and division. In *Drosophila,* LDs are ubiquitous organelles found in diverse cell types and represent major energy storage sites (Kuhnlein, 2012). A genome-wide RNA interference study in embryonic cells demonstrated that about 1.5% of all genes in the fly function in LD formation (Guo et al., 2008). Moreover, mass spectrometry-based proteomic studies have revealed a rather complex protein network present in fly LDs (Beller et al., 2006; Cermelli et al., 2006). Identified proteins on LDs are involved in diverse biological functions, including TAG metabolism, membrane trafficking and signaling. Other proteins identified on LDs included chaperones, ER-resident proteins and histones.

Virtually all mammalian cell types have the ability to synthesize and store TAG within cytoplasmic LDs. LDs have been widely studied in mammalian cells and tissues.

For our purposes, LDs will be investigated in mammalian (Chapter 2-4) cell lines, as well as in human tissue (Chapter 5).

The largest depot of TAG is found in the adipose tissue, an organ specialized in long-term energy storage (Zechner et al., 2012). During increased energetic demand (e.g fasting or prolonged exercise), TAG in adipocytes are massively mobilized by hydrolytic enzymes called lipases and the resulting FFA are transported to peripheral tissues as a source of fuel (Lafontan & Berlan, 1993; Raclot & Groscolas, 1995). TAG can be synthesized from *de novo* lipogenesis (fatty acid synthesis) or from esterification of dietary fatty acids, which comprise between 30-40 % of our energy intake (Blundell et al., 1993; Saleh et al., 1999). Upon absorption through the gastronintestinal tract, long-chain fatty acids are esterified and are transported as part of TAG-rich chylomicrons to peripheral tissues such as adipose tissue, skeletal muscle and the heart (Lopez-Miranda et al., 2007) (Frohnert, Prog Lipid Res, 2000). In plasma, lipoprotein lipases (LPL) hydrolyse the chylomicron TAG into fatty acids, which are taken up by muscle cells for β-oxidation or adipocytes for storage (Lopez-Miranda et al., 2007). The chylomicron remnants are subsequently removed from the circulation after being taken up by the liver.

In the liver, LDs not only serve as a storage site for neutral lipids, but also provide substrates by lipolysis for the formation of mature very low-density lipoproteins (VLDL) (Wang et al., 2007; Ye et al., 2009). Therefore, LDs in the liver participate in lipoprotein metabolism.

The heart and the muscle cells utilize LD-derived fatty acids for mitochondrial β-oxidation and generation of adenosine triphosphate (ATP) (Ducharme & Bickel, 2008; Frohnert & Bernlohr, 2000). During endurance exercise, LDs in skeletal muscle cells are a major source of fuel for fat oxidation and contribute to energy requirements. Under resting conditions or after an overnight fast, the heart utilizes long-chain fatty acids as its primary source of energy to support cardiac contractions (Frohnert & Bernlohr, 2000; Taegtmeyer & Harmancey, 2008).

LDs can also be found in abundance within macrophages, which store large amounts of cholesterol from lipoproteins, such as low-density lipoproteins (LDL). LDs are highly abundant in macrophage-derived foam cells in atherosclerotic plaques and in infected leukocytes, and are sites of eicosanoid (e.g prostaglandins and leukotrienes) synthesis. Thus, LDs are highly involved in inflammatory processes.

1.2.3 Lipid droplet structure, composition and biogenesis

LDs are structurally similar to circulating lipoproteins and chylomicrons in that they have a core of esterified lipids (i.e TAG and cholesteryl esters) and a monolayer membrane comprised of polar lipids and proteins (Tauchi-Sato et al., 2002) (Figure 1.1). However, LDs are generally much larger (diameter from 100 nm to 100 µm) than lipoproteins (~30-60 nm for very low-density lipoproteins; 22-29 nm for low-density lipoproteins; <20 nm for high-density lipoproteins) and chylomicrons (~200-500 nm) (Colhoun et al., 2002; Sacks & Campos, 2003; Wood et al., 2006). Noteworthy, LDs in adipocyte and non-adipocytes greatly differ in size (Suzuki et al., 2011). While most adipocytes contain a single LD (unilocular) with a diameter of up to 100 µm, non-adipocytes contain a much higher number of smaller LDs, generally with a diameter between 0.5 and 1 µm (Suzuki et al., 2011).

Biochemical and ultrastructural studies have shown that LDs are formed in ER (Jacquier et al., 2011). It is hypothesized that LDs form as a result of the accumulation of neutral lipids between the two leaflets of the ER: neutral lipids bulge from the cytoplasmic leaflet and bud off the ER (Murphy & Vance, 1999). Following the budding, LDs may completely detach from the ER or remain connected to it. According to this model, it was assumed that the surface of LDs is a monolayer derived from the cytoplasmic leaflet of the ER. Accordingly, by using cryoelectron microscopy, Tachi-Sauti and colleagues confirmed that the LD surface was covered by a phospholipid monolayer (Tauchi-Sato et al., 2002). Moreover, they demonstrated that the lipid (e.g fatty acid) composition of the monolayer was distinct from that of the ER. In comparison to the ER, LDs had a higher content of free cholesterol. These results showed that the LD surface is phospholipid monolayer but is compositionally different from the ER membrane, from which it is derived. In yeast and mammalian cells, LDs mainly consist of neutral lipids (95 – 98%). Phospholipids account for 1-2% of the total LD lipidome (Bartz et al., 2007). Mass spectrometric analyses have shown that the most abundant phospholipids in the LD membrane are phosphatidylcholine (PC) and phosphatidylethanolamine (PE), followed by phosphatidylinositol (PI) (Bartz et al., 2007). In contrast, LDs are deficient in sphingomyelin, phosphatidylserine, phosphatidic acid and cardiolipin.

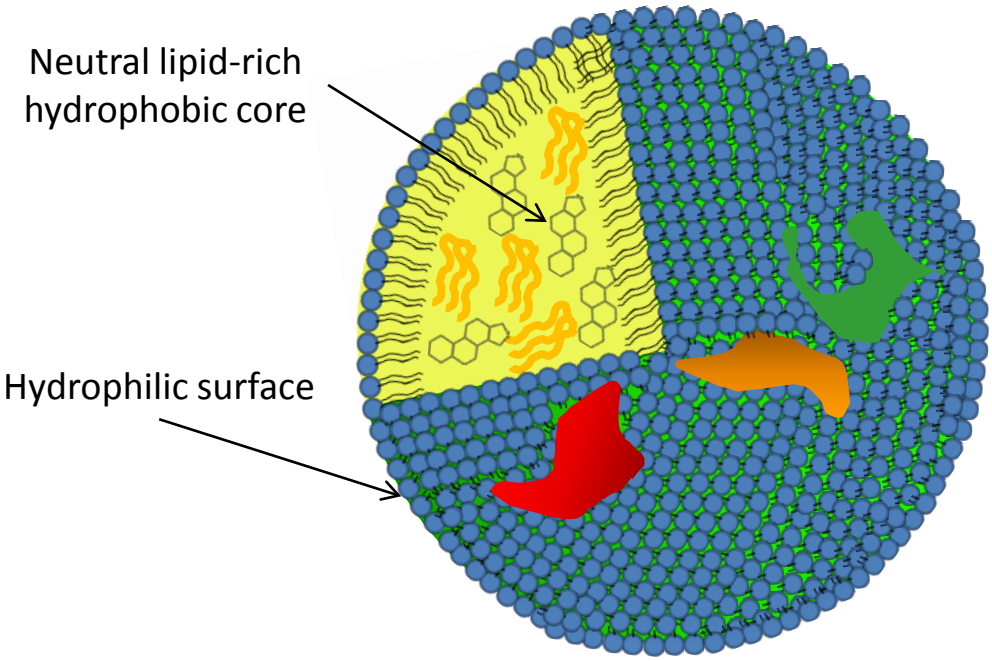

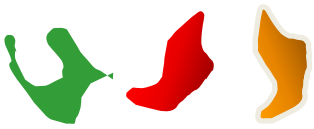

LD proteins
(Perilipins, lipases)

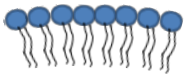

Phospholipid
monolayer

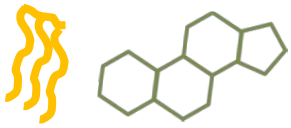

Neutral lipids

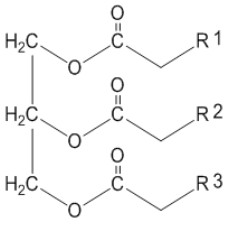

Triacylglycerol

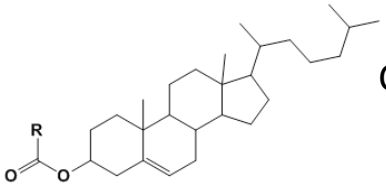

Cholesterol
ester

Figure 1.1 Lipid droplet structure and composition

The structure of a LD consists of a core (yellow) enriched with neutral lipids, such as triacylglycerol (TAG) and cholesterol esters. The core is surrounded by a phospholipid monolayer (blue) and a multitude of structural and signaling proteins, and metabolic enzymes, such as TAG lipases. Recent lipidomic studies have revealed the presence of a highly diverse population of lipid species within LDs. Of LD proteins, the PAT family members (perilipin-1, 2, and 3) have been widely studied. Other LD-associated proteins, such as FSP27, have recently attracted much interest.

LD biogenesis and growth requires biosynthesis of neutral lipids including TAG and cholesteryl esters (Kuerschner et al., 2008). TAG synthesis plays an important role in many physiological processes including intestinal dietary fat absorption, storage of excess fatty acids in the postprandial state and protective roles against lipotoxicity (Cardell et al., 1967; Fruhbeck et al., 2001; Listenberger et al., 2003). There are two major biochemical pathways leading to TAG biosynthesis: the glycerol-3-phosphate (G-3-P) pathway and the monoacylglycerol (MAG) pathway (Figure 1.2) (Yen et al., 2008). Both pathways start with the acylations of G-3-P and MAG with fatty acyl-CoA by glycerol-3-phosphate acyltransferase (GPAT) and monoacylglycerol acyltransferase (MGAT), respectively. The two pathways share the final step in TAG synthesis where diacylglycerol (DAG) is converted to TAG in an acylation reaction catalyzed by diacylglycerol acyltransferase (DGAT). The other neutral lipid in LDs, cholesteryl ester, is synthesized by cholesterol from acyl-coenzyme A: cholesterol acyltransferase (ACAT), an enzyme catalyzing the esterification of cholesterol (Chang et al., 2009). In mammals, ACAT and DGAT exist in two isoforms and are localized to the ER membrane, the site of LD biogenesis. The other enzymes involved in TAG synthesis are also found in the ER membranes including MGAT, GPAT, 1-acylglycerol-3-phosphate acyltransferase (AGPAT) and phosphatidic acid phosphatase 1 (PAP) (Takeuchi & Reue, 2009).

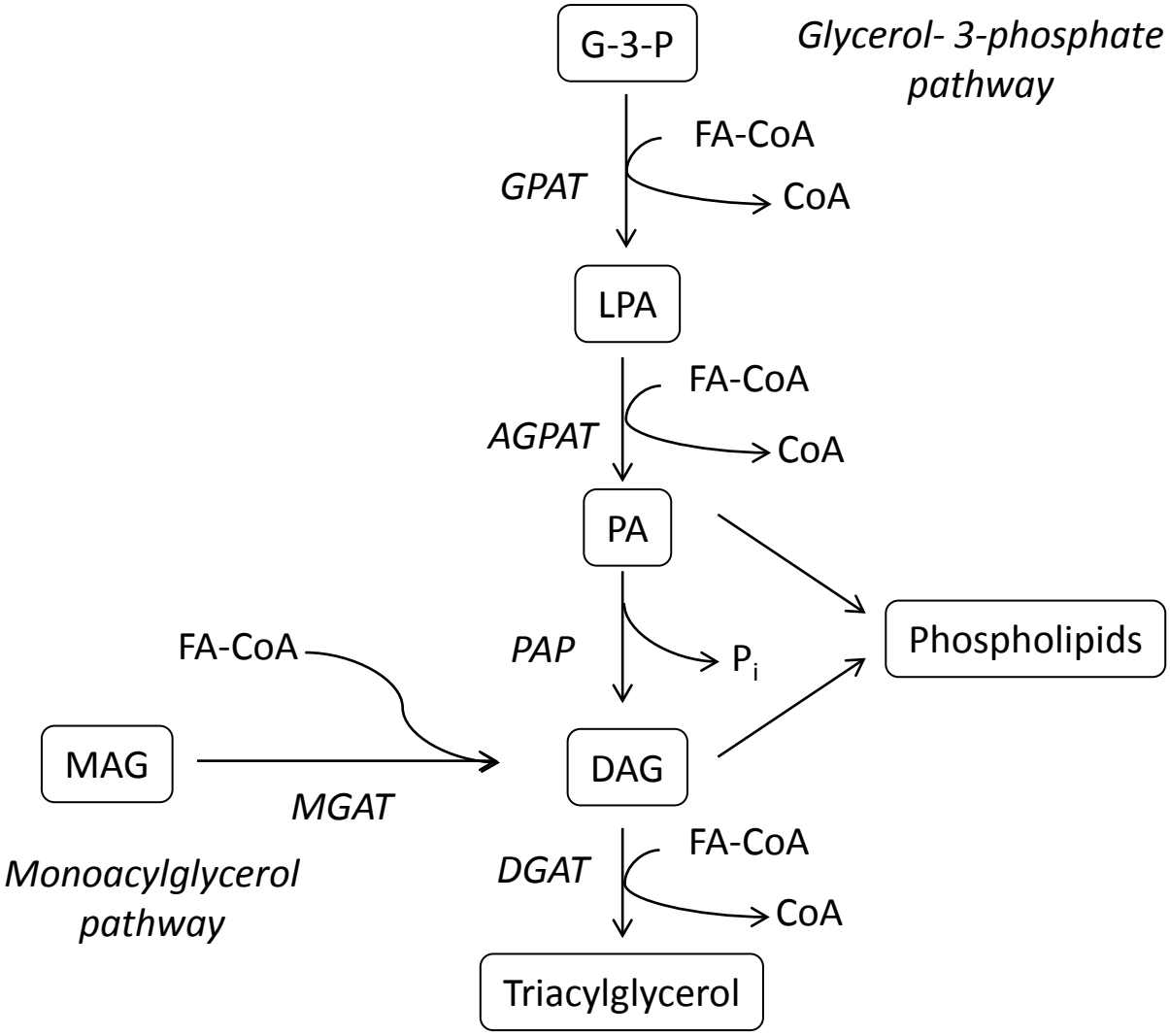

Figure 1.2 Pathways of triacylglycerol biosynthesis

Triacylglycerols (TAG) are synthesized from two major biosynthetic pathways: the glycerol-3-phosphate (G-3-P) and the monoacylglycerol (MAG) pathways. The G-3-P pathway begins with the acylation of G-3-P with a fatty acyl-CoA to yield lysophosphatidic acid (LPA), followed by further acylation and dephosphorylation reactions, leading to diacylglycerol synthesis. The final step is the acylation of DAG by diacylglycerol transferase (DGAT), which converts DAG to TAG. The MAG pathway is characterized by the converstion of MAG to DAG by fatty acyl-CoA, followed by further acylation by DGAT.

1.2.4 Imaging of lipid droplets

Imaging of LDs is critical for understanding their dynamics, formation, and subcellular distribution. In order to better understand LDs under physiological or pathological conditions, we imaged them and related changes occurring in their status to cellular function.

LDs can be detected by different optical imaging techniques including light microscopy (e.g dark field, differential interference contrast, and brightfield), conventional fluorescence microscopy and confocal microscopy. Several hydrophobic fluorescent dyes are commercially available and may be used to image LDs (see Figure 1.3). Oil Red-O is used to stain LDs in fixed cells and is visible by light microscopy (Koopman et al., 2001). However, Oil-Red-O staining is known to cause fusion of small LDs and artifactual appearance of LDs (Fukumoto & Fujimoto, 2002). Other fluorescent lipophilic probes, such as Nile Red and BODIPY 493/503, are commonly used for LD imaging in living or fixed cells and tissues (Greenspan et al., 1985; Listenberger & Brown, 2007). BODIPY 493/503 is highly selective for cellular neutral lipids and emits a bright green fluorescence. The relatively narrow emission (λ_{ex} = 493; λ_{em} = 503) facilitates the use of BODIPY 493/503 in dual labeling studies with other fluorescent markers in red. However, one should also consider the fact that BODIPY 493/503 also emits in red under certain conditions (Ohsaki et al., 2010). By contrast, Nile Red has a broad emission spectrum and also emits green fluorescent in certain cellular environments (Listenberger & Brown, 2007). Therefore, it is difficult to perform dual labeling with Nile Red and another green or red fluorescent marker.

Confocal microscopy is preferable for LD imaging because it produces images with a lower background fluorescence signal, greater axial and lateral resolution and improved contrast (Smith, 2001). Moreover, the optical sectioning along the *z* axis in confocal microscopy allows 3D-recontruction of the cell and of its constituents such as organelles, membranes and proteins (Strohmaier et al., 1997). Confocal microscopy also offers the possibility of doing colocalization analyses between different organelles or between organelles and proteins. Confocal imaging has served as a valuable tool to better

understand LD formation, metabolism and dynamics (Krahmer et al., 2011; Kuerschner et al., 2008).

For our purposes, LD imaging was mostly done by confocal imaging with the use of lipophilic fluorophore BODIPY 493/503. The use of this dye allowed us to perform dual labeling of LDs and other organelles (e.g mitochondria, lysosomes) or proteins (e.g perilipin-2).

Other approaches have also been used to detect and study LDs. High resolution LD imaging can be achieved by different electron microscopy (EM) techniques including conventional transmission EM (Almahbobi et al., 1992), cryo-EM (Tauchi-Sato et al., 2002), freeze fracture EM (Blanchette-Mackie et al., 1995), scanning EM (Fraenkel et al., 2008), and wet SEM (Thiberge et al., 2004). Most importantly, EM has provided valuable information on LD structure and on functional interactions between LDs and other organelles such as mitochondria (Pu et al., 2011). A relatively new vibrational imaging method based on coherent anti-Stokes Raman scattering (CARS) can be used for non-invasive LD imaging in living cells. This label-free imaging technique offers the advantage of rapid image acquisition and long-term observations. So far, CARS microscopy has been used to study LD dynamics, LD formation and even LD composition (Nan et al., 2003; Rinia et al., 2008).

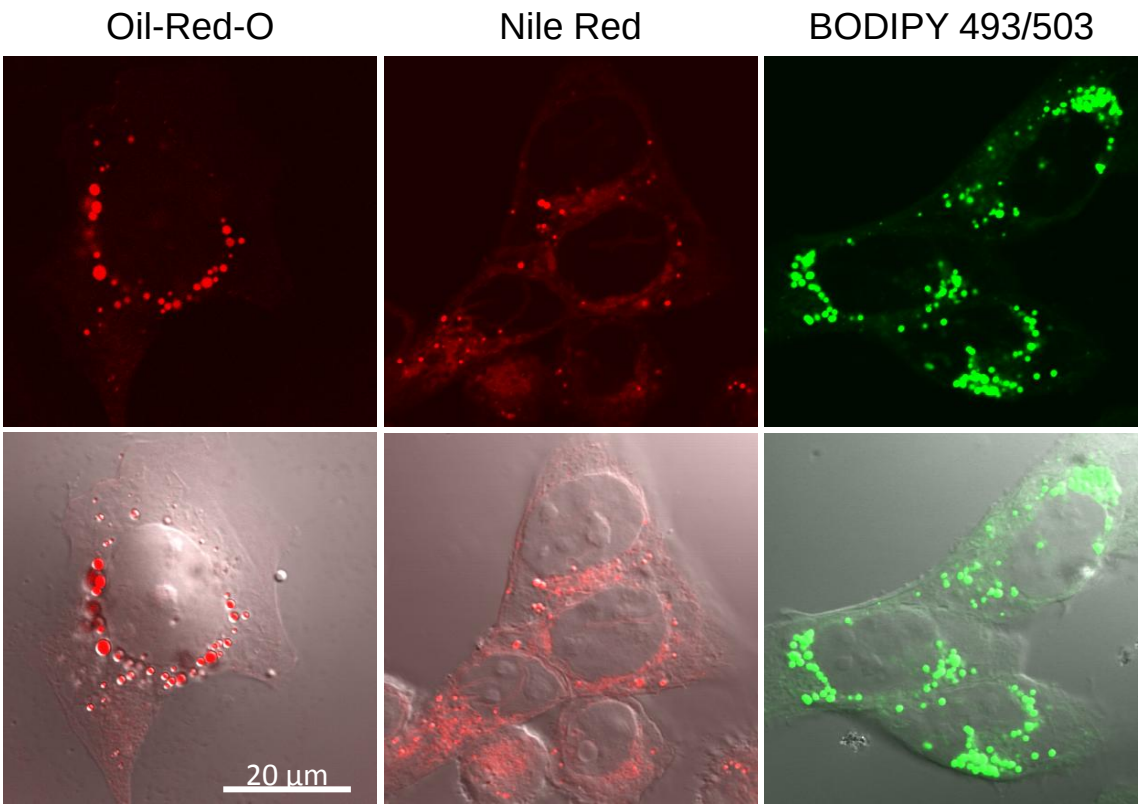

Figure 1.3 Detection of lipid droplets with lipophilic fluorcescent probes.

LDs can be detected by using different commercially available lipophilic fluorescent dyes, Oil-Red-O, Nile Red and BODIPY 493/503. These confocal images show LDs stained in pancreatic cell lines (Panc 2.13). Cells shown here were fixed with 4% paraformaldehyde. Scale bar, 20 µm. Unpublished experiments (2007).

1.2.5 Lipid droplet-associated proteins

LD-associated proteins play essential roles in regulating TAG storage and mobilization. In our studies, we mainly focused on adipose-differentiation related protein (ADRP), also known as adipophilin or perilipin-2, the most recent name of the protein. Perilipin-2 is constitutively present on LDs and is often used as a marker for LD accumulation in cells. Before going into the details, we will give an overview of prominent LD-associated proteins.

1.2.5.1 Discovery of PAT family proteins

The surface proteins of LDs play multiple roles including LD mobilisation, stabilization, biogenesis, and trafficking. The existence of proteins on the surface of LDs was reported for the first time about two decades ago. The group of Costantine Londos identified in 1991 a protein associated with LDs which could be regulated by phosphorylation in response to lipolytic stimuli: the protein was perilipin (Greenberg et al., 1991). In 1997, adipose-differentiation related protein (ADRP) (also known as adipophilin), which shares extensive sequence similarity with perilipin in the amino terminus, became the second protein found to be associated with the surface of LDs (Brasaemle et al., 1997). Three additional LD-associated proteins with sequence similarity to perilipin and ADRP were identified; these proteins are tail-interacting protein 47 (Tip47) (or PP17) (in 2001), S3-12 (in 2003) and myocardial LD protein (MLDP)/OXPAT/LSDP5 (in 2006) (Wolins et al., 2001; Wolins et al., 2003; Yamaguchi et al., 2006). The amino acid sequence of Tip47 is 43% identical to ADRP and shows an even higher sequence identity (60%) in the amino terminus (Wolins et al., 2001). Hence, they were grouped as a family called the "PAT protein family", named after the three members, **p**erilipin, **A**DRP and **T**ip47 (Miura et al., 2002). Two additional non-mammalian PAT proteins with conserved sequences in the N-terminus were identified in insects, lipid storage droplet-1 and -2 (LSD1 and LSD2) (Gronke et al., 2003; Patel et al., 2005).

1.2.5.2 A unifying nomenclature for the PAT family lipid droplet-associated proteins

Recently, a unifying nomenclature for the PAT family of proteins was established (Kimmel et al., 2010). The purpose of replacing the old nomenclature was to reduce confusion over the multiple names given to each member, and also to establish consistency and precision. Hence, each family member is now numbered sequentially in the following order:

Perilipin-1 for perilipin; Perilipin-2 for ADRP/adipophilin; Perilipin-3 for Tip47/PP17; Perilipin-4 for S3-12; Perilipin-5 for MLDP/OXPAT/LSDP5. Accordingly, we will henceforth refer to the PAT family proteins by the names established in this new nomenclature.

1.2.5.3 Tissue distribution and subcellular localization of PAT proteins

PAT proteins may differ from one another with respect to size, tissue distribution, subcellular localization, transcriptional regulation and post-translational regulation (Wolins et al., 2006). Indeed, perilipin-2 and -3 are ubiquitously expressed in almost all mammalian cell types, whereas perilipin-1, -4 and -5 are expressed in a tissue-specific manner (Bickel et al., 2009). Perilipin-1 is predominantly expressed in adipocytes and steroidogenic cells, but can also be found to be expressed at low levels in other cell types (Londos et al., 1995). Perilipin-4 is primarily expressed in the white adipose tissue and to a lesser degree in the heart and skeletal muscle (Wolins et al., 2005). On the other hand, the expression of perilipin-5 is limited to tissues capable of high rates of fatty acid oxidation (β-oxidation), including the heart, fasted liver, brown adipose tissue and oxidative muscle (Dalen et al., 2007; Yamaguchi et al., 2006). PAT family proteins also differ in their subcellular distribution.

While perilipin-1 and -2 are constitutively present on the surface of LDs, the other members demonstrate exchangeable LD binding (Wolins et al., 2006). They are highly unstable when not bound to LDs and are rapidly degraded by post-translational mechanisms involving the ubiquitin/proteasome machinery (Brasaemle et al., 1997; Xu et al., 2005). Upon lipid loading (e.g fatty acids), newly synthesized neutral lipids stabilize

perilipin-1 and -2, protecting them from proteasomal degradation. Unlike perilipin-1 and -2, the other PAT family proteins are stable in the cytosol when not bound to LDs and translocate to the surface of LDs to participate in the incorporation of fatty acids into TAG (Wolins et al., 2006).

1.2.5.4 Functions and regulation of perilipin-2

Perilipin-2 plays an essential role in cellular neutral lipid accumulation and, in particular in LD structural stability. In our work, we were specifically interested in the implication of perilipin-2 in LD formation under stressful cellular conditions and also in human pathology.

Initial evidence for the role of perilipin-2 in lipid storage came from studies showing that perilipin-2 overexpression leads to TAG accumulation and LD formation in different cell types (Imamura et al., 2002; Larigauderie et al., 2004; Magnusson et al., 2006). On the other hand, knockdown of perilipin-2 using a small interfering RNA approach (siRNA) results in reduced fatty acid storage and cytosolic LD accumulation (Larigauderie et al., 2004; Magnusson et al., 2006). Listenberger and colleagues investigated the mechanisms by which perilipin-2 stimulates lipid storage and LD formation (Listenberger et al., 2007). They found that perilipin-2 stabilizes LDs and prevents their turnover by reducing the LD association of adipose triglyceride lipase (ATGL), an important enzyme for TAG hydrolysis. Human kidney embryonic cells transfected with perilipin-2 displayed an increased level of total TAG and a slower rate in TAG hydrolysis. In these cells, transient expression of perilipin-2 reduced the association of ATGL with the surface of LDs, as shown by confocal microscopy. In addition to its role in slowing down TAG hydrolysis in LDs, perilipin-2 may affect LD accumulation in other ways as well, such as by participating in the synthesis of new LDs. Taken together, these mechanisms may explain the reduced liver TAG content in the liver of perilipin-2-null mice and their resistance to diet-induced fatty liver (Chang et al., 2006).

Perilipin-2 is regulated by transcriptional and post-translational mechanisms. It was reported that peroxisome proliferator activated proteins (PPAR) play an important role in the regulation of perilipin-2 gene expression. A number of studies have shown that treatment with selective ligands for PPARα, PPARγ and PPARδ results in increased expression of perilipin-2 (Bildirici et al., 2003; Edvardsson et al., 2006; Fan et al., 2009; Schadinger et al., 2005). A PPAR response element (PPRE) was identified in the promoter region of perilipin-2 and was shown to mediate perilipin-2 transcription following PPAR activation (Targett-Adams et al., 2005). Long chain fatty acids such as oleic acid stimulate perilipin-2 expression in a PPAR-dependent manner (Fan et al., 2009; Suzuki et al., 2009; Tobin et al., 2006).

As mentioned previously, degradation of perilipin-2 by the ubiquitin-proteasome system is a major mode of its post-translational regulation. In fact, perilipin-2 is stabilized when it is associated with LDs, but is destabilized and degraded by the proteasome in cells devoid of neutral lipids (e.g TAG) (Masuda et al., 2006; Xu et al., 2005). Accordingly, regression of cellular TAG content is accompanied with increased levels of polyubiquitinated perilipin-2. Conversely, oleic acid treatment, which induces TAG synthesis, blunts the appearance of polyubiquitinated perilipin-2 and leads to an increase in perilipin-2 content and perilipin-2 association with LDs (Xu et al., 2005).

In summary, perilipin-2 may be regulated both at the transcriptional and post-transcriptional levels. Therefore, an increase in perilipin-2 levels may be a consequence of either increased gene expression or a decrease in its proteasomal degradation when it is bound to LDs.

1.2.6 Interactions of lipid droplets with other organelles

LDs have been reported to undergo heterotypic interactions with other cellular organelles and even homotypic interactions with other LDs (Murphy et al., 2008). These interactions are more prominent in non-adipocytes, since LDs are smaller and more mobile as compared to LDs in adipocytes. To date, LDs have been shown to interact with the ER, mitochondria, peroxisomes, lysosomes, autophagosomes and endosomes (Murphy et al.,

2008; Singh et al., 2009). Given that many of these organelles are involved in fatty acid metabolism, such interactions may play important functions in cellular lipid metabolism. For instance, close apposition of LDs with mitochondria facilitates the coupling of TAG hydrolysis to mitochondrial fatty acid oxidation. More recently, interplay between lipid metabolism and autophagy has been discovered showing that LDs can be mobilized by a process called macrolipophagy, resulting in FFA release and utilization (Singh et al., 2009). In this regard, lysosomes seem to be implicated in LD degradation and recycling of LD lipids.

In the presented work, we have examined LDs-lysosome (Chapter 2) and LD-mitochondria (Chapter 4) interactions (or close apposition) under different cellular conditions. More specifically, we questioned the biological role of such interactions during oxidative stress and inflammation.

1.3. Physiological regulation of lipid droplet formation

As part of our studies, we examined LD formation under physiological conditions, as well as pathological conditions. Some dietary long-chain fatty acids, such as 18:1 monounsaturated oleic acid (Figure 1.5), may induce TAG synthesis and LD formation in various non-adipose tissue cells (see Figure 1.4).

Dietary long chain fatty acids were previously shown to be major physiological inducers of LD formation (Fujimoto et al., 2006). Upon digestion of TAG in the intestine, the resulting fatty acids and monoacylglycerols are absorbed by the enterocytes through simple diffusion (Tso & Balint, 1986). In enterocytes, fatty acids are re-esterified into TAG molecules and are sequestered into LDs, which are further processed in the Golgi apparatus and released in the form of chylomicrons into the circulation (Tso & Balint, 1986). Plasma lipoprotein lipases hydrolyze chylomicron TAGs into fatty acids which are taken up by muscle cells for oxidation and adipocytes for long-term storage (Havel, 1997). The chylomicron remnants are subsequently taken up by the liver.

Upon entry into cells, long-chain fatty acids are activated by fatty acyl-CoA synthetase (ACSL) to form fatty acyl-CoA (Mashek et al., 2007). This activation is necessary and channels fatty acids to metabolic pathways such as mitochondrial β-oxdiation (see Figure 1.4) or synthesis of complex lipids such as cholesteryl esters, phospholipids, ceramides, and TAG (Li et al., 2010). When there is an excess of fatty acyl-CoAs, these are esterified and stored in LDs in the form TAG and CE. The storage of the excess fatty acyl-CoAs is very important, because it serves as a protective mechanism against fatty acid-induced cytoxicity (Li et al., 2010).

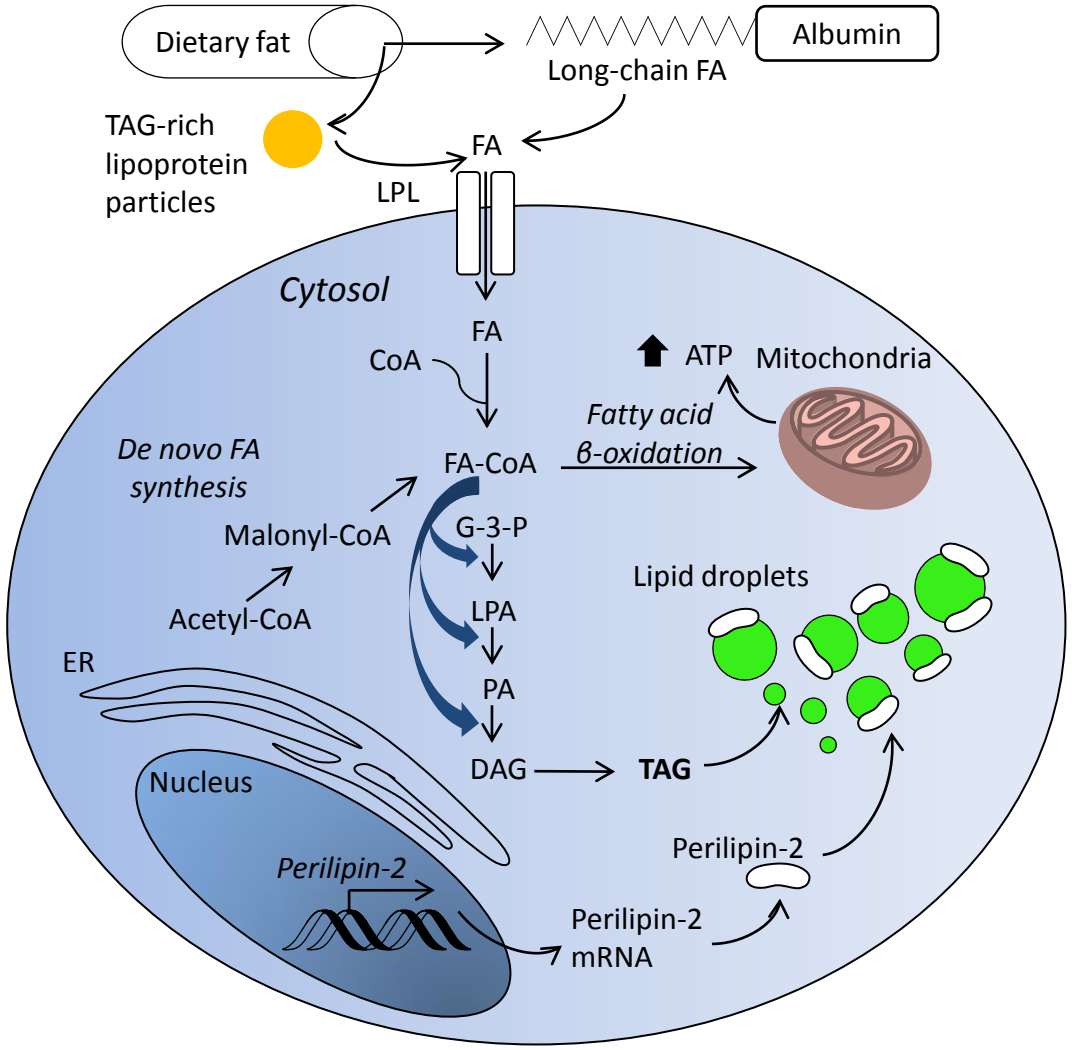

Figure 1.4 Regulation of lipid droplet formation by dietary or *de novo* synthesized long-chain fatty acids

Upon their internalization, long chain fatty acids (FA) are activated by coenzyme-A (CoA) to become long-chain fatty acyl-CoA, which are used either as substrates for TAG synthesis by the G-3-P pathway or oxidized via mitochondrial β-oxidation in order to produce ATP. Fatty acids may also be synthesized *de novo* from acetyl-CoA. TAGs are synthesised in the ER and enclosed within nascent LDs. Perilipin-2 and other perilipin proteins sabilize LDs by preventing lipase-induced TAG hydrolysis.

The ability of fatty acids to induce LD formation depends on both the length and the degree of saturation of the hydrocarbon chain. In fact, unsaturated fatty acids and fatty acids with longer hydrocarbon chain (> twelve carbons) are more efficient at inducing LD formation, compared to shorter chain (< twelve carbons) or saturated fatty acids (Fujimoto et al., 2006; Yonezawa et al., 2004). This finding might be explained by the fact that unsaturated and long-chain fatty acids are incorporated more efficiently into TAGs than short-chain or saturated fatty acids (Aardema et al., 2011; Listenberger et al., 2003). A well-known example of a long-chain unsaturated fatty acid with a great capacity to induce LD accumulation is oleic acid (18:1 n-9), naturally occurring in olive oil and sunflower oil (Fujimoto et al., 2006; Perez-Jimenez et al., 1995). On the other hand, palmitic acid (Figure 1.5), a saturated fatty acid also very abundant in our diet, is poorly incorporated into TAGs and has a low LD-inducing capacity (Listenberger et al., 2003).

Oleic acid (Figure 1.5) is a major plasma fatty acid (Quehenberger et al., 2010). Due to its ability to stimulate LD formation, oleic acid is commonly used in LD studies and serves as a standard control for LD induction. To date, oleic acid has been shown to induce LD formation in a diverse array of cell types including hepatocytes (Fujimoto et al., 2006), mammary epithelial cells (Yonezawa et al., 2004), fibroblasts (Nakamura et al., 2005), enterocytes (Bouchoux et al., 2011), leukocytes (Bozza & Viola, 2010) and cardiomycoytes (Bartels et al., 2010). Long-chain polyunsaturated fatty acids such as linoleic acid (18:2 n-6) and docosahexaenoic acid (DHA) (22:6 n-3) (Figure 1.5) may also induce LD formation (Yonezawa et al., 2004).

In the body, synthesis of TAG in such organs as liver, muscle and adipose tissue is a highly regulated process and is determined by the balance between fat synthesis (lipogenesis) and fat breakdown (lipolysis) (Wang et al., 2008). Insulin, a major anabolic hormone, stimulates lipogenesis in the liver and the adipocytes (Kersten, 2001). Upon binding to its membrane receptor, insulin stimulates glucose uptake, glycolysis, and activation of lipogenic enzymes and gene expression (Iozzo et al., 2003; Moustaid et al., 1996). Glucose itself is a substrate for lipogenesis: after being glycolytically converted to acetyl CoA, glucose promotes fatty acid synthesis (Del Boca & Flatt, 1969).

In sum, LD formation is regulated by diverse physiological stimuli including some dietary fatty acids and metabolic hormones.

Palmitic acid (16:0)

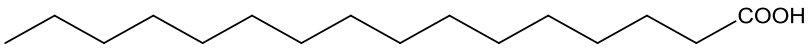

Oleic acid (18:1 (n-9))

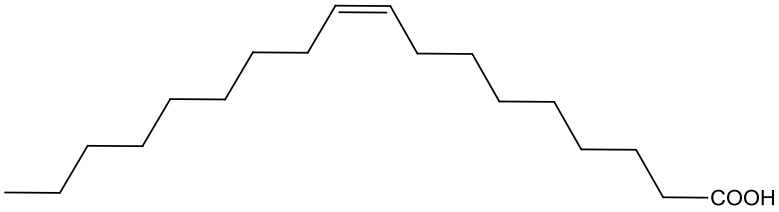

Docosahexaenoic acid (22:6 (n-3))

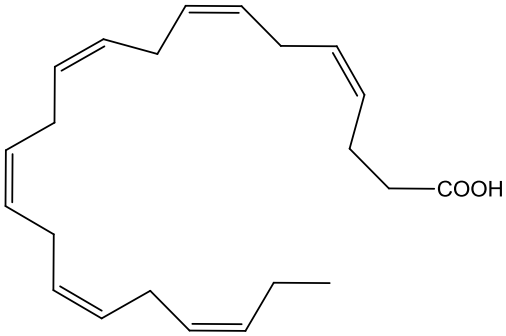

Figure 1.5 Structures of palmitic acid, oleic acid and docosahexaenoic acid.

Palmitic acid (16:0, saturated) and oleic acid (18:1, monounsaturated) are two major fatty acids in the blood. Docosahexaenoic acid (DHA), a polyunsaturated fatty acid, is much less abundant in the plasma. These fatty acids can be obtained from dietary sources, such as olive oil (oleic acid), palm oil (palmitic acid) and fish (DHA). The effects of these fatty acids on cells were examined under different conditions in our studies in Chapters 2 to 4.

1.4 Lipid droplets under stressful conditions and their implication in pathology

The key objective of this thesis was to understand the role of LDs under stressful conditions and in human metabolic disorders (e.g obesity/T2DM). Accumulation of TAG-rich LDs is a well-conserved process among eukaryotes. In plants (e.g algae), for instance, cytoplasmic LDs accumulate in response to a variety of environmental stressors, such as osmotic stress or nitrogen deprivation (Murphy, 2001). In mammals, LD accumulation is associated with several pathologies including obesity, T2DM, atherosclerosis, steatosis and bacterial infections (Bozza et al., 2009; Greenberg et al., 2011).

We investigated the role of LDs in oxidative stress (Chapter 2) and inflammation (Chapter 3 and 4). Furthermore, we studied the implication of pancreatic LDs in human T2DM (Chapter 5).

This section describes the current understanding of the implication of LDs in pathology, in particular in metabolic disorders such as obesity and T2DM, and provides background material for the experimental studies presented in Chapters 2 to 5.

1.4.1 A historical perspective of lipid droplet accumulation in pathology

LD accumulation in mammalian tissues under stressful conditions has been known since the 19th century. In 1867, Dr Hillier examines the liver of a patient poisoned with phosphorus and notes a remarkable accumulation of “oil globules of different sizes” in hepatic cells (Hillier, 1867). Decades later, Dr. Wells found that noxious agents like hydrazine and phosphorus could cause a high degree of “fatty change” or “fatty degeneration” in the liver of poisoned dogs (Wells, 1910). “Fatty degeneration” referred to the accumulation of fat induced by the toxic agent. Histological examination revealed that hepatocytes of hydrazine intoxicated dogs contained large amounts of cytoplasmic LDs. Other studies indicated the presence of fatty degeneration in peripheral and central organs in human diseases (Cotton, 1915; Reye et al., 1963). In 1963, Reye and his colleagues described the clinical and pathological features of twenty-one children with

encephalopathy and fatty degeneration of viscera (Reye et al., 1963). Extensive accumulation LDs was observed in hepatocytes and kidney cells, and to a lesser extent in the pancreas and myocardium. The aetiology of this disorder remains unknown, and is known as Reye's syndrome. Similar observations of fatty degeneration were shown to occur in other disease states and experimental conditions. In 1962, Herman and Fitzgerald observed LD accumulation in degenerating pancreatic acinar cells in rats injected ethionine, a methionine analog (Herman & Fitzgerald, 1962). Although most of the observations of LD accumulation were made in peripheral organs, a small number of studies have seen this phenomenon occurring also in central and peripheral nervous system. For instance, LD accumulation was observed in rat neural cells following radiation injury and exposure to tellurium (de Estable-Puig & Estable-Puig, 1973; Goodrum et al., 1990).

1.4.2 Lipid droplet accumulation by stress agents

One of the aims in this thesis was to investigate LD formation under oxidative stress in cells exposed to stress agents, more specifically exogenous metallic nanoparticles and ROS (e.g hydrogen peroxide). Accumulation of LDs by stress agents has been widely reported in the literature. For instance, LD accumulation has been observed in cells exposed to chemotherapeutic agents and ER-stress inducing agents (Delikatny et al., 2002; Lee et al., 2012; Schmitz et al., 2005). Noteworthy, increased LD content has been reported under different stressful conditions such as in hypoxic or apoptotic cells. In many studies, the accumulation of LDs correlated with increased production of ROS and mitochondrial damage. In our studies, we will also measure cellular ROS levels and examine subcellular structures in cells exposed to stress agents (i.e toxic nanoparticles and hydrogen peroxide).

1.4.2.1 Oxidative stress

Oxidative stress plays a fundamental role in the pathogenesis of many diseases, such as metabolic and neurodegenerative diseases (Emerit et al., 2004; Furukawa et al., 2004). It occurs when there is an imbalance between the production of ROS and cellular antioxidant defences (Jones, 2006). The imbalance in cellular redox state is accompanied by an overall increase in ROS such as superoxide radical ($^{\bullet}O_2^-$), hydroxyl radical ($HO^{\bullet}$), and hydrogen peroxide (H_2O_2) (Jones, 2008). These highly reactive molecules are deleterious to cells due to their ability to cause arbitrary oxidative damage to lipids, deoxyribonucleic acid (DNA) and proteins. These events may lead to cellular dysfunction or, when damages are too severe, to cell death. Alternatively, the cell may initiate an adaptive response to the stress by up-regulating key antioxidant enzymes, such as glutathione peroxidase, and repair the damages inflicted by ROS (Davies, 2000). This antioxidant defense system may prevent cells from undergoing apoptosis during oxidative stress.

Noteworthy, ROS induced by stress agents can trigger the activation of diverse specific signaling pathways, such as mitogen-activated protein kinases (MAPK) (McCubrey et al., 2006). In mammalian cells, the MAPK family is comprised of extracellular signal-regulated kinases (ERK), the c-Jun N-terminal kinase and the p38 MAPKs. These serine/threonine kinases activate many transcription factors, which can stimulate expression of genes involved in various cellular functions.

In Chapter 2 and 3, we will be examining the activation of c-Jun N-terminal kinase (JNK) and p38 MAPKs and elucidate their role in the regulation of LD formation under stressful conditions.

1.4.2.2 Intracellular sources of reactive oxygen species

Under physiological conditions, ROS are continuously generated from different intracellular sources and function as signalling molecules in cell proliferation and

apoptosis (D'Autreaux & Toledano, 2007). It is suggested that the majority of cellular ROS during normal metabolism is derived from mitochondria. Complex III in the mitochondrial electron transport chain is a major source of superoxide radical ($^{\bullet}O_2^-$) production (Chen et al., 2003). After being generated, O_2^- is enzymatically converted to H_2O_2 by superoxide dismutase (SOD). Other important intracellular sources of ROS are the peroxisomes, cytochrome P450 metabolism, and NADPH oxidase (Thannickal & Fanburg, 2000).

1.4.2.3 Exogenous sources of reactive oxygen species

A variety of exogenous stress stimuli are known to enhance ROS production either directly or indirectly through cellular mechanisms. A rise in ROS levels can be caused by xenobiotics, carcinogens, herbicides, pesticides, heavy metals, ionizing radiation, thermal shock and chemotherapeutic agents (Valko et al., 2006). Growth factors, hormones and inflammatory cytokines are also considered to be important ROS increasing factors. Among environmental agents, ultrafine particles and nanoparticles have also been shown to stimulate ROS production and cause oxidative stress (Muller et al., 2010). In Chapter 2, we will be using one such nanoparticle as stress inducing agent.

1.4.2.4 Nanoparticles as environmental stressors

Nanotechnology is a rapidly growing industry using engineered nanomaterials in a variety of technology and industry sectors such as electronics, information technology, cosmetics, sustainable energy applications (e.g solar panels), biomedical imaging and drug delivery (Salata, 2004). However, the increasing prevalence of nanotechnologies has augmented the risk of exposure to environmental nanoparticles and several toxicological studies have shown that some carbon-, metal- and semiconductor-based nanoparticles may pose a risk to human health and to the environment (Buzea et al., 2007; Nel et al., 2006). Due to their unique optical and physical properties, quantum dots (QD) have been widely used in live cell and animal imaging (Michalet et al., 2005). These fluorescent

nanocrystals with sizes between 2-100 nm are typically comprised of a metallic core, which is surrounded by a shell that renders QDs bioavailable (Bruchez et al., 1998). The core of QDs is often made of semiconductor metal complexes such as Cd-Te, cadmium-selenium (Cd-Se), zinc sulfide (Zn-S) and zinc selenium (Zn-Se) (Biju et al., 2008). The cytotoxicity of QDs has been extensively studied both *in vitro* and *in vivo* (Cho et al., 2007; Hauck et al., 2010; Lewinski et al., 2008; Lovric et al., 2005; Lovric et al., 2005). In these studies, increasing doses of certain types of QDs, namely those lacking a shell or without surface coating were strongly associated with increased cytotoxicity. This apparent cytotoxicity can be attributed to QD surface oxidation, which leads to the release of toxic metals (e.g Cd^{2+}) from the core. Conversely, QDs with a protective shell (e.g ZnS) or with a surface coated with bioconjugates were more stable and relatively nontoxic (Cho et al., 2007).

In Chapter 2, we used cytotoxic nanoparticle containing cadmium telluride (CdTe) and studied LD formation in cells exposed to them.

1.4.3 Lipid droplets in inflammation

Increased LD biogenesis within leukocytes under inflammatory conditions was observed more than thirty years ago (Dvorak et al., 1983). Clinical studies have reported LD accumulation in leukocytes under diverse inflammatory states including inflammatory arthritis (Weinstein, 1980), bacterial sepsis (Pacheco et al., 2002), acute respiratory distress syndrome (Triggiani et al., 1995) and atherosclerosis (Ross, 1995). *In vitro* and *in vivo* experimental studies further showed that LD accumulation in leukocytes could be induced by a wide variety of proinflammatory stimuli including pathogen-derived endotoxin (e.g lipopolysaccharides) (Pacheco et al., 2002), cytokines or chemokines (Bandeira-Melo et al., 2001; Bozza et al., 1998), platelet-activating factor (PAF) (Bozza et al., 1996) and modified low-density lipoproteins (e.g oxidized/acetylated LDL) (McGookey & Anderson, 1983; Tontonoz et al., 1998). Of note, leukocyte LD accumulation occurs in a highly regulated manner and is cell- and stimuli- dependent phenomenon (Bozza et al., 2009).

LPS is a major component of the outer surface of Gram-negative bacteria. Its structure consists of a polysaccharide moiety and a lipid A moiety, which is responsible for its biological activity (Caroff & Karibian, 2003). *In vivo* studies have shown that LPS stimulates LD accumulation in leukocytes in a time- and dose-dependent manner, by acting through its receptor, Toll-like receptor 4 (TLR4) (Pacheco et al., 2002; Pacheco et al., 2007). In fact, LPS failed to induce LD accumulation in TLR4-mutated mice. Other TLRs were also shown to be implicated in leukocyte LD formation during bacterial infections (D'Avila et al., 2006; Mattos et al., 2010).

The biological functions of LDs in activated leukocytes were previously investigated. They are known to be involved in cellular signaling, lipid metabolism, membrane trafficking, and synthesis of inflammatory lipid mediators (e.g eicosanoids) (Bozza et al., 2009). Importantly, LDs have been for long regarded as sites involved in eicosanoid generation (Bozza et al., 2011; Weller & Dvorak, 1994). This is supported by the fact that LD accumulation in activated leukocytes correlates with enhanced generation of prostaglandins and leukotrienes (Pacheco et al., 2002). Furthermore, many enzymes involved in eicosanoid synthesis, such as cytoplasmic phospholipase A_2, cyclooxygenases and lipoxygeneases were found to be localized on the surface of LDs (Bozza et al., 1997; Moreira et al., 2009). In addition to eicosanoid-forming enzymes, LDs in leukocytes compartmentalize a diverse set of structural, signaling and membrane trafficking proteins. Like in many other cells, the PAT family proteins perilipin-2 and -3 associate with LDs in leukocytes and participate in LD biogenesis under inflammatory conditions (Feingold et al., 2010; Wan et al., 2007). In fact, many intracellular signaling proteins such as PI3K (Yu et al., 2000), ERK 1/2 MAPK (Yu et al., 1998) and protein kinase C (PKC) (Chen et al., 2002) also associate with LDs, suggesting that LDs are implicated in cellular signaling.

In Chapter3, we will explore the regulation and dynamics of LD formation in LPS-stimulated microglia, the resident immune cells in the brain. These neural cells are the guardians of the central nervous system (CNS) as they constantly screen the brain

microenvironment and become reactive following CNS injury, bacterial infections and exposure to endotoxin (Rivest, 2009). While the role and accumulation of LDs inflammatory macrophages have been previously extensively investigated, their role in neuroinflammation and their status in reactive microglia (i.e microglia) remain unclear. Interestingly, findings from a recent study suggest that LDs in microglia may serve an important function in neurodegeneration (Ebert et al., 2009). It was shown that activated microglia in a mouse model of inherited retinal degeneration contained large number of LDs. Analysis of retinal lipid composition revealed decreased levels of docosahexaenoic acid (DHA), a n-3 polyunsaturated fatty acid. Noteworthy, supplementation with DHA attenuated microglial activation and promoted cell survival. While the anti-inflammatory properties of DHA are well established, the mechanisms underlying its anti-inflammatory effects still remain unclear.

In Chapter 4, we will elucidate the mechanisms underlying the anti-inflammatory properties of DHA in LPS-stimulated microglia. In particular, we will study the role of LDs and their contribution to the immunomodulating effect of DHA.

1.4.4 Lipid droplets in obesity, type 2 diabetes mellitus and metabolic syndrome

One of the key aims in our work was to understand the role of LDs and LD associated proteins in human metabolic disorders, namely obesity and T2DM. We sought to examine the impact of T2DM and obesity on LDs and LD-associated protein, perilipin-2, in human pancreatic tissue, more specifically, in pancreatic islets. Lipotoxicity in pancreatic islet β-cells is considered to be an important contributor to β-cell dysfunction or death.

Obesity is characterized by excessive lipid storage in the adipose tissue and is strongly associated with the development of T2DM and cardiovascular disease (Lavie et al., 2009) . When the amount of fat in the adipose tissue is excessive, fatty acids spill-over and accumulate in non-adipose tissues such as the liver, pancreas, heart and muscle (Schaffer, 2003). This phenomenon is known as ectopic fat accumulation and is associated with lipotoxicity in the affected cells and tissues (van Herpen & Schrauwen-Hinderling, 2008)

(See Figure 1.6). In this section, we will briefly describe the pathogeneses of type 2 diabetes and obesity. Subsequently, we will focus on the implication of LDs and LD-associated proteins in the development of these metabolic diseases.

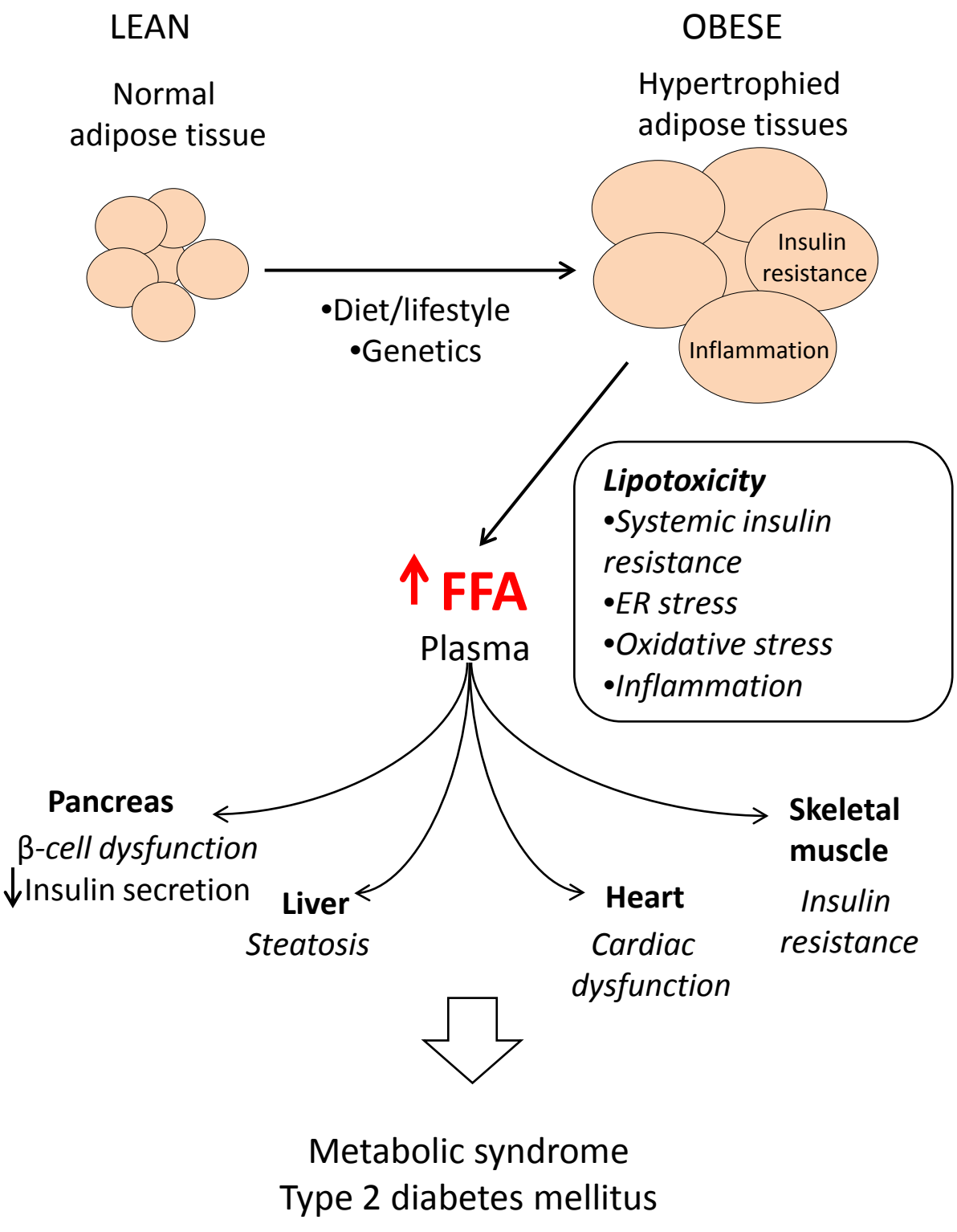
LEAN
Normal adipose tissue
OBESE
Hypertrophied adipose tissues
Insulin resistance
Inflammation
•Diet/lifestyle
•Genetics
Lipotoxicity
•Systemic insulin resistance
•ER stress
•Oxidative stress
•Inflammation
↑ FFA
Plasma
Pancreas
β-cell dysfunction
↓Insulin secretion
Liver
Steatosis
Heart
Cardiac dysfunction
Skeletal muscle
Insulin resistance
Metabolic syndrome
Type 2 diabetes mellitus

Figure 1.6 Obesity, ectopic fat accumulation and metabolic complications

Excess fat accumulating in the adipose tissue may spill out from adipocytes and enter the circulation. Of note, chronic excess of lipids has been previously shown to be associated with macrophage infiltration in adipose tissue, leading to local inflammation, which may eventually develop into a systemic inflammation. Chronically elevated fatty acid levels have been linked to insulin resistance, endoplasmic reticulum (ER) stress, oxidative stress and inflammation, and associated with several pathologies. Ensuing lipotoxicity leads to cellular dysfunction, for instance impaired insulin secretion from pancreatic β-cells. This hyperlipidaemic state is an important component of the metabolic syndrome, and when combined with diabetic hyperglycemia, may become much more deleterious.

1.4.4.1 Obesity

It is estimated that about one-quarter of Canadian adults and over one third of adults in the United States are obese according to measurements of body mass index (BMI) (BMI $\geq$30 kg m^{-2}) (National Center for Health Statistics (NCHS) Data Brief, 2012; Public Health Agency of Canada & Canadian Institute for Health Information, 2011). The prevalence of overweight (BMI $\geq$ 25 kg m^{-2}) and obesity is increasing worldwide and has now reached epidemic proportions globally, with 1.4 billion adults overweight and 500 million of them clinically obese (World Health Organization (WHO), 2012). The global increase in obesity seems to be driven by changes in the global food system, which is producing more processed, affordable and effectively marketed food than ever before (Swinburn et al., 2011). Many factors contribute to obesity including behavioural (diet, physical activity), environmental, genetic and socio-economical factors.

Obesity is essentially caused by a positive energy balance resulting from excess calorie intake, insufficient physical activity, or the combination of both (Wells & Siervo, 2011). The energy excess is stored in the form of fat in subcutaneous and visceral (or intra-abdominal) adipose tissue. It is recognized that excess visceral adipose tissue is strongly associated with fat deposition in other tissues, insulin resistance and other obesity-associated complications (Lebovitz & Banerji, 2005). Conversely, subcutaneous adipose tissue might serve as a metabolic sink to buffer the excess energy and protect the other organs from fat deposition (Porter et al., 2009). Therefore, individuals with subcutaneous fat accumulation may be protected from the development of metabolic complications. It was hypothesized that the appearance of insulin resistance among individuals with excess visceral adiposity may be caused by the increased plasma fatty acid concentrations (Klein, 2004). In fact, this is supported by the observation that levels of circulating fatty acids are elevated in most obese individuals (Boden, 1997). Chronically elevated plasma fatty acid levels may impair carbohydrate and lipid metabolism in the liver, reduce insulin sensitivity in skeletal muscle, and, on the long term, cause pancreatic β-cell dysfunction (McGarry & Dobbins, 1999; Poitout, 2004)

1.4.4.2 Type 2 diabetes mellitus

The past three decades have seen a striking increase in the prevalence of T2DM worldwide both in developed and developing countries (Zimmet et al., 2001). As of 2011, diabetes affected 25.6 million adults aged 20 years or older in the U.S, equivalent to 11.3 % of all people in this age group (Centers for Disease Control and Prevention, 2011). In adults, T2DM accounted for about 90-95 % of all diabetes cases. Almost 2.4 million Canadians (6.8 % of population) were living with diabetes in 2009, T2DM accounting for 90-95 % of the cases (Public Health Agency of Canada, 2011). If the incidence rate is maintained, it is estimated that the number of Canadians with diabetes will reach 3.7 million by 2019. The increasing prevalence of T2DM is of major concern, because it is a major independent risk factor for cardiovascular disease, a predominant cause of death among T2DM patients (Mazzone et al., 2008; Panzram, 1987).

The fundamental problem in T2DM, or *non-insulin dependent diabetes*, is peripheral insulin resistance, which results in impaired plasma glucose clearance and postprandial hyperglycemia (American Diabetes Association, 2011). Impaired glucose uptake by skeletal muscle or fat cells is perceived as one of the major contributors to hyperglycemia in T2DM patients (DeFronzo & Tripathy, 2009). Increased gluconeogenesis and glucose output from the liver is another important contributor to hyperglycemia in T2DM (Gastaldelli et al., 2000). At the earlier stages of T2DM, as the tissues become unresponsive to insulin, pancreatic β-cells compensate by secreting more insulin. Such compensation leads to a hyperinsulinemic state and is commonly observed in insulin resistant obese individuals (Shanik et al., 2008). At this stage, a twofold increase in basal insulin level is common in patients with insulin resistance associated with T2DM or obesity.

1.4.4.3 Association between obesity and type 2 diabetes mellitus

Obesity is strongly associated with insulin resistance and T2DM (Astrup & Finer, 2000). In fact, it is estimated that 80-90% of patients with T2DM are overweight or obese

(Astrup & Finer, 2000). Thus, the dramatic increase in the prevalence of T2DM over the last 20 years may be explained by the global epidemic of obesity. Other factors, such as sedentary lifestyle, over nutrition and stress are regarded, along with obesity, to be important risk factors for T2DM. Noteworthy, not all obese subjects develop T2DM, and not all T2DM patients are obese. This suggests that the development of T2DM also depends on other factors such as genetic susceptibility.

1.4.4.4 Metabolic syndrome

Metabolic syndrome, also known as the Insulin Resistance syndrome or Syndrome X, is a cluster of risk factors for cardiovascular disease (Elliott et al., 2002). The risk factors include central (abdominal) obesity, dyslipidaemia, hypertension and insulin resistance/glucose intolerance (Alberti et al., 2005). The dyslipidaemia in metabolic syndrome is characterized by elevated circulating triglycerides (hypertriglyceridemia) and low HDL-cholesterol. The increasing prevalence of metabolic syndrome has become a major public health burden and will certainly exert a negative impact on the occurrence of T2DM and cardiovascular disease.

1.4.4.5 Ectopic fat accumulation in obesity, type 2 diabetes mellitus and metabolic syndrome

It is well known that obesity is associated with increased basal and hormonally stimulated lipolysis, resulting in increased systemic FFA and leading to lipid accumulation in non-adipose tissues (Coppack et al., 1994) (See Figure 1.6). It is now known that high levels of circulating FFA play a key role in development of insulin resistance in muscle and adipocytes and induce produce lipotoxicity (van Herpen & Schrauwen-Hinderling, 2008) . The excess FFA entering non-adipose tissues are shunted into LDs, where they are stored as TAG. In the last decade, LDs and LD-associated proteins have emerged as organelles highly involved in metabolic diseases (Greenberg et al., 2011).

In Chapter 5, we will investigate the impact of ectopic fat accumulation on the expression of perilipin-2 in the pancreas and, more specifically, in pancreatic islet β-cells. This will be examined in lean and obese subjects, either without or with T2DM. The study will provide us w with additional piece of information about the implication of LDs (or perilipin-2) in the pathogenesis of T2DM in humans.

It is well established that prolonged exposure of β-cells to excess levels of FFAs plays an important role in islet β-cell deterioration through lipotoxic events (McGarry & Dobbins, 1999). It was also postulated that the combination of chronic hyperglycemia (glucotoxicity) and hyperlipidemia (lipotoxicity) is synergistically detrimental and plays a critical role in β-cell failure in T2DM (Poitout, 2004). The relationship between lipid accumulation (lipotoxicity) in pancreatic islets and β-cell dysfunction was examined *in vivo* for the first time about two decades ago by the group of Unger. In the Zucker diabetic fatty (ZDF) rat, plasma FFA levels markedly increased in the weeks preceding hyperglycemia (Lee et al., 1994). Furthermore, a robust and abrupt increase in islet TAG content was observed prior to hyperglycemia. At this stage, LDs were detected in sections of diabetic islets. Caloric restriction in obese pre-diabetic rats was associated with a marked attenuation of hyperglycemia and accumulation of fat in islets. The results from this study support a lipotoxic model for obesity-related β-cell impairment and subsequent T2DM.

While the contribution of lipotoxic mechanisms to β-cell dysfunction/death is well known, the role of LDs in β-cell lipotoxicity remains obscure. As in other cell types, β-cells accumulate a large number of LDs in them when incubated with unsaturated fatty acids, such as oleic acid (Cnop et al., 2001; Collins et al., 2008; Moffitt et al., 2005). LDs are also present in islet non-β-cells, but they are not as abundant as in β-cells (Cnop et al., 2001; Winborn, 1963). It was postulated that the ability of β-cells in rodents to form TAG-rich LDs might be a protective mechanism against FFA-induced cytotoxicity (Cnop et al., 2001). An increasing number of studies showed increased LD deposition in the exocrine and endocrine pancreas of obese rodents with T2DM (Lee et al., 1994; Lee et al., 2010; Man et al., 1997). It was shown that the accumulation of LDs in islet β-cells may occur before the onset of T2DM, during the hyperinsulinemic phase, likely as the

result of increased influx of FFA into β-cells (Fex et al., 2007; Lee et al., 1994). Whether this occurs also in humans is not known, and will be one of our key objectives in Chapter 5. Moreover, it will be important to determine whether islet LD accumulation in humans with T2DM plays a protective role, or rather contributes to lipotoxic mechanisms.

1.4.4.6 Lipid droplet-associated proteins in type 2 diabetes mellitus and obesity

As mentioned before, LD-associated proteins are able to regulate lipolysis in the adipose tissue, and therefore serve an important function by controlling the release of FFA from adipocytes into the circulation. Variations in the expression of LD-associated proteins may contribute to dysregulated lipolysis in adipocytes and impair lipid homeostasis. Noteworthy, LDs and its proteins are also abundant in some non-adipose tissue, such as liver and muscle, and dysregulations in LDs in such tissue may also play an important role in metabolic disorders like insulin resistance. Several studies have already revealed LD abnormalities in liver, muscle and kidney of T2DM or obese rodents and humans (Minnaard et al., 2009; Mishra et al., 2004; Motomura et al., 2006). To gain a better understanding of the role of LD- associated proteins in human metabolic diseases, we will study (Chapter 5) the expression and status of perilipin-2 in the pancreas in human T2DM and obesity. As far as we know, this is the first study questioning the status of perilipin-2 expression in the pancreas of obese and diabetic individuals.

1.4.4.6.1 Perilipin-1

Due to its important role in lipolysis, it was hypothesized that variations in perilipin-1 in the obese adipose tissue might contribute to aberrant lipolysis in these individuals. Indeed, two independent studies have shown that perilipin-1 expression in adipose tissue was significantly lower in obese compared to non-obese individuals (Mottagui-Tabar et al., 2003; Wang et al., 2003). Low perilipin-1 content in these subjects was associated with increased *in vivo* lipolytic activity, possibly due to increased basal lipolysis.

Collectively, these studies indicate that lack of perilipin-1 leads to uncontrolled lipolysis, which may cause peripheral insulin resistance.

1.4.4.6.2 Perilipin-2

Perilipin-2 is the predominant LD-associated protein in non-adipose tissue. An increasing number of studies suggest that perilipin-2 might plays a role in ectopic fat accumulation in obesity/T2DM (Minnaard et al., 2009; Motomura et al., 2006; Varela et al., 2008). Perilipin-2 expression was up-regulated in liver of obese/diabetic mice (ob/ob mice) and in patients with fatty liver (Motomura et al., 2006). Similarly, an increase in perilipin-2 expression was observed in liver steatosis induced by high fat diet (HFD). Interestingly, inhibition of perilipin-2 expression in animals fed with a HFD reduced TAG and prevented hepatic insulin resistance in these animals (Varela et al., 2008). These results demonstrated a strong link between perilipin-2 and diet-induced insulin resistance in the liver. Perilipin-2 might also play a role in the development of insulin resistance in skeletal muscle (Minnaard et al., 2009). Muscle perilipin-2 expression was considerably increased in ZDF rats during the progression of T2DM, as compared to lean control rats.

1.4.4.6.3 Fat-specific protein 27

In 2007, Puri et al. identified a new LD-associated protein, fat-specific protein 27 (FSP27), also named CIDEC (cell death-inducing DFF45-like effector C), which is predominantly expressed in white and brown adipose tissue (Puri et al., 2007). FSP27 functions in TAG synthesis and LD accumulation, and also seems to be an important positive regulator of LD size. Accordingly, adipocytes from FSP27 knockout mice contain smaller or fragmented LDs, and show increased lipolysis and mitochondrial oxidative phosphorylation (Puri & Czech, 2008). These mice were protected from diet-induced obesity and insulin resistance.

Thus far, there have been no studies investigating perilipin-2 or FSP27 in the diabetic or obese pancreas. In Chapter 5, we will assess the expression of perilipin-2 in human pancreatic tissue (and pancreatic islets) from T2DM and obese donors. We will examine

its distribution in islets and assess it abundance in β-cells. The study will show, for the first time, the impact of T2DM and obesity on the status of pancreatic perilipin-2 in humans. We will additionally measure the expression of several genes involved in islet function, metabolism, LD regulation (e.g FSP27) and antioxidant defense.

1.4.5 Oxidative stress in obesity and type 2 diabetes mellitus

Obesity and T2DM are characterized by increased systemic and local oxidative stress (Furukawa et al., 2004; Meigs et al., 2007). Oxidative stress is known to impair many key physiological processes including glucose transport in muscle, insulin secretion by pancreatic β-cells and adipokine secretion by adipose tissue (Blair et al., 1999; Furukawa et al., 2004; Robertson, 2004). Excess levels of FFA in adipocytes increase ROS production, and this correlates with systemic oxidative stress and insulin resistance (Furukawa et al., 2004; Meigs et al., 2007). Chronic oxidative stress has been proposed to play a critical role in the development of T2DM (Robertson, 2004). In fact, chronic hyperglycemia can increase ROS production and cause oxidative stress in different cell types, including in pancreatic β-cells (Leahy et al., 1992). This results in β-cell dysfunction, which is characterized by selective loss of glucose-induced insulin secretion (Leahy et al., 1992). Chronic hyperglycemia is also strongly implicated in long-term complications of T2DM, including microvascular, macrovascular and peripheral nerve injuries (Stratton et al., 2000).

In Chapter 5, we examined the impact of obesity and T2DM on the expression of genes involved in oxidative stress and antioxidant defense. Our objective was to establish a relationship between pancreatic oxidative stress, islet function, and perilipin-2 expression.

Alterations in pro-oxidant and anti-oxidant enzymes have been reported in T2DM and obese subjects. For instance, expression and activity of NADPH oxidase complex was shown to be increased in cells and tissues of obese and T2DM individuals (Furukawa et al., 2004; Huang et al., 2011). On the other hand, abnormalities in activity and expression of several anti-oxidant enzymes such as glutathione peroxidase (GPx) and superoxide

dismutase (SOD) were also reported in T2DM and obesity (Beltowski et al., 2000; Kesavulu et al., 2001). Heme oxygenase-1 (HO-1) is a stress-responsive enzyme that catalyzes the degradation of heme to free iron, carbon monoxide (CO), and biliverdin in mammalian cells (Morse & Choi, 2005). Alterations in HO-1 activity and expression have been reported in T2DM and obese subjects (Avogaro et al., 2003; Bao et al., 2010; Li et al., 2008). Upregulation of HO-1 seems to play a protective role against oxidative stress and inflammation (Exner et al., 2004; Kruger et al., 2006).

1.4.6 Lipid droplet size alterations under pathological conditions

The biological function of a given LD is affected by its size. For instance, very large LDs in adipocytes (up to 100 μm) play a much different role compared to much smaller (about 1 μm) LDs in non-adipocytes (Suzuki et al., 2011). Furthermore, in a given LD population in non-adipocytes, small LDs differ from large LDs with respect to the type of proteins associated with them (Wolins et al., 2006). Interestingly, a marked enlargement of LDs has been reported under some pathological conditions such as inflammation, hepatic steatosis and T2DM (D'Avila et al., 2008; Fraenkel et al., 2008; Suzuki et al., 2011). For instance, LD size is characteristically increased in pro-inflammatory leukocytes (D'Avila et al., 2008).

In Chapter 3 and Chapter 4, we investigated changes in LD sizes in inflammatory cells and examined the biological implications of such alterations.

Connecting text between Chapter 1 and Chapter 2

In Chapter 1, we provided a description of the physiological roles of LDs and also of their implication in pathology. Since we were particularly interested in understanding their functions in pathological states, we investigated them under oxidative stress in rat pheochromocytoma cell line (PC12), neuronal-like cells that can be differentiated into cholinergic cells. Because PC12 cells are highly susceptible to different stressors, they have often been used as a model system to study oxidative stress and mechanisms involved in cell death (Piga et al., 2007). In Chapter 2 and in Appendices (I-V), we show that exogenous stressors (e.g cytotoxic nanoparticles and hydrogen peroxide) induce oxidative stress and increase cellular LD and perilipin-2 content. To determine whether LD formation per se is protective under stressful conditions, we primed the cells with LD-inducing dietary fatty acid, oleic acid, which protected cells against serum-starvation and stress-induced cell death. Our results indicate that induction of LDs by physiological stimuli (e.g oleic acid) may play a protective role against nutrient deprivation and/or oxidative stress that occurs in pathogenesis.

CHAPTER 2

Lipid droplets: their role in nanoparticle-induced oxidative stress

Armen Khatchadourian and Dusica Maysinger

Molecular Pharmaceutics (American Chemical Society), 2009, 6 (4), 1125-1137

2.1 Abstract

Lipid droplets are cytoplasmic organelles found in almost all cells under physiological or pathological conditions. Certain nanoparticles can induce lipid droplet formation under oxidative stress conditions. Small metallic nanoparticles such as cadmium telluride (CdTe) nanoparticles, particularly those with incompletely protected surfaces, induce oxidative stress and may inflict damages to several intracellular organelles. The objective of this study was to assess formation of lipid droplets in cells treated with CdTe nanoparticles and relate their status to cell function (mitochondrial activity and cell viability). Multicolor labeling of cellular organelles (lipid droplets and lysosomes) showed that lipid droplets formed in pheochromocytoma (PC12) cells following nanoparticle or oleic acid treatment. Some lipid droplets were found closely apposed to lysosomes suggesting possible communication between these organelles during severe oxidative stress. Combination of microscopy of living cells with cell viability assays showed that oleic acid-induced lipid droplets not only serve as intracellular storage sites, but also play a protective role in starving stressed cells. Results from these studies suggest that oleic acid-induced LD in PC12 cells are dynamic and adaptive organelles, which provide energy to starving cells and facilitate their rescue under starvation and exposure to metallic nanoparticles.

2.2 Introduction

Lipid droplets are cytoplasmic organelles found in most cell types, but their number and sizes vary from one cell type to another. They consist of two major compartments: a core filled with neutral lipids, such as triacylglycerides (TG), diacylglycerol and cholesterol esters, and a surrounding phospholipid monolayer, which contains free cholesterol and proteins (Murphy, 2001). During periods of nutrient shortage, lipolysis causes FFA to be released from the TG stored in LD (Ducharme & Bickel, 2008; Schmitz & Grandl, 2008; Smirnova et al., 2006). Although adipocytes are the cells specialized in lipolysis, all tissues must be able to convert their TG sources to FFA during starvation periods. Initially, LDs have been regarded as static organelles mainly involved in fat storage, but

more recently they were proposed to be dynamic bodies interacting with other cellular compartments. Recently, Goodman and Murphy reviewed different roles of LD and their dynamic interactions with several organelles (Goodman, 2008; Murphy et al., 2008). LDs are highly motile organelles and undergo microtubule-dependent bidirectional movements in the cytoplasm (Valetti et al., 1999). Their communication with other cellular compartments is supported by the presence of many membrane traffic regulating proteins, such as Rab and ARF1 (ADP- ribosylation factor), on their surfaces (Goodman, 2008). Close apposition between LDs and organelles such as the mitochondria, peroxisomes and the endoplasmic reticulum (ER) have been detected by fluorescence resonance energy transfer (FRET) analysis, confocal and electron microscopy (Binns et al., 2006; Ozeki et al., 2005; Sturmey et al., 2006). However, the studies employing multiple labeling of LD and other organelles using organelle-specific fluorescent dyes are rare.

In this study, we used organelle-specific dyes to investigate the status and the role of both LDs and lysosomes under nanoparticle-induced oxidative stress conditions and trophic factor deprivation in live PC12 cells. These are a well established cell line in neuroscience and they have been used for studying cytotoxicity of different nanoparticles (Lovric et al., 2005). Recent studies suggest that metallic nanoparticles containing cadmium, tellurium or mercury can induce oxidative stress (Cho et al., 2007; Choi et al., 2007; Lovric et al., 2005; Lovric et al., 2005; Maysinger, 2007; Seleverstov et al., 2006; Stern et al., 2008; Zabirnyk et al., 2007). It was proposed that enhanced formation of LDs could be a common cellular response to stress inducing nanomaterials (Maysinger, 2007; Seleverstov et al., 2006). With growing production of different nanomaterials including nanoparticles and their possible slipping past cell security, it is of interest to explore nanoparticle interactions with different organelles and relate them to changes in cellular functions (Hardman, 2006; Verma et al., 2008; Xia, 2008). It is of particular interest to investigate consequences of long term exposure of cells to hardly detectable nanoparticles since their insult to individual cellular organelles could lead to irreversible untoward changes to cellular organelles and eventually cell death (Cho et al., 2007; Choi et al., 2007; Maysinger & Lovric, 2007). We used PC12 cells to examine a possible role of LD formation in the presence and absence of nanoparticles and also with and without

monounsaturated fatty acid, oleic acid. LD formation is commonly induced by long-chain unsaturated fatty acids such oleic acid (C18:1) (Fujimoto et al., 2006; Yonezawa et al., 2004). We selected oleic acid because it is a major component of the plasma and is commonly used to induce LDs in different cell types without causing cytotoxicity when applied within a physiological concentration range (Artwohl et al., 2004; Falconer et al., 1994; Fujimoto et al., 2006; Guo et al., 2008).

Fluorescence-based detection of LDs is commonly achieved in fixed cells with oil-red-O (ORO) and in live cells with Bodipy 493/503 and Nile Red (Diaz et al., 2008; Guo et al., 2008; Tavian & Colombo, 2007). These hydrophobic dyes are useful because they help to evaluate LD number, surface, volume and cellular distribution (Guo et al., 2008; Tavian & Colombo, 2007). Detecting changes in LD formation, size, and examining interactions between LDs and other organelles may be useful to elucidate the underlying mechanisms leading to the development of diseases in which lipid metabolism is impaired, such as obesity and diabetes (Bakker et al., 2000; Cheng et al., 2006).

Results from the present studies suggest that cadmium telluride nanoparticles can induce formation of LD and cause marked changes in their morphology and proximity to lysosomes. We show that oleic acid treatment prior to the nanoparticle-induced oxidative stress enhances cell survival and prevents enlargement of lysosomes. Studies of interactions between nanoparticles and other nanomaterials with cellular organelles will eventually (i) aid in defining the most suitable structural properties which cause the least cellular damage, and (ii) define efficient ways of enhancing intrinsic cellular defenses to achieve maximal protection from possible nanomaterial insults.

2.3 Materials and Methods

Cell Cultures

Rat pheochromocytoma cells (PC12) (ATCC, Rockville. MD,USA) were cultured (37°C, 5 % CO_2) in RPMI1640 (Gibco, Burlington, ON, Canada) medium containing 10% fetal bovine serum (FBS)(Gibco) and 0.01 M Hepes buffer (Gibco).

Colocalization of LDs and lysosomes in live cells

Live PC12 cells seeded (7.5 $X10^3$ /well) in poly-d-lysine coated chambers slides (Lab-Tek, Nalge Nunc International, Rochester, NY, USA) were stained with Bodipy 493/503 (38 µM/ 10 min) in RPMI1640. Cells were washed with PBS and then lysosomes were stained with Lysotracker Red DND-99 (L-7528, MP) (500 nM/ 3 min) in RPMI1640. Cells were washed with PBS and taken to the confocal microscope for live imaging.

Lysotracker DND99 (LTR) and monodansylcadaverine (MDC) staining in live cells

PC12 cells were seeded in 24 well plates (Sarstedt, #83.1836) at a density of $5X10^4$ cells/well and cultured overnight in complete culture medium. Cells were treated as indicated in Figure legends, washed with PBS and stained with LTR (500 nM) for 3 min or MDC (Sigma, #30432) (50 µM) for 10 min at 37°C in RPMI1640. The dye was removed and cells were washed with PBS. Images of subcellular compartments labeled with LTR and MDC were acquired at 40X with a Leica DFC350FX monochrome digital camera connected to a Leica DMI4000B inverted fluorescence microscope. Images were acquired and pseudo-colored using Leica Application Suite (LAS) software. Relative fluorescence intensity of LTR in treated PC12 was measured with ImageJ (1.38) software.

Quantification of lipid droplet (LD) number

PC12 were seeded ($5X10^4$/well) on 24 well-plates (Sarstedt, #83.1836) and cultured overnight in serum containing media. Cells treated as indicated in Figure legends were washed with PBS and stained with Bodipy 493/503 (32 µM/ 10 min). Nuclei were labelled with Hoechst 33342 (10 µM/ 30 min). Fluorescent images of nuclei and LDs were acquired at 40X with a Leica DFC350FX monochrome digital camera connected to a Leica DMI4000B inverted fluorescence microscope. Images were acquired and pseudo-colored using Leica Application Suite (LAS) software. LDs were counted using ImageJ (1.38) software.

Detection of reactive oxygen species (ROS) and superoxide anion

Superoxide detection. PC12 cells seeded ($2.5X10^4$/well) on 96 well-plates (Costar,#3603) were treated with nanoparticles and hydrogen peroxide as described in the figure legends

and incubated with dihydroethidium (DHE) (MP, D-11347) (50 μM) for 30 min at 37°C. Fluorescence of DHE was determined with a Fluostar Optima spectrofluorometer (BMG LabTech) using excitation and emission wavelengths of 544 and 590 nm, respectively. *ROS detection.* PC12 cells seeded ($5X10^4$/well) on 24-well plates (Sarstedt) were treated as described in the figure legends and stained with 2',7'-dichlorodihydrofluorescein diacetate (DCFH-DA) (MP, D-399) (20μM) for 30 min at 37°C.

Oleic acid and palmitic acid preparation

Oleic acid/BSA complex was formed by the addition of 30 mg oleic acid (Sigma) and 50 mg palmitic acid (Sigma) to fatty acid free 5% BSA (Sigma, A6003) solution. The stock solution concentration was adjusted to 4 mM oleic acid or palmitic acid after determination with the NEFA C method kit (Wako). Aliquots of oleic and palmitic acid stocks (4 mM) were stored at -20 °C.

Synthesis of CdTe- nanoparticles

All chemicals for CdTe nanoparticle preparation were from Sigma-Aldrich (Oakville, ON, Canada). $NaBH_4$ (Sigma-Aldrich, Oakville, ON, Canada) (0.8 g, 21.15 mmol) was dissolved in water (20 ml) at 0°C. Tellurium powder (1.28 g, 10.03 mmol) was added portion-wise, and the mixture was stirred at 0°C under N_2 for 8 h, yielding a purple solution. The reaction mixture yielded NaHTe which was kept at 4°C in the dark. $Cd(ClO_4)_2$ (0.25 ml, 1 M aqueous solution), and 3-mercaptopropionic acid (MPA; 0.2 g, 1.884 mmol) were dissolved in water (200 ml). The pH of the solution was adjusted to 10.5 using 1 M KOH prior to addition of NaHTe solution (0.1 ml). The reaction mixture became light brown in color and was heated to reflux. Aliquots were taken as the reaction proceeded, and the fluorescence spectra were recorded to monitor the nanoparticle growth as a function of reaction time. The maximum emission wavelength after 25 minutes (λ_{em} = 530 nm) shifted to longer wavelengths as the reaction proceeded. The diameter of the CdTe nanoparticle core was determined by absorption/emission studies as described previously (Yu et al., 2003).

MTT assay for cell viability

PC12 cells seeded in 24-well plates ($5X10^4$ cells/well) were culture overnight in serum–containing media. Serum-deprived cells were treated with oleic acid (400 μM) and

palmitic acid (400 μM) for 24h before exposure to CdTe nanoparticles (23 nM) for 48h. MTT (3-(4,5-dimethylthiazol-2-yl)-2,5-diphenyl tetrazolium bromide, Sigma) was performed to assess the mitochondrial activity of cells. Treated cells were incubated with MTT (0.5mg/ml) for 1h at 37 °C, after which media were removed and cells were lysed with DMSO (Sigma). Absorbance was measured at 595 nm using a Benchmark microplate reader (Bio-Rad, Mississauga, ON, Canada). All measurements were performed in quadruplicates.

Confocal microscopy

Images were acquired with a Zeiss LSM 510 NLO inverted microscope. Lysosomes were stained with Lysotracker Red DND-99 (λ_{ex} 577 nm, λ_{em} 590 nm) and imaged with the HeNe 543 nm laser using a LP 560 filter. LDs stained with Bodipy 493/503 (λ_{ex} 493 nm, λ_{em} 503 nm) were visualized using Argon 488 laser and the BP 505-550 filter. Images were acquired at a resolution of 1024 × 1024.

Transmission Electron Microscopy (TEM)

The status of PC12 cell subcellular organelles was assessed by JEOL JEM-2000FX TEM operating at an accelerating voltage of 80 kV. Cells in monolayers with or without CdTe nanoparticle treatment were fixed with 4% paraformaldehyde, and cut using an Ultracut-E ultramicrotome (Reichert-Jung, Leica Microsystems, Austria). The ultrathin sections were transferred onto 200-mesh copper grids (Electron Microscopy Sciences). The grids were then doubly stained with uranyl acetate (negative stain for background) and Reynolds lead citrate stain (provides contrast for cellular membranes).

Statistics

Statistical analysis was performed using Systat (version 10.2). Two sample T-test was used when only two groups were being compared. Multiple comparisons were done with one way ANOVA, followed by Bonferroni's correction post-hoc test. All data are presented as group means ± SEM. $p<0.05$ was considered significant.

2.4 Results

2.4.1 Increased production of reactive oxygen species (ROS) following CdTe nanoparticle treatment

CdTe spherical nanoparticles (diameter=2.8nm) consist of a cadmium telluride core and do not have a zinc sulfide protecting cap, commonly used to stabilize the nanoparticle (Derfus et al., 2004). The coating with mercaptopropionic acid (MPA) increases nanoparticle hydrophilicity and renders the surface negative. It was previously shown that ROS are produced in PC12 cells exposed to CdTe nanoparticles (Lovric et al., 2005). In order to demonstrate generation of superoxide anion (O_2^-), dihydroethidium (DHE) was used. DHE oxidation by O_2^- results with ethidine, which intercalates with cellular DNA, yielding bright red, fluorescent nuclear staining. Hydrogen peroxide (H_2O_2) (10 μM), known for its capacity to generate ROS such as O_2^- in different cell types, was used as a positive control during DHE staining experiments (Satoh et al., 1997; Viola et al., 2007). Spectrofluorometric measurements of ethidine fluorescence showed significant increase in fluorescence intensity in cells treated with CdTe nanoparticles (23 nM) (26 %, $p<0.001$) and H_2O_2 (52%, $p<0.001$) relative to non-treated (serum deprived cells) (Figure 2.1A). These data are supported by fluorescent micrographs of DHE-stained cells under similar conditions (Figure 2.1B). In order to examine production of total intracellular ROS, we stained the cells with a general marker for ROS, 2',7'-dichlorodihydrofluorescein diacetate (DCFH-DA). Within the cell, DCFH-DA is deacetylated and easily oxidized to 2',7'-dichlorofluorescein (DCF), a highly fluorescent compound (excitation: 485nm, emission:530 nm)(Bland et al., 2001). Fluorescent micrographs of DCFH-DA-stained cells show increased DCF fluorescence intensity inside individual cells following serum starvation (24h), and incubation with CdTe nanoparticles and H_2O_2 (Figure 2.1C). An assessment of DCF fluorescence intensity shows an increase of about 2-fold in serum deprived cells and of more than 4-fold when cells were incubated with CdTe nanoparticles and H_2O_2, when compared with cells cultured in serum (Figure 2.1D).

2.4.2 Status of lipid droplets and lysosomes in cells exposed to CdTe nanoparticles

We first examined LD formation under nanoparticle-induced oxidative stress by staining the cells with Bodipy 493/503, a neutral lipid selective dye (Tavian & Colombo, 2007). LDs are sparse but detectable in PC12 grown in serum containing medium, whereas they are very low in serum starved cells in the absence of CdTe nanoparticles (23 nM,24h) or H_2O_2 (10 μM,24h) (Figure 2.2A). Average LD number per cell (LD/cell) decreased by about 4-fold in cells deprived of serum, as compared to cells cultured in serum-containing media (Figure 2.2B). In contrast, LDs were formed in serum deprived cells exposed to CdTe nanoparticles, H_2O_2 or oleic acid (Figure 2.2A). LD/cell was increased by 5 fold ($p<0.05$) and by about 6 fold ($p<0.05$) in cells exposed to CdTe nanoparticles and H_2O_2, respectively, when compared to serum starved cells. Oleic acid treatment (100 μM, 24h), which served as a positive control, caused almost a 20-fold increase in LD/cell in serum starved cells ($p<0.001$) (Figure 2.2B). To demonstrate that increased LD formation is caused by oxidative stress, cells were pre-treated with antioxidant molecule N-acetylcysteine (2mM). The pre-treatment significantly ($p<0.05$) reduced LD formation in cells exposed to CdTe nanoparticles, compared to non-pretreated cells (Figure 2.2C).

We next examined mitochondrial and lysosomal status in cells exposed to nanoparticles in starved PC12 cells. The mitochondrion is the metabolic center and the major free radical-producing compartment of the cell (Chaturvedi & Beal, 2008). Lysosomes are the central components of the autophagic degradative pathway and are highly susceptible to oxidative stress (Butler & Bahr, 2006). Examining the morphology of lysosomes and their cellular distribution may provide new information on the impact of CdTe nanoparticles on lysosomal integrity. Electron microscopy data (Figure 2.3A, B) show that CdTe nanoparticles induce ultrastructural changes in PC12, including disrupted mitochondrial cisternae (Figure 2.3B, black arrows) and appearance of large phagosomes (Figure 2.3B, white arrows) suggesting increased autophagy. Some metallic nanoparticles were recently reported to be inducers of autophagy (Seleverstov et al., 2006; Stern et al., 2008; Zabirnyk et al., 2007). The impact of CdTe nanoparticles on cellular lysosomal content and morphology in living PC12 cells was assessed by lysotracker DND99 (LTR) staining. LTR fluorescence intensity increased by 2.43 ± 0.38 ($p<0.05$) fold in serum-deprived cells and by 3.23 ± 0.31 fold ($p<0.05$) in rapamycin-treated cells, as compared to control cells (Figure 2.3C, D). CdTe nanoparticle treatment caused enlargement of

lysosomes, whereas serum starvation and rapamycin treatment seem to increase their number, but not their size (Figure 2.3C). Such large structures in CdTe nanoparticle-exposed cells were also detected with monodansylcadaverine (MDC) (Figure 2.3E, arrows), an autofluorescent dye specific to acidic autophagic vacuoles (Bampton et al., 2005).

We hypothesized that LDs and lysosomes in CdTe nanoparticle-stressed PC12 cells may be found in close proximity. Interactions of LDs with various organelles were reported in several cell types, but the biological functions behind these interactions are not fully understood. We therefore examined changes in proximity between LDs and lysosomes in cells undergoing oxidative stress. As shown previously, LDs were not detected in serum-starved PC12 cells (Figure 2.4). LDs were formed in cells incubated with CdTe nanoparticles (23 nM, 24h), but did not colocalize with lysosomes. However, LDs detected in cells exposed to nanoparticles for 48h were found in the proximity of lysosomes suggesting possible colocalization between these two organelles. A similar pattern was also seen in cells exposed to highly toxic “aged”CdTe nanoparticles in (23 nM, 24h) (Figure 2.4 and Supplementary figure 2.1). In order to validate our observations on the colocalization of lipid droplets with lysosomes at the 24h timepoint, we performed 3D isosurface reconstruction of the organelles using the image analysis software Imaris (Bitplane Inc.) (Supplementary figure 2.1B). The analysis clearly shows that some of the lipid droplets are found within the lysosomes, thereby supporting the colocalization seen in confocal micrographs. Oleic acid (400 μM) also induced LD formation, but these LDs did not colocalize with lysosomes (Supplementary figure 2.2).

2.4.3 Cell viability, LD status and lysosomal morphology in oleic acid primed cells

LD biogenesis was recently shown to be cytoprotective during stress induced by glucose-deprivation (Gubern et al., 2009). In order to examine possible role of LD in PC12 cell survival under oxidative stress, we tested the effects of oleic acid and palmitic acid (PA) preconditioning in nanoparticle-treated and serum starved cells. We set the control (cells grown in serum containing medium) to 100 % and expressed the other values as a percent

of control. Trophic factor withdrawal (48h) led to a significant decrease in cell viability (40.6 ± 0.6%, $p<0.001$), compared to cells grown in complete medium (100 ± 1.5%), as determined by MTT reduction (Figure 2.5A). Priming the cells with oleic acid (400 µM) partially prevented serum withdrawal-induced decrease in cell viability (76.4 ± 1.4 %, compared to 40.6 ± 0.6%, respectively, $p<0.001$). Priming with PA, a saturated fatty acid (400 µM), however, exerted the opposite effect of oleic acid: PA induced cell death (11.7 ± 1.4%, $p<0.001$), whereas oleic acid preconditioning significantly rescued cells (59.5 ± 1.7, $p<0.001$) from CdTe nanoparticle/serum withdrawal- induced cell death (20.0 ± 1 %, $p<0.001$). The gain of cell viability by oleic acid priming under serum withdrawal and nanoparticle/serum withdrawal treatment was not much different (36 % and 40 %). In order to examine the rescue by oleic acid from toxicity alone, we exposed cells to CdTe nanoparticles while keeping them in serum containing media. The viability of untreated cells cultured in the presence of serum was set as control (100%). Priming with oleic acid (95.6 ± 1.1%) prevented some of the CdTe nanoparticle induced-cell death (82.8 ± 0.4%) following 48h treatment (Supplementary figure 2.3). However, priming with PA further decreased cell viability (36.9 ± 3.4%) under CdTe nanoparticle treatment. These results suggest that the protective effect of oleic acid is at least partly due to the rescue from CdTe NP-inflicted toxicity. It was previously proposed that triglycerides in LDs may be utilized as fuel and prolong cell survival during starvation and oxidative stress (Du et al., 2008; Ducharme & Bickel, 2008; Gubern et al., 2009). An assessment of LD using Bodipy 493/503 staining after 48h of incubation with CdTe nanoparticles revealed presence of many LDs only in cells primed with oleic acid (Figure 2.5B).

In order to determine whether the protection by oleic acid could be due to the prevention of CdTe nanoparticle-induced lysosomal membrane destabilization (organelle enlargement) (see Figure 2.3), we investigated lysosomal morphology during long term serum deprivation (48h) and CdTe nanoparticle treatment (48h) with or without oleic acid preconditioning. Serum-deprived PC12 showed a weak lysosomal staining (Figure 2.5C, first row), which was increased in cells preconditioned with oleic acid (Figure 2.5C, second row). CdTe nanoparticles caused excessive enlargement of lysosomes (Figure 2.5C), as previously observed (Figure 2.3C), which was prevented by oleic acid preconditioning, suggesting that priming with oleic acid improved stability of lysosomes.

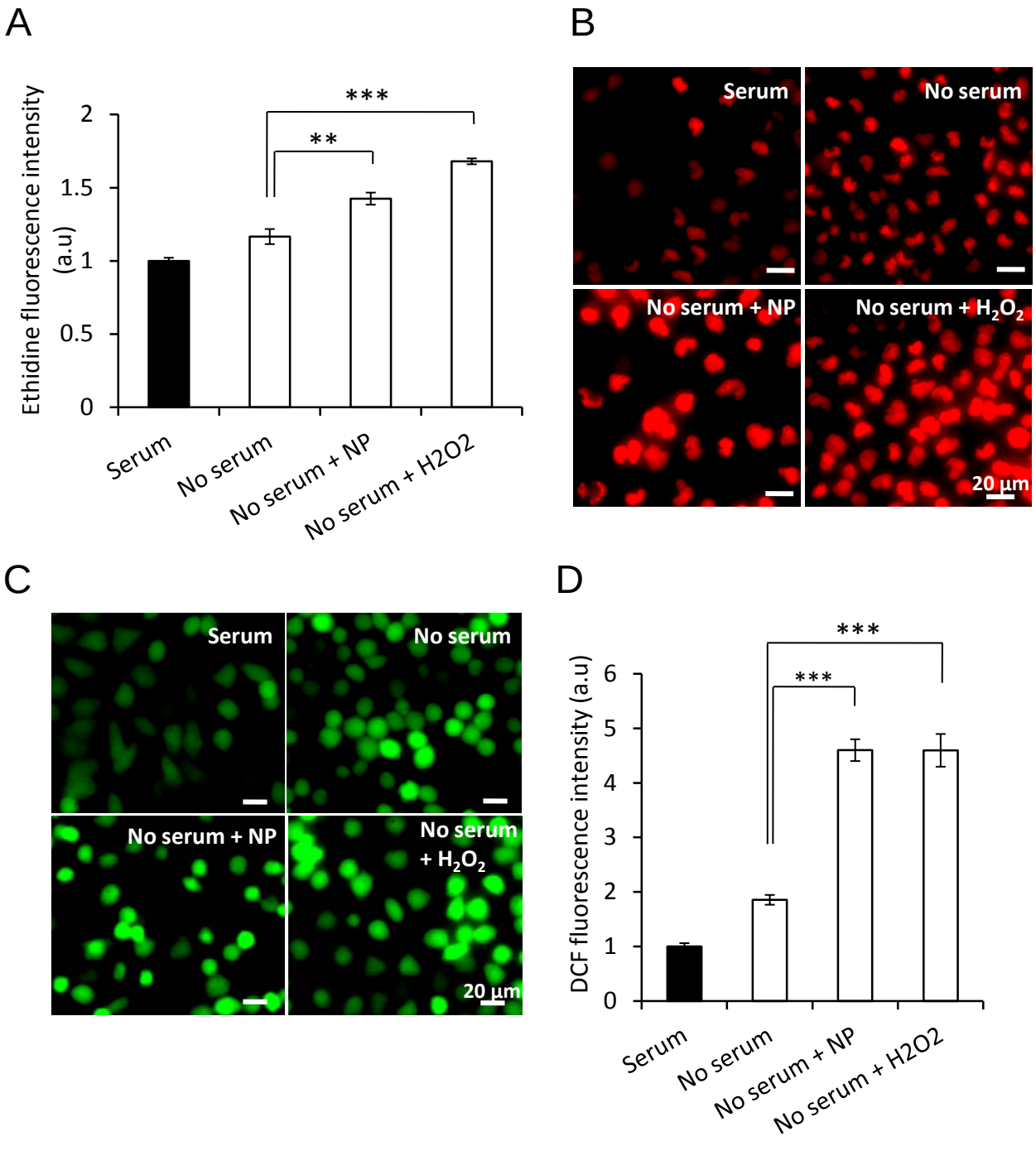
A
Ethidine fluorescence intensity (a.u)
2
1.5
1
0.5
0
***
**
Serum
No serum
No serum + NP
No serum + H2O2
B
Serum
No serum
No serum + NP
No serum + H2O2
20 µm
C
Serum
No serum
No serum + NP
No serum + H2O2
20 µm
D
DCF fluorescence intensity (a.u)
6
5
4
3
2
1
0
***
***
Serum
No serum
No serum + NP
No serum + H2O2

Figure 2.1 Increased oxidative stress in CdTe nanoparticle-treated cells.

(A) Increased superoxide anion (O_2^-) production in PC12 cells exposed to CdTe nanoparticles. Spectrofluorometric detection and quantification of dihydroethidium (DHE) staining in PC12 cultured in the presence or absence of serum and incubated with or without CdTe nanoparticles (23 nM, 24h) and H_2O_2 (10 μM) for 24h. Mean ethidine fluorescence intensity (arbitrary units) was normalized to number of cells and expressed relative to intensity of control (cells cultured in serum-containing medium). SEM was calculated from two independent experiments. Statistically significant differences are indicated by ***$p<0.001$ or **$p<0.005$.

(B) Fluorescent microscopy of DHE stained PC12 cells under similar conditions as in Figure 2.1A. Scale bar, 20 μm.

(C) Enhanced production of reactive oxygen species (ROS) in CdTe nanoparticle-treated cells. Fluorescent micrographs showing DCFH-DA stained PC12 cultured in the presence or absence of serum and incubated with or without CdTe nanoparticles (23 nM, 24h) and H_2O_2 (10 μM) for 24h. Cells were stained with DCFH-DA (20 μM, 30 min) Scale bar, 20 μm.

(D) Semi-quantification of DCF fluorescence intensity (arbitrary units) from experiments performed as described in Figure 2.1C. Fluorescence intensity was measured with ImageJ and normalized to number of cells. Bar graphs indicate the mean fold increase in the fluorescence intensity (arbitrary units) of DCF over the control (cells cultured in serum-containing medium). Statistically significant differences are indicated by ***$p<0.001$ and were calculated from at least two independent experiments (n=4 in each experiment).

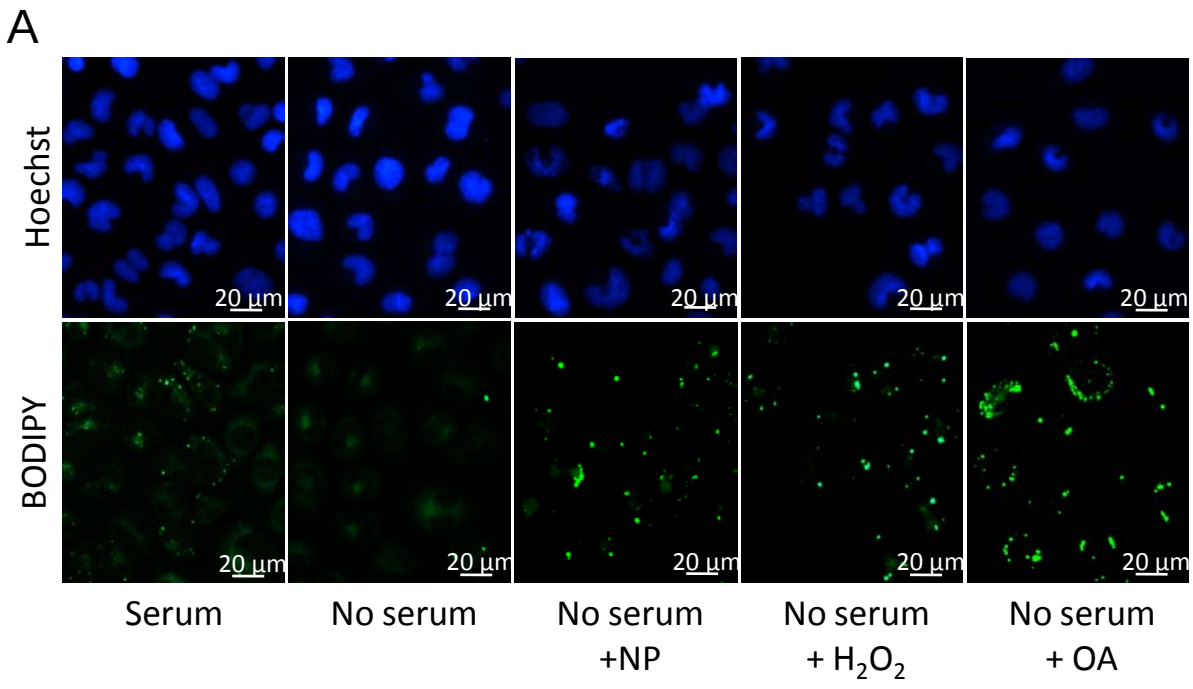
A
Hoechst
BODIPY
20 µm
Serum
No serum
No serum +NP
No serum + H_2O_2
No serum + OA

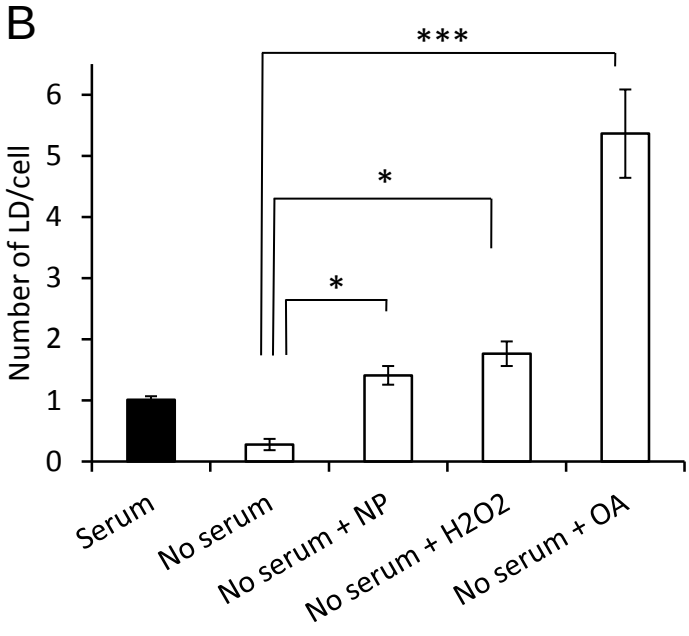
B
Number of LD/cell
0
1
2
3
4
5
6
***
*
*
Serum
No serum
No serum + NP
No serum + H2O2
No serum + OA

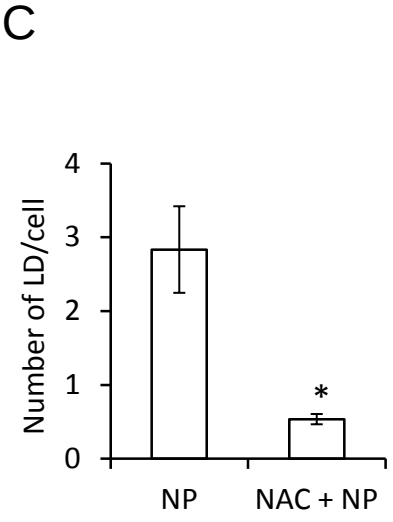
C
Number of LD/cell
0
1
2
3
4
*
NP
NAC + NP

Figure 2.2 LD formation is induced by CdTe nanoparticles and H2O2 and blocked by antioxidant treatment.

A) LD staining in PC12 cultured in serum or deprived of serum and incubated with CdTe nanoparticles (23 nM), H_2O_2 (10 μM) and oleic acid (OA) (100 μM) for 24h. Nuclei and LDs were stained with Hoechst 33342 (10 μM) and Bodipy 493/503 (32 μM), respectively, as described in *Experimental Section*. Scale bars, 20 μm.

B) Quantification of average LD number per cell from treatments in (A). LDs counted in each field (6 fields/well) were normalized to the number of cells present in the field. Counting was performed with Image J software (1.38).

C) Reduced LD formation in cells pretreated with antioxidant NAC. PC12 cells were treated with NAC (2 mM) for 2h before exposure to CdTe nanoparticles. Bar graphs show the mean of LD/cell and standard error of the means from at least two independent experiments (n=4 in each experiment)**.** Statistically significant differences are indicated by * ($p<0.05$) or *** ($p<0.001$).

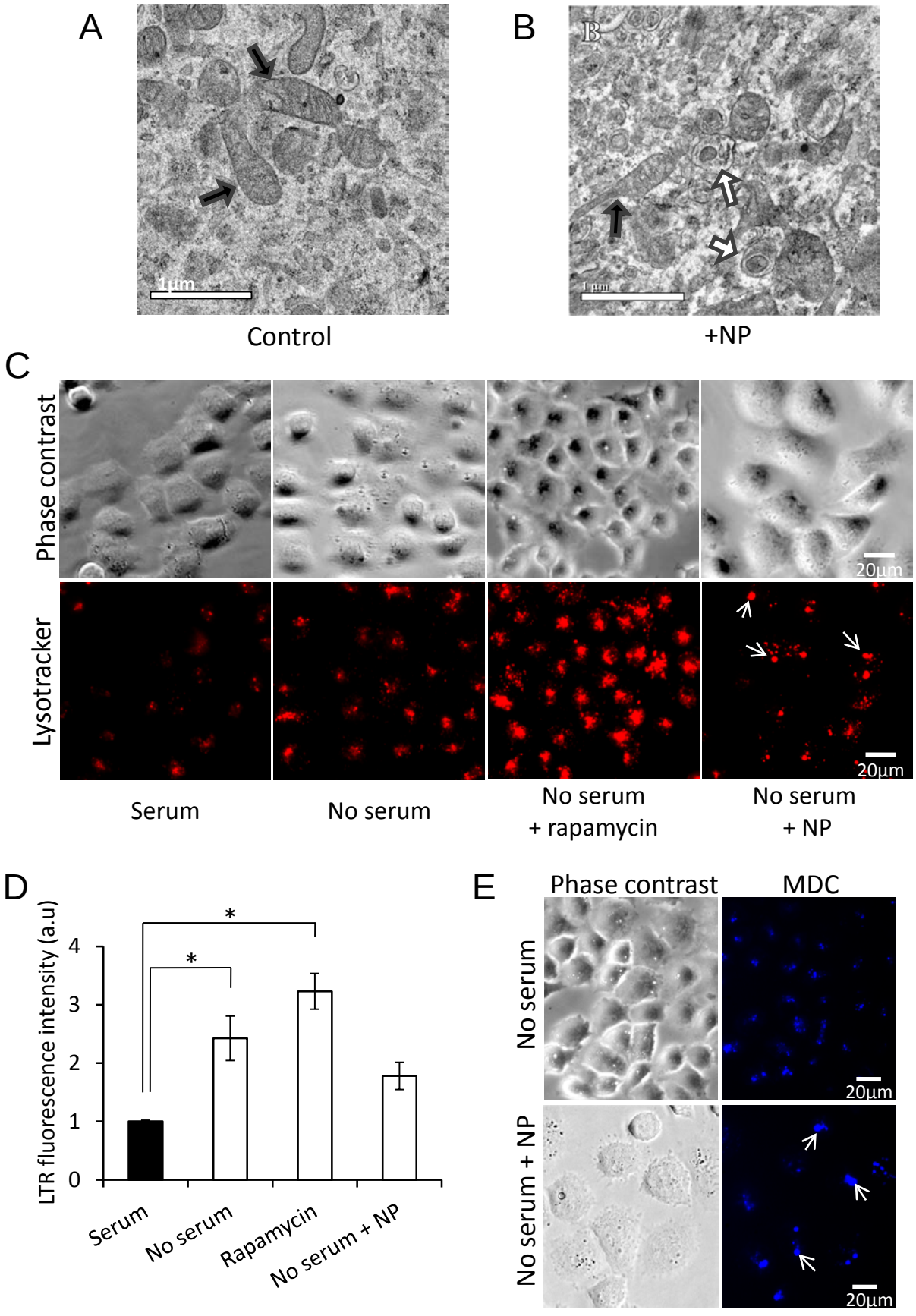
A
1µm
Control
B
B
1 µm
+NP
C
Phase contrast
Lysotracker
20µm
20µm
Serum
No serum
No serum
+ rapamycin
No serum
+ NP
D
LTR fluorescence intensity (a.u)
0
1
2
3
4
*
*
Serum
No serum
Rapamycin
No serum + NP
E
Phase contrast
MDC
No serum
No serum + NP
20µm
20µm

Figure 2.3 Phagosome appearance and enlargement of lysosomal compartments in PC12 cells exposed to nanoparticles.

A) and B) Electron micrographs showing ultrastructural changes in nanoparticle-treated cells. PC12 cells were cultured in serum containing media (control) or deprived of serum and incubated with CdTe nanoparticles (23 nM) for 24h. Mitochondrial structure (black arrows) is disrupted and phagosomes (white arrows) appear in nanoparticle-treated cells. Scale bar, 1 μm.

C) CdTe nanoparticles cause enlargement of acidic lysosomal compartments in PC12 cells. Cells were cultured in serum containing media or deprived of serum and treated with either rapamycin (200 nM) or CdTe nanoparticles (23 nM) for 24h. Fluorescent micrographs show lysosomes (red) stained with lysotracker DND99 (LTR) (500 nM). Scale bars, 20 μm.

D) Quantification of LTR fluorescence intensity (arbitrary units) in images from Figure 2.1C. LTR fluorescence intensity was measured with ImageJ and normalized to number of cells. Standard errors of the means were calculated from at least two independent experiments (n=3 in each experiment) and expressed as fold increase over the control (cells cultured in serum). Statistically significant differences are indicated by *$p<0.05$.

E) Nanoparticle-induced enlargement of acidic autophagic vacuoles detected by monodansylcadaverine (MDC) staining. PC12 cells were deprived of serum and incubated with CdTe nanoparticle (23 nM) for 24h. Acidic autophagic vacuoles are stained with blue autofluorescent dye MDC (50 μM) for 10 min. Scale bars, 20 μm.

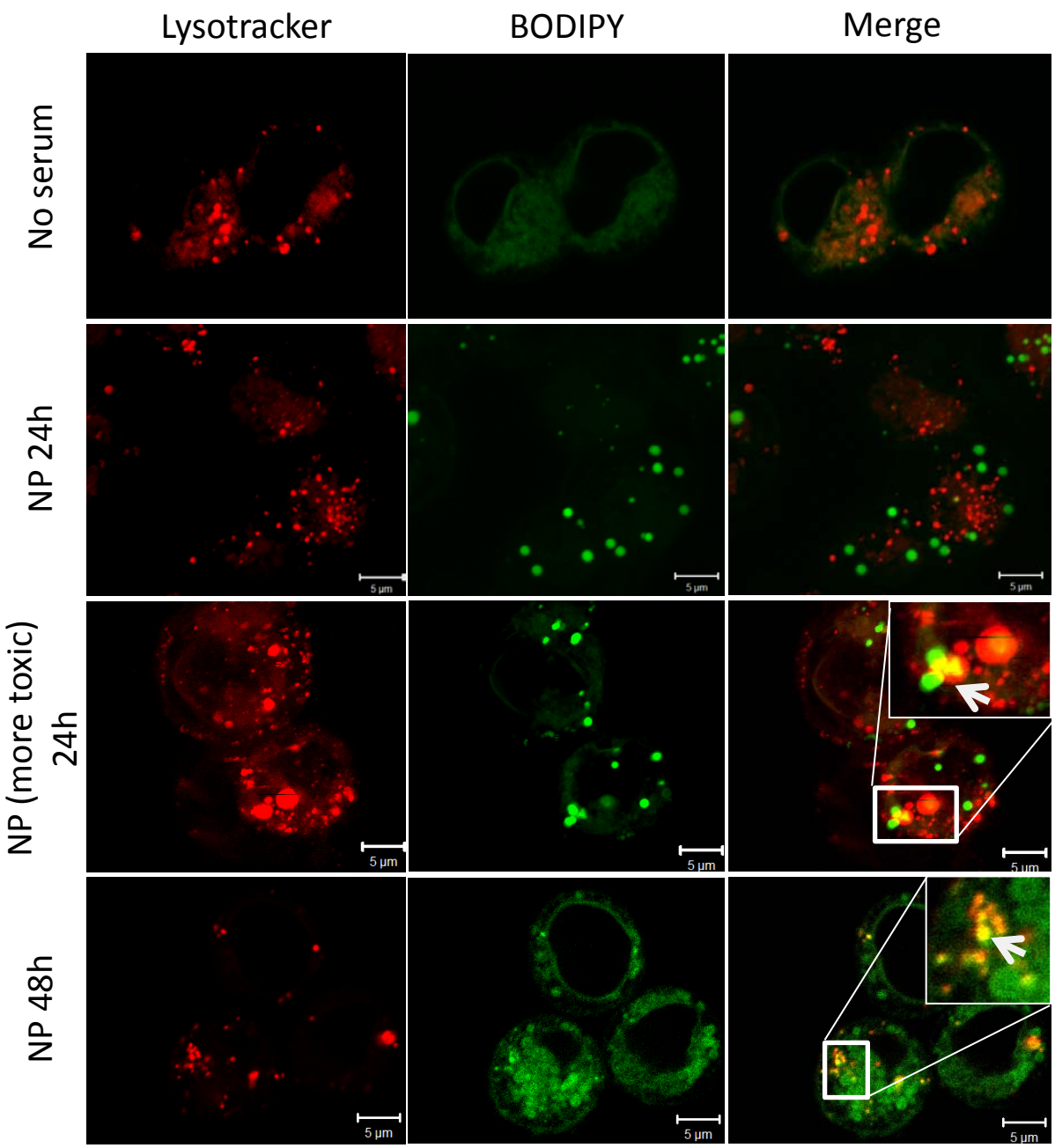
Lysotracker
BODIPY
Merge
No serum
NP 24h
NP (more toxic) 24h
NP 48h
5 µm

Figure 2.4 Relative localization of LDs and lysosomes in cells exposed to CdTe nanoparticles.

PC12 cells seeded on confocal chamber slides were deprived of serum and incubated with CdTe nanoparticles (23 nM) for 24h and 48h. LDs were labeled with Bodipy 493/503 (38 μM) and lysosomes with LTR (500 nM). LD-lysosomal colocalization is indicated by white arrows in the insets. Colocalization between the organelles was detected under long term (48h) and short term (24h) with treatment of highly toxic "aged" CdTe nanoparticles. Scale bars, 5 μm.

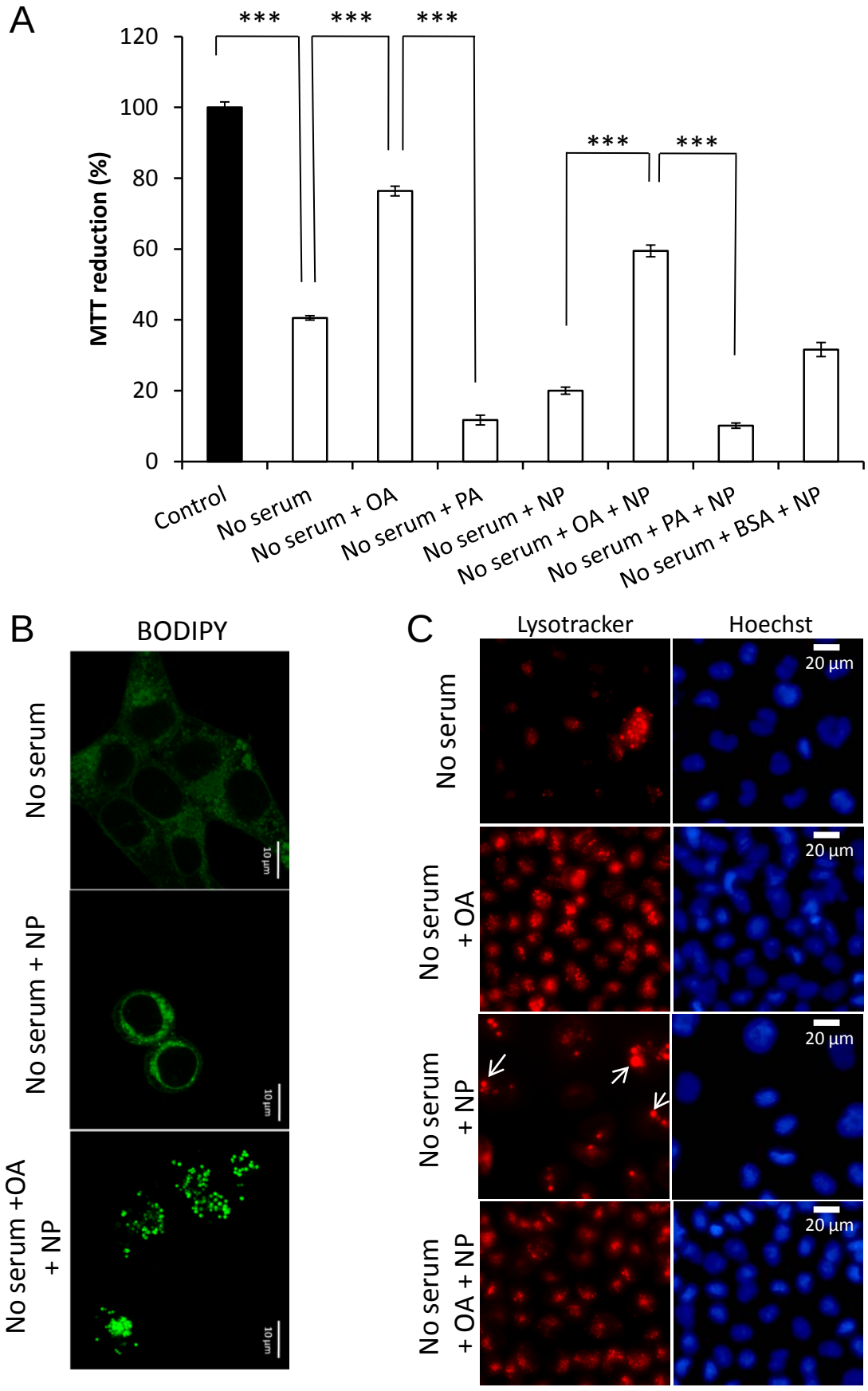
A
***
***
***
***
***
120
100
80
60
40
20
0
MTT reduction (%)
Control
No serum
No serum + OA
No serum + PA
No serum + NP
No serum + OA + NP
No serum + PA + NP
No serum + BSA + NP
B
BODIPY
No serum
No serum + NP
No serum +OA + NP
10 µm
C
Lysotracker
Hoechst
No serum
No serum + OA
No serum + NP
No serum + OA + NP
20 µm

Figure 2.5 Nanoparticle-induced cell death and oleic acid-mediated rescue during long-term oxidative stress.

A) PC12 cells preconditioned with oleic acid (OA), but not palmitic acid (PA) are partially rescued from CdTe nanoparticle-induced cell death. Cells were primed with oleic acid (400 μM), palmitic acid (400 μM) or BSA (0.5%) for 24 h in the absence of serum. They were washed and incubated in serum free media for 48h with or without CdTe nanoparticle treatment (23 nM). Cell viability was determined by using the MTT reagent. Data obtained from three independent experiments (n=4 in each experiment) are expressed as the mean (%) ± standard error of the mean. Statistically significant differences are indicated by *** $p<0.001$.

B) LDs are maintained only in oleic acid-primed cells. All treatments were carried out in serum-free media with or without nanoparticle treatment. Confocal imaging of Bodipy 493/503 staining shows the presence of numerous LDs in oleic acid (OA) + CdTe nanoparticles panel. Scale bars,10 μm.

C) Effect of oleic acid preconditioning on lysosomal morphology in serum starved and nanoparticle-treated cells. Note that enlarged lysosomes (No serum + nanoparticles) are normalized in cells pretreated with oleic acid (No serum + OA + nanoparticles). Nuclei and lysosomes were stained with Hoechst 33342 (10μM) and lysotracker DND99 (LTR) (500nM), respectively, and images were acquired by widefield fluorescent microscope. Scale bars, 20 μm.

2.5 Discussion

Results from these studies show that some metallic, i.e. CdTe "naked" nanoparticles induce lipid droplet formation. Oleic acid treatment also induced LD formation and it provides fuel needed for survival under starvation conditions; it also prevents excessive expansion of lysosomal membranes under nanoparticle-induced oxidative stress, thereby providing cytoprotection under such conditions.

Several studies, including ours, have shown that some nanoparticles can induce oxidative stress leading ultimately to cell death (Choi et al., 2007; Lovric et al., 2005). CdTe nanoparticle-induced oxidative stress is partly caused by the release of cadmium ions from the nanoparticle core, but the concentration of the cadmium ions in the medium did not induce significant LD formation (unpublished observation). An early *in vivo* study proposed that high tellurium ion concentrations cause LD formation in Schwann cells and that their accumulation can be explained by an increase in the cholesterol precursor, squalene (Goodrum et al., 1990). This mechanism is unlikely because free tellurium concentrations here are far below those reported to induce LDs. Oxidative stress-induced LD accumulation is well studied and has been demonstrated under hypoxic conditions, irradiation and treatments with chemotherapeutic agents (de Estable-Puig & Estable-Puig, 1973; Delikatny et al., 2002; Witt & Flower, 2006; Zoula et al., 2003). Recently, Gubern et al. demonstrated that triglyceride synthesis and LD biogenesis during stress mainly takes place from pre-existing fatty acids and is dependent on group VI phospholipase A_2 (PLA_2-VIA) manner (Gubern et al., 2009). One possible explanation for LD accumulation is the impairment in mitochondrial fatty acid β-oxidation, resulting from mitochondrial membrane damage, and leading to an increase in triglyceride storage (Hashimoto et al., 1999; Lovric et al., 2005; Vickers et al., 2006).. Results from our studies suggest that assessment of LD accumulation may serve as a biological marker of oxidative stress and indicate disrupted lipid homeostasis by nanomaterials.

Lysosomes are major organelles for degradation of damaged intracellular organelles (e.g. mitochondria) in autophagy and they are fierce responders to oxidative stress (Kurz et al., 2008; Levine & Yuan, 2005). Autophagy (cell "self-eating") usually occurs in nutrient or growth factor deprived cells (Levine & Yuan, 2005). It was shown that autophagy plays

an instrumental role in serum deprivation-induced cell death in PC12 cells, and that lysosomes are involved in this process (Guillon-Munos et al., 2005; Isahara et al., 1999; Shibata et al., 1998). In the present work, serum starved PC12 cells showed a significant increase in lysosomal staining relative to non-starved controls (Figure 2.3C, D), suggesting an increased in autophagy. Similarly, rapamycin, commonly used to induce autophagy significantly increased the fluorescence intensity of the lysosomal marker lysotracker DND99 (Rubinsztein et al., 2007; Stern et al., 2008). Electron micrographs of CdTe nanoparticle-treated PC12 cells revealed membrane-bound vacuoles containing cytoplasmic structures. Such vacuoles were previously observed in serum-starved PC12 cells and identified as autophagosomes or autolysosomes (Uchiyama, 2001). In the autophagic-lysomal pathway, cytoplasmic contents are engulfed by the autophagosomes and degraded in the autolysosomes upon their fusion with lysosomes (Shacka et al., 2008). The enlargement of acidic compartments in cells exposed to CdTe nanoparticles (Figure 2.3C, 5C) could be caused by lysosomal membrane destabilization under oxidative stress or by the overflow of cytoplasmic contents (e.g organelles) into lysosomes due to an increased autophagy (Maysinger, 2007; Ono et al., 2003; Shacka et al., 2008). Lysosomal membrane impairments are partly caused by free cadmium ions released from the CdTe nanoparticle core (Cho et al., 2007). An excessive damage of the lysosomal membranes by cytotoxic nanoparticles could lead to the leaching of hydrolytic enzymes outside of the organelle, leading to apoptotic or necrotic cell death (Kroemer & Jaattela, 2005; Kurz et al., 2008).

Lipid droplets are currently considered to be metabolically active organelles and their behavior in stressed cells is intriguing, as lipid metabolism is impaired during oxidative stress (Cutler et al., 2004; Furukawa et al., 2004). Only very limited information is available about communications between lysosomes and LD. Liu et al. identified proteins that are common between LD and lysosomes, such as Rab7 and SNAP, suggesting a possible link between these organelles (Liu et al., 2004). LD are consistently associated with phagolysosomes in macrophages during *in vivo* infection, and some are even internalized by the phagolysosomes (Melo et al., 2006). In the present study, we examined colocalization of LD with lysosomes in starved PC12 cells exposed to CdTe nanoparticles for up to 48h. Lysosome-LD colocalization was detected after 24h exposure

to highly toxic nanoparticles, but considerably later (48h) with less toxic nanoparticles. The term “highly toxic” is used to indicate “aged” (degenerate) nanoparticles as compared to those used shortly after their preparation. Enlargement of lysosomal compartment in the cells exposed to ”aged” CdTe nanoparticles is striking and reflects excess cellular stress (Ono et al., 2003). The present study carried out with living PC12 cells suggests suggests close apposition between LD and acidic organelles (e.g lysosomes) labeled with lysotracker DND99; the identity of lysosomes should be confirmed in future studies by immunocytochemisty using LAMP1 antibodies or in cells expressing organelle-specific proteins tagged with green fluorescent protein (GFP) family members. Detailed studies employing these approaches in combination with wet electron microscopy could provide more information on lysosome-LD interactions and on their role in different cell functions.

Oleic acid is commonly used in investigations on LD biogenesis, morphology, proteomics and cytoplasmic distribution (Guo et al., 2008). In the current study oleic acid was used for induction of LD to assess their protective role in cells under oxidative stress and nutrient deprivation. Assessment of cell viability clearly shows that priming with oleic acid, but not with saturated fatty acid palmitic acid (PA), provides effective cell rescue, as evidenced by enhanced mitochondrial metabolic activity and cell viability (Figure 2.5A). PA exacerbates nanoparticle- and nutrient deprivation-induced cell death. Other groups have shown that PA, in similar concentrations (300 to 500 μM), exerts lipotoxic effects and induces apoptosis (Chai & Liu, 2007; Listenberger et al., 2001). Lipotoxicity resulting from the accumulation of long chain fatty acids seems to be caused predominantly by saturated fatty acids (Listenberger et al., 2001). Conversely, oleic acid supplementation is well- tolerated by the cells, leads to triglyceride (TG) accumulation and protects the cells against saturated fatty acid-induced lipotoxicity (Listenberger et al., 2003). Recently, Du et al. proposed that triglycerides stored within LD can be utilized for fuel in starving neurons, thereby increasing their viability (Du et al., 2008). Our studies are in line with these findings and suggest that LD TGs are also utilized in as fuel in starved cells exposed to nanoparticles.

The protection by oleic acid against nanoparticle-induced oxidative stress can be explained by multiple effects of oleic acid in living cells. For instance, aside from providing the fuel during starvation, oleic acid can also promote the activity of cellular antioxidant enzymes, such as superoxide dismutase and glutathione peroxidase (Duval et al., 2002; Xu et al., 2005). These two enzymes are part of the mitochondrial antioxidant system which promote mitochondrial integrity by scavenging free radicals (Moldovan & Moldovan, 2004). Nanoparticle cytotoxicity is largely mediated by the oxidation of lipids (lipid peroxidation) in subcellular membranes (Choi et al., 2007). Previous studies have shown that cells enriched in monounsaturated fatty acids (oleic acid), but not polyunsaturated fatty acids, were protected against oxidants, such as hydrogen peroxide and high oxygen (95%), suggesting reduced lipid peroxidation in cells loaded with oleic acid (Hart et al., 1997; Spitz et al., 1992). In our studies, oleic acid preconditioning prevented the enlargement of lysosomes in cells exposed to nanoparticles suggesting a beneficial effect of oleic acid on lysosomal integrity by indirectly reducing peroxidation of lysosomal membrane lipids (Kurz et al., 2008).

2.6 Conclusion

Results from these studies implicate that at least two different mechanisms could contribute to cell rescue and organelle adaptation by oleic acid in PC12 cells during starvation and nanoparticle-induced oxidative stress: (i) oleic acid-induced LDs serve as energy stores which at least in part prevent massive metabolic catastrophe in starved cells; (ii) oleic acid contributes to maintenance of lysosomal membrane integrity during a disturbance of the cellular redox balance initiated by CdTe nanoparticles.

In conclusion, our studies suggest that oleic acid priming and formation of lipid droplets could play a protective role in cells deprived from trophic factors and exposed to certain metallic nanoparticles and also likely to other nanomaterials disrupting homeostatic cellular redox balance.

2.7 Acknowledgments

We thank Ms Jacynthe Laliberté for her assistance with the confocal microscope. We are grateful to Cory Glowinsky and to the McGill Life Sciences Complex Imaging Facility staff for their technical assistance with the 3D isosurface reconstruction and for their precious advice. We thank Alexandre Moquin for the synthesis and characterization of CdTe nanoparticles, and H. Vali and J. Mui for technical assistance in electron microscopy. A.K is supported by the McGill Graduate Studies Fellowship. DM is supported by Canadian Institutes for Health Research (CIHR) and National Science and Research Council (NSERC, Canada).

A

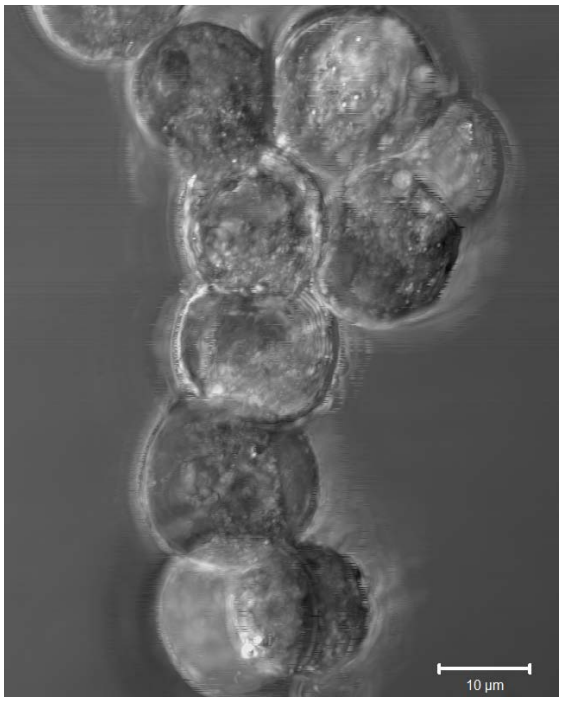

DIC

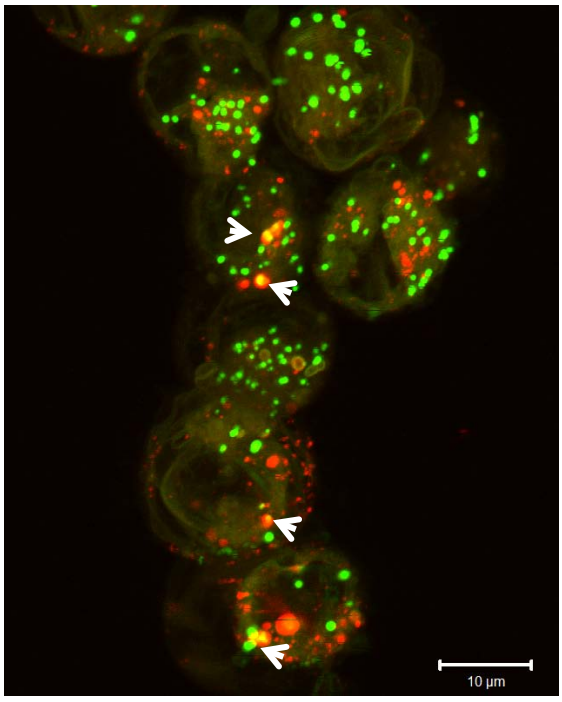

Lipid droplets (green)
Lysosomes (red)

B

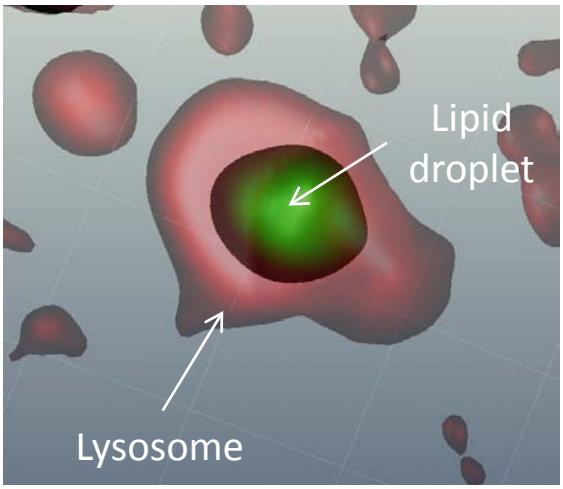

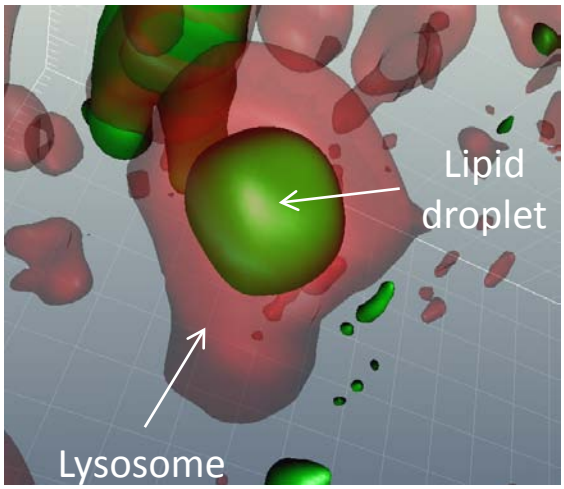

Supplementary figure 2.1 Relative localization of LDs and lysosomes in cells exposed to highly toxic “aged” CdTe nanoparticles.

A) PC12 cells seeded on confocal chamber slides were deprived of serum and incubated with CdTe nanoparticles (23 nM) for 24h. LDs were labeled with Bodipy 493/503 (38 μM) and lysosomes with LTR (500 nM). Yellow regions indicated by the white arrow heads suggest LD-lysosomal colocalization. Scale bars, 10 μm. Cells are shown in differential interference contrast (DIC) images.

B) 3D image isosurface reconstruction of lipid droplets found within lysosomes was done using the 3D image analysis software Imaris (Bitplane). The analysis strongly supports a colocalization of lipid droplets with lysosomes under highly toxic CdTe nanoparticle treatment.

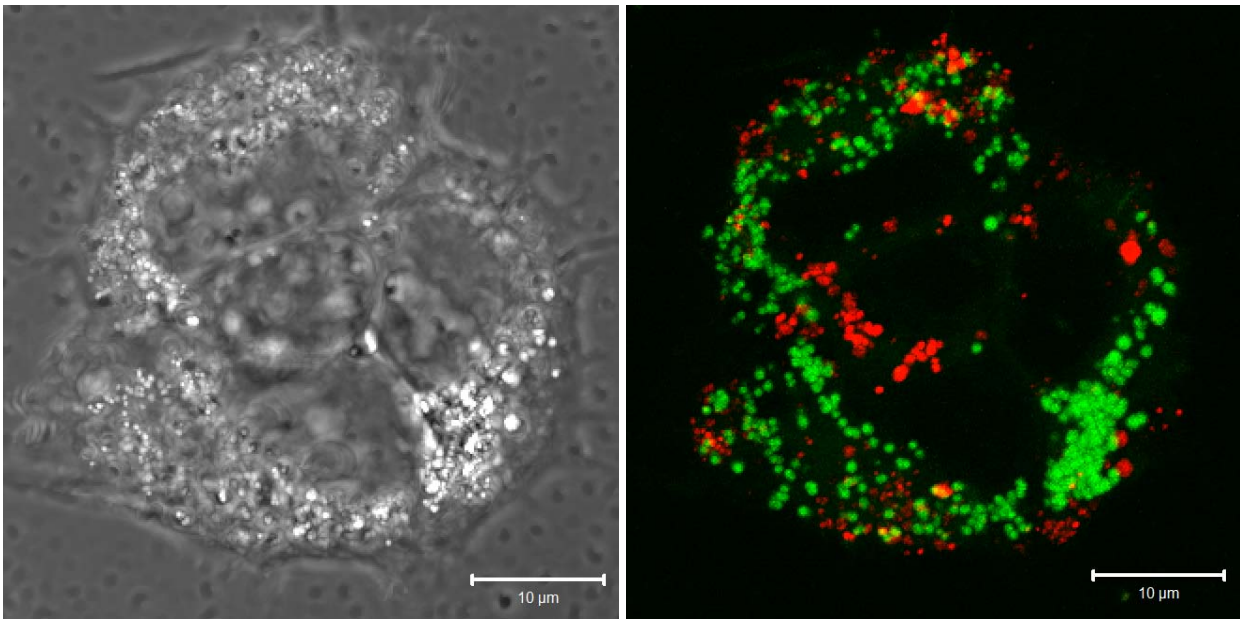

Supplementary figure 2.2

Assessment of LD-lysosome colocalization in oleic acid-treated PC12 cells.

Cells were cultured in the presence of OA (400 µM) for 24 h. LDs (green) and lysosomes (red) were stained with Bodipy 493/503 (38 µM) and lysotracker red (500 nM), respectively, and do not seem to be found in close proximity as suggested by the lack of colocalization. Differential interference contrast (DIC) shows the presence of four cells in the field. Scale bars, 10 µm.

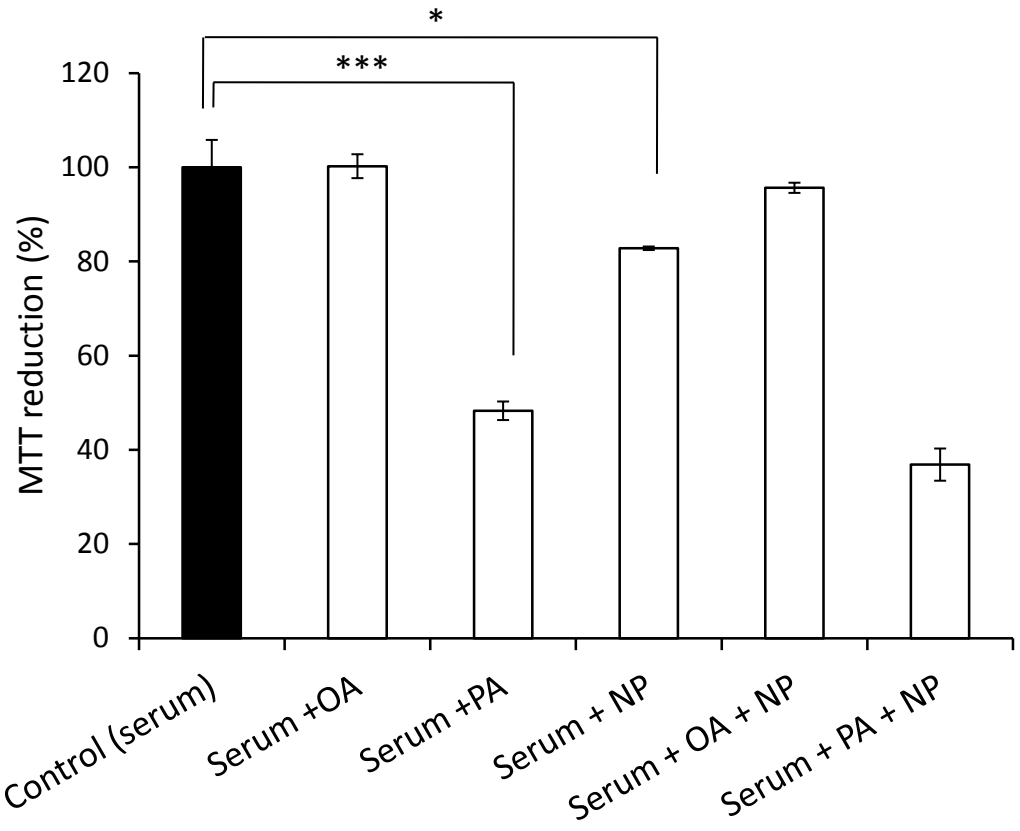

Supplementary figure 2.3

Effect of oleic acid pre-treatment on viability of cells treated with CdTe in serum containing media.

Cells were primed with oleic acid (400 μM), palmitic acid (400 μM) for 24 h. They were washed and incubated in serum-containing media for 48h with or without CdTe nanoparticle treatment (23 nM). Cell viability was determined by using the MTT reagent. Data are expressed as the mean (%) ± standard error of the mean. Statistically significant differences are indicated by *** $p<0.001$ or *$p<0.05$.

Connecting text between Chapter 2 and Chapter 3

Our investigations presented in Chapter 2 establish a clear relationship between LD accumulation and oxidative stress. We show that LDs can be induced both under physiological and pathological (stressful) conditions. The work from Chapter 2 was further extended and supplemental experiments were performed (see Appendix I-V).

In these additional experiments, our aim was to elucidate the mechanisms leading to LD formation under stressful conditions. First, we re-evaluated LD accumulation by confocal microscopy in order to obtain better quality (resolution, lower background) images of LDs and a more rigorous quantification of their numbers (Appendix I-II). We sought to examine alterations in perilipin-2 levels under oxidative stress (Appendix III). We then studied the role of mitogen-activated protein kinases (MAPK), c-Jun N-terminal kinase (JNK) and p38 in LD formation. This was achieved by using selective pharmacological inhibitors of JNK and p38. These additions helped us to better understand the cellular regulation of LDs under oxidative stress.

Oxidative stress is involved in a wide variety of pathologies and is commonly associated with inflammatory stress. The implication of LDs in inflammatory stress is well documented. LDs accumulate in leukocytes stimulated with pro-inflammatory agents, such as LPS. They are proposed to serve as intracellular sources of pro-inflammatory lipid mediator production. However, while LDs have been extensively investigated in peripheral leukocytes (e.g macrophages), so far they have not been explored in immune cells of the central nervous system (CNS). Microglia are the resident macrophages of the brain and become hyper-activated in response to brain injuries, infections and disease conditions. It remains to be clarified whether LDs in activated microglia play an important role in neuroinflammatory processes.

In the following chapter, we aim at understanding the regulation and the role of LDs in LPS-activated microglia. We studied the dynamics of LD accumulation and the role of p38 and JNK MAPKs in their formation. In particular, we sought to elucidate the role of LDs in pro-inflammatory eicosanoid synthesis. This study will shed light on the potential role of LDs in neuroinflammatory processes.

CHAPTER 3

Dynamics and regulation of lipid droplet formation in lipopolysaccharide (LPS)-stimulated microglia

Armen Khatchadourian, Simon D. Bourque, Vincent R. Richard, Vladimir I. Titorenko, Dusica Maysinger

Biochimica et Biophysica Acta. 2012 Apr;1821(4):607-17

3.1 Abstract

Lipid droplets are neutral lipid-rich organelles involved in many cellular processes. A well-known example is their accumulation in leukocytes upon activation by pro-inflammatory stimuli such as lipopolysaccharides (LPS) derived from gram-negative bacteria. A role of LDs and LD-associated proteins during inflammation in the brain is unknown, however. We have now studied their dynamics and regulation in microglia, the resident immune cells in the brain. We find that LPS treatment of microglia leads to the accumulation in them of LDs, and enhancement of the size of LDs. This induction of LDs was abolished by triacsin C, an inhibitor of triglyceride biosynthesis. LPS strongly activated c-Jun N-terminal kinase (JNK) and p38 MAPK stress signalling pathways and increased the expression of LD-associated protein perilipin-2 (ADRP) in a time-dependent manner. Immunostaining showed that perilipin-2 in LPS-treated microglia predominantly colocalized with LDs. Inhibitors of p38 α/β (SB203580) and PI3K/Akt pathway (LY294002), but not that of JNK (SP600125), reduced LPS-induced LD accumulation and eliminated the activating effect of LPS on perilipin-2. In addition, cytosolic phospholipase A_2 (cPLA$_2$-α), a key enzyme for arachidonic acid release, colocalized with LPS-induced LDs. These observations suggest that LDs may play an important role in eicosanoid synthesis in activated microglia; they provide a novel insight into the regulation of LDs in inflammatory cells of the brain and point to a potential role of p38 α/β in LPS-induced LD accumulation. Collectively, our findings imply that LD formation and perilipin-2 induction could be microglial biomarkers of inflammation in the central nervous system.

3.2 Introduction

Lipid droplets, also called lipid bodies, are dynamic intracellular organelles that contain a core rich in neutral lipids, such as triglycerides (TG) and cholesteryl esters (Murphy, 2001). Their surface is composed of a phospholipid monolayer with a unique phospholipid and fatty acid composition (Tauchi-Sato et al., 2002). Initially considered as inert neutral lipid-storage compartments, LDs have become intensively studied organelles, implicated, for example, in the pathology of atherosclerosis, obesity, insulin resistance, type 2 diabetes (Bell et al., 2008), hepatic steatosis (Motomura et al., 2006), cardiovascular disease, and inflammatory disorders (Bozza & Viola, 2010; Chang & Chan, 2007). The formation of LDs is a precisely regulated and inducible process which can be triggered by a variety of extracellular cues such as growth factors, long-chain fatty acids (Fujimoto et al., 2006), oxidized low density lipoproteins (Silva et al., 2009) or by various environmental insults such as oxidative stress (Gubern et al., 2009; Khatchadourian & Maysinger, 2009) and inflammatory stimuli (Bozza et al., 2009). LDs are rapidly induced under inflammatory conditions in leukocytes. In experimental models of sepsis, the interaction of bacterial lipopolysaccharide (LPS) with Toll-like receptor 4 (TLR4) leads to a considerable accumulation of LDs in macrophages (Pacheco et al., 2002). LDs were shown to contain esterified arachidonic acid in their phospholipid and neutral lipid pools and proposed to be intracellular sites involved in the metabolism of arachidonic acid into eicosanoids (Weller & Dvorak, 1994; Yu et al., 1998). Cytosolic phospholipase A_2-α (cPLA_2-α), also called group IVA PLA_2, is a central enzyme for the release of arachidonic acid from phospholipids and has been found to co-localize with LDs (Moreira et al., 2009). cPLA_2-α activation and release of proinflammatory lipid mediators are regulated by TLR4 signaling in LPS-activated macrophages (Qi & Shelhamer, 2005).

The surface of LDs is coated with various proteins, many of which regulate their formation, growth or turnover (Bickel et al., 2009). Members of the PAT family proteins, namely perilipin, adipocyte differentiation-related protein (ADRP) and tail-interacting protein 47 kDa (TIP47), share extensive amino acid sequence in their amino termini (PAT domain) and bind to LDs (Bickel et al., 2009). A recently implemented new

nomenclature for the PAT proteins has changed the names of perilipin, ADRP and Tip 47 to perilipin 1, 2 and 3, respectively (Kimmel et al., 2010). Perilipin-2 (ADRP) and perilipin-3 (Tip 47) are ubiquitously expressed in different cell types, including macrophages (Larigauderie et al., 2004; Robenek et al., 2005). Perilipin-2 is a prominent LD-associated protein, whose expression level rises concomitantly with an increase in both LD abundance and TG level (Xu et al., 2005). Perilipin-2 is a key regulator of LD formation and has been investigated in the context of metabolic syndrome and inflammatory diseases (Chang & Chan, 2007).

The present study sought to advance our understanding of the physiological roles of perilipin-2 and LDs in microglia, the resident macrophage population of the central nervous system (CNS) (Hanisch & Kettenmann, 2007). Microglia are of myeloid origin and share certain phenotypic characteristics with macrophages in their activated form. Upon activation microglia express cell surface markers that are also present on macrophages (Chan et al., 2007). They respond rapidly to pathological challenges in the CNS by acquiring a reactive state and secreting proinflammatory cytokines, nitric oxide (NO) and reactive oxygen species (Block et al., 2007; Hanisch & Kettenmann, 2007). Importantly, TLR4-initiated signalling underlies microglia-induced inflammation in the CNS (Buchanan et al., 2010). LPS-induced activation of TLR4 triggers an activating downstream signal to mitogen-activated protein kinases (MAPK), c-Jun N-terminal kinase (JNK) and p38 (Buchanan et al., 2010). Phosphorylation of p38 and JNK by upstream MAPK kinases leads to activation of transcription complex activator protein -1 (AP-1), which then induces the expression of proinflammatory cytokines (Wagner & Nebreda, 2009). In LPS-treated macrophages, stimulation of the binding of AP-1 to the Ets/AP-1 binding site results in increased perilipin-2 expression (Gu et al., 2008). Although the effect of LPS on perilipin-2 protein expression in macrophages has been previously examined (Feingold et al., 2010; Gu et al., 2008), this has not been investigated in microglia.

In the current study, we investigated the effects of LPS on LD status and perilipin-2 expression in murine N9 microglia cells. These cells express TLR4 and many other pathogen recognition receptors and rapidly respond to bacterial endotoxins (McKimmie

et al., 2006). The effect of LPS was compared with that of oleic acid (OA), a major plasma fatty acid (Quehenberger et al., 2010). In cells, OA is esterified and stored as triglyceride inside LDs. OA and other long chain fatty acids induce LD formation and perilipin-2 expression (Fujimoto et al., 2006; Wei et al., 2005). In the brain, OA is synthesized by astrocytes and acts as a neurotrophic factor for neurons (Medina & Tabernero, 2002). Although induction of LD formation and perilipin-2 expression in response to OA has been assessed in different cell types, it has not been studied so far in microglia.

We hypothesised that stimulation of microglia with LPS may alter LD status and perilipin-2 expression via JNK and/or p38 MAPK. We show that LPS stimulation greatly increases microglial LD and TG content and induces perilipin-2 expression. We also demonstrate that pharmacological inhibition of p38 downregulates perilipin-2 expression and LD accumulation. OA-driven LD accumulation was not accompanied by p38 or JNK activation. In order to better understand the role of microglial LDs in the production of proinflammatory lipid mediators, we examined colocalization of $cPLA_2$-α with LDs. Our findings imply that LPS-driven changes in LD biogenesis and perilipin-2 expression could contribute to microglia-mediated inflammation in the CNS.

3.3 Materials and methods

Lipidomics analysis

Lipid analysis was performed as previously reported (Bourque & Titorenko, 2009). Prior to lipid extraction, internal standards were added corresponding to each lipid class, lipids were then extracted from whole cells by a modified Bligh and Dyer method, samples were dried under nitrogen and resuspended in chloroform. Immediately prior to injection the extracted lipids were combined with 2:1 methanol:chloroform with 0.1% (v/v) ammonium hydroxide. This was injected directly into a Q-TOF 2 mass spectrometer (Waters, Milford, MA) using a nano-esi spray source at 1µl/min. Spectra were obtained in positive-ion mode ($PC+H^+$, $TAG+NH_4^+$) and negative-ion mode ($FFA-H^+$,$PA-H^+$,PE-

H^+, PG-H^+, PI-H^+,PS-H^+,CL-$2H^+$). Acquired spectra were centroided using the Masslynx software then deconvoluted and deisotoped with excel macros.

Cell culture and treatments

Murine N9 microglia were cultured in Iscove's Modified Dulbecco's Medium (IMDM) (+ L-glutamine, + 25 mM HEPES) (Gibco) supplemented with 5% (v/v) fetal bovine serum (FBS) (Gibco) and 1% (v/v) penicillin/streptomycin (Gibco). Subconfluent cells were treated with lipopolysaccharides (LPS) (Escherichia coli, strain 055:B5) (Sigma, #62326) in medium containing 1% FBS as described in the figure legends. In experiments with oleic acid, control group cells were treated with bovine serum albumin (BSA) alone (0.1% w/v). Pharmacological inhibitors SP600125 (Calbiochem, #420119), SB203580 (Sigma, S8307) and LY294002 (Cell Signaling, #9901) were added 30 min prior to the addition of LPS (10 μg/ml). For every 10 μM of SP600125, 0.1 % of DMSO was added to the cultures, as recommended by the supplier.

OA/BSA complex preparation

OA/BSA complex was formed by mixing 30 mg of sodium oleate (Nu-Check Prep, S-1120) with fatty acid-free BSA solution (5 % w/v) (Sigma, A6003) for 5h at 37 °C. After the incubation, the pH of the solution was adjusted to pH 7.4 and the solution was filtered through a 0.22 μm filter. Non-esterified OA concentration in this solution was determined with the NEFA C method kit (Wako). The final molar ratio of OA to BSA was approximately 4.4:1. Aliquots of the stock solution were stored at -20 °C.

Staining of lipid droplets

LDs in cells fixed with 4% paraformaldehyde were stained with the neutral lipid-staining fluorophores BODIPY 493/503 (4,4-difluoro-1,3,5,7,8-pentamethyl-4-bora-3a,4a-diaza-s-indacene) (Invitrogen, D-3922) or HCS LipidTOX (Invitrogen, H34477). Stock solution of BODIPY 493/503 was made by dissolving the powder in DMSO. Protected from light cells were incubated with BODIPY 493/503 (20 μM, diluted in PBS) for 10 min or with HCS LipidTOX (1:200 in PBS) for 30 min at room temperature. Cells were washed at least twice with PBS.

Confocal microscopy

Images were acquired with a Zeiss LSM 510 NLO inverted confocal microscope using a Plan Achromat 63X/1.4 Oil DIC objective. Microglial cells were seeded on confocal chamber slides (Lab-Tek, Nalge Nunc International, Rochester, NY, USA) at a density of 1.5×10^4 cells/well (area of well = 0.8 cm^2) or on coverslips (area = 1.1 cm^2) at a density of 2×10^4 cells/coverlsip. Surfaces were coated with rat tail collagen (Sigma, C7661) prior to seeding. Coverslips were mounted on glass microscope slides (Fisher Scientific, 12-550-14) using glycerol-free mounting media Vectashield H-1000 (Vector) and were sealed around the perimeter with clear nail polish. Images of BODIPY 493/503-labelled LDs were acquired using an Argon 488 nm excitation laser and a 500-550 band pass (BP) filter. HCS LipidTOX-labelled LDs were detected using the HeNe 633 nm laser and a long pass (LP) 650 filter. Alexa Fluor 594 (red) was detected using HeNe 543 excitation laser and BP 565-615 IR filter. Each Z-stack image consisted of 10 to 20 optical slices taken at 0.3 μm intervals and had dimensions of 73.1×73.1×5.7 μm (x, y, z) when zoomed by a factor of 2, and 97.5 x 97.5 x 5.7 μm (x, y, z) when zoomed by a factor of 1.5. All images were acquired at a resolution of 1024 × 1024 pixels.

Analysis of LD volume and number

Confocal Z-stack images of fluorescently labelled LDs were analyzed using the software Imaris (Bitplane). LDs were visualized as point-like structures by selecting "Spots object". Prior to spot (i.e. LD) detection, the background of the image was subtracted. The threshold of spot detection was adjusted such that only spots associated with lipid droplets were considered in the analysis. The number, radius (μm), and volume (μm^3) of LDs were calculated by the software. A minimum of 9 fields were analyzed for each condition. The number of LDs per cell was calculated by dividing the number of LDs in the field by the number of cells present in the field. Data computed in Imaris were used to calculate the size distribution in the total LD population that included all LDs detected by microscopy. Small (diameter < 0.5 μm), medium (diameter > 0.5 < 1.0 μm) and large (diameter > 1 μm) LDs in their different populations were determined using the histogram analysis in Microsoft Excel's (2007).

Nitric oxide (NO) production

Release of NO from microglia in cultures was measured using the Griess reagent (Sigma, G-4410). Cells seeded at a density of 2×10^5/well in 24-well culture plates (Sarstedt #83.1836) were treated with LPS (10 μg/ml) or OA (50 μM) for 24h in 1% FBS-containing media. At the end of treatments, supernatants (50 μl) were collected and incubated with the Griess reagent (50 μl) for 15 min, after which the absorbance at 540 nm was measured with a spectrophotometer. In each experiment, a standard curve with different concentrations of nitrite (NO_2^-) was used to calculate the concentration of NO detected in the culture media. Each measurement was carried out in quadruplicate samples from two independent experiments.

Western blot analysis

Whole cell extracts made by lysing the cells in NP-40 buffer (50 mM Tris pH 8.0, 137 mM NaCl, 1% NP-40, 10% glycerol) were supplemented with complete protease inhibitor cocktail (Roche Applied Science) (1 tablet per 25 ml of lysis buffer) and with phosphatase inhibitors sodium orthovanadate (1 mM) and sodium fluoride (1 mM). Cell lysates were boiled in 6 × sample buffer (12 % SDS, 30% glycerol, 0.2 % bromophenol blue (w/v), 12% 2-mercaptoethanol, 0.375 M Tris HCl pH 6.8) at a 5:1 (cell lysate:sample buffer) ratio for 5 min, and proteins were resolved by SDS-PAGE and then transferred (1h, 100V, in ice-cold transfer buffer) to nitrocellulose membranes (Hybond, Amersham Bioscience). Blocking of the membranes was performed by incubating them in 5% milk or BSA (in TBS-T). Membranes were incubated with primary antibodies to perilipin-2 (guinea pig polyclonal) (1:2000) (Fitzgerald Ind. 20R-AP002), JNK (rabbit polyclonal) (1:1000) (Santa Cruz, sc-571), phospho-JNK (rabbit monoclonal) (1:1000) (Cell Signaling, #4668), p38 (rabbit polyclonal) (1:500) (Santa Cruz, sc-535), phospho-p38 (rabbit monoclonal) (1:1000) (Cell Signaling #9215), $cPLA_2$-α (mouse monoclonal (1:500) (Santa Cruz, sc-454, 4-4B-3C) or actin (mouse monoclonal) (1:1000) (Millipore, MAB1501R) overnight at 4°C. Following incubation with primary antibodies, membranes were incubated with horse radish peroxidise-linked secondary antibodies anti-rabbit IgG (Amersham Biosciences, NA 934), anti-guinea pig IgG (Sigma, A5545) and anti-mouse IgG (GE Healthcare, NXA931). The binding of the secondary antibody to the primary antibody was visualized by using an ECL Plus detection kit and HyBlot autoradiography films (Denville). Films were scanned (greyscale at 16 –bits) and relative

intensities of the immunoreactive bands were analyzed using the gel analyzer tool in the software Image J (1.42).

Immunocytochemistry of perilipin-2 and $cPLA_2$

Microglia were seeded at a density of 1.5×10^4 cells/well on coverslips coated with rat tail collagen (Sigma, C7661). Paraformaldehyde-fixed (4%, 15 min) cells were permeablized with Triton X-100 (0.1%) (Amersham Biosciences, # 17-1315-01) for 5 min and blocked with goat serum (10%) (Sigma, G9023) for 1h for perilipin-2 or 2h for $cPLA_2$ experiments. Immunostaining was performed by incubating the cells with a primary antibody to perilipin-2 (guinea pig polyclonal, 1:200) (Fitzgerald Ind. 20R-AP002) or $cPLA_2$-α (mouse monoclonal, 1:100) (Santa Cruz, sc-454, 4-4B-3C). Primary antibodies were targeted with anti-guinea pig (goat) (Invitrogen, A11076) or anti-mouse (goat) (Invitrogen, A11005) Alexa Fluor 594-conjugated secondary antibodies. Coverslips were mounted on glass microscope slides (Fisher Scientific, 12-550-14) using glycerol-free mounting media Vectashield H-1000 (Vector).

MTT assay for cell viability

The MTT assay was performed as described previously (Khatchadourian & Maysinger, 2009). N9 microglia were seeded in 24-well plates ($5 \text{ X } 10^4$ cells/well, area per well = 2 cm^2) (Sarstedt, 83.1836), cultured overnight and then treated with the inhibitors, oleic acid and LPS for 12h as described in the figure legends. Mitochondrial metabolic activity in viable cells was determined by conversion of MTT (thiazolyl blue tetrazolium bromide) (M2128, Sigma) to formazan. The absorbance from dissolved formazan in DMSO was measured spectrophotometrically at 594 nm.

Statistical analysis

Statistical analysis was performed using Systat (version 13). Comparisons between multiple groups were done by ANOVA, followed by post hoc tests such as Tukey's or Dunnett's. T-tests were used when comparing only two groups. All data are presented as group means ± SEM. The Fischer exact test (two-tail) was used to test for differences in proportions of small, medium and large LDs between their different populations in 2×2 tables. In all statistical tests, values of $p < 0.05$ were considered significant.

3.4 Results

3.4.1 LPS induces LD accumulation, alters LD size distribution and increases triglyceride content.

Binding of LPS to TLR4 leads to the activation of TLR4 signal transduction pathways known to induce NO synthase expression. Therefore, we measured the concentration of NO in the culture media following LPS (10 μg/ml) treatment for 6 and 24h. LPS treatment resulted in a dramatic increase in NO release (55.5 ± 1.8 μM) when compared with untreated cells (0.4 ± 0.6 μM) ($p<0.005$) (Supplemental figure 3.1). We sought to assess LD dynamics during microglial activation by examining changes in LD numbers and volumes. Using confocal microscopy, we monitored the dynamics of microglial LDs, which were visualized with the neutral lipid-selective fluorescent dye BODIPY 493/503. Cells treated with LPS (10 μg/ml) for 12h displayed significantly elevated number of LDs, as compared to non-stimulated microglial cells (Figure 3.1A). OA, a monounsaturated long chain fatty acid, is known to be a potent inducer of LDs (Fujimoto et al., 2006) and was therefore used as a positive control. We observed a marked accumulation of LDs in cells supplemented with OA (50 μM) for 12h (Figure 3.1A). In contrast to LPS, however, OA did not stimulate NO release from microglia (Supplemental figure 3.1). The number of LDs per cell (#LD/cell) was determined at each of the different timepoints (3, 6, 9, 12 and 24h) following LPS or OA treatment. LPS caused a time-dependent increase in #LD/cell, with a maximum number observed by 12h of LPS treatment (8.7 ± 0.7 vs. 4.6 ± 0.6 in untreated cells) ($p<0.05$) (Figure 3.1B). OA treatment rapidly increased LD content in microglial cells, causing a ~16-fold increase in #LD/cell (113 ± 13 in treated vs. 7 ± 2 in untreated) after 3h ($p<0.005$) (Supplemental Figure 3.2A). Typically, LDs are heterogeneous with respect to their sizes, as well as their lipid (Bartz et al., 2007; Rinia et al., 2008) and protein content (Straub et al., 2008). In N9 microglia, LDs with a diameter ranging from ~250 nm to 2 μm or even greater can be detected by confocal microscopy (our unpublished observations). In addition to an induction of LD number by inflammatory stimuli, an increase in LD size has also been seen in inflammatory macrophages (Melo et al., 2006). Therefore, we assessed the effect of LPS on the size distribution of LDs in microglial cells. After 12h of LPS treatment, we

observed a significant reduction (-19.8%, $p<0.005$) in the relative abundance of small LDs, accompanied by an increase in the relative abundance of medium (+18.6%, $p<0.005$) and large (+1.2%, not significant) LDs (Figure 3.1C). OA exerted a pronounced effect on LD size distributions (Supplemental figure 3.2B). A reduced relative abundance of small LDs (-26%, $p<0.005$) and concomitant increase of medium and large LDs (24%, $p<0.005$ and 2%, $p<0.005$, respectively) were seen within three hours (Supplemental figure 3.2B). These findings imply that LPS alters LD size distribution in microglia, although to a much lesser extent than OA. Our data show that LPS-activated microglia have a higher LD content than untreated microglial cells and that LPS and OA greatly differ in the extent to which they induce LD accumulation and alter LD sizes.

To further demonstrate that LPS leads to LD accumulation, we performed mass spectrometry-based lipidomic analysis to determine changes in the levels of triglycerides (TG), the major neutral lipids found in LDs. Following their extraction from microglia treated with LPS for 9h, TG levels were measured by quantitative electrospray ionization mass spectrometry (ESI-MS). Cells treated with LPS displayed a significant increase in total cellular TG levels (Figure 3.1D) and in TG species 52:2 and 54:3, thereby supporting the observed increase in LD content in activated microglia. TG synthesis requires incorporation of long-chain fatty acyl CoAs into glycerol-3-phosphate, monoacylglycerol and diacylglycerol (Buhman et al., 2001). Triacsin C, an inhibitor of long-chain acyl-CoA synthetase (ACSL), inhibits *de novo* synthesis of TG from glycerol and diacylglycerol (Igal et al., 1997). Treatment with triacsin C abolished the increase in LDs induced by LPS, suggesting that *de novo* synthesis of TGs was required under this condition (Figure 3.1E and Supplemental figure 3.1B).

3.4.2 LPS-induces activation of JNK and p38 MAPK and stimulates perilipin-2 expression. JNK and p38 MAPKs are key players in LPS-induced inflammatory response of microglia (Sanchez-Tillo et al., 2007). JNK activation leads to transcriptional activation of AP-1, a heterodimeric transcriptional complex (Wagner & Nebreda, 2009). It has been reported that LPS-induced perilipin-2 expression is in part mediated by an increased binding activity of AP-1 to the Ets/AP-1 element on the perilipin-2 gene

promoter (Gu et al., 2008). We first explored the effect of LPS on p38 and JNK by determining the extent of their phosphorylation by Western blot analysis. LPS induced a significant increase in p38 phosphorylation after 15 min of treatment ($p<0.01$) (Figure 3.2A & B). LPS also caused a rapid (15 min), transient and robust increase in JNK phosphorylation ($p<0.005$) (Figure 3.2C & D). In contrast, neither p38 nor JNK were activated following OA treatment at any timepoint between 0 and 120 min (Supplemental figure 3.2C).

Perilipin-2 has been reported to stimulate neutral lipid accumulation and LD formation in macrophages and fibroblasts (Imamura et al., 2002; Larigauderie et al., 2004). In macrophages, LPS increases perilipin-2 expression leading to LD accumulation (Feingold et al., 2010; Gu et al., 2008). To date, the role of perilipin-2 has not been investigated in neural cells. We hypothesized that activation with LPS will increase perilipin-2 protein levels in microglia. Following LPS stimulation, perilipin-2 levels increased in a time-dependent manner with a peak at 9h after LPS addition corresponding to a ~ 3-fold increase ($p<0.05$) over the control (Figure 3.3A & B). Immunostaining experiments of perilipin-2 indicated that the protein colocalizes with LDs in LPS-treated cells (Figure 3.3C). In the experiments with our positive control, we observed a significant increase (> 3-fold, $p< 0.05$) in perilipin-2 expression after 3h of OA treatment (Supplemental figure 3.3A & B). Moreover, perilipin-2 extensively colocalized with LDs (Supplemental figure 3.3C). Altogether, the above data imply that LPS rapidly activates MAPK pathways and leads to an increase in perilipin-2 expression in microglia.

3.4.3 LPS-induced LD formation is blocked by inhibitors of p38 and PI3K, but not by an inhibitor of JNK.

To investigate whether MAPK activation regulates LD formation, LPS-stimulated microglia were treated with selective inhibitors of JNK (SP600125) and p38 (SB203580). We found that in the presence of LPS, SP600125 (10 μM) further increased the LD number/cell (Figure 3.4A & B). In contrast, SB203580 (10 μM) reduced the LD number/cell ($p<0.005$) (Figure 3.4A & B). However, SB203580 also reduced the LD

number/cell under basal conditions ($p<0.005$). We also examined whether inhibition of p38 downregulates perilipin-2 expression in LPS-stimulated microglia. Indeed, SB203580 treatment, though not SP600125 treatment, significantly decreased perilipin-2 expression in LPS-treated microglia (Figure 3.4C). It has been demonstrated that SB203580, when used at concentrations above 2-3 μM, can block the phosphorylation and activation of Akt/protein kinase B (PKB) by inhibiting 3-phosphoinositide-dependent protein kinase 1 (PDK1) (Lali et al., 2000). Akt/PKB, a serine-threonine kinase is activated by growth factors and plays a central role in cell survival, growth and proliferation. Interestingly, Akt/PKB was also shown to promote accumulation of LDs in *Drosophila* nurse cells (Vereshchagina & Wilson, 2006). To examine whether Akt/PKB is a regulator of LD formation, we treated microglia with an inhibitor (LY294002) of class I phosphatidylinositol 3-kinase (PI3K), an upstream activator of Akt/PKB. LPS-induced LD accumulation in microglia was blunted by LY294002 treatment ($p<0.005$) (Figure 3.4A & B). The inhibitor also reduced perilipin-2 expression (Figure 3.4C). Together, these data implicate the p38 MAPK and PI3K/Akt pathways in the regulation of LD formation in LPS-treated microglial cells.

3.4.4 p38 and PI3K inhibitors do not block OA-induced LD formation, but decrease the size of LDs

Roles for p38 MAPK and PI3K activation in OA-induced LD formation have been previously reported for epithelial cells (Moreira et al., 2009). To examine whether p38 and PI3K regulate OA-induced LDs in microglia, we tested their effect on LD formation by confocal microscopy. SB203580 or LY294002 did not block the induction of LDs by OA (Supplemental figure 3.5 A&B), but they did markedly decrease the average size (volume) of LDs ($p<0.01$).

3.4.5 In microglia, cytosolic phospholipase A_2 ($cPLA_2$) colocalizes with LPS-induced LDs, but not with OA-induced LDs.

LDs in leukocytes were previously shown to contain significant amounts of esterified arachidonate in their triglyceride and phospholipid pools (Yu et al., 1998). Different eicosanoid-synthesizing enzymes, including the key enzyme for the release of arachidonic acid, cPLA$_2$-α, compartmentalize at LDs in human monocytic (U937) and rat intestinal (IEC-6) epithelial cells (Moreira et al., 2009; Yu et al., 1998). We asked whether or not the newly formed LDs in LPS-treated microglia play a function in eicosanoid synthesis. To address this question, we examined by confocal microscopy the colocalization of cPLA$_2$-α with LDs in LPS-treated microglia. Colocalization of cPLA$_2$-α with LDs could not be assessed in untreated cells, because LDs were almost entirely absent (Figure 3.5A). LPS induced the formation of many LDs which colocalized with cPLA$_2$-α (Figure 3.5A, bottom row). In contrast, OA-induced LDs did not colocalize with cPLA$_2$-α. Treatment with LPS or OA did not alter the protein levels of cPLA$_2$-α (Figure 3.5B). Taken together, these findings suggest that LDs in microglia can potentially be involved in the generation of eicosanoids under inflammatory conditions.

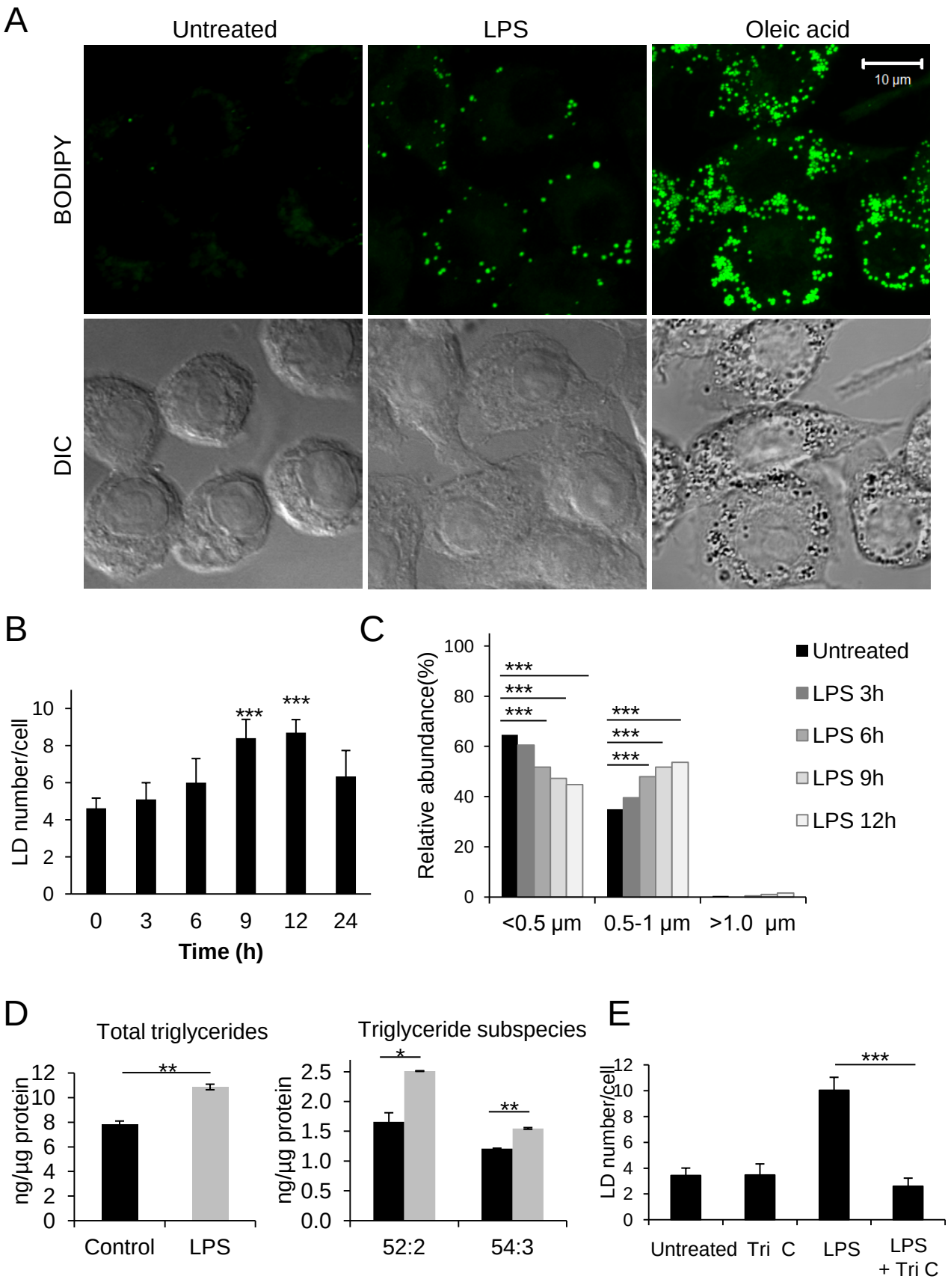
A
Untreated
LPS
Oleic acid
BODIPY
DIC
10 μm
B
LD number/cell
Time (h)
0
3
6
9
12
24
***
C
Relative abundance(%)
Untreated
LPS 3h
LPS 6h
LPS 9h
LPS 12h
<0.5 μm
0.5-1 μm
>1.0 μm
D
Total triglycerides
ng/μg protein
Control
LPS
**
Triglyceride subspecies
52:2
54:3
*
E
LD number/cell
Untreated
Tri C
LPS
LPS + Tri C

Figure 3.1 LPS treatment induces LD accumulation and increases cellular triglyceride content in microglia.

(A) Representative confocal images showing LDs in microglia treated with LPS (10 µg/ml) or OA (50 µM) for 12h. LDs were labelled with BODIPY 493/503 (green) and cells were visualized by differential interference contrast (DIC). Scale bar = 10 µm.

(B) Assessment of the average number of LDs per cell in cells treated with LPS for 3, 6, 9, 12 and 24h.

(C) Temporal changes in the relative abundance of small, medium and large LDs in LPS-treated microglia. LDs were divided into the small (< 0.5 µm diameter), medium (> 0.5 <1 µm diameter) and large (> 1 µm diameter) categories. Data show the relative abundance (% of the total LD population) of LDs of different sizes over time.

(D) Total triglycerides and triglyceride species (52:2 and 54:3) in microglia treated with LPS for 9h, as determined by ESI-MS.

(E) Triglyceride biosynthesis inhibitor, triacsin C, blocks LPS-induced LD accumulation. Cells were incubated with triacsin C (1 µM, 30 min) and treated with LPS for 9h. Statistically significant differences are indicated by * ($p < 0.05$), ** ($p < 0.01$) and *** ($p<0.005$).

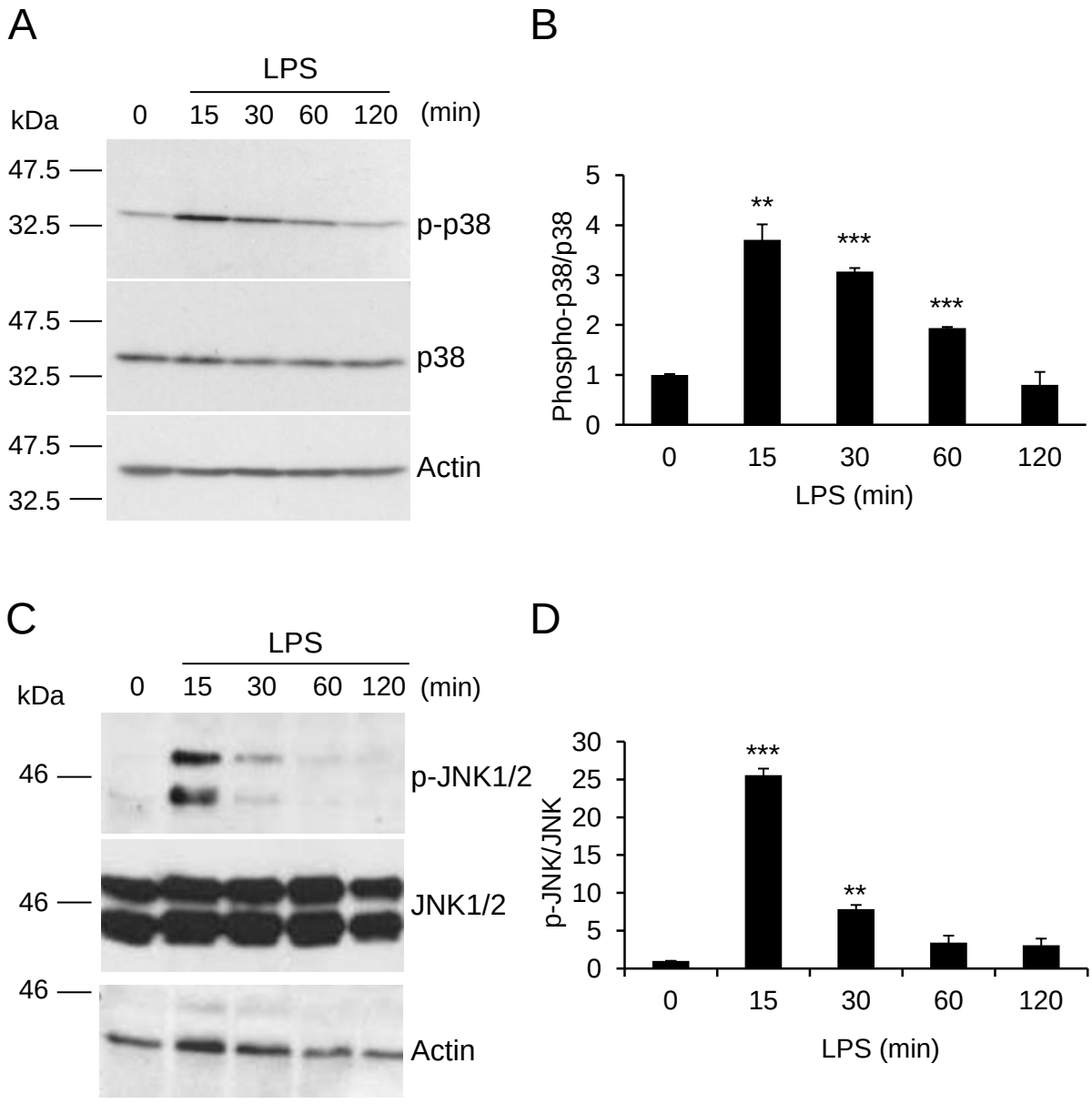
A
LPS
kDa
0
15
30
60
120
(min)
47.5
32.5
p-p38
47.5
32.5
p38
47.5
32.5
Actin
B
Phospho-p38/p38
5
4
3
2
1
0
**
***
***
0
15
30
60
120
LPS (min)
C
LPS
kDa
0
15
30
60
120
(min)
46
p-JNK1/2
46
JNK1/2
46
Actin
D
p-JNK/JNK
30
25
20
15
10
5
0
***
**
0
15
30
60
120
LPS (min)

Figure 3.2 LPS activates JNK and p38 MAPK in microglia.

(A) Western blot analysis of phosphorylated p38 (p-p38) in LPS-stimulated microglia. Cells were incubated with LPS (10 μg/ml) for 15, 30, 60 and 120 min.

(B) Quantification of p-p38. P-p38/p38 is expressed as fold increase over the untreated group. Quantification of the immunoreactive bands was performed by densitometric analysis using Image J. Bars represent mean values ± SEM from two independent experiments (n=2 in each experiment).

(C) Western blot analysis of phosphorylated JNK (p-JNK) in LPS-stimulated microglia. Cells were incubated with LPS (10 μg/ml) for 15, 30, 60 and 120 min.

(D) p-JNK/JNK is expressed as fold increase over the untreated group. Bars represent mean values ± SEM from two independent experiments (n=2 in each experiment). Statistically significant differences are indicated by ** ($p< 0.01$, vs. untreated) and *** ($p<0.005$, vs. untreated).

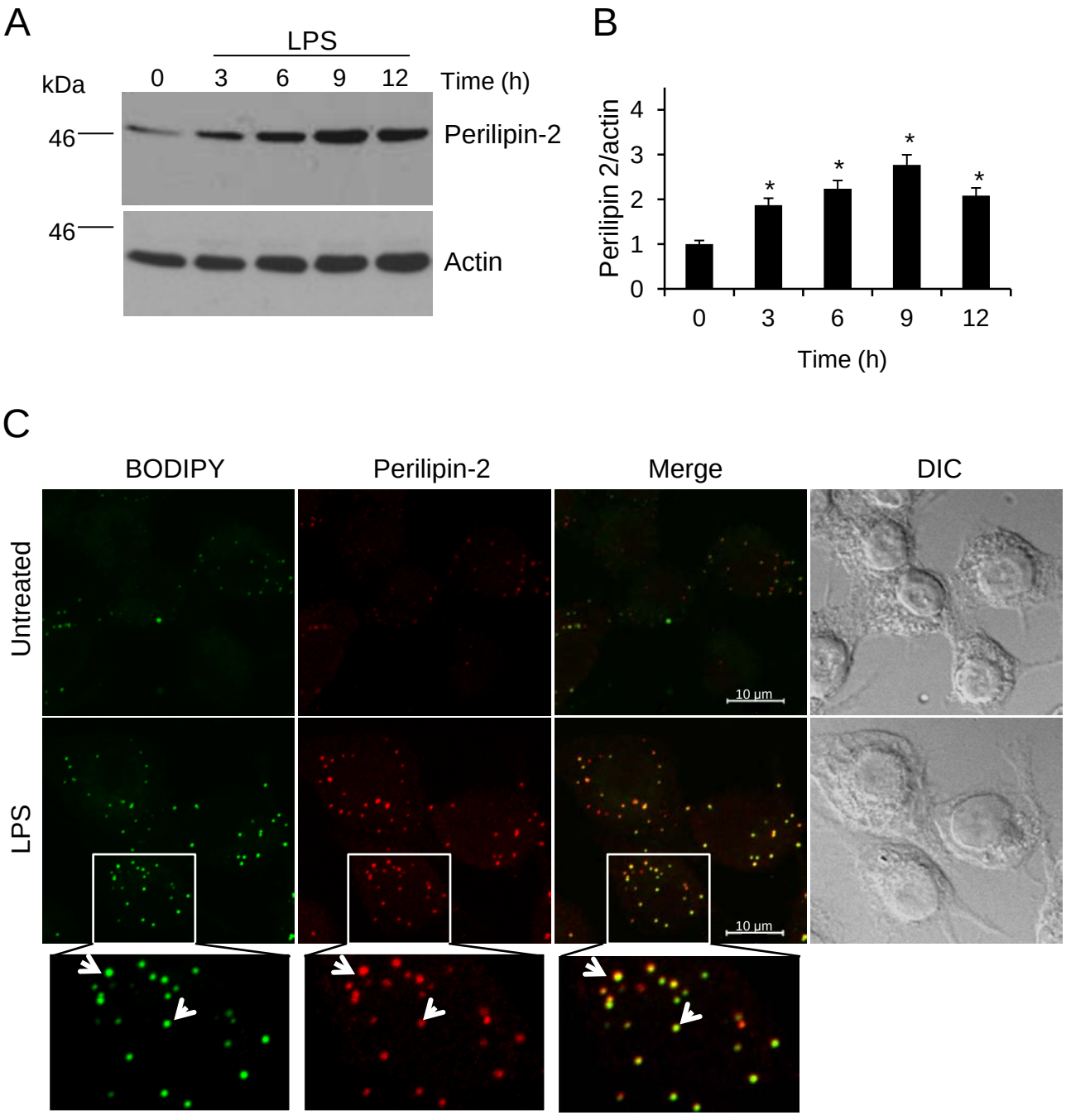
A
LPS
kDa
0
3
6
9
12
Time (h)
46
Perilipin-2
46
Actin
B
Perilipin 2/actin
0
1
2
3
4
*
*
*
*
0
3
6
9
12
Time (h)
C
BODIPY
Perilipin-2
Merge
DIC
Untreated
LPS
10 μm
10 μm

Figure 3.3 Perilipin-2 is induced after LPS stimulation and colocalizes with LDs.

(A) Western blots showing perilipin-2 protein expression in microglia treated with LPS (10 µg/ml) for 3, 6, 9 and 12 h.

(B) Quantification of perilipin-2 expression. Perilipin-2/actin is expressed as fold increase over untreated cells. Bars represent mean values ± SEM from at least two independent experiments (n=2 in each experiment). Statistically significant differences are indicated by * ($p < 0.05$, vs. untreated).

(C) Immunostaining of perilipin-2 in untreated or LPS-treated (9h) microglia. Cells were double-labelled for LDs with BODIPY (493/503) (green) and perilipin-2 (red). White arrows indicate colocalization of perilipin-2 with LDs. Scale bar = 10 µm.

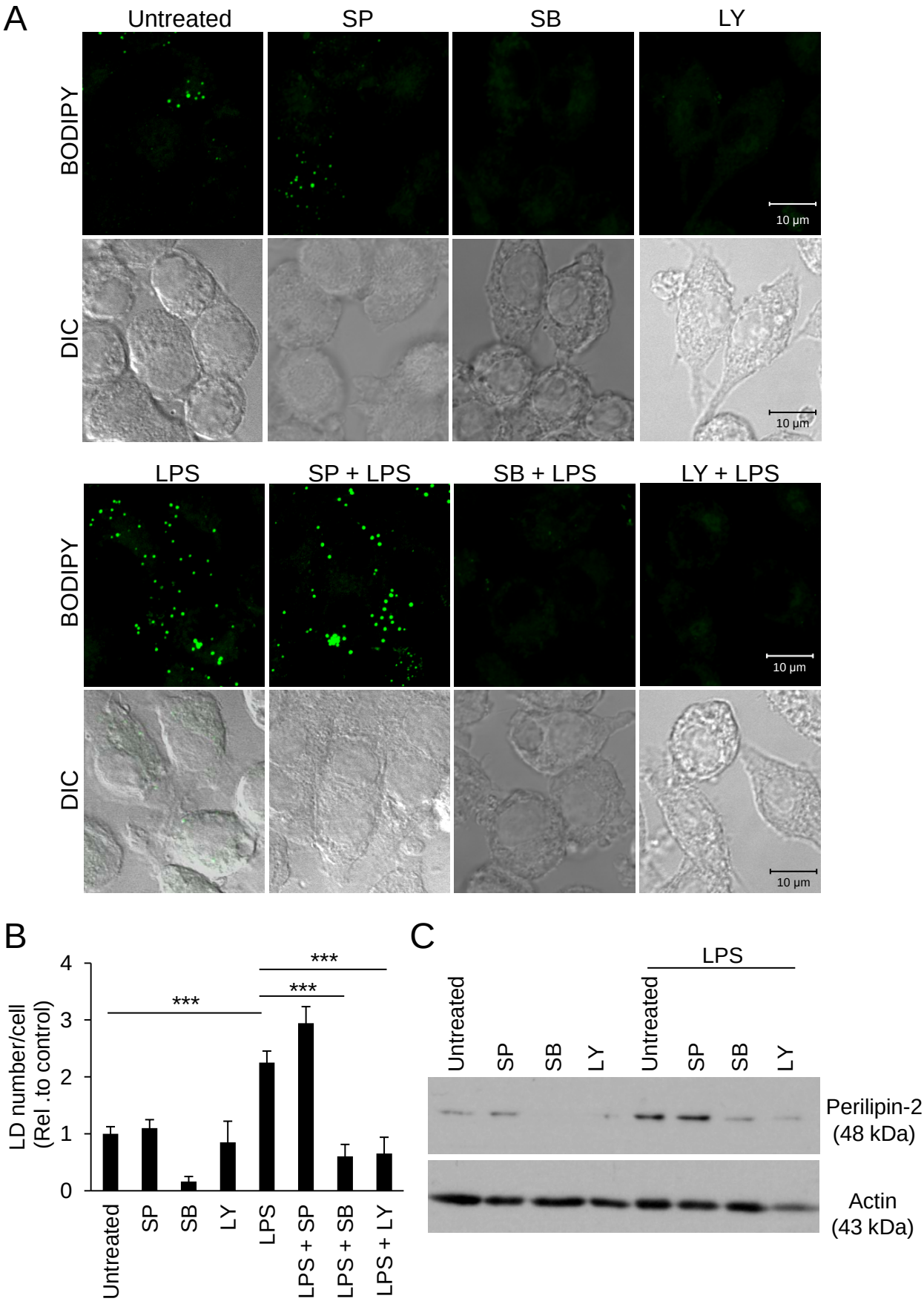
A
Untreated
SP
SB
LY
BODIPY
DIC
10 μm
LPS
SP + LPS
SB + LPS
LY + LPS
B
LD number/cell
(Rel .to control)
***
***
***
Untreated
SP
SB
LY
LPS
LPS + SP
LPS + SB
LPS + LY
C
LPS
Perilipin-2
(48 kDa)
Actin
(43 kDa)

Figure 3.4 Inhibition of p38 MAPK and PI3K, but not of JNK, abolishes LPS-induced LD accumulation and perilipin-2 expression.

(A) Representative confocal micrographs of LDs in cells treated with LPS (10 µg/ml, 12h) in the presence or absence of SP600125 (10µM), SB203580 (10µM) and LY294002 (10 µM). LDs were labelled with BODIPY 493/503. Scale bar = 10 µm.

(B) Assessment of LD/cell in cultures incubated with the inhibitors in the presence or absence of LPS. Bars indicate mean values ± SEM from two independent experiments (n=3 per experiment). Statistically significant differences are indicated by * ($p< 0.05$) and *** ($p<0.005$).

(C) Western blot analysis of perilipin-2 expression in cells treated with LPS and inhibitors. Perilipin-2 expression was determined after 9h of LPS treatment. Inhibitors were added to cultures 30 min before stimulation with LPS. Actin was used as a loading control.

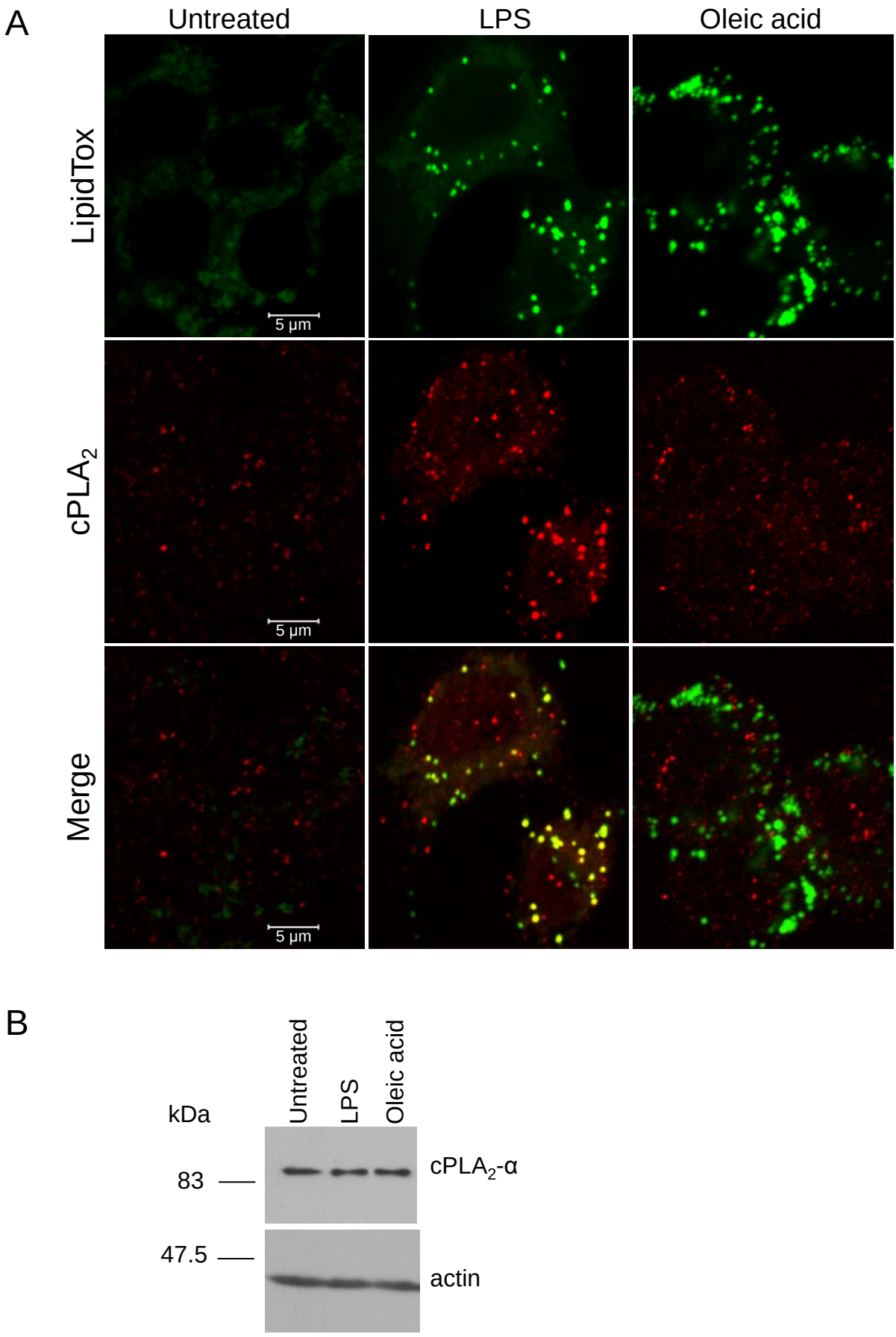
A
Untreated
LPS
Oleic acid
LipidTox
cPLA2
Merge
5 µm
5 µm
5 µm
B
Untreated
LPS
Oleic acid
kDa
83
47.5
cPLA2-α
actin

Figure 3.5 Cytosolic phospholipase A_2-α ($cPLA_2$-α) colocalizes with LDs induced by LPS, but not with LDs induced by OA treatment.

(A) Microglia were treated with LPS (10 µg/ml) or OA (50 µM) for 9h. Confocal images show LDs labelled with HCS LipidTox (pseudocolored green) and immunolabeled $cPLA_2$-α (red). Note that $cPLA_2$-α colocalized with LDs (merged images; bottom row, middle panel). Images are representative of two independent experiments. Scale bar = 5 µm.

(B) Western blot analysis of $cPLA_2$-α in cells treated with LPS (10 µg/ml) or OA(50 µM). Actin was used as a loading control.

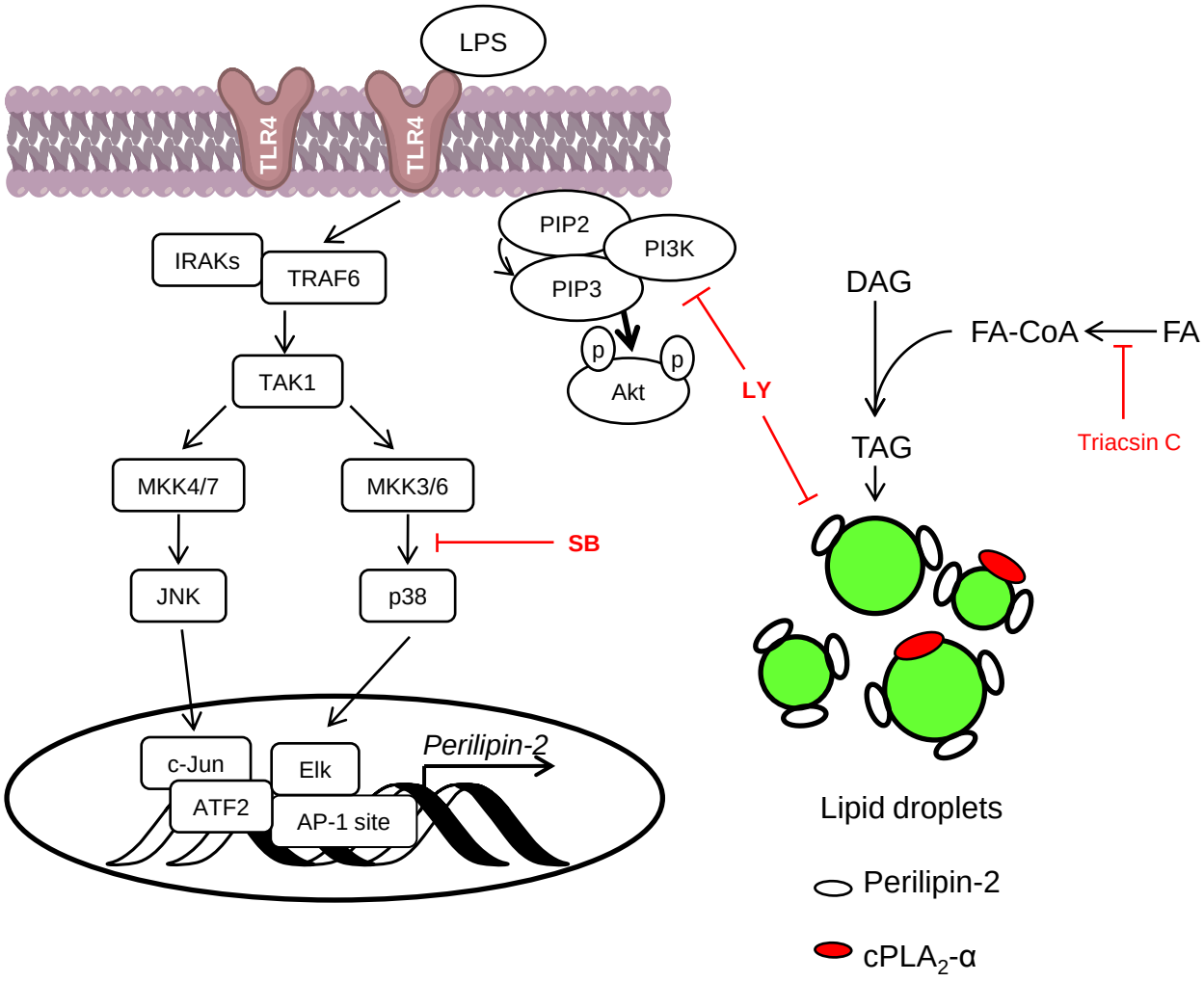
LPS
TLR4
TLR4
IRAKs
TRAF6
TAK1
MKK4/7
MKK3/6
JNK
p38
SB
PIP2
PI3K
PIP3
p
p
Akt
LY
DAG
FA-CoA
FA
Triacsin C
TAG
Lipid droplets
c-Jun
ATF2
Elk
AP-1 site
Perilipin-2
Perilipin-2
cPLA2-α

Figure 3.6 Proposed processes involved in LD formation following microglia stimulation by LPS.

Activation of TLR4 by LPS results in the activation of TGFβ-activated kinase 1 (TAK1), leading to an activation of MAP kinase kinases (MKKs), and subsequent phosphorylation of JNK and p38 MAPKs. AP1 (c-Jun/ATF2) and ELK1 are downstream targets of JNK and p38. SB203580 (p38 inhibitor) and LY294002 (PI3K inhibitor) suppress perilipin-2 expression and LD induction by LPS. cPLA-α, a key arachidonic acid-releasing enzyme, colocalized with LDs. The induction of LDs by LPS was blocked by triacsin C, an inhibitor of triglyceride biosynthesis.

3.5 Discussion

In this report we show that LPS-induced TLR4 activation in microglia is accompanied by marked changes in intracellular lipid droplet (LD) status as manifested by an increase in the number and volume of LDs in the cells. LPS also increased the expression of perilipin-2, a major LD surface-associated protein. We attribute this effect of LPS on LDs to the activation of p38 MAPK, since inhibition of p38 suppressed LPS-induced perilipin-2 expression and LD formation. Taken together, our results suggest that LDs are actively involved in LPS-induced inflammatory response in microglia.

We first demonstrated that LPS-mediated TLR4 activation in microglia leads to LD accumulation. In vivo studies in mice have demonstrated that LD number in leukocytes is increased following LPS administration (Pacheco et al., 2002). Because of their implication in the innate immune response, LDs were described as “inflammatory organelles” that can serve as key markers of cell activation (D'Avila et al., 2008) We showed that in LPS-challenged microglia, the increase in the LD number was significant. However, temporal analysis of LDs over a 24h period following LPS stimulation demonstrated that the initial increase in LD number does not persist; after reaching a peak following 12h of LPS treatment, the number of LDs decreased. This decrease could be explained by increased fusion between LDs, leading to larger, but fewer LDs in the cells. LD fusion is an inducible process (Bostrom et al., 2007; Murphy et al., 2010). In fact, LPS did cause marked changes in the LD size distribution pattern in microglia, shifting the balance towards larger LDs and reducing the abundance of small-sized LDs. We speculate that the enlargement of LDs in LPS-stimulated microglia was caused, at least in part, by activated homotypic fusion of their smaller forms. Treatment with LPS resulted in a significant increase in cellular TG levels in microglia. The effect of LPS on lipid synthesis in macrophages has been previously examined (Funk et al., 1993; Posokhova et al., 2008). It was demonstrated that macrophages (RAW 264.7) treated with LPS accumulate TG, but not cholesterol esters (CE) (Funk et al., 1993). An *in vivo* study showed that LPS increased both TG and CE levels in peritoneal macrophages (Posokhova et al., 2008). In microglia, LD accumulation triggered by LPS required TG biosynthesis, since triacsin C, an inhibitor of long-chain acyl-CoA synthetase (ACSL) activity, blocked

the induction of LDs by LPS. Whether CE levels increase concurrently with TG levels in LPS-treated microglia should also be determined in future studies.

In parallel with LPS, we supplemented microglia with OA, a dietary monounsaturated fatty acid. As expected, OA strongly induced LD formation and caused marked changes in the pattern of LD size distribution. Upon entering the cell, unsaturated FFAs are rapidly activated by becoming converted to their CoA esters. TGs consist of three fatty acid chains attached to a glycerol backbone by ester bonds. In the final reaction of TG synthesis, a fatty acyl-CoA and diacylglycerol are covalently attached in an esterification reaction catalyzed by the enzyme acyl-CoA:diacylglycerol acyltransferase (DGAT) (Yen et al., 2008). The esterification-driven conversion of FFAs into stored TGs is considered a protective mechanism against FFA-induced lipotoxicity (Listenberger et al., 2003). In the present study, OA treatment in microglia did not induce cytotoxicity and displayed no activating effect on JNK and p38 MAPK.

We further demonstrated that LPS treatment increases perilipin-2 protein expression. The increase in perilipin-2 expression took place before the increase in the number of LDs, suggesting that new perilipin-2 protein synthesis was required for LPS-induced LD formation. In fact, using actinomycin D and cycloheximide, Gu et al. demonstrated that in RAW 264.7 macrophages LPS-induced perilipin-2 expression was stimulated at the transcriptional level and was mediated by new protein synthesis (Gu et al., 2008). Post-translational mechanisms were shown to regulate perilipin-2 via the ubiquitin/proteasome proteolytic pathway (Xu et al., 2005). Increased cellular neutral lipids (e.g triglyceride) stabilize perilipin-2 and prevent its degradation by the proteasome (Masuda et al., 2006). Therefore, similar mechanisms could contribute to increased perilipin-2 levels in microglia accumulating TGs.

We observed a robust induction of perilipin-2 in OA-supplemented microglia. Fatty acids can bind peroxisome proliferator activated receptors (PPAR) α- and – γ and thereby regulate gene expression (Kliewer et al., 1997). A PPAR response element (PPRE) is located in the promoter region of perilipin-2 (Targett-Adams et al., 2005) and regulates perilipin-2 expression in OA-treated cells (Fan et al., 2009). OA was also shown to affect the post-translational regulation of perilipin-2 (ADRP). Indeed, OA treatment reduced

levels of polyubiquitinated perilipin-2 and prevented its proteolytic degradation (Xu et al., 2005).

JNK and p38 MAPKs play an important role in the pro-inflammatory actions of microglia and macrophages (Lee et al., 1994; Waetzig et al., 2005). Their activity is highly regulated by TLR4-generated signals. TLR4 agonists, such as LPS, induce homodimerization of the TLR4/MD-2 complex and trigger a downstream signaling cascade involving IRAK and TAK1. This leads to activation of MAPK kinases (MKK) 3, 4, 6 and 7 (Wagner & Nebreda, 2009). MKK3/6 mainly phosphorylate p38, whereas MKK 4/7 phosphorylate JNK. Phosphorylation of c-Jun and ATF2 by JNK and p38 increase the transcriptional activity of AP-1, leading to expression of inflammatory cytokines (Wagner & Nebreda, 2009). The effects of LPS on microglia have been previously investigated (Oh et al., 2009; Zhou et al., 2006). In BV2 microglia, LPS-induced activation involves iNOS expression, NFκB activation, p38 phosphorylation, reactive oxygen species production and cyclooxygenase -2 expression (Oh et al., 2009). Interestingly, OA showed an anti-inflammatory effect by reducing the proinflammatory effects of LPS. In agreement with these studies, we showed that in N9 microglia LPS caused rapid and transient stimulation of JNK and p38 MAPK and increased NO production. OA treatment had virtually no stimulating effect on JNK, p38 and NO release. Taken together, these findings reveal differential effects of OA and LPS on the TLR4-initiated signal transduction pathway.

We demonstrated that the inhibition of p38 MAPK or PI3K, but not the inhibition of JNK, downregulates LPS-induced perilipin-2 expression and LD accumulation. SP600125 inhibits JNK 1/2 with high specificity (Bennett et al., 2001). SP600125 treatment further increased LD formation in LPS-stimulated microglia, contrary to our expectations. The growing body of evidence implies the existence of a crosstalk between JNK and other kinases. Activation of the PI3K/Akt pathway and ERK1/2 following inhibition of JNK with SP600125 have been reported in macrophages and neurons (Sanchez-Tillo et al., 2007; Yeste-Velasco et al., 2009). Of note, ERK 1/2 and Akt/PI3K signalling pathways were implicated in regulating LD formation in macrophages (Pacheco et al., 2007). It is conceivable, therefore, that under LPS treatment,

pharmacological inhibition of JNK causes a compensatory activation of either ERK1/2 or Akt/PI3K pathway, leading to increased LD formation. The inhibitor of 38 MAPK, SB203580, abolished the increase in perilipin-2 expression and LD accumulation caused by LPS treatment. It was previously shown that SB203580 inhibits LPS-induced activation of p38 MAPK and transcription factor AP-1 in macrophages (Chen et al., 1999). Considering that LPS can enhance perilipin-2 promoter activity by activating AP-1, the suppression of peilipin-2 by SB203580 in LPS-treated microglia could have been mediated by the inhibition of AP-1. In the absence of LPS, SB203580 also reduced the number of LDs. This could have been caused by the off-target inhibitory effect of SB203580 on the Akt/PKB signalling pathway, as previously reported in experiments applying the inhibitor at concentrations above 2- 3 μM (Lali et al., 2000).

3.6 Conclusion

In summary, our study revealed that both LPS and OA can stimulate LD formation and perilipin-2 expression in microglia, but with different dynamics and to a remarkably different extent. OA is a much more potent inducer of LD formation and perilipin-2 expression, as compared to LPS. Our results reveal at least two distinct signalling pathways involved in LD formation in microglia. Whereas OA induces LD formation in a MAPK independent manner, LPS induces LD accumulation by strongly activating p38. The presence of colocalization between $cPLA_2$-α and LPS-induced LDs indicates a potential role for these organelles in the regulation of eicosanoid synthesis in activated microglia.

We suggest that LDs induced by LPS play an important regulatory role in the microglial inflammatory response. Altogether, our findings imply that in the central nervous system, specific changes in the biogenesis of LDs and their proteins may contribute to regulation of pathologies associated with inflammation.

3.7 Acknowledgements

We acknowledge the financial assistance from Canadian Institute of Health Research (CIHR) (DM). VIT is a Concordia University Research Chair in Genomics, Cell Biology and Aging. Centre for Biological Applications of Mass Spectrometry at Concordia University is acknowledged for outstanding services. VRR is supported by a scholarship from the CIHR. This work was also supported by the Concordia University Chair Fund (VIT). We thank G. Yeretssian for his careful and critical reading.

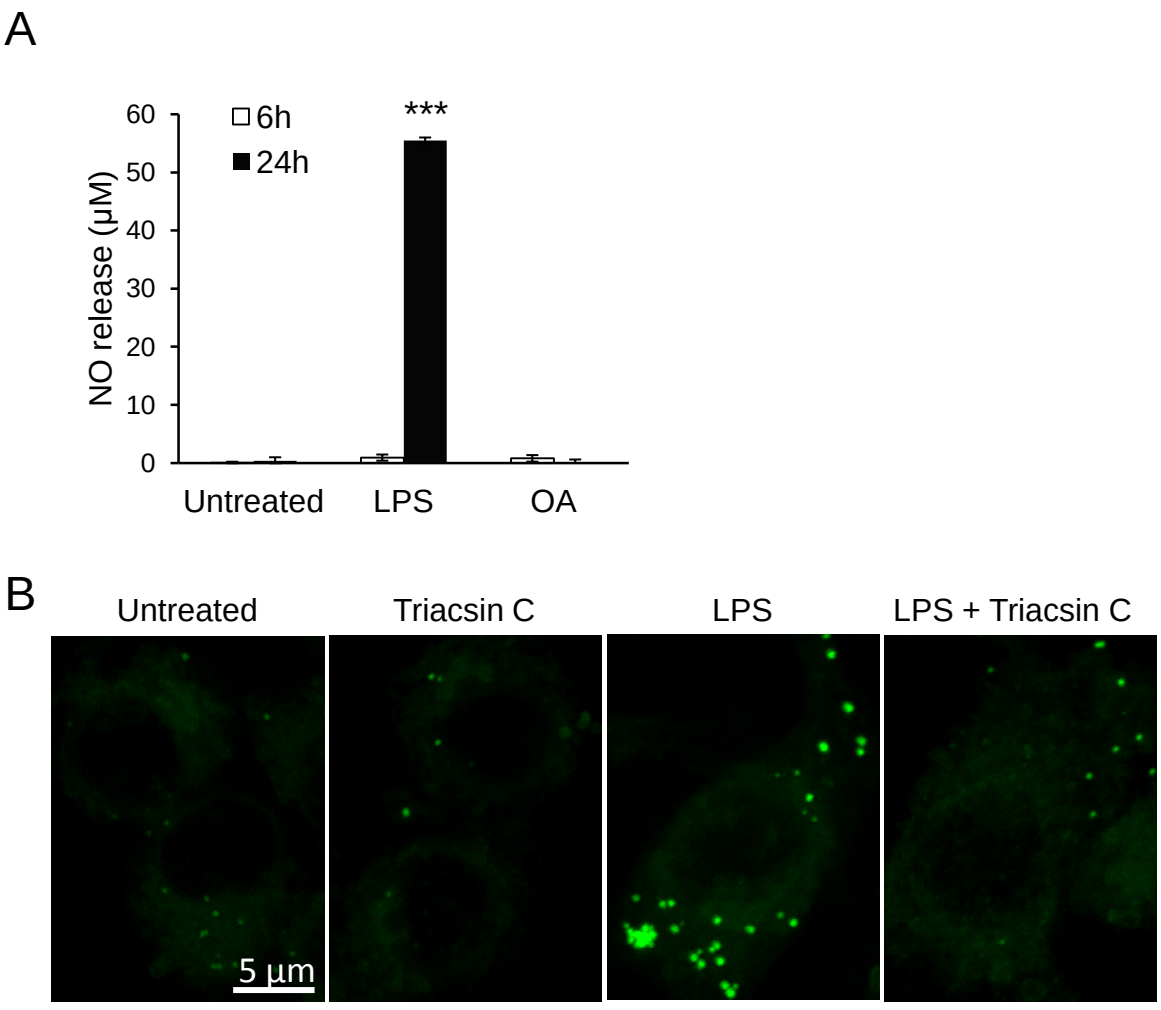

Supplementary figure 3.1

Effect of LPS on nitric oxide release and inhibition of LD formation by triacsin C.

(A) Nitric oxide (NO) release from microglia exposed to LPS (10 µg/ml) or OA (50 µM) for 6 and 24h. NO is expressed as a concentration (µM). Bars represent means ± SEM from two independent experiments and quadruplicate (n=4) samples. Statistically significant differences are indicated by *** ($p<0.005$, vs. untreated).
(B) Effect of triacsin C on LPS-induced LD accumulation. Cells were incubated with triacsin C (1 µM, 30 min) and treated with LPS for 9h. Representative confocal images (Z-stacks) show LDs in untreated and treated cells. Scale bar = 5 µm.

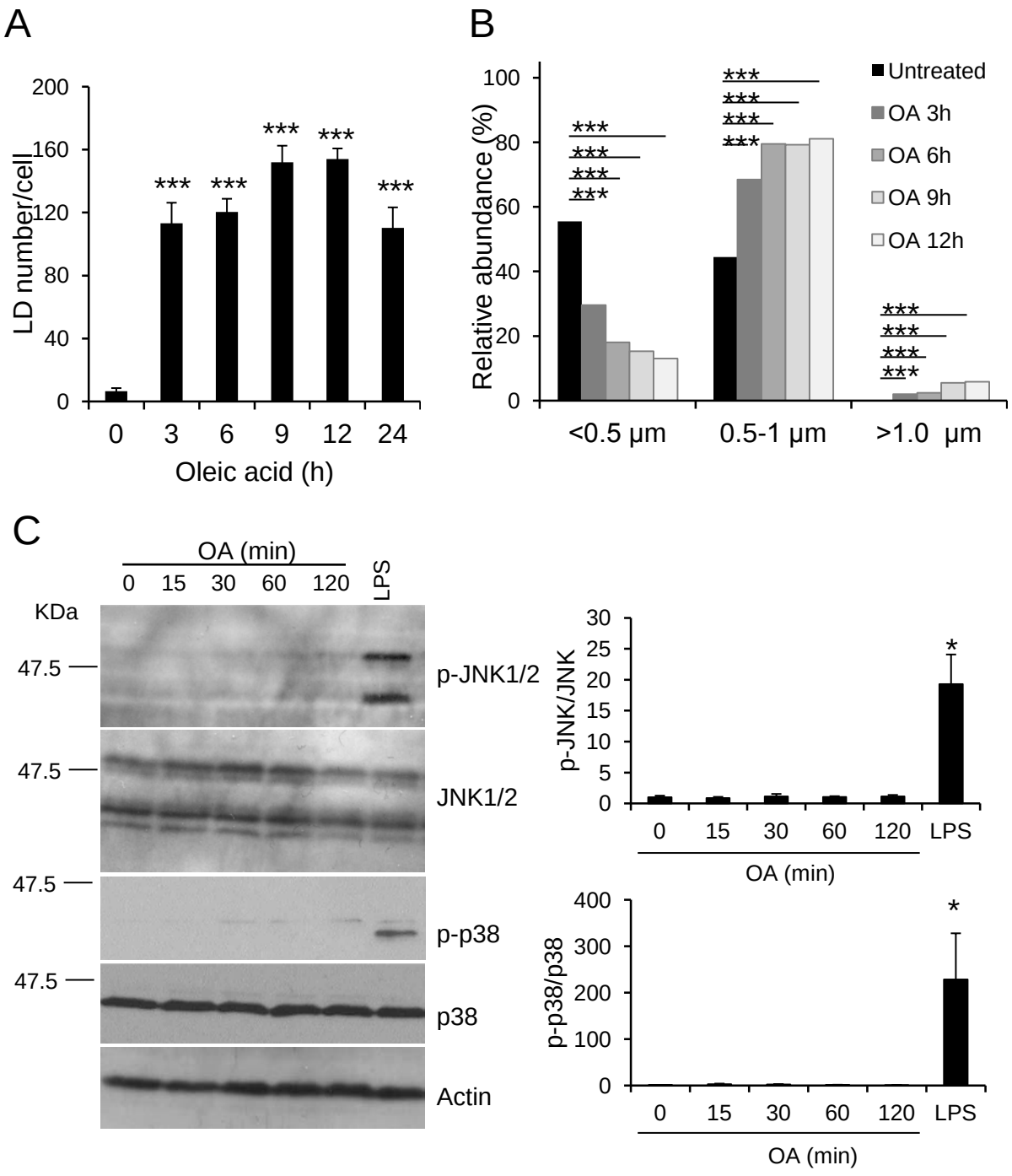
A
LD number/cell
200
160
120
80
40
0
***
0
3
6
9
12
24
Oleic acid (h)
B
Relative abundance (%)
100
80
60
40
20
0
Untreated
OA 3h
OA 6h
OA 9h
OA 12h
<0.5 μm
0.5-1 μm
>1.0 μm
C
OA (min)
0
15
30
60
120
LPS
KDa
47.5
p-JNK1/2
JNK1/2
p-p38
p38
Actin
p-JNK/JNK
p-p38/p38
*

Supplementary figure 3.2 Oleic acid quickly induces LD formation and shows no activating effect on JNK nor p38 MAPK.

(A) Temporal changes in the average LD number per cell after OA (50 µM) treatment.

(B) Temporal changes in the relative abundance of small, medium and large LDs in OA-treated cells. Statistically significant differences are indicated by *** ($p<0.005$, vs. untreated). (C) Western blot analysis of phosphorylated JNK and p38 in OA-treated cells. Cells were incubated with OA (50 µM) for 15, 30, 60 and 120 min or LPS (10 µg/ml) for 15 min. Quantification of p-p38 and p-JNK. Bars represent mean values ± SEM from two independent experiments. Statistically significant differences are indicated by * ($p< 0.05$, vs. untreated).

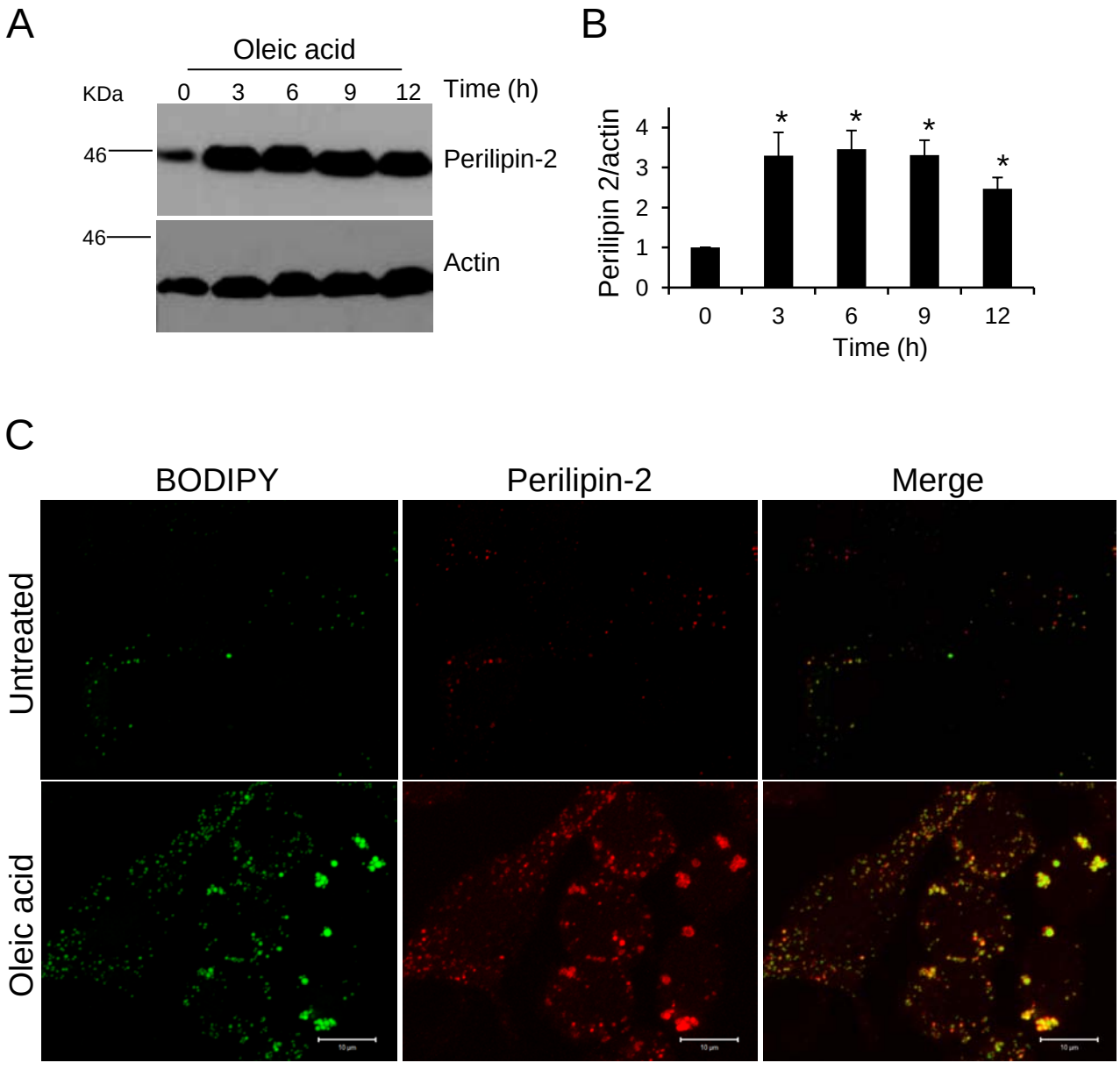
A
Oleic acid
KDa
0
3
6
9
12
Time (h)
46
Perilipin-2
46
Actin
B
Perilipin 2/actin
4
3
2
1
0
*
*
*
*
0
3
6
9
12
Time (h)
C
BODIPY
Perilipin-2
Merge
Untreated
Oleic acid

Supplementary figure 3.3 Perilipin-2 colocalizes with lipid droplets and is rapidly induced following oleic acid treatment.

(A) Perilipin-2 protein expression in microglia treated with OA (50 µM) for 3, 6, 9 and 12 h.

(B) Quantification of perilipin-2 expression. Perilipin-2/actin is expressed as fold increase over untreated cells. Bars represent mean values ± SEM from at least two independent experiments (n=2 per experiment). Statistically significant differences are indicated by * ($p < 0.05$, vs. untreated).

(C) Immunostaining of perilipin-2 in untreated or OA-treated (9h) microglia. Cells were labeled for LDs with BODIPY (493/503) (green). Note that perilipin-2 (red) colocalizes with LDs, as indicated by the overlap of red and green signals (yellow spots). Scale bar = 10 µm.

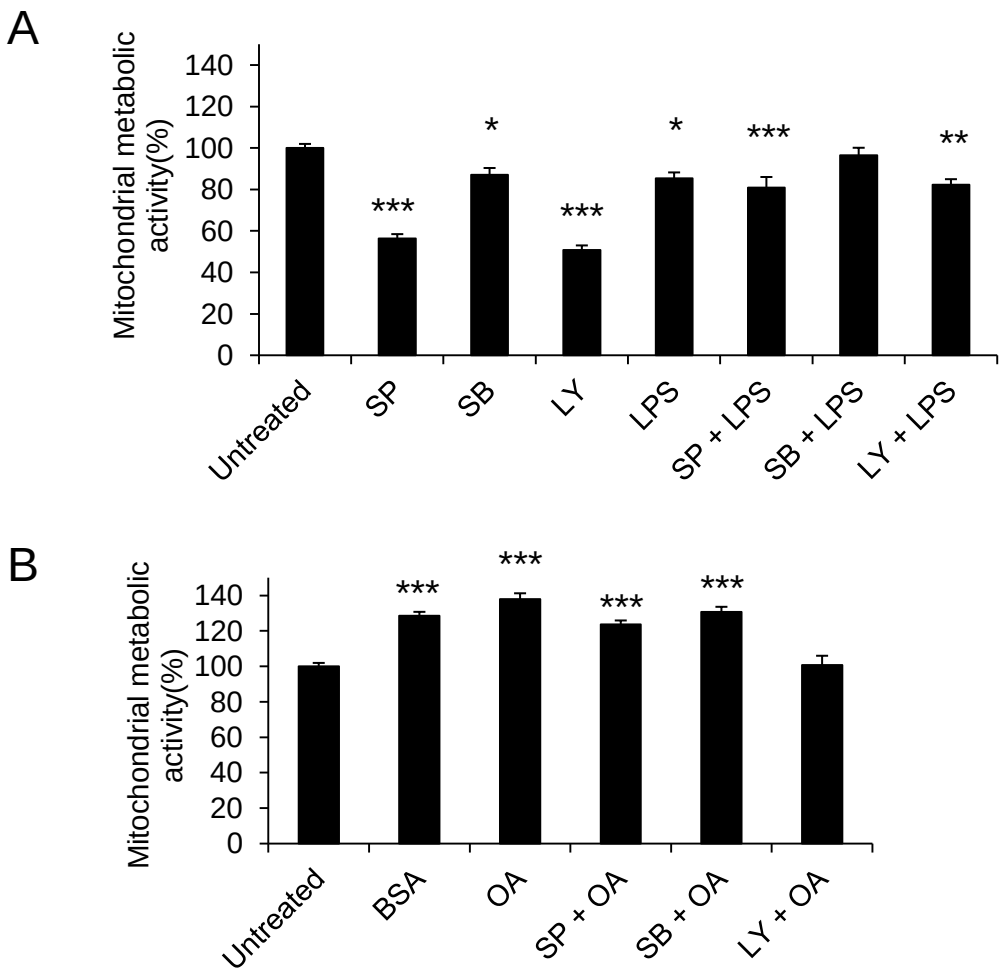

Supplementary figure 3.4 Effect of oleic acid, LPS and pharmacological inhibitors on microglial cell viability.

(A) Effect of inhibitors (SP600125, SB203580 and LY294002) and LPS on cell viability. Cells were treated with inhibitors (10 µM) and LPS (10 µg/ml), alone or in combination, for 12h.

(B) Effect of oleic acid and inhibitors on cell viability. Cells were treated with oleic acid (50 µM) in the presence or absence of inhibitors. Cell viability was assessed by measuring the mitochondrial metabolic activity using the MTT reduction assay. Bars represent mean values (± SEM) and were expressed as a percentage (%) of the value in the untreated group. Statistically significant differences are indicated by *** ($p<0.005$, vs. untreated).

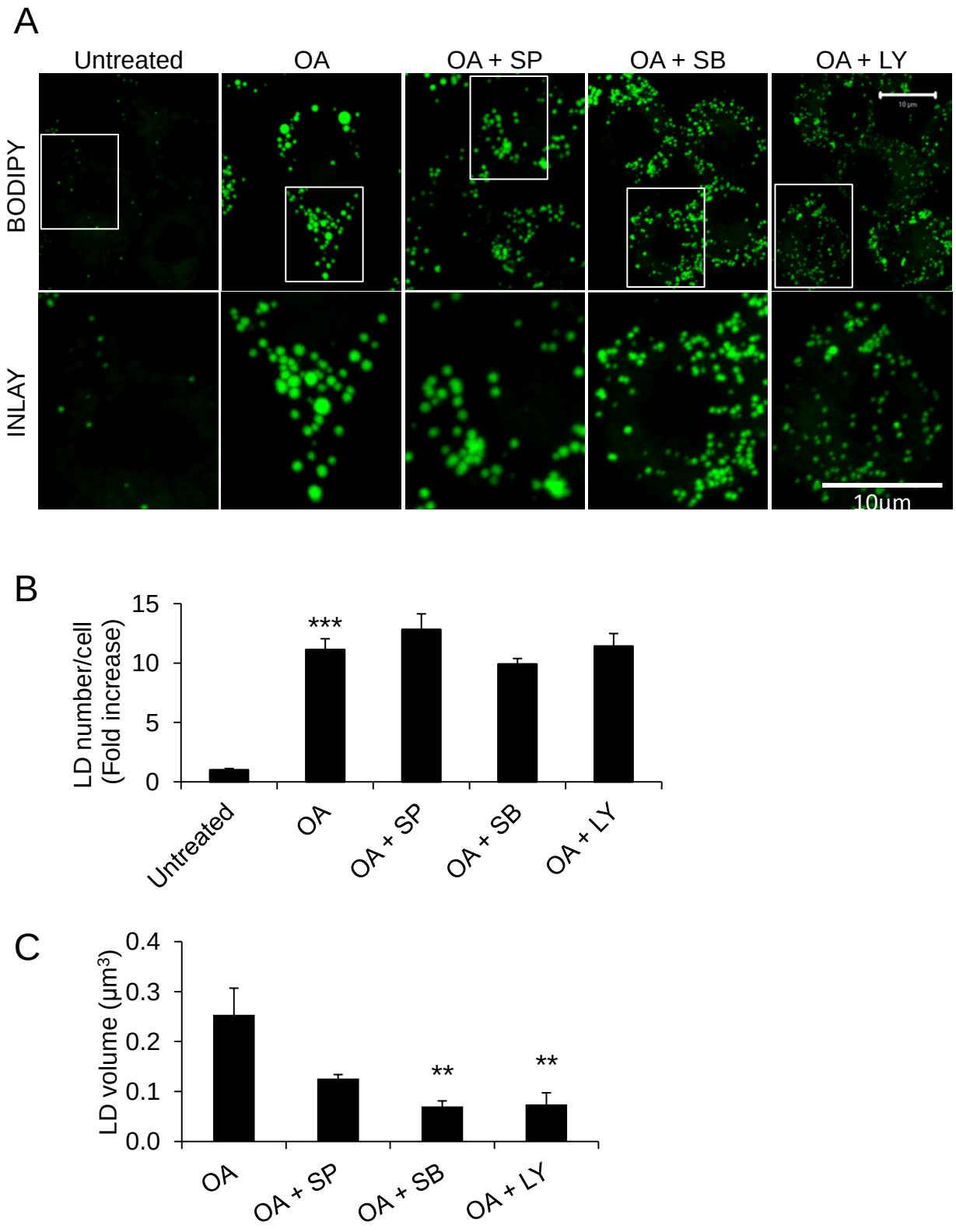
A
Untreated
OA
OA + SP
OA + SB
OA + LY
BODIPY
INLAY
10μm
B
LD number/cell
(Fold increase)
15
10
5
0
***
Untreated
OA
OA + SP
OA + SB
OA + LY
C
LD volume (μm³)
0.4
0.3
0.2
0.1
0.0
**
**
OA
OA + SP
OA + SB
OA + LY

Supplementary figure 3.5 SB203580 and LY294002 do not inhibit oleic acid-induced LDs but affect their sizes.

(A) Representative confocal micrographs of LDs in cells treated with OA (50 µM, 12h) in the presence or absence of SP600125 (10µM), SB203580 (10µM) and LY294002 (10 µM). Scale bar = 10 µm.

(B) Assessment of the number of LDs per cell. Bars indicate the average number of LD/cell expressed relative to the untreated group ± SEM from two independent experiments (n=4 per experiment). Statistically significant differences are indicated by *** ($p<0.005$).

(C) The inhibitors of p38 (SB203580) and PI3K (LY294002) reduce the size of OA-induced LDs. Individual LD volumes (μm^3) from at least 3 fields were measured and analyzed using the software Imaris. Bars show the mean LD volume ± SEM. Statistically significant differences are indicated by ** ($p<0.01$).

Connecting text between Chapter 3 and Chapter 4

In Chapter 3, our findings implied that the inflammatory response in LPS-stimulated microglia is due in part to specific changes in the biogenesis and proliferation of LDs, and also in the recruitment of cytosolic phospholipase A_2-α (cPLA_2-α) to LDs. In contrast, LDs induced under physiological conditions (e.g. by dietary fatty acid, oleic acid), did not harbour cPLA_2-α on their surface. This suggests that LDs may act as double-edged swords, playing either an inflammatory or non-inflammatory role, depending on the type of stimulus.

Some aspects of LD abundance, morphology and function have been recently studied in the mouse model of retinal degeneration and in activated BV-2 microglia. Activated microglia contained prominent LDs and analysis of the retinal lipid composition showed decreased docosahexaenoic acid (DHA) levels.

DHA, an n-3 polyunsaturated fatty acid that is abundant in the brain, is enriched in health-improving Mediterranean diets. Numerous *in vitro* and *in vivo* studies have demonstrated beneficial health effects of DHA to organisms experiencing pathological conditions accompanied by inflammation. Although dietary DHA has been shown to reduce the extent of neurodegeneration in a mouse model of retinal degeneration, the effect of this n-3 polyunsaturated fatty acid on the spatiotemporal dynamics of LDs and inflammation-related signaling cascades in LPS-stimulated microglial cells have not been investigated yet.

In Chapter 4, we will investigate how DHA impacts pro- and anti-inflammatory cellular processes in microglia.

CHAPTER 4

Docosahexaenoic acid (DHA): a modulator of lipid droplet proliferation and a facilitator of their interaction with mitochondria in hyperactive microglia

Dusica Maysinger*, Armen Khatchadourian*, Vincent R. Richard, Noura Al-Hajaj, Simon D. Bourque, Vladimir I. Titorenko

*: these authors contributed equally to this work

Submitted to NeuroMolecular Medicine

4.1 Abstract

Docosahexaenoic acid (DHA), an n-3 polyunsaturated fatty acid abundant in the brain and enriched in health-improving diets, is a potent immunomodulator. Although its beneficial effects in the nervous system have been reported, the mechanisms underlying these effects remain unclear. We have studied how DHA affects the inflammatory response in lipopolysaccharide (LPS)-stimulated microglia, the resident macrophage population in the central nervous system. Our findings implicate lipid droplets (LDs) as playing a key role in the amelioration by DHA of this glial response. The study focused on how DHA treatment of LPS-stimulated microglia (i) influences the size and number of LDs and expression of perilipin-2, an LD-associated protein; (ii) impacts the proximity of LDs to mitochondria and thereby their ability to alter mitochondrial metabolic activity; (iii) alters cellular lipidome; (iv) influences the recruitment of cytosolic phospholipase A_2-α (cPLA_2-α) to LD surface; (v) impinges on downstream protein components of the Toll-like receptor 4 (TLR4) signaling network; and (vi) affects the levels of inflammatory proteins secreted by microglial cells, levels which relate to the extent of nitric oxide release from microglia and to their phagocytic ability. Our findings suggest a model for a DHA-governed regulatory network that attenuates the inflammatory response in LPS-stimulated microglia. Overall, the DHA-initiated changes in LD dynamics and cellular lipidome weaken LPS-induced microglial activation by specifically altering mitochondrial metabolism and signaling, by modulating the flow of information through the TLR4 signaling network.

4.2 Introduction

A chronic activation of inflammation-related signaling cascades within cells eventually impairs physiological functions of multiple organs in the body (Goris et al., 1985). This activation can be averted or attenuated with the help of certain anti-inflammatory pharmaceuticals, and also of some healthy diets (Dinarello, 2010; Galland, 2010). Numerous *in vivo* studies have demonstrated beneficial effects of docosahexaenoic acid (DHA) and of its derivatives on organisms experiencing pathological conditions accompanied by inflammation (Hong et al., 2003; Raederstorff et al., 1996). DHA, an n-3 polyunsaturated fatty acid that is abundant in the brain, is enriched in health-improving Mediterranean diets (Dyall & Michael-Titus, 2008; Galland, 2010; Innis, 2007). However, clinical trials conducted to test effects of DHA on neurological disorders provided controversial data, likely due to the inherent complexity of these disorders, the diversity of populations used in these trials, and the different dosages and formulations and other confounding factors (Berson et al., 2004; Quinn et al., 2010).

The present study sought to investigate how DHA impacts pro- and anti-inflammatory cellular processes in microglia. These neural cells play a pivotal role in cerebral functions and act as major guardians of brains threatened by pathogens and the pro-inflammatory endotoxins they produce (Hughes, 2012). Microglial cells exhibit a striking functional plasticity and display a very low threshold of activation (Hanisch & Kettenmann, 2007). Although in the healthy central nervous system (CNS) microglia do not normally operate as macrophages, certain stimuli can convert them into macrophage-like cells able to perform immunological functions (Graeber, 2010). Lipopolysaccharide (LPS), an endotoxin produced by gram-negative bacteria, is one of the most potent of such stimuli (Nakamura et al., 1999). The activation of microglia by LPS is initiated by LPS binding to the two surface receptors, cluster of differentiation 14 (CD14) and Toll-like receptor 4 (TLR4) (Jack et al., 2005). LPS binding to these triggers an activating downstream signal to phosphatidylinositol 3-kinase (PI3-K) and to a serine/threonine-specific protein kinase called Akt (Saponaro et al., 2012). Downstream target of Akt is the forkhead box protein O1 (FOXO1), which is a key regulator of cell metabolism, cell cycle and cell death. Its activity is tightly regulated by the phosphoinositide-3-kinase-

AKT (PI3K-Akt) pathway. In addition to the transient Akt activation, the LPS-induced TLR4 pathway leads to an activation of c-Jun N-terminal kinase (JNK) and p38 (Guha & Mackman, 2001); DHA attenuates activation of both these protein kinases (Antonietta Ajmone-Cat et al., 2012; Xue et al., 2006). In LPS-stimulated microglial cells, DHA also inhibits nuclear import of the p65 protein component of the nuclear factor kappa-light-chain-enhancer of activated B cells (NFkB), thereby mitigating NFkB-driven transcription of genes encoding pro-inflammatory cytokines (Kang & Weylandt, 2008; Kong et al., 2010). Following their release by LPS-stimulated microglial cells, these pro-inflammatory cytokine proteins can act (if unopposed) on other microglia in a paracrine manner, and can also affect neurons (Hanisch, 2002). Furthermore, DHA has been demonstrated not only to inhibit the synthesis and release of pro-inflammatory cytokines but also to promote the production of neuroprotective anti-inflammatory cytokines (e.g. interleukin-10) and neuroprotectin D1 (Bazan, 2005; Neff et al., 2011), and to impair surface presentation of the LPS receptors CD14 and TLR4 (De Smedt-Peyrusse et al., 2008).

LDs are organelles found in almost all eukaryotic cells, and their number and size vary in different cell types (Farese & Walther, 2009; Martin & Parton, 2006). In the so-called “surveying” state, microglial cells exhibit only a few LDs, but their numbers significantly increase following cell exposure to microbial toxins (e.g. LPS) or unsaturated fatty acids (Ebert et al., 2009; Khatchadourian et al., 2012). Similarly, LDs are abundant in peripheral macrophages of animals and humans exposed to bacterial toxins and various other pro-inflammatory molecules (Bandeira-Melo et al., 2001; Pacheco et al., 2002). LDs consist of two major sub-compartments, a core filled with neutral lipids, mainly triglycerides (TGs) and cholesteryl esters, and a surrounding phospholipid monolayer, which contains free cholesterol and proteins (Murphy, 2001; Tauchi-Sato et al., 2002). The phospholipid composition of LDs is remarkably complex, with more than 160 molecular species of phospholipids: phosphatidylcholine (PC) and phosphatidylethanolamine (PE) are the most abundant classes (Bartz et al., 2007). A label-free quantitative method has revealed the existence of several classes of LDs, which markedly differ from each other with regard to size and lipid composition (Rinia et al., 2008).

A regulated lipolysis of the neutral core of LDs releases stored free fatty acids (FFAs), phospholipids and cholesterol, thereby providing energy via mitochondrial β-oxidation of FFA during times of nutrient deprivation, and both maintaining homeostasis of membrane lipids during cell growth and division and modulating the levels of free cholesterol inside and outside of the cell (Ducharme & Bickel, 2008; Guo et al., 2009; Martin & Parton, 2006). Moreover, recent studies have shown that LDs can serve both as an intracellular signaling compartment and an organizing platform for proteins (Welte, 2007). Physical interactions between LDs and other organelles (e.g. ER, mitochondria) have been previously reported (Murphy et al., 2009; Zehmer et al., 2009). It is suggested that these interactions may promote delivery of proteins and exchange of lipids between LDs and other cellular compartments (Welte, 2007; Zehmer et al., 2009).

A recent study showed that fully activated microglia in a mouse model of retinal degeneration contained a large number of LDs in them (Ebert et al., 2009). Although dietary DHA has been shown to reduce the extent of neurodegeneration in a mouse model of retinal degeneration and to suppress LD accumulation (Ebert et al., 2009), its effects on the spatiotemporal dynamics of LDs and inflammation-related signaling cascades in LPS-stimulated microglial cells have not yet been investigated. In this study we elucidated how the exposure of LPS-treated or non-stimulated (naïve) microglial cells to DHA (i) influences the size and number of LDs; (ii) affects the abundance of perilipin-2, a prominent LD-associated protein essential for LD growth and proliferation; (iii) impacts the proximity of LDs to mitochondria and mitochondrial metabolic activity; (iv) alters cellular lipidome; (v) influences the recruitment of cytosolic phospholipase 2 to LD surface promoted by LPS; and (vi) impinges on numerous downstream protein components of the TLR4 signaling network that modulates the neuroinflammatory effects induced by LPS. Based on our findings, we propose a model for a DHA-governed regulatory network that attenuates the inflammatory response in LPS-stimulated microglia.

4.3 Materials and methods

Cell culture and treatments. Murine microglia (N9) cells were seeded in Iscove's Modified Dulbeco's Medium (IMDM) (12440, Gibco) containing 5% fetal bovine serum (26140, Gibco) and1% penicillin–streptomycin (15140, Gibco). Cells were maintained at 37 °C in a humidified atmosphere containing 5% CO_2. Adherent cells were treated with lipopolysaccharides (LPS) (10 μg/ml) (Sigma, 62326), docosahexaenoic acid (DHA) (50 μM) (Nu-Chek Prep, U-84-A) and/or fluosphere polysterene microspheres (Microsph) (15 x $10^{\wedge 6}$ microspheres/ well) (Invitrogen, F13083) as described in the figure legends.

DHA/BSA complex preparation. DHA/BSA complex was prepared by adding 25 mg of DHA (Nu-Check Prep, U-84-A) to ~ 20 ml of fatty acid-free BSA (Sigma, A6003) solution (5% w/v, in KRBH buffer). The DHA/BSA solution was incubated for 5h at 37 °C. After the incubation, the pH of the solution was adjusted to pH 7.4 and the solution was filtered through a 0.22 μm filter. Non-esterified DHA concentration in the solution was determined with the NEFA C method kit (Wako). The final molar ratio of OA to BSA was approximately 6:1. Aliquots of the stock solution were flushed with argon to prevent oxidation of DHA and were stored at -80 °C.

Nitric oxide release. Nitric oxide released from treated cells was measured using Griess reagent (G4410, Sigma). Briefly, cells were seeded in 24-well plates (Sarstedt 83.1836) at a density of 2×10^5 cells/well. Following treatment, 50 μl of cell supernatant from each well were collected and transferred into 96 well plates. 50 μl of Griess reagent was added to each well and incubated at room temperature for 15 min. Absorbance of the produced nitrite was measured using spectrophotometer at 540 nm. In each experiment, a standard curve with different concentrations of nitrite (NO_2^-) was used to calculate the concentration of NO detected in the culture media.

Measurement of mitochondrial metabolic activity. Mitochondrial metabolic activity in treated cells was assessed by measuring the extent of MTT (thiazolyl blue tetrazolium bromide) (M2128, Sigma) reduction to formazan. Cells were seeded in 24-well plates (Sarstedt 83.1836) at a density of 5×10^4 cells/well. Following treatments, media was removed and replaced with serum-free media containing MTT (0.5 mg/ml). After 30 min

of incubation at 37° C, media was aspirated from each well and formazan crystals were dissolved in dimethylsulfoxide (DMSO) (154938, Sigma). The formazan obtained from the reduction of MTT was measured by using a Benchmark microplate reader (Bio-Rad, Canada) at 595 nm. All measurements were done in triplicates three or more times.

Enzyme-linked immunosorbent assays (ELISA). Cells were seeded in 24-well plates (3526, Costar) at a density of 1×10^5 cells/well. Production of TNF-α and IL-1β was assessed using commercial ELISA kits (SABiosciences). Briefly, following treatment the supernatants were collected and the amount of cytokine released into the media was quantified according to the supplier's protocol. Activity of Akt and p38 were determined using commercial ELISA assays (R & D, Minneapolis) according to the supplier's instructions. Results are expressed as mean ± SEM obtained from at least three independent experiments performed in triplicates.

Phagocytosis. Cells were seeded in 24-well plates (3526, Costar) at a density of 2×10^4 cells/well on coverslips (Fisher) coated with rat-tail collagen (Sigma, C7661). Following treatment, cells were washed with 1X PBS and nuclei were stained with Hoechst 33342 (H1399, Invitrogen) (10 µM, 10 min). Coverslips were mounted on glass microscope slides (Fisher Scientific, 12-550-143) using Poly aqua mount (Polysciences, 18606). Fluorescence micrographs were acquired with a Leica DFC350FX monochrome digital camera connected to a Leica DMI4000B inverted fluorescence microscope using a DAPI-1160A (Nuclei) and CY3 (Microsph) filters. Images were acquired in grey scale using Leica Application Suite (LAS). The average number of microspheres per cell was counted and analyzed using Image J software. Results are expressed as mean ± SEM obtained from at least three independent.

Confocal microscopy. Images were acquired with a Zeiss LSM 510 NLO inverted confocal microscope using a Plan Achromat 63X/1.4 Oil DIC objective. Microglial cells were seeded at a density of 1×10^4 cells/well in confocal chamber slides (Lab-Tek, Nalge Nunc International, Cat # 155411) or on coverslips at a density of 1.5×10^4 cells/well. Coverslips were mounted on glass microscope slides (Fisher Scientific, 12-550-14) using glycerol-free mounting media Vectashield H-1000 (Vector) and were sealed around the perimeter with clear nail polish. Images of BODIPY 493/503-labelled LDs were acquired

by using the Argon 488 nm excitation laser. Imaging of Mitotracker Deep Red 633-labelled mitochondria was done using HeNe 633 nm excitation laser. Alexa Fluor 594 (red) was detected using HeNe 543 excitation laser. All images were acquired at a resolution of 1024 × 1024 pixels and a zoom factor of at least 1.5. Z-stack images consisted of 15 to 20 optical slices and were taken at intervals of 0.3 μm (Z).

Lipid droplet staining. LDs in cells fixed with 4% paraformaldehyde were visualized with the neutral lipid staining fluorophores BODIPY 493/503 (4,4-difluoro-1,3,5,7,8-pentamethyl-4-bora-3a,4a-diaza-s-indacene) (Invitrogen, D-3922) or HCS LipidTOX ™ Deep red (Invitrogen, H34477). Stock solution of BODIPY 493/503 (4 mM) was made by dissolving the powder in DMSO. Cells were incubated with BODIPY 493/503 (20 μM, in PBS, 10 min) or with HCS LipidTOX (1:200 in PBS, 30 min). Cells were washed with PBS prior to confocal imaging.

Double labeling of mitochondria and LDs. Live microglial cells were incubated with Mitotracker Deep Red 633 (M22426, MP) (500 nM) for 3 min at 37 °C. After a wash with sterile PBS, cells were incubated with BODIPY 493/503 (prepared in cultured media, 20 μM) for 10 min at 37 °C. Cells were washed with PBS and then incubated in culture media during the imaging session.

Transmission electron microscopy. Microglial cells were treated with LPS, DHA or the two agents in combination as specified in Figure legend. Cells exposed only to the drug carrier (BSA in the cell culture medium) were used as controls. All samples were fixed (60 minutes) according to the procedure consisting of 1 % paraformaldehyde, 1,25 % glutaraldehyde, and 25 mg calcium chloride, in 0.1 M sodium cacodylate buffer at pH 7,4. After removal of fixatives cells were washed three times with phosphate saline buffer and embedded in Epon. Thin and ultrathin section were cut using microtome and analyzed by electron microscope (Joel 100/120kV) at different magnifications similar to common procedures (Holloway et al., 2011; Le Lay et al., 2010).

Lipidomic analysis. Lipid analysis was performed as previously reported (Bourque & Titorenko, 2009). Prior to lipid extraction, internal standards were added corresponding to each lipid class, lipids were then extracted from whole cells by a modified Bligh and

Dyer method, samples were dried under nitrogen and resuspended in chloroform. Immediately prior to injection the extracted lipids were combined with 2:1 methanol:chloroform with 0.1% (v/v) ammonium hydroxide. This was injected directly into a Q-TOF 2 mass spectrometer (Waters, Milford, MA) using a nano-ESI spray source at 1µl/min. Spectra were obtained in positive-ion mode ($PC+H^+$, $TAG+NH_4^+$) and negative-ion mode ($FFA-H^+$,$PA-H^+$,$PE-H^+$, $PG-H^+$, $PI-H^+$,$PS-H^+$,$CL-2H^+$). Acquired spectra were centroided using the Masslynx software then deconvoluted and deisotoped with excel macros.

Analysis of LD volume and number. Confocal images of fluorescently labeled LDs were analyzed using the software Imaris (Bitplane). LDs were visualized as point-like structures by selecting "Spots object". Prior to spot (i.e. LD) detection, the background of the image was subtracted. The threshold of spot detection was adjusted such that only spots associated with lipid droplets were considered in the analysis. The number, radius (µm), and volume (μm^3) of LDs were calculated by the software. A minimum of nine fields were analyzed in each treatment group. The average number of LDs per cell was calculated by dividing the apparent number of LDs in the field by the number of cells. The number of small (diameter < 0.5 µm), medium (diameter > 0.5 < 1.0 µm) and large (diameter > 1 µm) LDs in their different populations were determined using the histogram analysis in Microsoft Office Excel (2007).

Western Blot analysis. Whole cell extracts made by lysing the cells in NP-40 buffer (50 mM Tris pH 8.0, 137 mM NaCl, 1% NP-40, 10% glycerol) were supplemented with complete protease inhibitor cocktail (Roche Applied Science) (1 tablet per 25 ml of lysis buffer) and with phosphatase inhibitors sodium orthovanadate (1 mM) and sodium fluoride (1 mM). Cell lysates were boiled in 6 × sample buffer (12 % SDS, 30% glycerol, 0.2 % bromophenol blue, 12% 2-mercaptoethanol, 0.375 M Tris HCl pH 6.8) at a 5:1 (cell lysate : sample buffer) ratio for 5 min, and proteins were resolved by SDS-PAGE and then transferred (1h, 100V, in ice-cold transfer buffer) to nitrocellulose membranes (Hybond, Amersham Bioscience). Blocking of the membranes was performed by incubating them in 5% milk or BSA (in TBS-T). Membranes were incubated with primary antibodies to perilipin-2 (ADRP) (guinea pig polyclonal, Fitzgerald Ind. 20R-

AP002), perilipin- 3 (TIP47) (guinea pig polyclonal, Progen GP30), p38 (rabbit polyclonal) (1:500) (Santa Cruz, sc-535), phospho-p38 (rabbit monoclonal) (1:1000) (Cell Signaling #9215), actin (mouse monoclonal) (1:1000) (Millipore, MAB1501R) overnight at 4°C. Following incubation with primary antibodies, membranes were incubated with horse radish peroxidase-linked secondary antibodies anti-rabbit IgG (Amersham Biosciences, NA 934), anti-guinea pig IgG (Sigma, A5545) and anti-mouse IgG (GE Healthcare, NXA931). The binding of the secondary antibody to the primary antibody was visualized by using an ECL Plus detection kit and HyBlot autoradiography films (Denville). Films were scanned (greyscale at 16 –bits) and relative intensities of the immunoreactive bands were analyzed using the gel analyzer tool in the software Image J (1.42).

Immunocytochemistry of cPLA$_2$ and perilipin-2. Microglia were seeded at a density of 1.5 × 10^4 cells/well on coverslips (Fisher) coated with rat tail collagen (Sigma, C7661). Paraformaldehyde-fixed cells were permeabilized with Triton X-100 (0.1%) (Amersham Biosciences, # 17-1315-01) for 5 min and blocked with goat serum (10%) (Sigma, G9023) for 2h at room temperature. Immunostaining was performed by incubating the cells with a primary antibody recognizing cPLA$_2$-α (mouse monoclonal, 1:100) (Santa Cruz, sc-454, 4-4B-3C) or perilipin-2 (guinea pig polyclonal, 1:200) (Fitzgerald Industries #20R-AP002) at 4°C (overnight), followed by an incubation with goat anti-mouse (Invitrogen, A11005) or goat anti-guinea pig (Invitrogen, A11076) antibodies conjugated to Alexa Fluor 594. Coverslips were mounted on glass microscope slides (Fisher Scientific, 12-550-14) using glycerol-free mounting media Vectashield H-1000 (Vector).

Immunocytochemistry of RelA (p56) and FOXO1. Microglia were seeded at a density of 5 × 10^4 cells/well on coverslips (Fisher) coated with rat-tail collagen (Sigma, C7661). Paraformaldehyde-fixed cells were permeabilized with Triton X-100 (0.1%) (Amersham Biosciences, # 17-1315-01) for 5 min and blocked with goat serum (10%) (Sigma, G9023) for 75 min at room temperature. Immunostaining was performed by incubating the cells with a primary antibody recognizing RelA (P65) (rabbit monoclonal, 1:50) (Cell signaling, #4764S, C22B4) or FOXO1 (rabbit monoclonal, 1:250) (Cell signaling,

#2880S) at 4°C (overnight), followed by an incubation with goat anti-rabbit (Invitrogen, A11070) antibody conjugated to Alexa Fluor 488. Nuclei were stained with DRAQ5 (Immunochemistry technology, DR50050) (5 μM, 5 min). Coverslips were mounted on glass microscope slides (Fisher Scientific, 12-550-143) using Poly aqua mount (Polysciences, 18606).

Statistical analysis. All experiments were performed at least twice and all samples were analyzed in triplicates. Data are expressed as means +/- SEM and analyzed by ANOVA using Tukey's and Dunnett's post hoc test for multiple comparisons. Significant differences are indicated by * ($p < 0.05$), ** ($p < 0.01$) and *** ($p < 0.001$).

4.4 Results

DHA treatment causes proliferation of LDs and greatly elevates the level of perilipin-2

In this study we investigated changes occurring in LD number and size, and in LD dynamics, upon exposure of microglia to LPS or DHA or to the two agents in combination. LDs were detected by fluorescent labeling of living cells with the lipophilic dye BODIPY 493/503 (bright green), and were visualized using confocal laser scanning microscopy.

We found that although both LPS and DHA significantly increased the number of LDs in microglial cells, the increase was much more pronounced in cells exposed to DHA: a ~37-fold rise) in LD number/cell compared to a ~ 5-fold increase for LPS (Figure 4.1 A,B). Our reconstruction of the individual confocal Z-stack images of fluorescently labeled LDs and subsequent quantitation of LD volumes revealed that an exposure of microglial cells to DHA alone leads to a significant increase of the average volume of LDs (from 0.05 ± 0.011 μm^3 to 0.183 ± 0.02 μm^3, $p<0.001$), while treatment with LPS alone added a significantly lower increase (to 0.104 ± 0.016 μm^3, $p<0.01$) (Figure 4.1C).

Comparison of LD size distribution following LPS and DHA treatments revealed differences in the proportions of small (2r: <0.5 μm) and medium (2r: 0.5-1 μm)-sized LDs (Supplementary figure 4.1A). Treatment with LPS may have slightly reduced the relative abundance of small LDs (-14.9%, n.s) and concomitantly increased the proportion of medium-sized LDs (+13.2%, n.s) in microglial cells. However, exposure of these cells to DHA alone resulted in a significantly more dramatic reduction in the relative abundance of small LDs (-45.0%%; $p < 0.001$) and in a significantly more pronounced rise of medium-sized LDs (+42.2 %; $p < 0.001$). Notably, our electron microscopical analysis clearly demonstrated that these medium-sized LDs in microglial cells exposed to DHA actually represent aggregates of small-sized LDs (Figure 4.2).

Perilipin-2 (formerly known as ADRP) and perilipin-3 (formerly known as TIP47) are LD-associated proteins essential for LD growth and proliferation (Bulankina et al., 2009; Imamura et al., 2002). An exposure of macrophages and microglial cells to LPS added alone led to a rise in the level of perilipin-2 and caused the accumulation of LDs (Feingold et al., 2010; Khatchadourian et al., 2012). We performed western blotting to compare how LPS and DHA influence the levels of perilipin-2 and -3 in microglial cells. DHA added alone elevated the level of perilipin-2 to a significantly higher extent (~17 fold; $p < 0.001$) than that observed in microglial cells exposed to LPS (~3 folds; $p < 0.05$) (Figure 4.1D,E). In contrast, neither DHA nor LPS caused a significant change in the level of perilipin-3 in microglial cells. Immunocytochemical analysis of perilipin-2 in microglia showed that the protein is confined to LDs and that its expression is increased following treatment with LPS or DHA (Supplementary figure 4.2). However, the pattern of immunopositive signal was different: in DHA, but not LPS-treated cells, perilipin-2 was more diffuse in DHA-treated cells than in cells exposed to LPS.

The effects of DHA on the number of LDs, their volumes and their size distribution, as well on the abundance of perilipin-2, were stronger than those caused by LPS. Indeed, an exposure of microglia to the mixture of DHA and LPS yielded a DHA-like pattern (but not an LPS-like pattern) of changes for each of these hallmark features of LD dynamics (Figure 4.1A-E).

DHA suppresses the LPS-induced increase in the distance between LDs and mitochondria and elevates mitochondrial metabolic activity

LDs have been previously shown to form membrane contact sites with different organelles, including mitochondria (Goodman, 2008; Jagerstrom et al., 2009). These close contact sites are known to facilitate the coupling of triglyceride (TGs) hydrolysis in LDs to fatty acid β-oxidation in mitochondria, thereby promoting mitochondrial ATP production. The substantial changes in the number, volume and size distribution of LDs that we observed in microglial cells exposed to LPS and to DHA, or to their mixture, prompted us to examine possible associated changes in the extent of physical contacts between LDs and mitochondria also.

Using confocal fluorescence microscopy of BODIPY 493/503-labeled LDs and Mitotracker-visualized mitochondria, we found that these two organelles are closely apposed to each other in microglial cells exposed to DHA or to DHA and LPS combined, but not to LPS alone (Figure 4.2A). Our electron microscopical analysis of untreated microglial cells validated this conclusion by revealing that only a small number of small LDs in these cells are located in the vicinity (often at distances < 300 nm) of mitochondria .

Exposure of microglial cells to LPS added alone led to a significant increase in this distance (Figure 4.2B,C), but in contrast, DHA treatment did not. Of note, mitochondria in untreated cells exhibited extensive and regularly occurring cristae (Figure 4.2B); this arrangement of cristae was impaired by LPS treatment but not by DHA (Figure 4.2B). Electron microscopical analysis revealed another interesting result; the medium-sized LDs detected by confocal microscopy in cells exposed to DHA were actually aggregates of small-sized LDs (Figure 4.2B).

It should be stressed that mitochondrial metabolic activity in microglial cells inversely correlated with the distance between LDs and mitochondria and was proportional to the extent of regularity in mitochondrial cristae arrangement. Exposure of these cells to LPS alone resulted in a significant reduction of mitochondrial metabolic

activity (Figure 4.2D), while DHA treatment alone led to an increase in mitochondrial metabolic activity (Figure 4.2D). It is conceivable that the increased mitochondrial metabolic activity seen in DHA treated cells was due to the observed ability of this anti-inflammatory agent to elevate the levels of various molecular forms of cardiolipin (Supplementary figure 4.3), a signature lipid of the inner mitochondrial membrane known to play a pivotal role in regulating a number of essential cellular processes (Osman et al., 2009; Osman et al., 2011).

Overall, an exposure of microglia to the mixture of DHA and LPS yielded a DHA-like pattern (but not an LPS-like pattern) of mitochondrial morphology (i.e. the cristae arrangements) and function (i.e. mitochondrial metabolic activity).

LPS and DHA alter the lipidome of microglial cells

Because exposure of microglial cells to LPS or DHA, separately or as a mixture, altered the dynamics of LDs, a depot of neutral lipids, and elevated the level of cardiolipin in the inner mitochondrial membrane, we used a quantitative mass spectrometric analysis to examine possible changes in microglial lipidome following such an exposure.

Our mass spectrometry-based quantification of changes in the lipidome of microglial cells treated only with LPS revealed significantly increased total levels of free fatty acids (FFAs) (Figure 4.3A), especially of their 16:1, 16:0, 18:1, 18:0 and 22:6 molecular forms (Figure 4.3B). Unlike LPS treatment, a treatment of microglial cells with DHA added alone did not lead to an increase in total levels of FFAs (Figure 4.3A) or their 16:1, 16:0 and 18:1 species (Figure 4.3B). This effect of DHA was epistatic (dominant over) to that caused by LPS. Indeed, an exposure of microglia to the mixture of DHA and LPS yielded a DHA-like pattern (but not an LPS-like pattern) of changes for total levels of FFAs (Figure 4.3A) and for the levels of their 16:1, 16:0 and 18:1 species (Figure 4.3B). However, akin to the effect of LPS treatment, a treatment of microglial cells with DHA alone caused only a moderate though significant increase in the level of the 18:0 molecular form of FFAs (Figure 4.3B). Furthermore, an exposure of microglial

cells with DHA, a C22:6 form of FFAs, added alone or together with LPS led to a rise in its cellular level (Figure 4.3B).

Our mass spectrometric quantification of the lipidome of microglia cells exposed to LPS alone did not reveal significant changes in total levels of the phospholipids phosphatidylserine (PS) (Figure 4.3C), phosphatidylcholine (PC), phosphatidylethanolamine (PE), phosphatidylinositol (PI), phosphatidic acid and phosphatidylglycerol (data not shown). However, the total level of PS was significantly increased in microglial cells treated with DHA, added alone or together with LPS (Figure 4.3C). The only three molecular forms of PS (out of its 23 forms detected by mass spectrometry) that displayed such a pattern in DHA- and DHA/LPS-treated microglial cells were the following species of PS: (i) C34:0 (*i.e.*, a PS form carrying the C16:0-C18:0 acyl chains); (ii) C36:0 (*i.e.*, a PS form carrying the C18:0-C18:0 acyl chains); and (iii) C40:6 (*i.e.*, a PS form carrying the C18:0-C22:6 acyl chains; the C22:6 polyunsaturated fatty acid chain originates from DHA) (Figure 4.3D). According to our quantitative lipidomic analysis, these three molecular forms of PS constituted more than 80% of its total cellular membrane pool, while each of the other 20 molecular species of PS was present at 1% of the total pool of this membrane phospholipid. Noteworthy, despite PC, PE and PI being much more abundant phospholipid constituents of cellular membranes than PS, their total levels were not altered in DHA- and DHA/LPS-treated cells (data not shown). The total levels of other membrane phospholipids, PA and PG, also remained unaltered in microglial cells exposed to DHA, added alone or together with LPS (data not shown).

Our mass spectrometry-based quantitation of changes in the lipidome of microglial cells treated only with LPS revealed significantly increased total levels of TGs (Figure 4.3E), especially of their 52:2 and 54:3 molecular forms (Figure 4.3F). Unlike LPS treatment, a treatment of microglial cells with DHA alone did not lead to an increase in total levels of TGs (Figure 4.3E) or their 52:2 and 54:3 species (Figure 4.3F).

DHA modulates a pro-inflammatory signaling network that governs LPS-stimulated inflammation in microglial cells

Our recent study demonstrated that the stimulation of LD proliferation observed in microglial cells exposed to the pro-inflammatory endotoxin LPS relies on the transient activation of serine/threonine-specific protein kinase Akt and p38 MAPK (Khatchadourian et al., 2012). These protein kinases are essential components of the TLR4 signaling network that governs LPS-stimulated inflammation in microglial cells (Barton & Medzhitov, 2003; Bauerfeld et al., 2012). Because the present study revealed that an exposure of microglial cells to separately added LPS and DHA or to their mixture alters the dynamics of LDs, we investigated how DHA (added alone or together with LPS) influences protein kinase activities of Akt and p38 and the extent of p38 phosphorylation. Our ELISA-based quantitative protein kinase assay revealed that an exposure of microglial cells to LPS alone causes a transient increase in activities of both Akt and p38, with both protein kinase activities reaching a maximum at 15 min post LPS addition (Figure 4.4A,B). It should be emphasized that an overnight pre-treatment of microglial cells with DHA prevented such LPS-driven transient activation of Akt and p38 (Figure 4.4A,B). We also found that an exposure of microglial cells to DHA alone promoted a significantly more moderate and less lasting increase in the extent of dual (*i.e.*, Thr180/Tyr182) phosphorylation of p38 than that observed in microglial cells exposed to LPS alone (Figure 4.4C). Moreover, an overnight pre-treatment of microglial cells with DHA prevented such LPS-driven rise in the extent of p38 dual phosphorylation (Figure 4.4D).

It should be stressed that the observed effects of DHA (added alone or together with LPS) on the Akt and p38 upstream components of the TLR4 signaling network governing LPS-stimulated inflammatory processes in microglial cells are likely to underlie the effects of this n-3 polyunsaturated fatty acid on several essential processes downstream of this pro-inflammatory network, as outlined below.

Next, we examined the the recruitment of cytosolic phospholipase A_2 -α (cPLA_2-α) from the cytosol to the surface of LDs, where it is required for the release of arachidonic acid which is then converted into potent inflammatory mediators such as prostaglandins and

leukotrienes (Khatchadourian et al., 2012). In contrast to LPS, DHA did not trigger the recruitment of $cPLA_2$-α from the cytosol to the surface of LDs if added alone (Figure 4.5A). If added together with LPS, DHA suppressed such LPS-driven attachment of cytosolic $cPLA_2$-α to the LD surface (Figure 4.5A), where it is required for the formation of arachidonic acid, known to be then converted into such potent inflammatory mediators as prostaglandins and leukotrienes. In fact, about 33% of LDs were $cPLA_2$-α positive in LPS-stimulated microglia, and only 5% of LD were $cPLA_2$-α positive when DHA was added together with LPS.

We continued investigating how DHA impacted TLR4-initiated pro-inflammatory signaling by examining the nuclear/cytosolic distribution of NFκβ and FOXO1, two essential transcription factors operating downstream of the TLR4 signaling network, the production and secretion of inflammatory proteins and metabolites, and the phagocytic activity of microglial cells. Unlike LPS, DHA did not trigger the characteristic inflammation and subsequent release of NO by microglia (Figure 4.5D). However, added together with LPS, DHA significantly reduced the extent of NO synthesis and secretion by LPS-stimulated microglial cells. In contrast to LPS, DHA (added alone) did not stimulate a synthesis and subsequent secretion by microglia of the inflammatory cytokines TNF-α and IL1β, a hallmark event of the inflammatory process (Figure 4.5E, F). When added together with LPS, however, DHA caused a moderate but significant reduction in the LPS-stimulated production and secretion of TNF-α and IL1β by microglial cells.

Finally, unlike LPS, DHA did not stimulate the phagocytic activity of microglial cells if added alone (Figure 4.5G), but added together with LPS, it caused a reduction of phagocytosis (Figure 4.5G).

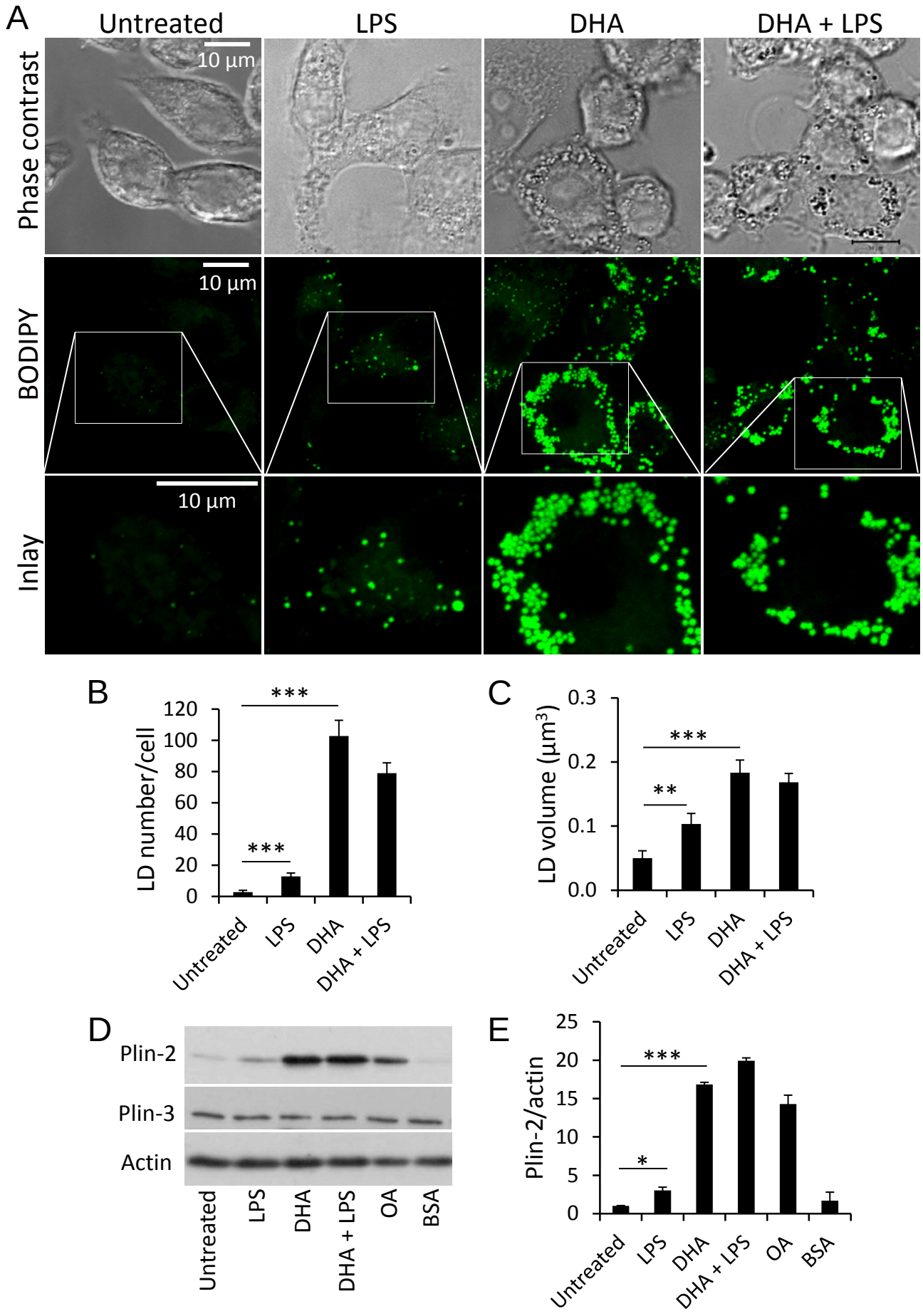
A
Untreated
LPS
DHA
DHA + LPS
Phase contrast
BODIPY
Inlay
10 µm
B
LD number/cell
***
***
Untreated
LPS
DHA
DHA + LPS
C
LD volume (µm³)
***
**
D
Plin-2
Plin-3
Actin
Untreated
LPS
DHA
DHA + LPS
OA
BSA
E
Plin-2/actin
***
*

Figure 4.1 Effect of LPS and DHA on LD formation, size and expression of LD-associated proteins.

(A) Confocal micrographs of LDs in microglia treated with LPS (10 μg/ml) and DHA (50 μM), alone or in combination, for 9h. Z-stack images of BODIPY 493/503-labelled LDs (green) were obtained from 20 optical slices (top row + inlay in middle row). Cells were imaged by differential interference contrast (bottom row). Scale bar = 10 μm.

(B) Quantification of number of LDs in cells treated with LPS and DHA as described in Figure 4.1A. Bar graphs show mean number of LDs per cell (LD/cell) ± standard error the means (SEM) calculated from two independent experiments. Statistically significant differences are indicated by *** ($p<0.001$).

(C) LD volume in microglia exposed to LPS, DHA, or LPS + DHA. Bar graphs show average LD volumes (μm^3) ± SEM. Statistically significant differences are indicated by ** ($p<0.05$) or *** ($p<0.001$).

(D) Immunoblotting of perilipin-2 and perilipin-3 in DHA and/or LPS – treated cells. Cells were treated as described in Figure 4.1A. Oleic acid (OA) (50 μM, 9h) treatment served as a positive control to induce perilipin-2 expression. Actin (43 kDa) was used as a loading control.

(E) Quantification of perilipin-2 signal from western blots shown in Figure 4.1D. Bar graphs represent the average (fold) increase in the signal of perilipin-2 (± SEM) expressed relative to the untreated group. Statistically significant differences are indicated by * ($p<0.05$) or *** ($p<0.001$).

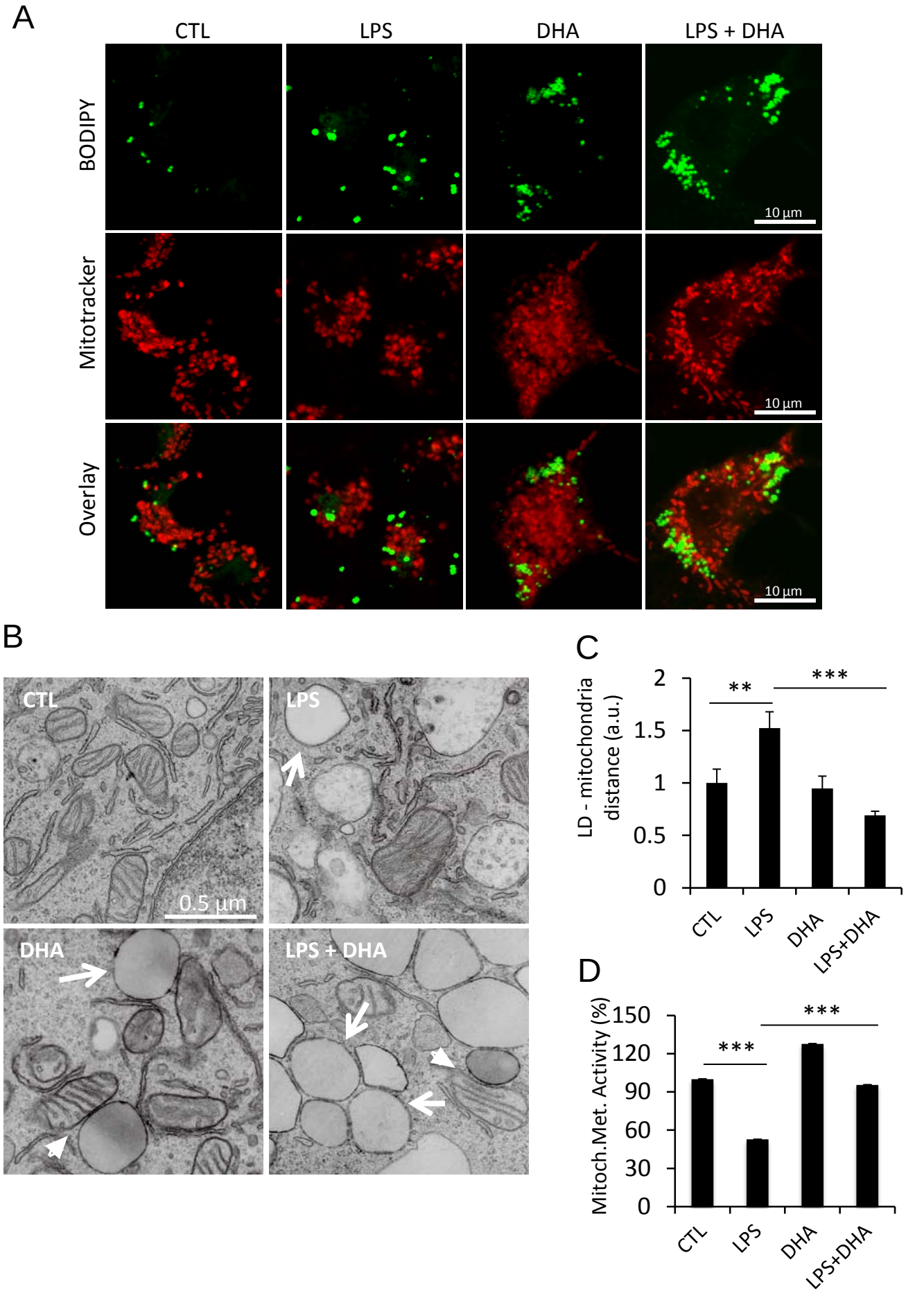
A
CTL
LPS
DHA
LPS + DHA
BODIPY
Mitotracker
Overlay
10 µm
10 µm
10 µm
B
CTL
LPS
DHA
LPS + DHA
0.5 µm
C
LD - mitochondria distance (a.u.)
2
1.5
1
0.5
0
**
***
CTL
LPS
DHA
LPS+DHA
D
Mitoch.Met. Activity (%)
150
120
90
60
30
0
***
***
CTL
LPS
DHA
LPS+DHA

Figure 4.2 Spatial and functional relationship between LD and mitochondria following LPS and DHA treatment.

(A) Confocal micrographs showing the effect of DHA and LPS on the cellular distribution of LDs (green) and mitochondria (red). Cells were left untreated (control) or treated with LPS (10μg/ml), DHA 50 (μM), or LPS + DHA for 9h. Cells were washed and stained with BODIPY 493/503 and Mitotracker Deep Red 633 sequentially. Mitochondria and LDs were detected by confocal microscopy. Images represent Z-stacks of 10 slices acquired at 0.3 μm intervals. Scale bar, 10 μm.

(B) Representative electron micrographs of microglia left untreated or treated with LPS, DHA, or LPS + DHA. Arrows indicate LDs; arrowhead points to closely apposed LD and mitochondria. Scale bar = 500 nm.

(C) Average distance (expressed as a.u) between LDs and mitochondria in untreated (control) and treated microglia. Distances were calculated using the EM pictures. Statistically significant differences are indicated by ** ($p<0.01$) and *** ($p<0.001$).

(D) Mitochondrial metabolic activity in LPS, DHA or LPS + DHA- treated cells as determined by the MTT reduction assay. Bar graphs show mean mitochondrial metabolic activity (± SEM) expressed as percentages (%) and relative to the value in untreated cells. Note the increased metabolic activity with DHA, which is counteracted by LPS. Statistically significant differences are indicated by *** ($p<0.001$)

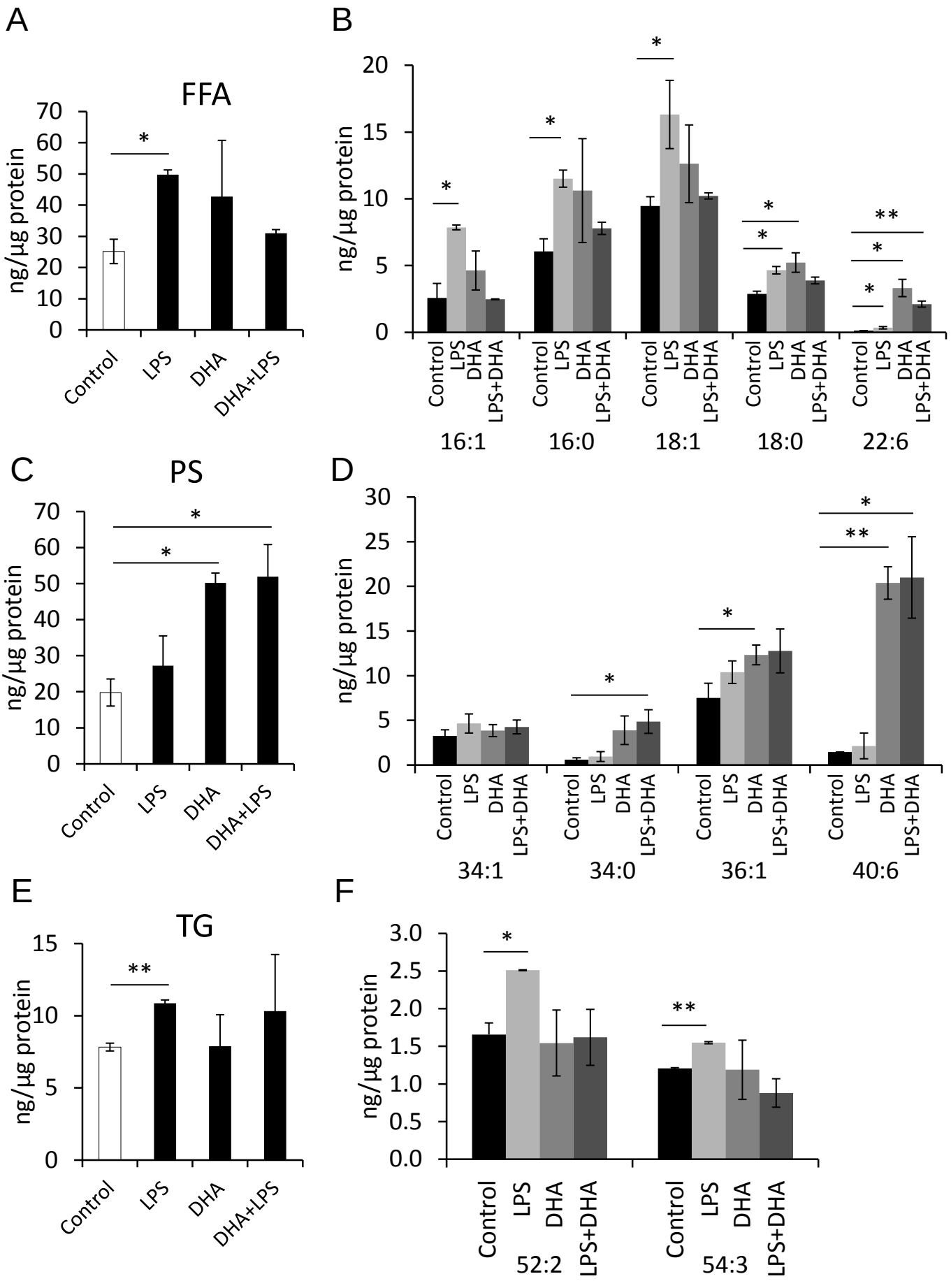
A
FFA
ng/µg protein
70
60
50
40
30
20
10
0
*
Control
LPS
DHA
DHA+LPS
B
ng/µg protein
20
15
10
5
0
*
**
Control
LPS
DHA
LPS+DHA
16:1
16:0
18:1
18:0
22:6
C
PS
ng/µg protein
70
60
50
40
30
20
10
0
*
Control
LPS
DHA
DHA+LPS
D
ng/µg protein
30
25
20
15
10
5
0
*
**
Control
LPS
DHA
LPS+DHA
34:1
34:0
36:1
40:6
E
TG
ng/µg protein
15
10
5
0
**
Control
LPS
DHA
DHA+LPS
F
ng/µg protein
3.0
2.5
2.0
1.5
1.0
0.5
0.0
*
**
Control
LPS
DHA
LPS+DHA
52:2
54:3

Figure 4.3 Effect of DHA and LPS on different molecular lipid species in microglia.

Microglia were treated with LPS (10 μg/ml) and DHA (50 μM) for 9h and lipid species were measured by ESI-MS.

(A) Measurement of total cellular FFA following treatments. Bar graphs represent the average cellular content of total FFA (ng/μg of protein) ± SEM. Statistically significant differences are indicated by * ($p<0.05$).

(B) Cellular levels of individual FFA species: 16:1, 16:0, 18:1, 18:0 and 22:6 following treatments. Statistically significant differences are indicated by * ($p<0.05$) or ** ($p<0.01$).

(C) Cellular levels of total phosphatidylserine (PS) following treatments. Bar graphs represent the average total content of PS (ng/μg of protein) ± SEM. Statistically significant differences are indicated by * ($p<0.05$).

(D) Levels of selected PS species (34:1, 34:0, 36:1 and 40:6) following treatments. Statistically significant differences are indicated by * ($p<0.05$) or ** ($p<0.01$).

(E) Total triglyceride (TG) content following treatments. Statistically significant differences are indicated by **$p<0.01$.

(F) Levels of selected TG species (52:2 and 54:3) following treatments. Statistically significant differences are indicated by * ($p<0.05$) or ** ($p<0.01$).

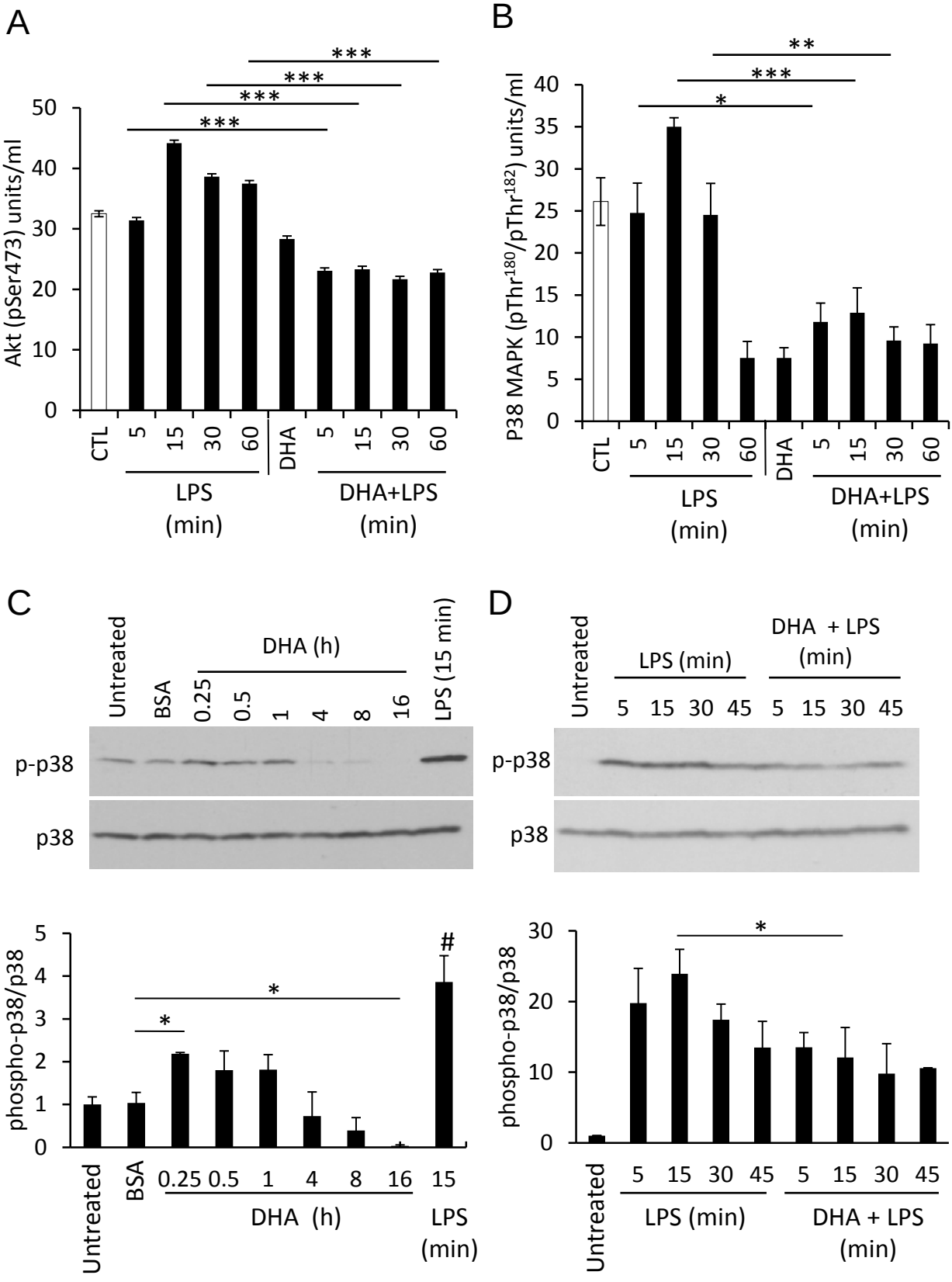
A
Akt (pSer473) units/ml
50
40
30
20
10
0
***
***
***
***
CTL
5
15
30
60
DHA
5
15
30
60
LPS
(min)
DHA+LPS
(min)
B
P38 MAPK (pThr180/pThr182) units/ml
40
35
30
25
20
15
10
5
0
**
***
*
CTL
5
15
30
60
DHA
5
15
30
60
LPS
(min)
DHA+LPS
(min)
C
Untreated
BSA
DHA (h)
0.25
0.5
1
4
8
16
LPS (15 min)
p-p38
p38
phospho-p38/p38
5
4
3
2
1
0
*
*
#
Untreated
BSA
0.25 0.5 1 4 8 16
DHA (h)
15
LPS
(min)
D
Untreated
LPS (min)
DHA + LPS
(min)
5 15 30 45 5 15 30 45
p-p38
p38
phospho-p38/p38
30
20
10
0
*
Untreated
5 15 30 45
LPS (min)
5 15 30 45
DHA + LPS
(min)

Figure 4.4 Effect of LPS and DHA on Akt activity and p38 activity and phosphorylation in microglia

(A) Phosphorylated Akt (pSer473) concentration and (B) Phosphorylated P38 MAP Kinase (pThr180/pThr182) concentration was measured using respective ELISA kit in cells pretreated with or without DHA (50 µM, overnight) and treated with LPS (10 µg/ml, 5-60 min). Following supplier established ELISA assay, concentration of Akt (pSer473) and P38 MAP Kinase (pThr180/pThr182) was calculated from their respective standard curves and expressed in units/ml. Bars represent mean values ± SEM (n=6). White bars represent control (CTL) non treated cells. Statistically significant differences are indicated by * ($p<0.05$), ** ($p<0.01$) and *** ($p<0.001$).

(C) Western blot analysis of phosphorylated p38 (p-p38) in DHA-treated cells. Cells were left untreated or treated with BSA (0.1%), DHA (50 µM) (for 15, 30, 60 min, 4h, 8h, and 16h) and LPS (10 µg/ml, 15 min). Phospho-p38/p38 is expressed as fold increase over the untreated group. Quantification of the western blots was performed by densitometric analysis using Image J. Bars represent mean values ± SEM (n=2). Statistically significant differences are indicated by * ($p<0.05$, compared with BSA group) and # ($p<0.05$, compared with untreated group).

(D) Western blot analysis of phosphorylated p38 in LPS-stimulated microglia in the presence or absence of DHA. After overnight (16h) incubation with DHA (50 µM), cells were treated with LPS (10 µg/ml) for 5, 15, 30, and 45min. p-p38/p38 is expressed as fold increase over the untreated group. Bars represent mean values ± SEM (n=2). Statistically significant differences are indicated by * ($p<0.05$) and *** ($p<0.001$).

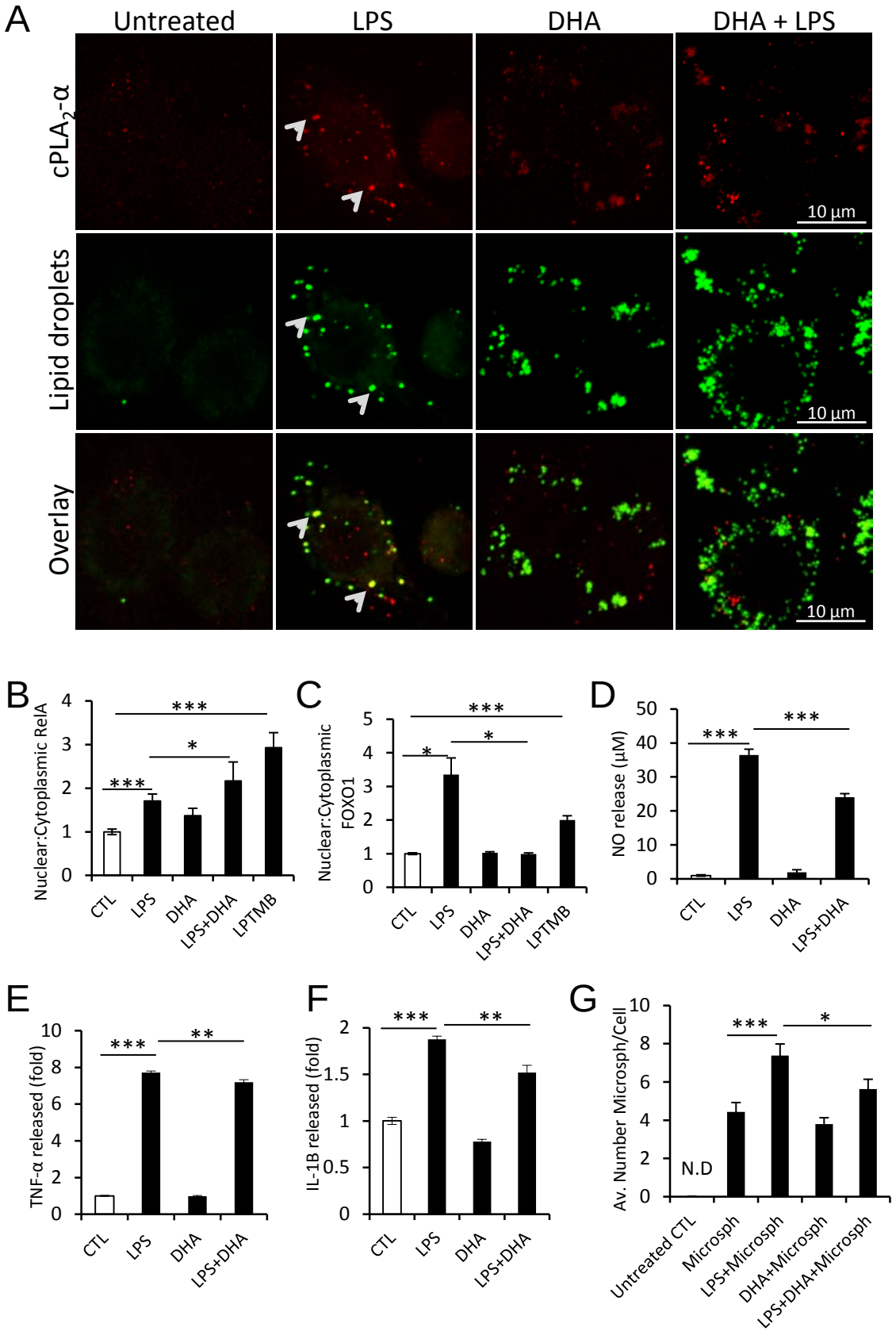
A
Untreated
LPS
DHA
DHA + LPS
cPLA2-α
Lipid droplets
Overlay
10 µm
B
Nuclear:Cytoplasmic RelA
CTL
LPS
DHA
LPS+DHA
LPTMB
C
Nuclear:Cytoplasmic FOXO1
D
NO release (µM)
E
TNF-α released (fold)
F
IL-1B released (fold)
G
Av. Number Microsph/Cell
N.D
Untreated CTL
Microsph
LPS+Microsph
DHA+Microsph
LPS+DHA+Microsph

Figure 4.5 Effect of DHA on $cPLA_2$-α recruitment to LDs, translocation of NFKB (RelA) and FOXO-1, cytokine release, nitric oxide release, and phagocytic activity in LPS-stimulated microglia

(A) Cellular distribution of $cPLA_2$-α in LPS and DHA-treated microglia. Confocal Z-stack images show immunostained $cPLA_2$-α (red) and LipidTOX™ -labeled LDs (green) in LPS (10 μg/ml, 9h) and/or (DHA 50 μM, 9h) - treated cells. Z-stack images were obtained from 10 optical slices at 0.3 μm intervals. Note the colocalizing regions between $cPLA_2$-α and LDs (white arrows) in LPS-treated microglia. Scale bar, 10 μm.

(B) Nuclear translocation of RelA (P65) in microglia treated with LPS (10 μg/ml, 1hr) and DHA (50 μM, 1 hr) alone or both together for 1hr. Leptomycin b (LPTMB, 40 nM, 3 hr) was used as a positive control for nuclear translocation. Relative fluorescence intensities were measured using image analysis software (ImageJ) and the ratio of nuclear to cytoplasmic mean grey intensities were plotted. Bars represent mean values ± SEM (n=18). White bars represent control (CTL) non treated cells. Statistically significant differences are indicated by * ($p<0.05$) and *** ($p<0.001$).

(C) Nuclear translocation of FOXO1 in microglia cells treated with LPS (10 μg/ml, 1hr) and DHA (50 μM, overnight) alone or both together. Leptomycin b (LPTMB, 40 nM, 3 hr) was used as a positive control for nuclear translocation. Relative fluorescence intensities were measured using image analysis software (ImageJ) and the ratio of nuclear to cytoplasmic mean grey intensities were plotted. Bars represent mean values ± SEM (n=18). White bars represent control (CTL) non treated cells. Statistically significant differences are indicated by * ($p<0.05$) and *** ($p<0.001$).

(D) Nitric oxide (NO) released from microglia cells treated with LPS (10 μg/ml, 24hr) and DHA (50 μM, 24hr) alone or both together was measured using Griess reagent (n=9). Bars represent mean values ± SEM (n=18). White bars represent control (CTL) non treated cells. Statistically significant differences are indicated by *** ($p<0.001$).

(E) Tumor necrosis factor-alpha (TNF- α) and (F) Interleukin 1-beta (IL1-β) cytokines released from microglia cells treated with LPS (10 μg/ml, 24hr) and DHA (50 μM, 24hr) alone or both together was measured using respective ELISA kit (n=9) and expressed as

fold change with respect to untreated cells (CTL) that were set to 1. Bars represent mean values ± SEM (n=18). White bars represent control (CTL) non treated cells. Statistically significant differences are indicated by ** ($p<0.01$) and *** ($p<0.001$).

(G) Average number of Microspheres per cell was analyzed from fluorescent images of microglia cells pre-treated with LPS (10 µg/ml, 3hr) and/or DHA (50 µM, overnight) alone or both together followed by treatment with fluorescent microspheres (Microsph) ($15 \times 10^{\wedge 6}$ microspheres/well, 3hr). N.D=non- detectable number of microspheres for untreated cells. Bars represent mean values ± SEM (n=12). Statistically significant differences are indicated by * ($p<0.05$) and *** ($p<0.001$).

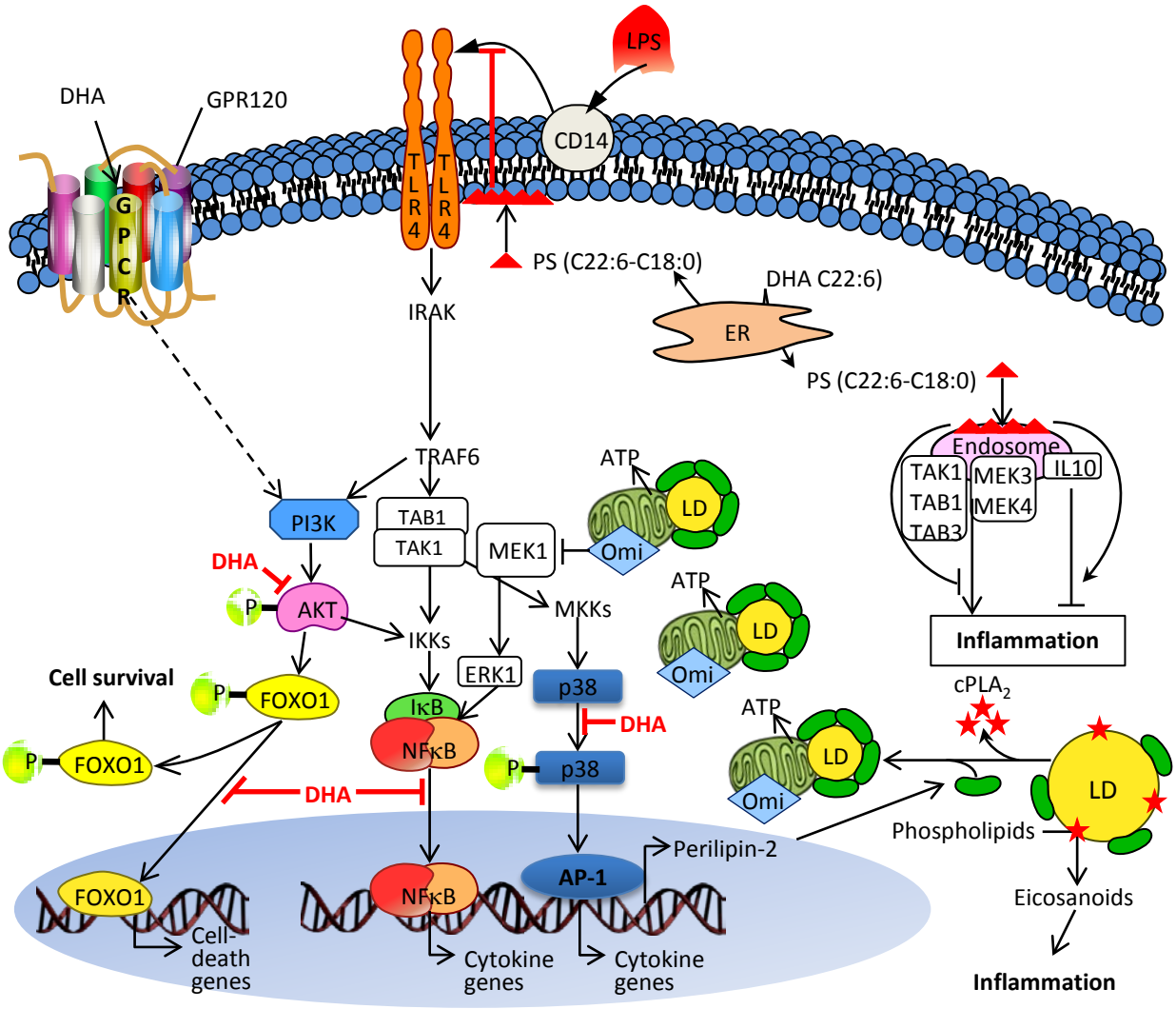
LPS
DHA
GPR120
CD14
TLR4
TLR4
GPCR
PS (C22:6-C18:0)
DHA C22:6)
ER
PS (C22:6-C18:0)
IRAK
TRAF6
Endosome
TAK1
TAB1
TAB3
MEK3
MEK4
IL10
ATP
LD
Omi
PI3K
TAB1
TAK1
MEK1
DHA
P
AKT
IKKs
MKKs
ERK1
p38
Inflammation
Cell survival
FOXO1
IκB
NFκB
DHA
cPLA2
Phospholipids
Perilipin-2
AP-1
Eicosanoids
Cell-death genes
Cytokine genes
Cytokine genes
Inflammation

Figure 4.6. Schematic illustration showing the mechanisms underlying the anti-inflammatory properties of DHA.

Our model proposes that both a direct activation by DHA of its G-protein coupled receptor GPR120 and an indirect modulation of the TLR4/CD14 signaling network (by PS species induced following DHA treatment and then delivered to the PM), are responsible for the anti-inflammatory effects triggered by DHA on several key downstream protein components of this signaling network known to modulate LPS-induced neuroinflammation. The direct and indirect action of DHA causes these anti-inflammatory effects in naïve and LPS-stimulated microglia by reducing protein kinase activities, thereby altering the extent of phosphorylation and causing redistribution between the nucleus and cytoplasm for several proteins downstream in the TLR4/CD14 signaling network. DHA also promotes the massive fragmentation of larger LDs into small and medium size LDs rich in perilipin-2. $cPLA_2$-α is recruited to the LD surface in response to microglia treatment with LPS leading to the release of arachidonic acid from LD phospholipids. The enrichment of DHA phospholipid species significantly weakens the association of $cPLA_2$-α with the surface of LDs, thereby stimulating a release of this phospholipase to the cytosol. The removal of $cPLA_2$-α molecules from the surface of LDs impairs the release of arachidonic acid and, therefore, their subsequent cyclooxygenase-dependent conversion into such potent inflammatory mediators as prostaglandins and leukotrienes.

4.5 Discussion

This study provides evidence that DHA exhibits profound effects on the spatiotemporal dynamics of numerous essential pro- and anti-inflammatory cellular processes in both non-stimulated and LPS-stimulated microglia. Our findings suggest a model (Figure 4.6) for a complex DHA-governed regulatory network that attenuates the inflammatory response in LPS-stimulated microglia by modulating and integrating these various inflammation-related cellular processes.

In our model, DHA promotes the proliferation of small and medium size LDs. Our data suggest that the greatly elevated level of perilipin-2 in microglial cells exposed to DHA and the subsequent recruitment of this key regulator of LD biogenesis and proliferation to the surface of LDs drives this observed proliferation of organelles. The insertion of numerous perilipin-2 molecules into the phospholipid monolayer enclosing LDs is likely to cause a massive fragmentation of large LD into small- and medium-sized LDs in DHA-treated microglial cells. Our findings suggest at least two important outcomes of such LD fragmentation triggered by DHA.

First, there is a significant reduction of the surface area of individual LDs upon DHA-induced fragmentation of their large forms, as well as (i) a considerable enrichment of perilipin-2 molecules within the phospholipid monolayer enclosing LDs, and (ii) a release of cPLA$_2$-α molecules from the surface of LDs (Figure 4.6). cPLA$_2$-α is recruited to the LD surface in response to microglia treatment with LPS, leading to the release of arachidonic acid from LD phospholipids (Khatchadourian et al., 2012). It is conceivable that the resulting removal of cPLA$_2$-α from its phospholipid substrates in the monolayer of LDs impairs the release of arachidonic acid and, therefore, their subsequent cyclooxygenase-dependent conversion into such potent inflammatory mediators as prostaglandins and leukotrienes. The reduced levels of these pro-inflammatory eicosanoids in microglia exposed to DHA is one of the mechanisms that may underlie its potent anti-inflammatory effect . Another (perhaps, equally important) factor responsible for the observed increase in DHA-treated microglial cells of cPLA$_2$-α molecules from the surface of LDs could be the enrichment of DHA, a C22:6 polyunsaturated fatty acid, in various phospholipid species known to be abundant in the membrane monolayer

enclosing LDs. We propose that the enrichment of DHA phospholipid species significantly weakens the association of $cPLA_2$-α with the surface of LDs, thereby stimulating a release of this phospholipase to the cytosol. In addition, recent studies using chiral MS/MS show that DHA is intracellularly converted into resolvins and protectins, which can attenuate inflammation (Weylandt et al., 2012).

Second, the observed significant increase in the number of LDs is likely to be responsible for the very close apposition of LDs and mitochondria in DHA-treated microglial cells; of note, we found that DHA suppresses a substantial LPS-induced increase of the distance between LDs and mitochondria (Figure 4.6), an increase which must significantly reduce interactions between the LDs and the mitochondria. Such interactions would also be promoted by an increase in the numbers of small- and medium-sized LDs like that observed in microglial cells exposed to DHA, leading to a significantly increased probability in the establishment of physical contacts between LDs and mitochondria. Furthermore, another (perhaps, equally important) factor responsible for the observed close apposition of LDs and mitochondria in DHA-treated microglial cells could be the enrichment of DHA in the various phospholipid species abundant in the LD membrane and also present in the mitochondrial outer and inner membranes.

Overall, the observed very close apposition of LDs and mitochondria in DHA-treated microglial cells is likely to be responsible for the following anti-inflammatory effects of DHA: (i) a facilitation of the coupling of TG hydrolysis by LD-confined lipases with mitochondrial beta-oxidation of FFAs formed during such hydrolysis, thereby causing the observed rise in mitochondrial metabolic activity and likely promoting ATP production in mitochondria; (ii) the activation of mitochondria-associated serine protease Omi , which has been recently shown to inhibit activation of microglia through the MEK-ERK-NFκβ signaling pathway (Hu et al., 2012) ; and (iii) the enrichment of DHA in various phospholipid species abundant in LD membrane monolayer and also present in the mitochondrial outer and inner membranes.

The proposed model (Figure 4.6) envisions the potent anti-inflammatory effect of DHA due in part to the greatly increased level of PS in microglia exposed to this n-3 polyunsaturated fatty acid. Our mass spectrometric quantitation of DHA-imposed

changes in the lipidome of microglial cells identified PS as the only membrane phospholipid whose level is significantly elevated in response to this intervention. Furthermore, the only three molecular forms of PS (out of its 23 forms detected by mass spectrometry) induced by DHA in microglial cells constituted more than 80% of its total cellular membrane pool, while each of the other 20 molecular species of PS was present at 1% of the total pool of this membrane phospholipid. PS has been shown to be the most abundant negatively charged phospholipid in eukaryotic membranes (Leventis & Grinstein, 2010). It is a unique membrane phospholipid because (i) PS is synthesized by the action of PS synthase PSS1 only in the endoplasmic reticulum (ER) (Levine, 2004; Voelker, 2005); (ii) PS serves as a precursor of two major membrane phospholipids, namely PE and PC (van Meer et al., 2008); (iii) due to the lack of an enzyme responsible for the conversion of PS to PE (this enzyme is called PE decarboxylase) in the ER membrane, PS is transported to the mitochondrial membranes (where it is converted to PE by the action of PE decarboxylase 1) and Golgi (where it is converted to PE by the action of PE decarboxylase 2) (Voelker, 2003); (iv) PS is transported from the place of its synthesis (*i.e.*, the ER) to mitochondria and Golgi via specialized ER domains known as membrane contact sites (MCS) or ER junctions (ERJ) – these domains represent narrow cytoplasmic gaps at which the MCS/ERJ domains of the ER and the target organellar membrane come into close apposition (Holthuis & Levine, 2005; Levine, 2004) (v) PS is also known to be transported via the MCS/ERJ domains from the ER to lysosomes, endosomes (EN) and the plasma membrane (PM) (Holthuis & Levine, 2005; Levine, 2004); and (vi) following its delivery to the PM, PS normally (*i.e.*, in the non-apoptotic cells) can be found only in the inner (cytosolic) monolayer (Holthuis & Levine, 2005; van Meer et al., 2008).

Due to these unique properties, PS may function as a membrane phospholipid which - after being synthesized in the ER (or following its delivery into a cell by exogenously added liposomes) and then rapidly transported to any of the aforementioned membranes (including the PM and EN membrane) – could regulate various membrane-associated processes, including signaling pathways implicated in the inflammatory response. According to our model, following the induction of their synthesis from FFA (including DHA as a C22:6 polyunsaturated fatty acid) in the ER of microglial cells exposed to

DHA, the C34:0, C36:0 and C40:6 species of PS are rapidly transported via the MCS/ERJ domains from the ER to the PM and EN membrane (Figure 4.6). Following their delivery to the PM, these molecular species of PS could cause specific changes in its biophysical properties (such as its fluidity, thickness, protein-protein and protein-lipid interactions, etc.), thereby affecting a signaling network that promotes the LPS-dependent neuroinflammatory effects in microglial cells. Following PS delivery to the EN membrane, the molecular species of PS induced by DHA may inhibit the downstream components of TLR-4 and may also promote the binding of interleukin-10 to EN membrane, thereby stabilizing this anti-inflammatory cytokine (Figure 4.6).

We propose that both a direct activation by DHA of its G-protein coupled receptor GPR120 and an indirect modulation of the TLR4/CD14 signaling network (by PS species induced following DHA treatment and then delivered to the PM), are responsible for the anti-inflammatory effects triggered by DHA on several key downstream protein components of this signaling network known to modulate LPS-induced neuroinflammation (Figure 4.6). The direct and indirect actions of DHA cause these anti-inflammatory effects in naïve and LPS-stimulated microglia by reducing protein kinase activities, thereby altering the extent of phosphorylation and causing redistribution between the nucleus and cytoplasm of several proteins downstream in the TLR4/CD14 signaling network. These suggestions are supported as follows:

First, the normalization of protein kinase activity of AKT seen in microglial cells exposed to DHA could be responsible for the observed retention of FOXO1 in the cytosol. Such a retention may not only attenuate the transcription, driven by a nuclear pool of FOXO1, of genes encoding several cell-death proteins, but may also promote certain pro-survival processes outside of the nucleus by a cytosolic pool of FOXO1 (Figure 4.6).

Second, a direct activation by DHA of its receptor (by PS species induced following DHA treatment and then delivered to the PM), and an indirect modulation of the TLR4/CD14 signaling network, could inhibit the translocation of transcription factor NFkB from the cytosol to the nucleus. In turn, this inhibition could attenuate the transcription (driven by a nuclear pool of NFkB) of genes encoding the inflammatory

cytokines TNFalpha and IL1beta, causing the observed substantial reduction of their secretion by microglial cells exposed to DHA (Figure 4.6). In addition, the inhibited translocation in DHA-treated microglia of transcription factor NFkB from the cytosol to the nucleus may be due to specific changes in mitochondrial signaling. Both the close apposition of LDs and mitochondria and the enrichment of DHA in various phospholipid species abundant in LD membrane monolayer and in the mitochondrial outer and inner membranes, could affect mitochondrial signaling by activating the mitochondria-associated protease Omi (Figure 4.6; see above). This serine protease has been recently shown to inhibit activation of microglia through the MEK-ERK-NFκβ signaling pathway by initiating a series of events that ultimately attenuate the translocation of NFkB from the cytosol to the nucleus (Hu et al., 2012). Further studies are required to confirm this mechanism in activated microglia treated with DHA.

Third, a direct activation by DHA of its receptor as well as an indirect modulation of the TLR4/CD14 signaling network could be responsible for a reduced phosphorylation of p38 MAPK seen in microglia exposed to DHA. The resulting attenuation of the import of p38 MAPK into the nucleus would likely reduce transcription of nuclear genes encoding inflammatory cytokines (Figure 4.6).

4.6 Conclusion

In summary, our model proposes an explanation for the profound changes in the spatiotemporal dynamics of numerous pro- and anti-inflammatory cellular processes in non-stimulated and LPS-stimulated microglial cells exposed to DHA. The proposed model envisions the existence of a complex DHA-governed regulatory network that attenuates the inflammatory response in LPS-stimulated microglia by integrating a number of essential inflammation-related cellular processes.

The major challenge now is to obtain a greater insight into the molecular and cellular mechanisms that in exposed to DHA naïve and LPS-stimulated microglial cells underly firstly, the dynamics of changes in the protein and lipid composition, protein-protein interactions and protein-lipid interactions taking place in the PM as well as in the

membranes of LDs, mitochondria and EN; and secondly, global alterations in the transcription pattern of numerous nuclear genes encoding various pro- and anti-inflammatory proteins. Future studies are anticipated to further progress our understanding of an inherent complexity of the DHA-governed regulatory network described here, one that attenuates the inflammatory response in naïve and LPS-stimulated microglia by integrating various inflammation-related cellular processes confined to different cellular compartments.

4.7 Acknowledgments

Mrs. B. Bruhl is acknowledged for sample processing and acquisition of electron micrographs. Confocal image analysis for this manuscript was performed in the McGill University Life Sciences Complex Imaging Facility. Purchase of equipment in the facility was made possible with funding from the Canadian Foundation for Innovaiton (CFI) and the Ministère du Développement économique, innovation et exportation Québec (MDEIE). DM was supported by the Canadian Institutes for Health Research (CIHR MOP 119425). VIT was supported by the Natural Sciences and Engineering Research Council of Canada (#283228-2009) and Concordia University Chair Fund. AK was supported in part by a Graduate Excellence Fellowship from McGill University. The authors thank Dr. J. Diamond for editorial assistance of the drafted manuscript. VRR was supported by a Frederick Banting and Charles Best Doctoral Scholarship Awards from the CIHR. VIT is a Concordia University Research Chair in Genomics, Cell Biology and Aging. We also thank Drs. Behrendt and Przybytkowski for preliminary experiments they performed.

A

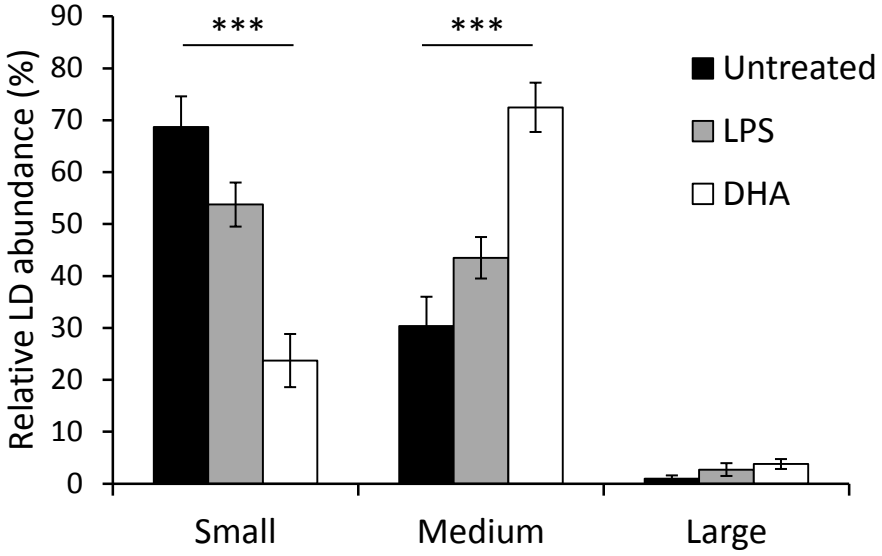
Relative LD abundance (%)
90
80
70
60
50
40
30
20
10
0
***
***
Untreated
LPS
DHA
Small
Medium
Large

B

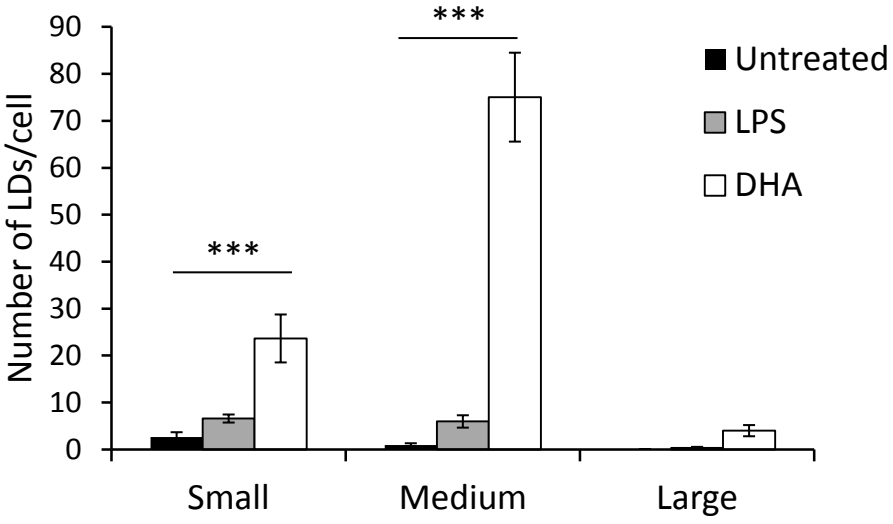
Number of LDs/cell
90
80
70
60
50
40
30
20
10
0
***
***
Untreated
LPS
DHA
Small
Medium
Large

Supplementary figure 4.1

Size distribution of LDs in microglia exposed to LPS or DHA.

(A) Relative abundance of LDs of different sizes in LPS or DHA –treated cells. The proportion of small (<0.5 μm), medium (0.5-1 μm) or large (>1.0 μm)–sized LDs per cell were calculated and are expressed as mean (%) ± SEM. Statistically significant differences are indicated by *** ($p<0.001$).

(B) Number of small, medium or large LDs. Number of LDs per cell was calculated by dividing total LD number per fiedl by number of apparent cells. Statistically significant differences are indicated by *** ($p<0.001$).

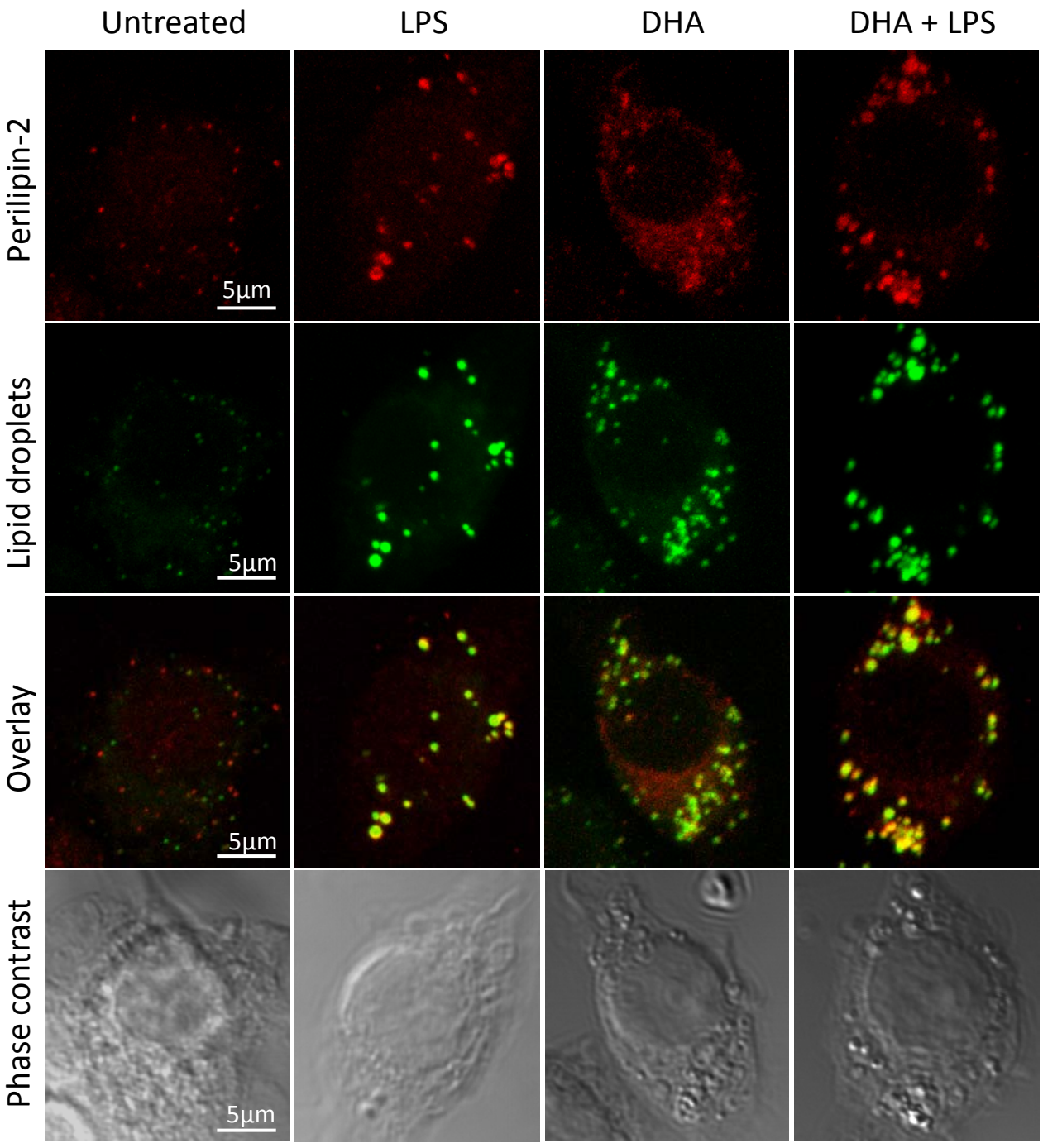
Untreated
LPS
DHA
DHA + LPS
Perilipin-2
Lipid droplets
Overlay
Phase contrast
5µm
5µm
5µm
5µm

Supplementary figure 4.2

Cellular distribution of perilipin-2 in microglial cells treated with LPS (10 μg/ml) and (DHA 50 μM), alone or in combination, for 9h.

Confocal micrographs show immunostained perilipin-2 (red) and lipid droplets (green). LDs were labelled with fluorescent dye HCS LipidTOX (pseudocolored green). Z-stack images were obtained from 15 optical slices at 0.3 μm intervals. Cells were imaged by differential interference contrast (bottom row). Scale bar, 5 μm.

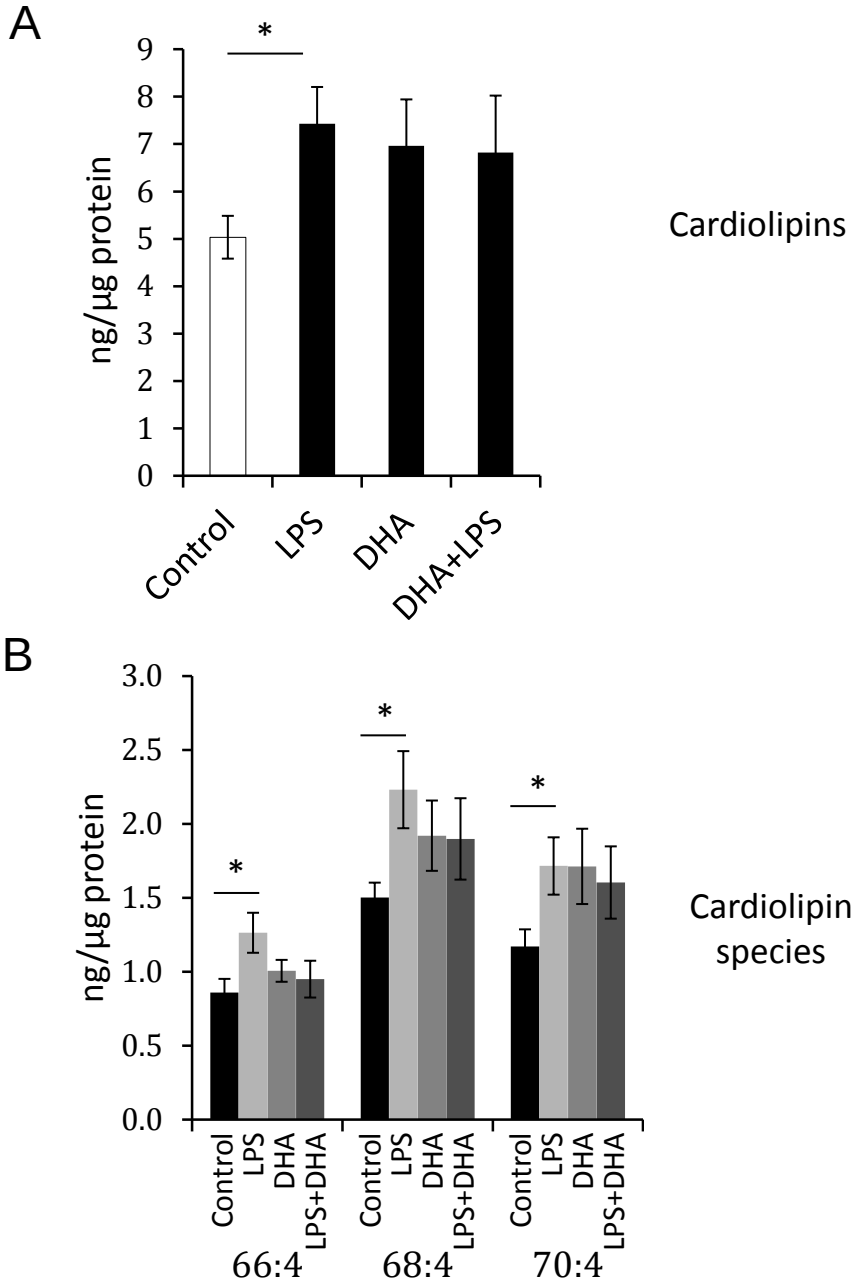
A
*
9
8
7
6
5
4
3
2
1
0
ng/µg protein
Control
LPS
DHA
DHA+LPS
Cardiolipins
B
3.0
2.5
2.0
1.5
1.0
0.5
0.0
ng/µg protein
*
*
*
Control
LPS
DHA
LPS+DHA
66:4
68:4
70:4
Cardiolipin species

Supplementary figure 4.3

Levels of total cardiolipin (A) and specific cardiolipin species (B) following LPS, DHA or LPS + DHA treatment as determined by ESI-MS. LPS and DHA, alone or combined, were added to the cells for 9h. Bars represent mean cardiolipin levels (ng/μg protein) ± SEM. Statistically significant differences are indicated by * ($p<0.05$).

Connecting text between Chapter 4 and Chapter 5

In Chapter 2- 4, we showed that LD accumulation in rodent cell lines could be induced by 1) environmental stressors, such as cytotoxic CdTe nanoparticles or hydrogen peroxide, and 2) by bacterial endotoxin (LPS). We showed that LD formation may also be induced by dietary unsaturated fatty acids, such as oleic acid and docosahexaenoic acid (DHA). Interestingly, the induction of LD formation by these fatty acids was harmless to the cells, and even protected them from either nanoparticle-induced toxicity or attenuated LPS-induced microglial activation. In Chapter 4, our findings implied that the anti-inflammatory effects of DHA in microglial cells are in part mediated by alterations in LD proliferation and dynamics.

Studies presented in Chapter 2-4 were done in rodent cell lines (e.g rat and mouse cell lines). Clearly, this limited our understanding of the implication of LDs under stressful conditions in human pathology. Therefore, we sought to study the implication of LDs in metabolic stress.

In order to gain insight into the implication of LDs in human pathology, we studied them in human pancreatic tissue obtained from T2DM and obese subjects. In particular, we examined the expression and distribution of perilipin-2 in human pancreatic islets by performing immunohistochemical staining. However, we could not directly stain for LD lipids by using BODIPY 493/503, since neutral lipids are dissolved by solvents such as xylene during the procedure. These studies were complemented by the assessment of mRNAs for the gene candidate implicated in the obesity, T2DM and LD regulation.

Our findings in Chapter 5 establish the link between LD-associated protein perilipin-2 and T2DM, suggesting new potential roles of LDs in the development of T2DM or obesity. Furthermore, LDs may serve as biomarkers of metabolic diseases that are characterized by oxidative stress and inflammation.A more advanced understanding of the role of LDs may lead to the development of novel therapeutic strategies for metabolic disorders.

CHAPTER 5

Human obesity and type 2 diabetes are associated with pancreatic upregulation of perilipin-2 and gene expression alterations

A. Khatchadourian, M. Petropavlovskaia, J. Patapas, J. Makhlin, L. Rosenberg, D. Maysinger

To be submitted

5.1 Abstract

Aims/hypothesis: Obesity and obesity-associated type 2 diabetes mellitus (T2DM) are characterized by an excess deposition of triacylglycerol (TAG) and subsequent lipid droplet (LDs) accumulation in non-adipose tissue. Perilipin-2 (PLIN2) is a ubiquitously expressed LD-associated protein that regulates TAG metabolism and LD formation. Alterations in PLIN2 expression in T2DM were previously reported in different tissues, such as muscle and liver. However, PLIN2 expression in the pancreas and its potential role in the pathogenesis of T2DM remain unknown. We hypothesized that PLIN2 is upregulated in the pancreas and pancreatic islets of obese and T2DM subjects as a protective response to reduce insult from toxic lipids. Changes in expression of various genes in the pancreas of obese versus lean and diabetic versus non-diabetic patients were also evaluated.

Methods: PLIN2 expression was measured by reverse transcription polymerase chain reaction (RT-PCR) in post-mortem pancreatic tissue from 1) non-diabetic normal (ND-N), 2) non-diabetic obese (ND-O), 3) type 2 diabetes normal (T2DN) and 4) type 2 diabetes obese (T2DO) donors. The distribution of PLIN2 in islet β-cells (colocalization with C-peptide) and in other areas surrounding the islets was evaluated by immunostaining on paraffin-embedded tissue sections.

Results: Immunohistochemical studies revealed increased islet and extra-islet PLIN2 expression in tissues from T2DN and T2DO donors, but not in ND-O donors. Data from RT-PCR analysis of T2DN and T2DO tissues confirmed the increase in PLIN2 expression and revealed significant alterations in several genes related to islet function, lipid/glucose metabolism, antioxidant defense and apoptosis.

Conclusions/interpretation: This is the first indication of increased PLIN2 expression in the pancreas of T2DM patients. We propose that PLIN2 protects from lipotoxicity by promoting the storage of toxic lipids within LDs.

5.2 Introduction

In the last decade, lipid droplets (LDs) have emerged as dynamic organelles implicated in metabolic disorders, such as obesity and T2DM (Greenberg et al., 2011). These organelles consist largely of TAG and cholesterol esters and serve as a major energy storage site in adipocytes. In obesity, excess lipids in adipocytes cause fatty acid spillover, leading to fat deposition in non-adipose tissue, a phenomenon known as ectopic fat accumulation (van Herpen & Schrauwen-Hinderling, 2008). The secretion of free fatty acid (FFA) from adipocytes is even more pronounced during insulin resistance, due to the loss of the anti-lipolytic activity of insulin on adipocytes. Consequently, this results in excessive accumulation of cytoplasmic LDs in skeletal muscle, liver or heart and is associated with lipotoxic events in these tissues.

LDs were shown to accumulate in the endocrine and exocrine pancreas in the Zucker diabetic fatty (ZDF) rat model, where excess amounts of TAG in pancreatic islets were associated with β-cell lipotoxicity (Lee et al., 1994; Lee et al., 2010). The metabolism of LD TAGs is highly regulated by perilipin-2 (PLIN2), formerly known as adipose differentiation-related protein (ADRP). PLIN2 stimulates cellular TAG accumulation and LD formation and can stabilize LDs by reducing the access of TAG lipases to their surface (Imamura et al., 2002; Listenberger et al., 2007). Being a ubiquitously expressed LD protein, it is highly expressed in mouse pancreatic islet β-cells (Faleck et al., 2010). In fact, PLIN2 is highly increased in β-cells of mice fed a high-fat diet and in human islets *in vitro* supplemented with fatty acids, suggesting that the protein is highly regulated by metabolic stimuli (Faleck et al., 2010). Interestingly, downregulation of PLIN2 reduced TAG accumulation and impaired metabolic processes such as lipolysis and fatty acid oxidation, and the ability of palmitate to increase insulin secretion.

PLIN2 expression is up-regulated in skeletal muscle and in kidneys of T2DM rodent models (Minnaard et al., 2009; Mishra et al., 2004). It is also increased in the liver of obese/diabetic mice (ob/ob mice) and in patients with fatty liver (Motomura et al., 2006). However, the status of PLIN2 in the pancreas of obese or T2DM subjects has not been examined so far. In this study, we sought to investigate the status of PLIN2 in human pancreatic tissue from T2DM and/or obese subjects. Furthermore, we evaluated T2DM-

and obesity-related alterations in expression of various genes involved in islet function, metabolism, antioxidant defense, and LD regulation.

5.3 Materials and Methods

Human pancreatic tissue

Pancreata from adult human cadaveric organ donors were obtained through the local organ procurement organization, Quebec Transplant, with prior consent for research of these tissues. The cold ischemia time, using refrigerated University of Wisconsin solution perfusion ranged from 3 to 8 h. Tissue samples were taken from the pancreatic tails and preserved in RNAlater^{TM} (Qiagen) for RNA extraction or fixed in 10% buffered formalin (Fisher Scientific) for IHC (immunostaining). Selection of samples for the study was based on the information provided by Quebec Transplant on donors' weight and height, and presence of T2DM (Supplementary tables 5.1-5.4). Four groups were formed based on the calculated BMI and the diabetic status: **ND-N** - Non-diabetic, normal (BMI 18<25, n=5), **ND-O** - Non-diabetic obese (BMI>30 n=6), **T2DN** - diabetic normal (n=5) and **T2DO** - diabetic obese (n=5)**.**

RT-qPCR

Samples stored at -80°C in RNAlater were homogenized in RLT buffer and processed in Qiacube^{TM} (Qiagen) using RNEasy mini kit, by following the manufacturer's protocol that included the DNAse 1 digestion step (all reagents were from Qiagen). Quality of RNA was assessed by $OD_{260/280}$ (all were >1.8) and by 1.5% agarose gel to ensure appearance of sharp 28S and 18S bands, as an indication of RNA integrity and suitability for quantification by real-time PCR. Primers (ordered from Integrated DNA Technologies (IDT)) were designed to span a splice site by one primer in each pair, except for somatostatin (SST), where primers were placed in different exons. Several primer pairs for each gene were designed and tested by thermal gradient and by the standard curve method using a wide range of serial dilutions. The selected primer pairs (Supplementary table 5.5) were found to anneal efficiently at 58-60°C and to amplify single products of the indicated sizes with efficiencies close to 100% (within the range of 95-105%). Equal amounts of RNA, based on OD_{260}, were reverse transcribed using oligo-dT primers and

Omniscript RT kit (Qiagen). 1 µl of cDNA was used for a 20 µl qPCR reaction performed with IQ™ SYBR® Green Supermix (Bio-Rad) in CFX96™ Real-Time System (Bio-Rad), CFX Manager software 1.1. PCR conditions included: activation for 3 min at 95°C; 40 cycles of 15s at 95°C, 15s at 58°C, 30s at 72°C; melt curve analysis from 65 to 95°C in 0.5°C increments. Multiple plates of experimental data, run with an inter-plate calibrator, were combined into one large gene study using GAPDH, β-Actin and SDHA as reference genes, and analyzed for relative quantities (ΔCt) and Fold Change in gene expression (ΔΔCt) using the data analysis software CFX Manager 2.0. ND-N group was used as a control. Selection of reference genes was based on their stability (M values<1.5, Supplementary table 5.6) across the samples determined with the geNorm method (Vandesompele et al., 2002)

Immunohistochemistry of PLIN2 and C-peptide

Samples were taken from the tail of the pancreas before isolation and stored at 4 °C in phosphate-buffered formalin. Paraffin-embedded tissue sections (5-µm) were deparraffinized in xylene, dehydrated in ethanol and then gradually rehydrated. Antigen retrieval was achieved by the heat-induced epitope retrieval method using citrate buffer (10 mM, 0.05% Tween 20, pH 6.0). After reaching boiling temperature, slides were maintained at sub-boiling temperature for 10 min. Sections were blocked in 10% goat serum/1% BSA (in tris buffer saline (TBS)) for 2 h and incubated with primary antibodies targeting C-peptide (mouse monoclonal, Meridian Life Science # E54094M) (1:100 dilution) and perilipin-2 (guinea pig polyclonal, Fitzgerald Industries #20R-AP002) (1:200 dilution) at 4°C (overnight). After removing the primary antibodies and washing the slides, sections were incubated for 1 h with secondary antibodies conjugated to Alexa Fluor 488 (goat anti-mouse IgG, Invitrogen, A-11029) (1:800 dilution) or Alexa Fluor 647 (goat anti-guinea pig IgG, Invitrogen, A-21450) (1:500 dilution). Slides (Fisher Scientific, 12-550-14) were mounted using Aqua-Poly/Mount (Polysciences, Inc, # 18-606).

Confocal microscopy

Confocal imaging was performed with Zeiss LSM 510 NLO inverted confocal microscope using a Plan Achromat 63X/1.4 Oil DIC objective. Fluorescent detection of Alexa Fluor 647-conjugated antibody was achieved by using a HeNe 633 nm laser and a long pass (LP) 650 filter. Alexa Fluor 488-conjugated secondary antibody was imaged using Argon 488 nm excitation laser and a 500-550 band pass (BP) filter. All images were acquired at a resolution of 1024 × 1024 pixels (x, y).

Statistical analysis

All data are expressed as means ± standard error of the mean (SEM). Statistical differences were analyzed by one way analysis of variance (ANOVA) followed by post-hoc Tukey's test. Statistical differences are indicated by * $p<0.05$ or ** $p<0.01$

5.4 Results

Assessment of PLIN2 expression in pancreatic islets

We first investigated the expression of PLIN2 in pancreatic tissue sections from different donor groups. Islets β-cells were detected by immunostaining for C-peptide. The PLIN2 immunofluorescence signal was low in non-diabetic normal (ND-N) and non-diabetic obese (ND-O) islets, whereas the signal was strongly enhanced in all type 2 diabetes normal (T2DN) and type 2 diabetes obese (T2DO) donor tissue, regardless of gender (Figure 5.1 A,B; Supplementary figure. 5.1). In these individuals, PLIN2 seemed to extensively colocalize with C-peptide (β-cells), whereas there was practically no such colocalization in ND-N and ND-O tissues. This suggests that PLIN2 accumulates in β-cells in T2 diabetic subjects. Our immunohistochemical studies also revealed a dramatic accumulation of PLIN2 in extra-islet microenvironments (Supplementary fig ure 5.2) and not only in the islets of Langerhans.

T2DM- and obesity-induced alterations in pancreatic gene expression

We investigated the effect of obesity and T2DM on the expression of several genes, more specifically the ones related to lipid/glucose metabolism, apoptosis, islet function, antioxidant defense and LD regulation. Consistent with our IHC data, the RT-qPCR analysis demonstrated that expression of PLIN2 was increased in T2DM but not in ND-O subjects (Figure 5.2). The expression of CAV1, which plays an important role in cholesterol transport, lipogenesis and LD biogenesis (Cohen et al., 2004) was also slightly increased. Another LD associated protein, FSP27, however did not follow the same pattern being highly upregulated in ND-O donors whereas in T2DM donors the change was not significant.

Aside from LD-associated genes, most change in expression in diabetic subjects was observed for the proteins involved in regulation of metabolism and associated with anti-oxidative response and apoptosis. The expression of several metabolic genes was significantly upregulated in diabetic subjects, including carnitine palmitoyltransferase 1A (CPT1A), uncoupling protein 2 (UCP2), peroxisome proliferator activated protein α (PPARα) and Forkhead box protein O1 (FOXO1) (Figure 5.2). Autophagy-related gene, sequestosome 1 (SQSTM1, or p62) was also upregulated in diabetic obese donors. Antioxidant defense genes, glutathione peroxidase 1 (GPX1) and heme oxygenase 1 (HMOX1) were significantly upregulated in ND-O, T2DN and T2DO. That seemed to correlate with upregulation of anti-apoptotic gene B-cell lymphoma 2 (BCL2) in diabetic subjects, albeit concomitant with an increase in the pro-apoptotic gene Bcl-2-associated X protein (BAX).

We also observed changes in the levels of islet hormones such as insulin, glucagon and somatostatin (Figure 5.2). Interestingly, insulin expression was increased about 3-fold in T2DO pancreas, whereas in ND-O and T2DN, no significant changes has been observed. No difference was found in the glucose transporter GLUT2 and the changes in glucokinase, although elevated in T2D donors, were not significantly different from control due to high variability. Glucagon mRNA was increased only in ND-O group, whereas somatostatin appeared to be slightly downregulated in T2D donors.

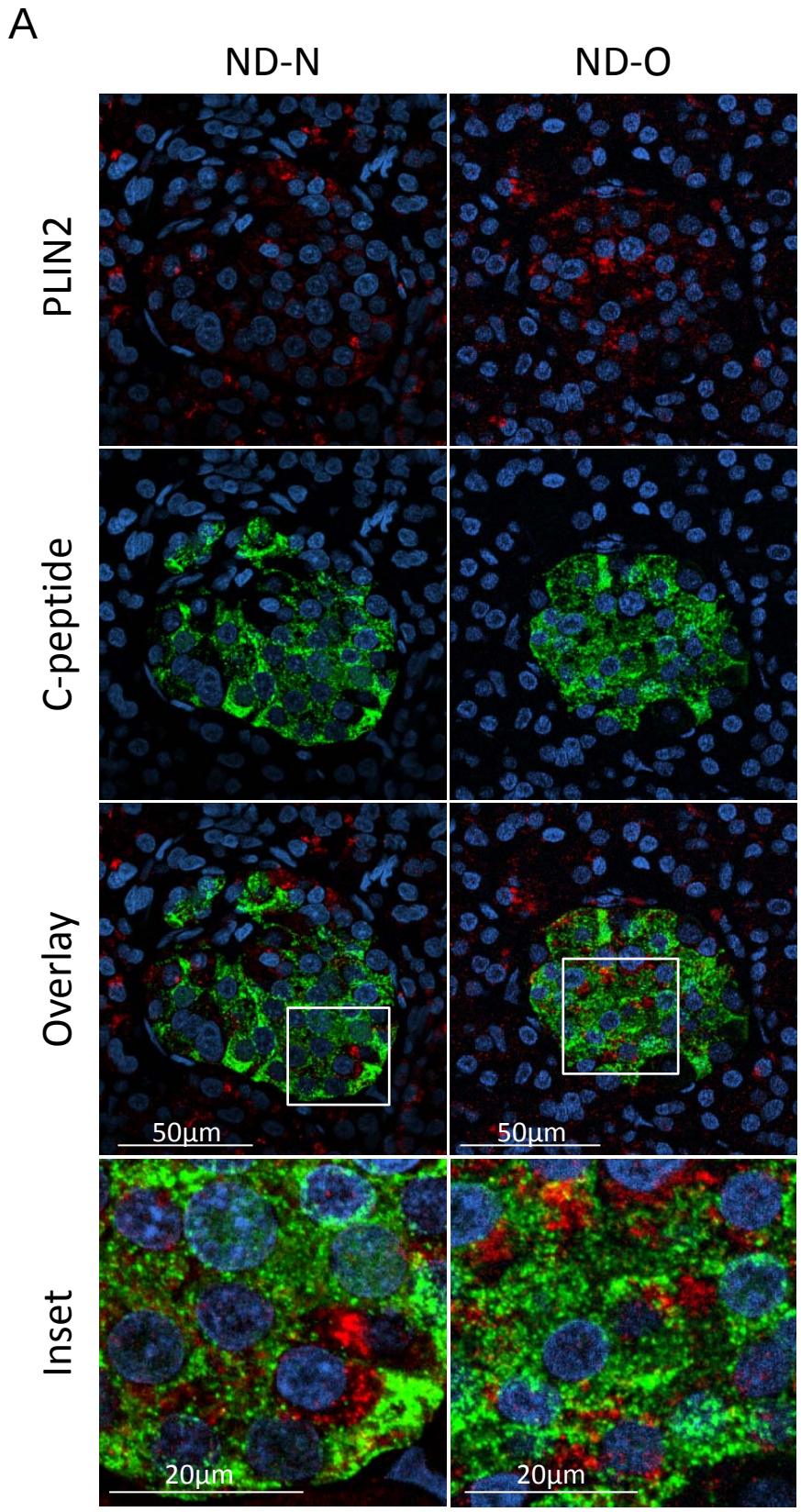
A
ND-N
ND-O
PLIN2
C-peptide
Overlay
Inset
50µm
50µm
20µm
20µm

B

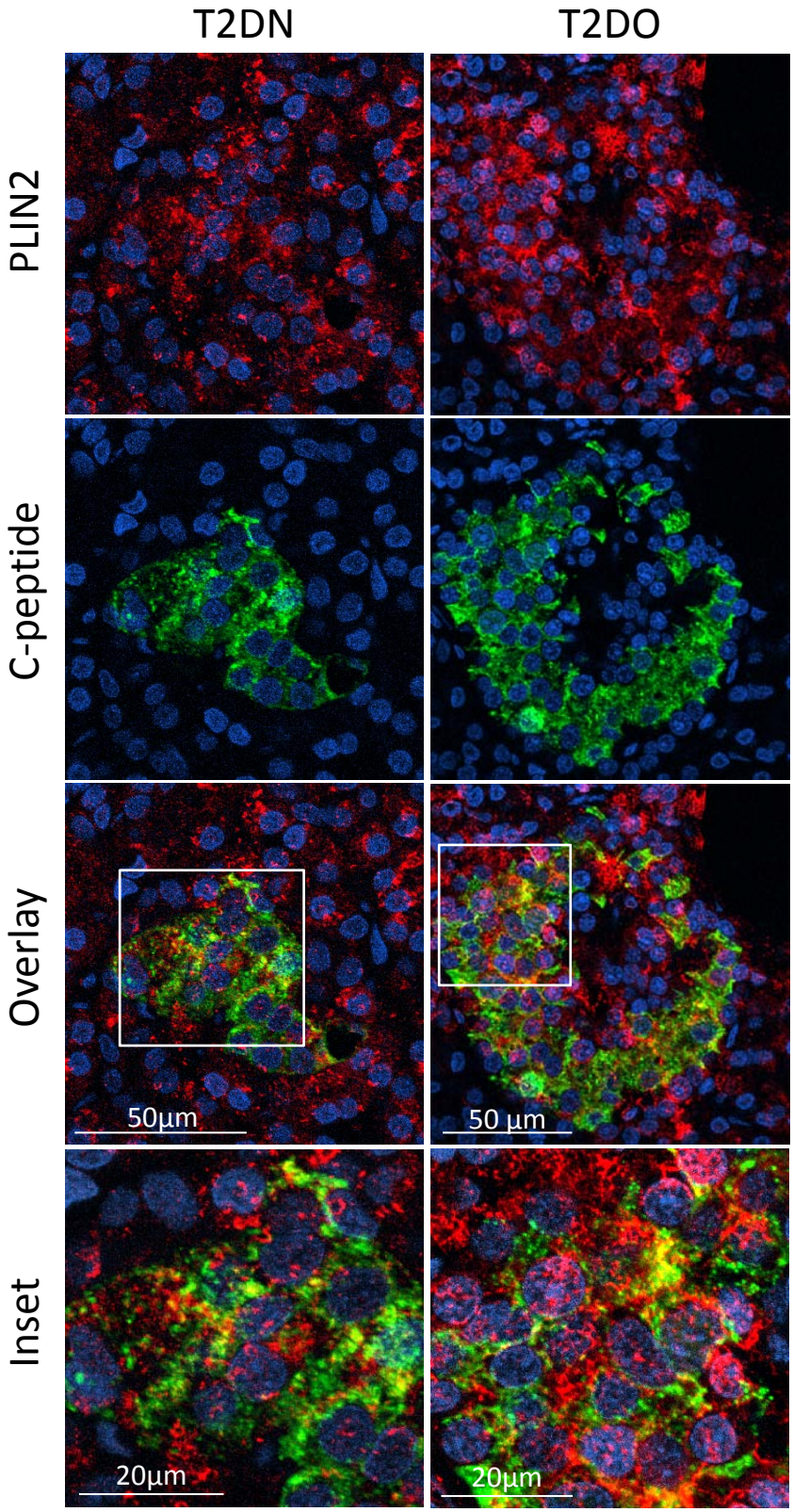

Figure 5.1 Expression of perilipin-2 in pancreatic islets of non-diabetic and T2 diabetic subjects.

Pancreatic sections obtained from different categories of male donors were immunostained, as described in Materials and methods, for perilipin-2 (Alexa Fluor 647, red) and C-peptide (Alexa Fluor 488, green) and examined by confocal microscopy.

(A) ND-N and ND-O donors.

(B) T2DN and T2DO donors.

Images represent Z-stacks of several optical sections (total thickness = 4 µm). Scale bars, 50 µm. Insets represent zoomed-in areas and reveal extensive colocalization of perilipin-2 with C-peptide in islets of T2 diabetic donors. Inset scale bars, 20 µm.

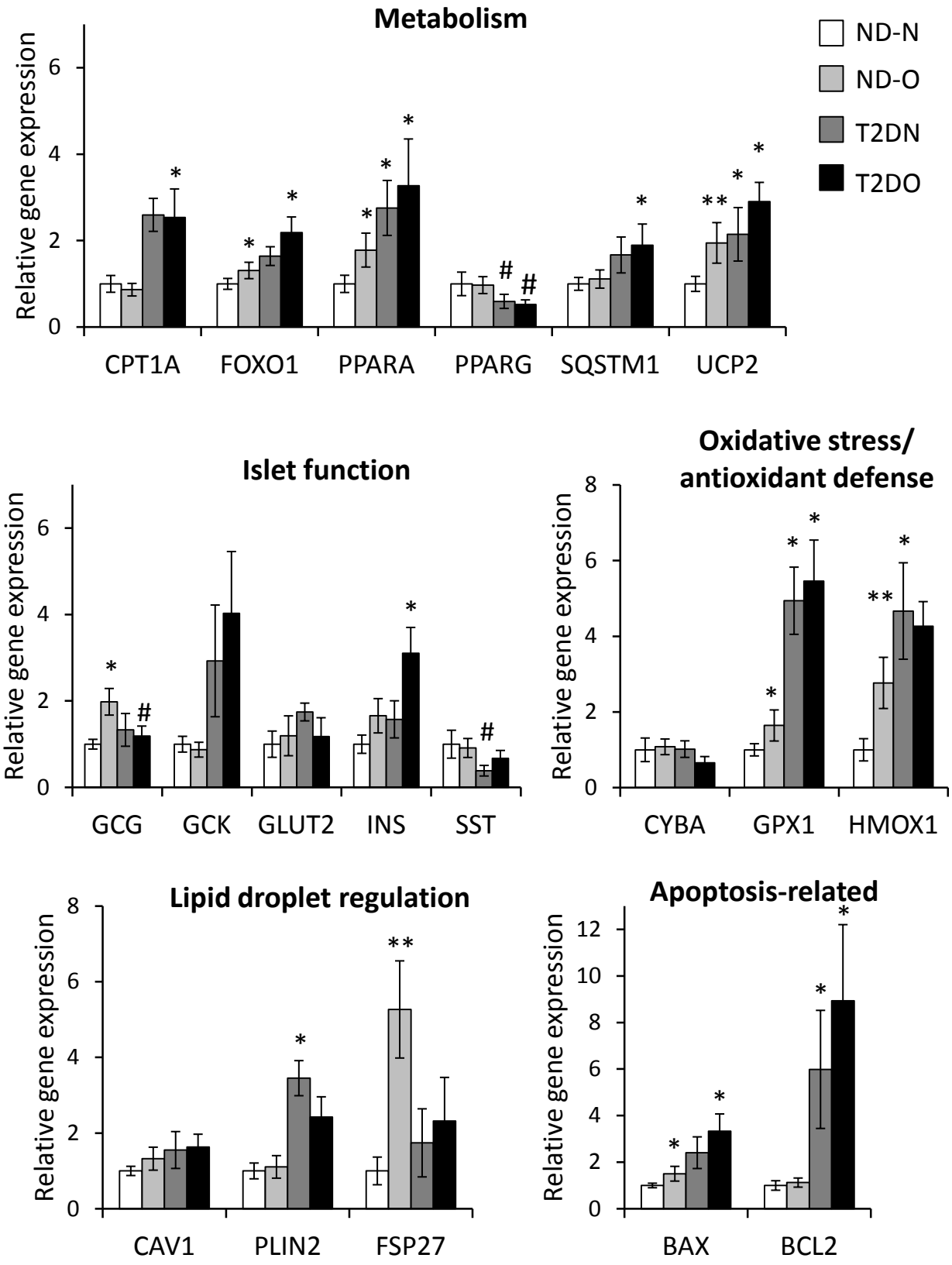
Metabolism
ND-N
ND-O
T2DN
T2DO
Relative gene expression
CPT1A
FOXO1
PPARA
PPARG
SQSTM1
UCP2
Islet function
GCG
GCK
GLUT2
INS
SST
Oxidative stress/
antioxidant defense
CYBA
GPX1
HMOX1
Lipid droplet regulation
CAV1
PLIN2
FSP27
Apoptosis-related
BAX
BCL2

Figure 5.2 Gene expression analysis in pancreatic tissue from non-diabetic and T2 diabetic donors.

Quantitative RT-PCR was performed as described in the Materials and methods. GAPDH, β-actin and SDHA were used as reference genes for calculations of the Normalized Fold Change in gene expression by the CFX Manager software (Biorad). Data are Shown as mean ± standard error of the mean (SEM) of Relative Gene Expression calculated a s a ratio over control (ND-N), which has a value of 1. Statistically significant differences were determined by performing one-way ANOVA of the Normalized Fold Change followed by post-hoc Tukey's test and are indicated by * (compared to ND-N), # (compared to ND-O). *or # $p<0.05$, and ** $p<0.01$.

5.5 Discussion

In the present study, we demonstrate that PLIN2 expression is considerably increased in human pancreas of T2DM individuals. Immunohistochemical analysis showed that the PLIN2 expression was upregulated in pancreatic islets, as well as in the extra-islet environment. Gene expression analysis using qPCR further confirmed the increase in PLIN2 and, concurrently revealed significant alterations in the expression of several genes involved in metabolism, islet function, LD regulation and antioxidant defense.

Alterations in PLIN2 expression were previously reported in other tissues such as muscle and kidneys of Zucker diabetic fatty (ZDF) rats and db/db mice, respectively (Minnaard et al., 2009; Mishra et al., 2004). In those hyperlipidaemic rodents, PLIN2 might facilitate the uptake of lipids (e.g long-chain fatty acids) from the extracellular environment and stimulate neutral lipid accumulation into LDs in muscle or kidney. An increase in PLIN2 in pancreatic islets might serve a similar function in T2 diabetic donors. Interestingly, PLIN2 expression did not seem to increase in response to high BMI (obesity), but it appeared to be only responsive to the diabetic condition, suggesting that chronic hyperglycemia may be a prerequisite for upregulation of PLIN2. In fact, it was shown that the esterification of fatty acids into neutral lipids (i.e TAG) depended on the presence of high glucose (Briaud et al., 2001). Given that PLIN2 stabilizes LDs and prevents leakage of FFAs from TAGs into the cytosol, its upregulation in T2 diabetic donor islets could play a protective role against lipotoxicity In agreement with this idea, overexpression of perilipin-1 (PLIN1), another prominent LD protein, was found to increase TAG storage and protect β-cells (INS-1 cell line) from palmitate-induced lipotoxicity (Borg et al., 2009). In fact, an inverse relationship was observed between FFA cytotoxicity and TAG accumulation in β-cells (Cnop et al., 2001). Collectively, these findings suggest that the intrinsic ability of β-cells to convert FFA into TAG and store them within LDs may represent an important cytoprotective mechanism. In line with this statement, increased expression of PLIN2 in skeletal muscle enhanced storage of FFA into TAG and was associated with improved insulin sensitivity (Bosma et al., 2012). Furthermore, overexpression of muscle PLIN2 *in vivo* resulted in LD accumulation and prevented high-fat diet-induced abnormalities in oxidative

phosphorylation. On the other hand, deficiency of PLIN2 and other LD-associated proteins impaired insulin signaling in the liver (Bell et al., 2008).

FSP27 is predominantly expressed in adipocytes and functions in TAG synthesis and LD accumulation. Our gene analysis by RT-qPCR revealed a significant upregulation in FSP27 in ND-O donors ($p<0.01$), suggesting an increased presence of adipocytes in the pancreas of these donors. It was reported that adipocyte infiltration in the pancreas correlates with pancreatic TAG content, but seems to be independent of diabetic status (Pinnick et al., 2008). It was somewhat unexpected to find that FSP27 was not significantly upregulated in T2DO donors characterized by stronger presence of LDs in the pancreas as compared to ND-O (Figure 5.1). Of note, FSP27 expression has been shown to be regulated by PPARγ, which also regulates expression of Cav1 and other lipid droplet associated proteins (Burgermeister et al., 2003; Dalen et al., 2004). Since PPARγ appears to be downregulated in diabetic patients in our study, this may explain, at least partially, the lack of increase in FSP27 mRNA in T2DO pancreas, as well as perhaps a weak response from CAV1 mRNA.

Gene analysis by RT-qPCR revealed significant alterations in many metabolic genes, but also in genes regulating islet function. For instance, INS was considerably upregulated in T2DO ($p<0.05$). It should be noted that the pathogenesis of T2DM does not involve an abrupt reduction in the beta cell mass, like in the case of T1DM, but is associated with a gradual decline in beta cell function often concomitant with hyperinsulinemia in early stages of the disease (Shanik et al., 2008). Given that most of the T2DM donors in our study were insulin independent (only one donor in each diabetic group received insulin), thus being in the early stage of the disease, we interpret the increase in insulin mRNA as an indication of a compensatory response in β-cells to the peripheral insulin resistance and the associated hyperglycemia.

Hyperglycemia is also consistent with the observed trend in an increase in expression of GCK (not significant) involved in metabolizing of glucose.

Interestingly, there was an increase in glucagon mRNA in ND-O donors, in line with the other report (Starke et al., 1984), but no change was detected in T2D donors. There was a

slight decrease in somatostatin mRNA but significant difference was found only between ND-O and T2DN donors. Taken together, our results show little difference in the expression levels of islet hormones (except for Insulin in T2DO donors) and glucose metabolism-related genes. It is important to note that no significant changes in these groups of genes was found in another study by profiling the gene expression in the laser capture microdissection (LCM)-derived, beta-cell enriched tissue from T2D subjects (Marselli et al., 2010).

Expression levels of other genes tested in our study appear to be consistent with the state of a metabolic stress associated with obesity and development of T2DM. For example, we show upregulation of PPARα, which is expressed in a wide range of tissues and controls glucose and lipid metabolism. Importantly, PPARα improves pancreatic adaptation to insulin resistance in obese and T2DM rodents (Lalloyer et al., 2006). Our data therefore suggest that it may play the same role in T2 diabetic humans. Though PPARγ was previously shown to be upregulated in the skeletal muscle of T2D donors (Park et al., 1997), it is not quite clear how its expression is regulated in the pancreas.

Diabetes is associated with high levels of reactive oxygen species (ROS) playing important role in the development of diabetic complications and leading to the generation of intracellular signals that ultimately lead to β-cell dysfunction. Consistent with this notion, expression of several genes, involved in oxidative phosphorylation (UCP2), fatty acid oxidation (CPT1), autophagy (SQSTM1/p62) were upregulated in samples analyzed in the present study. FOXO1, a critical factor in regulation of cellular oxidative stress response pathways (Ponugoti et al., 2012) and β-cell survival (Kousteni, 2012) was also altered. UCP2 dissipates the proton gradient across the inner mitochondrial membrane and thereby negatively regulates ATP production. It is also an important regulator of ROS signals (Robson-Doucette et al.). In agreement with our results, both UCP2 and CPT1 were also upregulated in db/db (obese T2 diabetic) mice (Kjorholt et al., 2005).

Interestingly, expression of both pro-apoptotic gene BAX and anti-apoptotic BCL2 was upregulated, adding to the complex state of affairs in the diabetic pancreas. Noteworthy, expression of HMOX and GPX1, antioxidant defense genes, were increased in obese and T2DM groups. Such adaptive enhancement of antioxidant genes may protect β-cells from

hyperglycemia- or hyperlipidemia- induced oxidative damage (Harmon et al., 2009; Lacraz et al., 2009).

5.6 Conclusion

Taken together, the gene expression profile of non-diabetic obese and T2DM lean and obese donors is consistent with dysregulation of cellular homeostasis that is characteristic of the disease. At the same time, our data suggest activation of pro-survival complementary pathways including previously reported ones and also PLIN2 as a critical LD stabilizing protein. We hypothesize here that accumulation of lipid droplets in the diabetic pancreas protects beta cells from lipotoxicity and as such it may aid in activation of pro-survival cellular mechanisms. If proven, this may lead to the development of drugs to take advantage of this potential protective effect, which will be a promising avenue for future therapeutic interventions.

5.7 Acknowledgements

These studies were supported by Canadian Institute for Health Research (DM), Canadian Diabetes Society (LR) and McGill University for contributing to the internal studentship (AK). We thank Dr S. Taylor (Biorad) for advice on the RT-qPCR study and Dr. J.Diamond for reading and editing the manuscript.

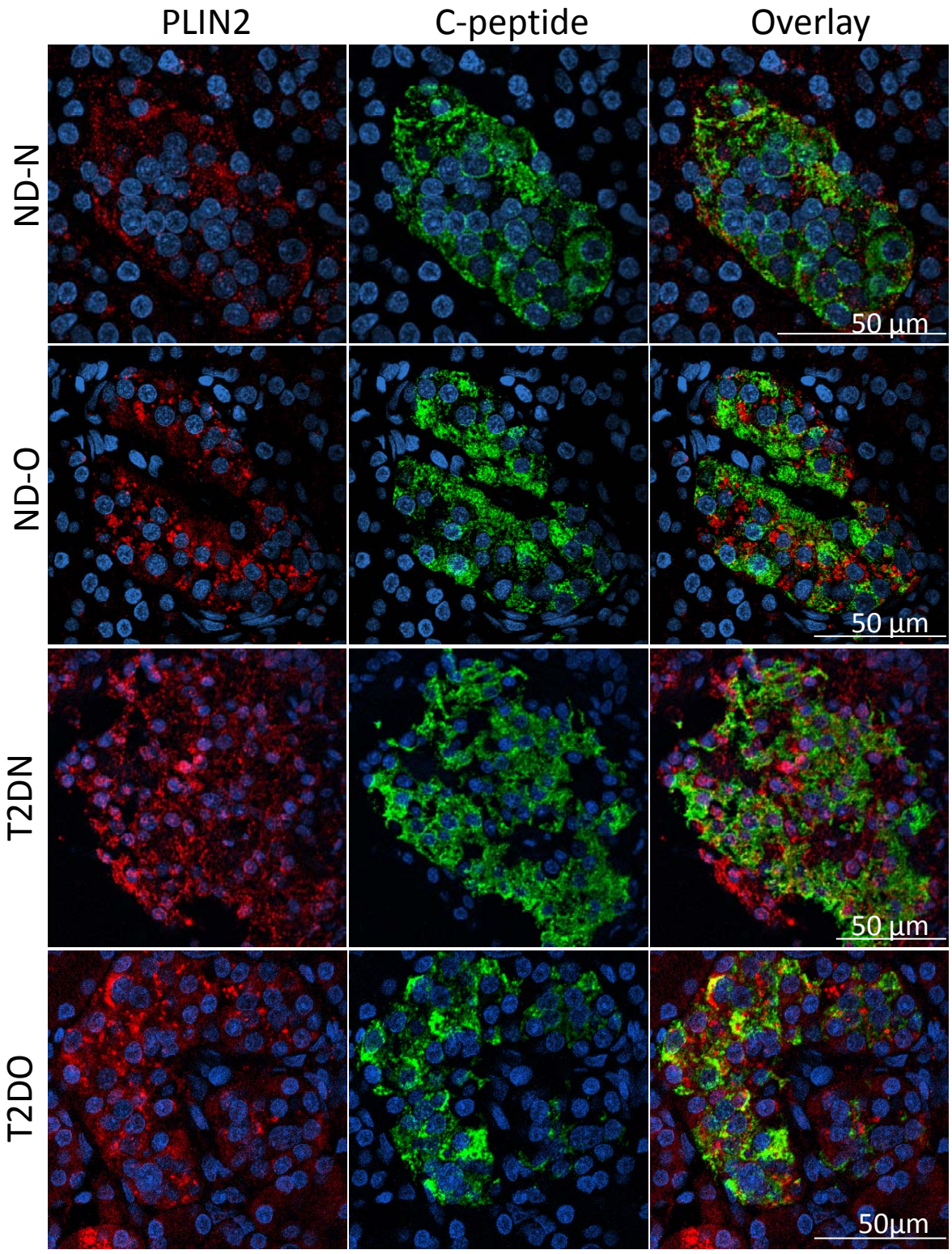
PLIN2
C-peptide
Overlay
ND-N
ND-O
T2DN
T2DO
50 µm
50 µm
50 µm
50µm

Supplementary figure 5.1 Perilipin-2expression in pancreatic islets of different female donor groups.

Immunofluorescent staining of perilipin-2 in islets in human pancreatic sections obtained from female donors. Confocal images show double immunostaining of perilipin-2 (red) and C-peptide (green) in lean or obese donors with or without T2DM. Images represent Z-stacks of several optical sections (total thickness = 4 μm). Scale bars, 50 μm.

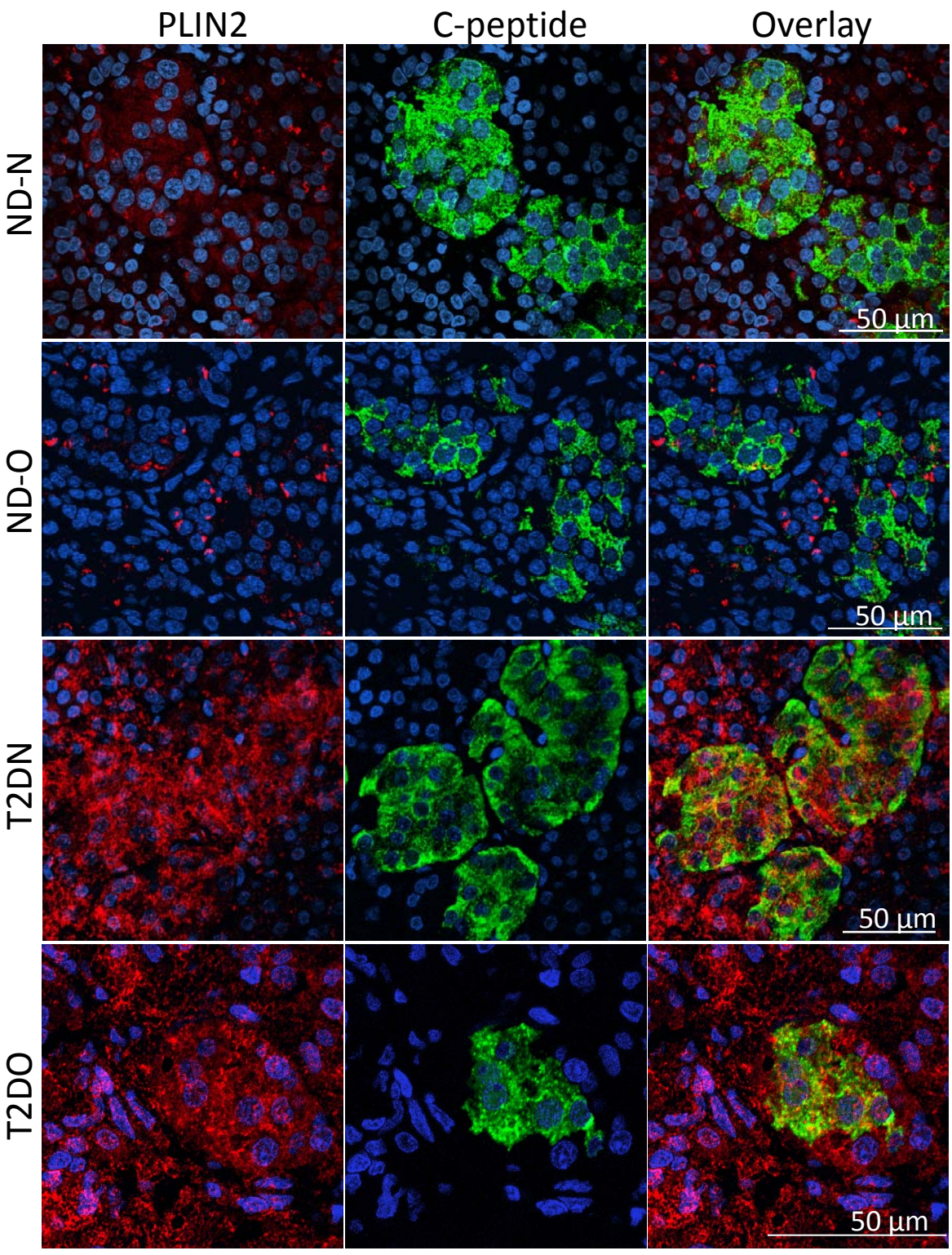
PLIN2
C-peptide
Overlay
ND-N
ND-O
T2DN
T2DO
50 µm
50 µm
50 µm
50 µm

Supplementary figure 5.2 Increased perilipin-2 expression in extra-islet environment in T2DM donor tissue

Accumulation of perilipin-2 in extra-islet environment in diabetic donors. Double immunostaining of perilipin-2 and C-peptide in tissue sections. Note the dramatic increase in perilipin-2 staining in T2DNand T2DO in islets as well as regions surrounding the islets of Langerhans. Images represent Z-stacks of several optical sections (total thickness = 4 μm). Scale bars, 50 μm

Supplementary table 1

Donor information for Figure 1

Sample	Age	Sex	BMI (kgm^{-2})	Weight (kg)	Height (cm)	Cause of death	PMHx	Rx
ND-N	50	M	22.1	-	-	-	-	-
ND-O	51	M	36.4	-	-	-	-	-
T2DN	49	M	24.2	82	184	anoxic encephalopathy	type 2 diabetes x 3yr, hypertension, hyperlipidemic, drinker	DiaBeta, Glucophage, insulin
T2DO	66	M	32.8	94.9	170	anoxia	type 2 diabetes x 15yr	Metformin

*PMHx – previous medical history

**Rx- drug treatment

Supplementary table 2

Donor information for Figure 2

Non-diabetic group

Sample	Age	Sex	BMI (kgm^{-2})	Weight (kg)	Height (cm)	Cause of death	PMHx*	Rx*
NDN1	74	unknown	22.4	61	165	Cranial trauma		
NDN3	50	M	22.1	70	178	Stroke		
NDN4	35	F	21.8	48	148	Stroke		
NDN5	26	F	24.2	70	170	Anoxia		
NDN6	52	F	20.2	53	162	Cerebral hemmorhage		
NDO1	62	F	31.8	82	160	Cerebral hemmorhage		
NDO2	51	M	36.4	118	180	Cerebral hemmorhage		
NDO3	70	F	35.2	90	160	Cerebral hemmorhage		
NDO4	60	F	36.5	90	157	Mesencephalic stroke		
NDO5	48	F	30.0	74	157	Anoxia		
NDO6	57	F	37.1	95	160	Cerebral hemmorhage		

Supplementary table 2 (continued)

Donor information for Figure 2.

T2D group

Sample	Age	Sex	BMI (kgm^{-2})	Weight (kg)	Height (cm)	Cause of death	PMHx*	Rx**
T2DN1	54	F	23.6	59	158	Cerebral hemorrhage	type 2 diabetes, hypertension, COPD, hyperlipidemia, smoker	Diabeta 5mg BID x1yr, Glucophage 500mg QD x1yr
T2DN2	54	M	25.2	80	178	Cranial trauma	type 2 diabetes x2.5yr, hypertension, hyperlipidemic	oral anti-hyperglycemics, then diet
T2DN3	63	M	24.2	70	170	Cranial trauma	type 2 diabetes x1yr controlled by diet, smoker, alcoholic	diet
T2DN5*	60	M	25.3	73	170	anoxic encephalopathy	type 2 diabetes, hypertension, hyperlipidemic, smoker, alcoholic	50 U/d insulin, DiaBeta, HLA DQ: 2, 5 DR: 52, 53
T2DN6	64	M	22.1	64	170	Cerebral hemorrhage	type 2 diabetes x3yr	Metformin
T2DO1*	54	F	30.5	83	165	Abdominal trauma	T2DM 5 years ago, 3 years on glucophage	Insulin
T2DO2	69	F	44.0	138	177	Cerebral hemorrhage		
T2DO3	60	M	37.9	113	173	Cerebral anoxia	recent type 2 diabetes, hypertension, smoker	Metformin
T2DO4	66	F	34.2	81	154	Sub-arachnoid hemorrhage	type 2 diabetes x3-4yr, manic depression, smoker	Metformin, Glyburide
T2DO5	66	M	32.8	95	170	Anoxia	type 2 diabetes x15yr	Metformin

Supplementary table 3

Donor information for Supplementary figure 1

Sample	**Age**	**Sex**	**BMI (kgm^{-2})**	**Weight (kg)**	**Height (cm)**	**Cause of death**	**PMHx**	**Rx**
ND-N	26	F	24.2	-	-	-	-	-
ND-O	48	F	30	-	-	-	-	-
T2DN	63	F	19.9	51	160	Cerebral hemorrhage	type 2 diabetes x2.5yr	Metformin
T2DO	57	F	34.1	90.6	163	Cerebral hemorrhage	type 2 diabetes x11yr, hypertension, hyperlipidemic, depression	Glucophage

Supplementary table 4

Donor information for Supplementary figure 2

	Age	Sex	BMI (kgm^{-2})	Weight (kg)	Height (cm)	Cause of death	PMHx	Rx
ND-N	52	M	22.1	-	-	-	-	-
ND-O	57	F	37.1	-	-	-	-	-
T2DN	64	M	22.2	64	170	Cerebral hemorrhage	type 2 diabetes x3yr	Metformin
T2DO	66	M	32.8	94.9	170	anoxia	type 2 diabetes x15yr	Metformin

Supplementary table 5

Selected primer pairs

Gene	Reference	Forward	Reverse	Amplicon(bp)
PLIN2	NM_001122	GCTGAGCACATTGAGTCACG	GCATTGCGGAACACTGAGTAGA	172
ACTB	NM_001101	TTCCTGGGCATGGAGTCCTGT	CTTGATCTTCATTGTGCTGGGTGC	188
BAX	NM_138761	TGCTTCAGGGTTTCATCCAGGA	CTGTCCAGTTCGTCCCCGAT	138
BCL2	NM_000633	TGCACCTGACGCCCTTCAC	TTCCACAAAGGCATCCCAGCC	244
CAV1	NM_001753	AGACTCGGAGGGACATCTCTACA	GTCATCGTTGAGGTGTTTAGGGTC	165
CPT1A	NM_001876	CGATGTTACGACAGGTGGTTTGAC	CGGAATGTTCGGATTGATGTCGC	200
GAPDH	NM_002046	AAGATCATCAGCAATGCCTCCTG	TGACCTTGCCCACAGCCTT	228
FSP27	NM_022094	ATCAGAACAGGGGACAAGGCA	CTTCACGTTCAGGCAGCCAATG	129
FOXO1	NM_002015	GACCTCATGGATGGAGATACATTGGA	GTGTAACCTGCTCACTAACCCTCA	128
GCK	NM_000162	GCTGAGATGCTCTTCGACTAC	CTTGGTCCAGTTGAGAAGGATG	152
GLUT2	NM_000340	GTGCTGCTGAATAAGTTCTCTTGG	GTCCACAGAAGTCCGCAATGTA	225
GCG	NM_002054	GACTACAGCAAGTATCTGGACTCC	TCTGGGAAATCTCGCCTTC	220
GPX1	NM_000581	GAATGTGGCGTCCCTCTGAG	TGCGTTCTCCTGATGCCCA	131
HMOX	NM_002133	GCAACAAAGTGCAAGATTCTGCC	TGGCATAAAGCCCTACAGCAACT	140
INS	NM_000207	CCATCAAGCAGATCACTGTCCT	GTGTAGAAGAAGCCTCGTTCC	180
PPARA	NM_001001928	ATTTGCTGTGGAGATCGTCCTGG	GCATCCGACTCCGTCTTCTTGAT	214
PPARG	NM_138712	TATCCGAGGGCCAAGGCTTC	AAACCTGGGCGGTCTCCACT	177
SST	NM_001048	CCAGACTCCGTCAGTTTCTG	GCCATAGCCGGGTTTGAGTTA	204
UCP2	NM_003355	GATACCAAAGCACCGTCAATGCCTAC	GGCAAGGGAGGTCATCTGTCAT	185
SQSTM1	NM_003900	ATCTCCCGCCAGAGGCTGA	GGATGCTTTGAATACTGGATGGTGTC	156
CYBA	NM_000101	ATCTACCTACTGGCGGCTGTG	TCCTCCTCGCTGGGCTTCTT	154
HPRT	NM_000194	CCTGGCGTCGTGATTAGTGATGAT	CAGAGGGCTACAATGTGATGGC	181
SDHA	NM_004168	GCAGAACCTGATGCTGTGTG	TTCCAGAGTGACCTTCCCAGTG	216

Supplementary table 6. Reference genes M-values

	GAPDH	Actin1	SDHA	**Normalisation Factor**
T2DMN1	1.00E+00	1.00E+00	1.00E+00	**0.8890**
T2DMN2	1.48E+00	1.45E+00	8.12E-01	**1.0720**
T2DMN3	2.10E+00	7.36E+00	1.04E+00	**2.2454**
T2DMN5	2.81E+00	5.74E+00	1.12E+00	**2.3300**
T2DMN6	3.20E+00	5.13E+00	1.40E+00	**2.5321**
T2DMO1	1.40E+00	1.47E+00	6.24E-01	**0.9684**
T2DMO2	3.79E-01	8.29E-01	3.49E-01	**0.4254**
T2DMO3	1.15E+00	1.84E+00	8.41E-01	**1.0770**
T2DMO4	1.22E+00	1.85E+00	6.55E-01	**1.0142**
T2DMO5	2.23E+00	3.20E+00	5.78E-01	**1.4277**
NDN1	8.24E-01	6.64E-01	7.53E-01	**0.6614**
NDN3	1.87E+00	2.14E+00	2.03E+00	**1.7863**
NDN4	1.23E+00	1.59E+00	1.61E+00	**1.3046**
NDN5	1.05E+00	2.14E+00	1.08E+00	**1.1950**
NDN6	9.73E-01	7.37E-01	8.89E-01	**0.7651**
NDO1	8.24E-01	6.64E-01	1.21E+00	**0.7740**
NDO2	6.75E-02	2.80E-02	4.41E-01	**0.0836**
NDO3	1.87E+00	2.14E+00	1.08E+00	**1.4476**
NDO4	1.23E+00	1.59E+00	1.01E+00	**1.1150**
NDO5	1.05E+00	2.14E+00	7.53E-01	**1.0597**
NDO6	9.73E-01	7.37E-01	9.79E-01	**0.7902**
M < 1.5	**0.813**	**1.074**	**1.200**	

CHAPTER 6

General Discussion

The work presented in this thesis describes the status and the regulation of LDs under stressful conditions. Although LD accumulation under stressful conditions was previously reported, their role in cellular stress responses remains largely unknown. To get a better understanding of this role and of the development of associated pathology, we investigated LDs in conditions of oxidative, inflammatory and metabolic stress (see summary Figure 6.1). Our findings should shed light on our current understanding of LDs in pathology generally.

In Chapter 2 and 3, we showed that LDs accumulate in rodent cells exposed to environmental stressors, such as metallic nanoparticles and bacterial pathogen (LPS). The main findings from these two chapters were:

1) Oxidative and inflammatory stress upregulate perilipin-2 expression and lead to LD accumulation.
2) Unstaruated fatty acid-induced LDs play a protective role in cells undergoing starvation or oxidative injury
3) Pharmacological inhibition of p38 MAPK reduces LD accumulation under stressful conditions.
4) LDs may play a role in eicosanoid synthesis in LPS-activated microglia, thereby contributing to neuroinflammation.

Thereafter, in Chapter 4 we examined the effects of an anti-inflammatory n-3 polyunsaturated fatty acid on pro-inflammatory signaling and LDs in microglial cells. We found that DHA-initiated changes in LD dynamics and cellular lipidome weaken LPS-induced microglial activation by:

1) Specifically altering mitochondrial metabolism and signaling
2) Modulating TLR4 signaling that governs the inflammation process
3) Reducing the intracellular and extracellular levels of several inflammatory proteins and metabolites.

Findings from the first three manuscripts prompted us to explore the functions of LDs in human metabolic stress. More precisely, we chose to investigate LDs in T2DM and obesity, disorders characterized by increased oxidative stress and inflammation. The main

objective was to examine how LDs within the human pancreatic islets are affected by T2DM and obesity.

In Chapter 5, we show that:

1) Perilipin-2 expression is up-regulated in pancreatic islets and in extra-islet tissue of T2DM subjects.
2) T2DM causes alterations in the expression of many genes associated with lipid metabolism, oxidative stress and LD regulation.

Collectively, these findings suggest that LDs are involved in cellular stress response, and in particular, in metabolic stress in humans. In the following Chapter, we will present a synthesis of our findings and relate them to the existing literature.

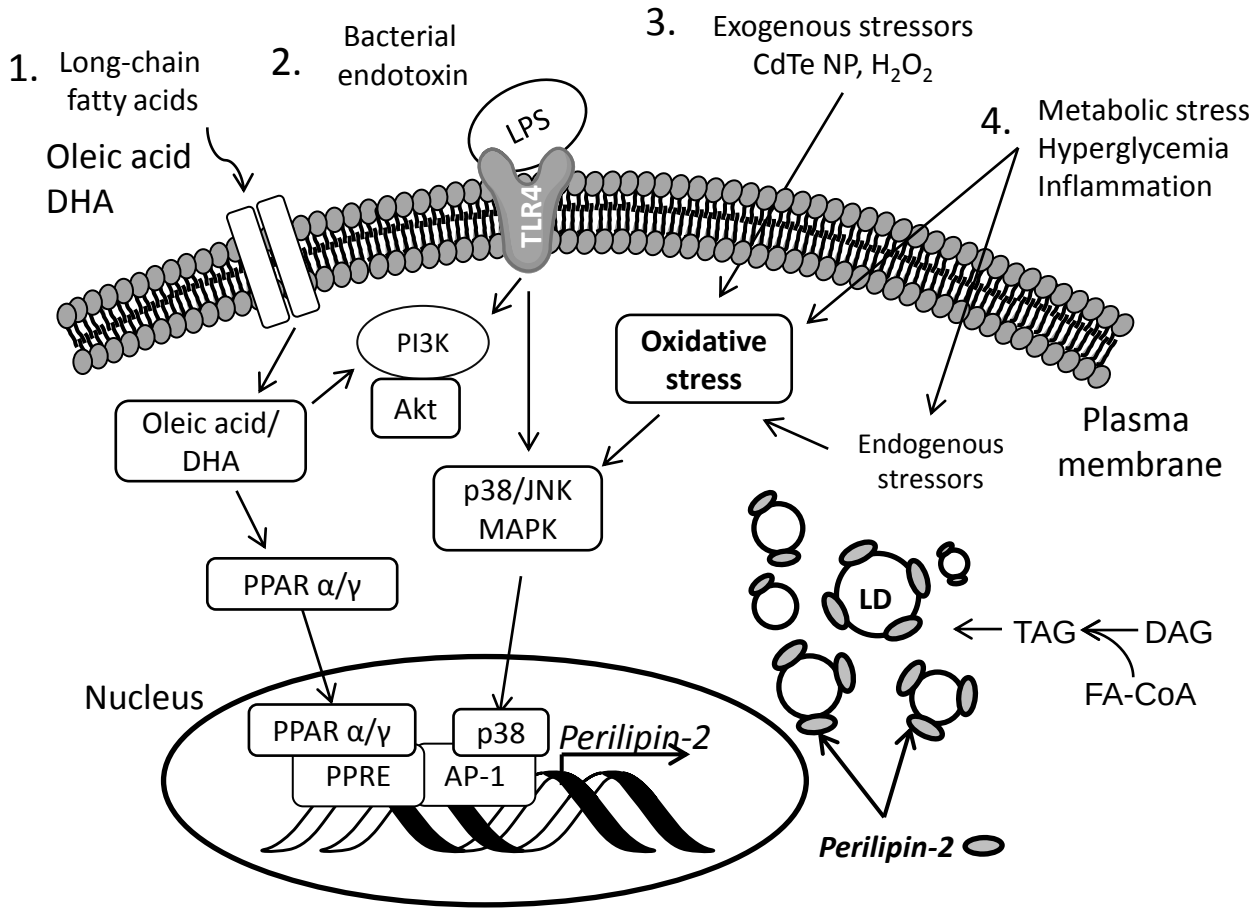

Figure 6.1. Schematic representation of LD formation induced by physiological or pathological stimuli.

In our studies, LDs were shown to be induced by either physiolgocial or pathological (stressful) stimuli. LD formation was increased upon treatment with 1) dietary fatty acids such as monounsaturated fatty acid, oleic acid, and polyunstaruated fatty acid, DHA, 2) bacterial endotoxin (e.g LPS), which binds to TLR4 and activates downstream inflammatory signaling pathways, 3) exogenous stressors (e.g CdTe nanoparticles and hydrogen peroxide), which induce oxidative stress and, finally, 4) hyperglycemia- and/or inflammation-induced metabolic stress during T2DM. ROS derived from endogenous sources of stress, such as mitochondria or NADPH oxidase, may contribute to LD accumulation.

6.1 Lipid droplets under oxidative stress: their regulation and function

In Chapter 2, we investigated the regulation and the roles of LDs under oxidative stress induced by exogenous stressors, H_2O_2 and cytotoxic CdTe nanoparticles. We showed that LDs accumulate under oxidative stress, even in the absence of an external source of fatty acids. Treatment with antioxidant NAC prevented LD accumulation (Chapter 2 and Appendix II). Additional data demonstrated that oxidative stress also increased the level of perilipin-2, which participates in LD formation (Appendix III).

In the following section, we will discuss potential mechanisms regulating LD formation in stressed cells and discuss our findings from Chapter 2.

6.1.1 Mechanisms involved in lipid droplet accumulation under stressful conditions

Recently, a number of studies reported LD accumulation under oxidative stress in different cell types (Gubern et al., 2009; Lee et al., 2012; Sekiya et al., 2008) . As we observed in our own studies, H_2O_2 treatment was reported to induce lipid accumulation (Sekiya et al., 2008). In adipocytes, a concentration of H_2O_2 similar to the one we used has been reported to induce LD accumulation, which was blocked by antioxidants such as NAC and flavonoids (Lee et al., 2012). Increased LD accumulation was strongly associated with increased ROS production and lipid accumulaton was associated with increased levels of ROS generated by pro-oxidant enzymes, such as NADPH oxidase 4 (NOX-4). Antioxidant treatment increased levels of antioxidant enzymes and prevented LD accumulation. Thus, these findings, together with our studies, establish causality between oxidative stress and LD accumulation.

Gubern et al. investigated LD biogenesis in Chinese hamster ovary (CHO-K1) cells exposed to various types of stress, including low pH, C_2-ceramide, tunicamycin and glucose deprivation (Gubern et al., 2009). All the treatments examined increased TAG synthesis and LD formation, and there was a strong correlation between the amount of TAG synthesised and LDs formed. Perilipin-2 expression was highly up-regulated in stressed cells. In stressed cells, LD biogenesis and TAG synthesis took place in the

absence of external source of fatty acid and did not require *de novo* fatty acid synthesis. The authors hypothesized that alterations in phospholipid metabolism in stressed cells may contribute to TAG synthesis. They found that TAG synthesis and LD biogenesis were dependent on pre-existing fatty acids released from phospholipid membranes by phospholipases.

Other studies have also suggested that alterations in phospholipid metabolism in stressed cells may lead to increased TAG synthesis (Al-Saffar et al., 2002; Iorio et al., 2003). Phospholipids are synthesized from diacylglycerol (DAG), which is a precursor to TAG (see Figure 1.2). It was proposed that in stressed cells, a reduction in phospholipid biosynthesis or the activation of specific phospholipases likely lead to increased levels of DAG, which are converted to TAG by an acylation reaction mediated by acyl-CoA transferase. If not converted to TAG, DAG may induce toxicity. Therefore, increased TAG synthesis in stressed cells may protect cells from DAG toxicity.

As mentioned in Chapter 1, LD accumulation following induction of apoptosis has long been known and reported in many different cell types (Al-Saffar et al., 2002; Boren & Brindle, 2012; Callies et al., 1993; Delikatny et al., 2002; Hakumaki & Kauppinen, 2000; Hakumaki et al., 1999; Schmitz et al., 2005). In Chapter 2, cell culture treatment with toxic CdTe nanoparticles was associated with a large accumulation of LDs in the cells and a concomitant decrease in cell viability. While we did not try to detect apoptosis in the treated cultures, we believe that many of the cells accumulating LDs were in a pre-apoptotic or apoptotic state, a proposal based on studies from our group which demonstrated that CdTe nanoparticle-related cytotoxic events may lead to apoptosis (Choi et al., 2007).

In our additional experiments described in Appendices IV and V, we showed a potential role for p38 MAPK in the regulation of LD accumulation. Treatments with CdTe nanoparticles and H_2O_2 strongly enhanced phosphorylation of p38 and JNK MAPKs and up-regulated perililin-2. We hypothesized that during oxidative stress, p38 MAPK and JNK may regulate LD formation by up-regulating the expression of perilipin-2. This hypothesis was based on evidence for perililpin-2 expression being regulated by activator protein -1 (AP-1) (Wei et al., 2005), a transcription factor activated by p38

MAPK. In fact, pharmacological inhibition of p38 MAPK, but not of JNK, reduced LD accumulation. These results suggest that p38 MAPK may mediate the accumulation of LDs in stressed cells and possibly under pathological conditions characterized by oxidative stress.

Mitochondrial damage, inhibition of mitochondrial B-oxidation, and lipid droplet accumulation

Toxic agents or stressful conditions that induce mitochondrial damage have been shown to lead to LD accumulation (Boren & Brindle, 2012; de Estable-Puig & Estable-Puig, 1973; Delikatny et al., 2002). In keeping with these reports, our studies indicated that mitochondrial disruption (cisternae disruption and decreased mitochondrial metabolic activity) in cells exposed to cytotoxic nanoparticles was also accompanied by LD accumulation (see Chapter 2). There is a growing body of evidence suggesting that inhibition of mitochondrial fatty acid β-oxidation diverts FFA to TAG synthesis, resulting in LD accumulation (Boren & Brindle, 2012). This process is mediated by acyl-CoA synthetase, an enzyme that catalyzes the ATP-dependent activation of FFA to fatty acyl-CoA. The inhibition of mitochondrial fatty acid β-oxidation may be explained by the increased mitochondrial ROS production in stressed cells (Boren & Brindle, 2012). In line with these findings, it is possible that LD accumulation in cells exposed to toxic CdTe nanoparticles was partly due to inhibition of mitochondrial fatty acid β-oxidation by ROS.

Other mechanisms leading to LD accumulation in stressed cells have also been suggested. Lysosomal processing of damaged mitochondrial membrane may lead to a large amount of fatty acids available for TAG synthesis (Delikatny et al., 2002; Griffin et al., 2003). In our studies in Chapter 2, we found that LDs and lysosomes colocalized in stressed cells, suggesting that there may be a functional communication between these organelles. In fact, it was recently shown that LDs may be delivered to lysosomes via autophagy, where lysosomal acid lipases process neutral lipids of LDs (Ouimet et al., 2011).

Another possible mechanism is that TAG synthesis is enhanced following uptake of fatty acids from extracellular sources of lipids, such as serum (Maurel et al., 2012). However,

this last mechanism cannot explain the accumulation of LDs in our experiments, since the cells were cultured in a serum-free environment.

6.1.2 Roles of lipid droplets produced as a consequence of oxidative stress

LDs may play different functions in cells undergoing oxidative stress. For instance, LD formation may be a survival strategy, achieved through increasing intracellular fuel stores in stressed cells (Gubern et al., 2009). In this scenario, fatty acids used for structural purposes, such as phospholipid membrane synthesis, are instead used for TAG synthesis and can be reused as fuel to provide energy.

A mounting body of evidence indicates that LD formation in stressed cells plays a protective role, since it prevents the accumulation of toxic lipids in the cytosol (Boren & Brindle, 2012; Hapala et al., 2011). Failure to store these lipids into TAG as non-toxic lipid species may lead to lipotoxicity and cell death.

It was suggested that LDs formed in stressed cells could serve as temporary hydrophobic storage sites for misfolded proteins and toxic lipids that accumulate in the endoplasmic reticulum (ER) and cause ER stress (Hapala et al., 2011). Translocation of misfolded proteins to the LDs may facilitate their degradation by the proteasome or by autophagy (Ohsaki et al., 2006). Thus, LDs may participate in relieving ER stress by sequestering toxic lipids and misfolded proteins.

6.1.2.1 Lipid droplets induced by stress versus lipid droplets induced by dietary fatty acid

In Chapter 2, we proposed that the induction of LDs under stressful conditions could represent a protective cellular response to stress. While it is well-known that LDs formed by fatty acids such as oleic acid likely serve as energy stores and provide energy to starving cells, it is less clear how stress-induced LDs could also play a protective role. These two types of LD populations likely differ in the manner by which they confer cytoprotection. The molecular composition of these LDs, such as the proteins and lipids present on/in these LDs, could possibly determine their function. In this regard,

proteomic and lipidomic studies on purified LDs could imporve our understanding of LD function following their induction by different stimuli (Yang et al., 2012).

6.1.3 Saturated versus unsaturated fatty acids

In Chapter 2, we demonstrated that unsaturated fatty acid (e.g. oleic acid) treatment stimulates LD formation and rescues cells from nanoparticle-induced cell death. Saturated fatty acids are poorly incorporated into TAG and are associated with cytotoxicity, apoptosis and insulin resistance (Cnop et al., 2001; Listenberger et al., 2003; Maedler et al., 2001; Storlien et al., 1991), whereas unsaturated (or monounsaturated) fatty acids (e.g. oleic acid) are readily incorporated into TAG and are associated with cytoprotection and cell proliferation (Cnop et al., 2001; Listenberger et al., 2003; Maedler et al., 2001). We too have observed striking differences between saturated (e.g palmitic acid) and unsaturated fatty acids (e.g oleic acid) on cell viability. Palmitic acid treatment of PC12 cells resulted in a dramatic decrease in cell viability (see Figure 2.5). Conversely, oleic acid treatment did not show toxicity and caused a strong accumulation of LDs. Interestingly, pre-treatment with oleic acid rescued cells from serum starvation and nanoparticle-induced toxicity, whereas palmitic acid treatment showed no protective effect whatsoever. Similarly, no toxicity was observed in oleic acid-treated microglial cells (Chapter 3). Thus, our findings point to a protective role of LD (or TAG) accumulation following unsaturated fatty acid treatment.

6.2 Lipid droplets in inflammatory cells

As mentioned earlier (in Chapter 1), accumulation of LDs in leukocytes following their stimulation with pro-inflammatory agents has been widely reported (Bozza et al., 2009). Given that LDs are highly abundant in inflammatory leukocytes, they are considered to be structural markers of inflammation. While LDs have been extensively studied in peripheral leukocytes and macrophages, they have rarely been investigated in immune cells in the central nervous system. This is what prompted us to investigate LDs in microglia (Chapter 3), the resident immune cells in the brain. Since we were particularly

interested in studying their roles under inflammatory conditions, LDs were studied in endotoxin (LPS) -stimulated microglia.

6.2.1 Features of lipid droplets in microglia

The presence of cytoplasmic LDs in human or rodent microglial cells has been known for a long time (Sturrock, 1984). In Chapter 3, we proposed that LD accumulation in activated microglia may be involved in pro-inflammatory lipid mediator synthesis and contribute to neuroinflammation. In line with this idea, other *in vivo* and *in vitro* studies also suggest an implication of LDs in neuroinflammation and neurodegenerative processes.

One piece of evidence in support of the implication of LDs in neuroinflammatory processes comes from a relatively recent study on retinal degeneration. Microglia were found to be highly activated in degenerating retina and contained a large number of LDs in them (Ebert et al., 2009). This was associated with upregulation of several genes involved in LD formation (e.g perilipin-2, PPARγ) and pro-inflammatory lipid synthesis (e.g leukotriene C4 synthase).

In a more recent study, mice fed an atherogenic diet showed accumulation of neutral lipids and LDs in the brain and this was associated with a recruitment of inflammatory cells and with microglial activation (Denes et al., 2012).

In another study, *in vivo* imaging following intranasal delivery of LPS-conjugated nanoparticles in mice showed robust microglial activation in the olfactory bulb (Lalancette-Hebert et al., 2010); a parallel *in vitro* study indicated the presence of large LDs in microglia exposed to these same nanoparticles.

In the past, accumulation of LDs in microglia has been observed under stressful and degenerative conditions e.g in degenerating white matter of cats or kittens after dorsal rhizotomy (Franson, 1985; Franson, 1988), following chronic administration of sodium valproate to rats (Sobaniec-Lotowska, 2005), during Wallerian (or anterograde) degeneration in the optic nerve of adult rats (Carbonell et al., 1991), in the developing

cerebellum of rats following X-ray irradiation (Das, 1976), and during degeneration of primary sensory neurons in newborn rats following capsaicin treatment (Jancso, 1978). Microglia containing large amounts of LDs were in a highly reactive state engaged in phagocytosis of degenerated neuronal debri (Jancso, 1978). On the basis of these observations, LDs seem very likely to be involved in the response of microglia to environmental stress (e.g neurotoxic injury).

6.2.2 Lipid droplets: compartments specialized in eicosanoid synthesis

Eicosanoids, such as prostaglandins and leukotrienes, are inflammatory lipid mediators derived from arachidonic acid, a n-6 (omega-6) polyunsaturated fatty acid. Several lines of evidence suggest that LDs are sites involved in eicosanoid synthesis during inflammatory processes (Accioly et al., 2008; Yu et al., 1998). The presence of several eicosanoid-forming enzymes on the surface of LDs supports this hypothesis. Accordingly, cPLA$_2$-α, leukotriene C4 (LTC4) synthase, 5- and 15-lipoxygenases (5- and 15-LOX), cycloxygenase-2 (COX-2) and prostaglandin E (PGE) synthase are some the eicosanoid-synthesizing enzymes shown to associate with LDs (Accioly et al., 2008; Dvorak et al., 1993; Meadows et al., 2005; Pacheco et al., 2002). Moreover, an important correlation between LD formation and increased synthesis of eicosanoids derived from LOX and COX enzymes has been observed, indicating that LD accumulation may increase the eicosanoid-generating capacity of leukocytes.

As in peripheral immune cells, microglia can synthesise eicosanoids from arachidonic acid and are involved in neuroinflammation (Matsuo et al., 1995; Tassoni et al., 2008). Following brain injury or infection, microglial cells become hyperactive and migrate to the affected site, where they secrete cytokines, chemokines, nitric oxide and eicosanoids (Rock et al., 2004). The prostaglandin and leukotriene released from microglia exert pro-inflammatory effects, mediate chemotaxis of leukocytes, increase ROS production and disrupt the blood brain barrier (Tassoni et al., 2008). The release of arachidonic acid from phospholipid membranes in neural cells, such as astrocytes and neurons, is mediated by different isoforms of PLA$_2$ (Sun et al., 2004). However, much less is known about PLA$_2$ in microglial cells, since it is more difficult to isolate sufficient amount of these cells to

perform biochemical analysis. $cPLA_2$-α, the cytosolic form of PLA_2, is activated in response to diverse types of pathogenic stimuli and contribute to the progression of neuroinflammation by increasing the release of arachidonic acid from phospholipid membranes (Farooqui & Horrocks, 2006; Farooqui et al., 2007).

TLR4 signaling pathway is essential for LPS-induced activation of $cPLA_2$-α and subsequent release of inflammatory lipid mediators (Qi & Shelhamer, 2005). Studies done in Chapter 3 and -4 revealed colocalization of $cPLA_2$-α with LPS-induced LDs in microglia. Interestingly, such colocalization of $cPLA_2$-α with LDs was virtually absent in microglia treated with with anti-inflammatory fatty acid DHA, and even with oleic acid. This finding suggested that the translocation of $cPLA_2$-α onto LDs may be an important component of the inflammatory response of microglia to endotoxin.

Colocalization of $cPLA_2$-α with LDs has previously been reported in other cells types such as human monocytic cells (Yu et al., 1998). In these cells, $cPLA_2$-α and its activating MAPK colocalized with cytoplasmic LDs, which were enriched with arachidonic acid. This suggested that compartmentalization of $cPLA_2$-α and its activating kinases at LDs may represent an efficient mechanism for eicosanoid formation in activated leukocytes.

In the light of these findings, we suggest that LDs might well play a role in arachidonic acid metabolism and eicosanoid formation in microglia. However, additional studies are needed in order to confirm these observations. First, eicosanoid release in the extracellular media in the presence or absence of inhibitors of LD formation would show a causal relationship between LD formation and eicosanoid synthesis. Second, we need to know whether other specialized eicosanoid synthesising enzymes downstream of cPLA2-α, such as 5-LOX and COX-2, are also associated with LDs in activated microglia. Finally, lipidomic analysis of purified LDs would confirm the presence of eicosanoid precursors (e.g arachidonic acid) in these organelles in microglia.

In Chapter 4, we continued investigating the roles of LDs in pro-inflammatory microglia and were particularly interested in exploring the anti-inflammatory effects of DHA, an n-3 polyunsaturated fatty acid, in LPS-stimulated microglia. Accordingly, because DHA

was previously shown to alter LD abundance in microglia (Ebert et al., 2009), we sought to understand the implication of LDs in the immunomodulating effects of DHA.

6.2.3 DHA: an anti-inflammatory fatty acid with lipid droplet modulating properties

In Chapter 4, our findings showed that alterations in LD dynamics and morphology were highly implicated in the anti-inflammatory effects of DHA in hyperactive microglia. DHA treatment attenuated LPS-induced microglial activation and caused marked alterations in LD size and accumulation. DHA increased the number of small and medium sized LDs in cells and significantly reduced the average distance between LDs and mitochondria. It also reversed the LPS-induced reduction in mitochondrial metabolic activity. Finally, DHA treatment modulated TLR4-initiated pro-inflammatory signaling in LPS-stimulated microglia.

Our observations are consistent with previous findings from Ebert et al., who also showed that DHA suppresses pro-inflammatory signaling *in vitro and in vivo* in microglia (Ebert et al., 2009). The authors also showed that DHA reduces LD accumulation in LPS-activated microglia *in vitro,* although they did not perform quantitative analysis of their sizes and number. They speculated that the suppression of LD formation by DHA dampens production of pro-inflammatory lipid mediators, such as prostaglandins and leukotrienes. In line with this idea, in Chapter 4 we showed that DHA treatment promotes the removal of eicosanoid-synthesizing enzymes $cPLA_2$-α from LDs, and suggested that this may prevent the conversion of arachidonic acid into prostaglandins or leukotrienes.

6.3 Lipid droplets and perilipin-2 in type 2 diabetes mellitus

As previously mentioned (Chapter 1), obesity and T2DM are characterized by excess lipid (e.g TAG) deposition in peripheral tissues such as muscle, heart, liver and pancreas (van Herpen & Schrauwen-Hinderling, 2008) (see Figure 1.6). This excessive lipid deposition in tissues, which is caused by increased levels of circulating FFA, may lead to cellular damage and cell death (lipotoxicity). However, sequestration of excess toxic FFA

within LDs in the form of TAG may partly prevent lipotoxicity (Cnop et al., 2001; Listenberger et al., 2003). In this regard, LD-associated proteins, namely perilipin-2, play a critical role in orchestrating TAG storage and LD formation.

In rodent models of T2DM, islet TAG increases during the progression of T2DM and is associated with β-cell lipotoxicity (Lee et al., 1994; Lee et al., 2010). Moreover, numerous cytoplasmic LDs can be seen in these same islets. These observations have suggested that LDs might play a role in lipotoxic events which contribute to functional impairments in β-cells. While the role of islet lipotoxicity in T2DM has been well documented in rodents, it remains to be shown whether this is also the case in human islets.

6.3.1 Upregulation of perilipin-2 in type 2 diabetes mellitus

In chapter 5, our immunohistochemical and gene expression studies revealed a marked increase in perilipin-2 in human post-mortem pancreas obtained from lean and obese T2DM individuals. Immunohistochemical analysis showed that perilipin-2 was highly increased in pancreatic islets, and that is strongly colocalized with insulin-secreting β-cells. To our knowledge, this was the first study investigating perilipin-2 in the pancreas of T2DM subjects.

Interestingly, alterations in perilipin-2 expression were previously reported in other tissues in obese T2DM rodents, such as ZDF rats and db/db mice. These rodent models of obesity/T2DM develop dyslipidemia (e.g hyperlipidemia), insulin resistance and hyperglycemia (Kobayashi et al., 2000; Lee et al., 1994). It was found that perilipin-2 levels were increased in muscle and kidneys of obese ZDF rats and db/db mice, respectively (Minnaard et al., 2009; Mishra et al., 2004). This was shown by gene exression profiling and by measurements of protein levels through immunohistochemistry and western blotting. The apparent increase in perilipin-2 occurred in parallel with a marked accumulation of cytoplasmic LDs in the examined tissues. It was suggested that perilipin-2 may facilitate the uptake of lipids (e.g long-chain fatty acids) from the extracellular environment and regulate lipid accumulation in muscle

or kidney during diabetes. In contrast to rodents, there was no difference in perilipin-2 and muscle lipid content between T2DM patients and BMI-matched control subjects (Minnaard et al., 2009; Phillips et al., 2005). The role of perilipin-2 in the development of insulin resistance in muscle remains unclear. While Minnaard et al. show that reduced levels of perilipin-2 in rodent muscle tissue are associated with improved insulin sensitivity following insulin sensitizer treatment, Phillip et al. show the opposite. They propose that in skeletal muscle, perilipin-2 sequesters FFAs into TAG and protects from detrimental effects of FFA on insulin signaling and glucose tolerance (Phillips et al., 2005).

6.3.2 Reglation of perilipin-2 by peroxisome proliferator activated receptors

It is known that perilipin-2 can be transcriptionally regulated by PPARα and -γ (Edvardsson et al., 2006; Fan et al., 2009), nuclear hormone receptors that bind fatty acid ligands and activate transcription of numerous genes involved in lipid metabolism. PPARγ is highly expressed in adipose tissue and participates in fatty acid uptake and lipid storage (e.g TAG synthesis). PPAR α is mostly expressed in tissues with high oxidative capacity and participates in fatty acid uptake and mitochondrial β-oxidation of FFAs (Martin et al., 2007).

In our studies, both perilipin-2 and PPARα expression were increased in the pancreas of obese and T2DM subjects. It is possible that the increased expression of perilipin-2 was caused by PPARα, which is known to regulate perilipin-2 expression by binding to a PPAR response element (PPRE) in the promoter region of perilipin-2 (Targett-Adams et al., 2005). Similar observations have been previously reported in other tissues. For instance, upregulation of perilipin-2 in the kidneys of db/db mice was accompanied with elevated expression of PPARα (Mishra et al., 2004).

Currently, there is sufficient evidence indicating a protective role of PPARα and -γ in metabolic disorders. A protective role for PPARα was has been reported in obesity-associated T2DM (Lalloyer et al., 2006). In fact, PPARα knockout mice developed

pancreatic β-cell dysfunction. Moreover, PPARα agonist treatment prevented fatty acid-induced lipotoxicity in human islets (Lalloyer et al., 2006).

6.3.3 Lipid droplet formation as a protective mechanism against lipotoxicity

We previously mentioned that peripheral insulin resistance increases lipolysis of TAG in adipose tissue, resulting in increased levels of plasma FFAs and leading to their accumulation in the form of TAGs (or LDs) in non-adipose tissues such as liver and muscle.

While TAG accumulation is often observed in pathologies characterized by lipotoxic events, it is suggested that it may serve, at least during the early stages of pathology, a protective role (Listenberger et al., 2003): increased synthesis of TAG from FFA accumulating in cells minimizes the increase in cytosolic toxic FFA levels (Choi & Diehl, 2008; Listenberger et al., 2003; Schaffer, 2003). Substantial evidence points to protective roles of LDs during obesity and insulin resistance (Choi & Diehl, 2008). Accorindingly, the ability of liver and muscle cells to store excess FFAs in the form of TAG is proposed to play a protective role in lipotoxicity and insulin resistance in skeletal muscle (Bosma et al., 2012; Choi & Diehl, 2008; Moro et al., 2008).

In light of the facts mentioned above, the TAG accumulation in pancreatic islet β-cells observed in the early stages of T2DM may serve a protective role. A growing number of studies indicate that sequestration of FFA into TAG protects pancreatic islets and β-cells from lipotoxicity (Borg et al., 2009; Cnop et al., 2001; Winzell et al., 2010). An inverse relationship was observed between FFA cytotoxicity and TAG accumulation in β-cells cells (Cnop et al., 2001). These findings are supported by a study done in transgenic mice over-expressing hormone-sensitive lipase (HSL) in β-cells (Winzell et al., 2010). Overexpression of HSL partly prevented accumulation of TAG in islets upon high-fat diet feeding and was associated with lipotoxicity and ensuing β-cell dysfunction. However, this protection may be eventually lost during prolonged TAG accumulation *in vivo* (Cnop et al., 2001), leading to lipotoxic events.

Role of perilipin proteins in protection against lipotoxicity

LD-associated proteins perilipin-1 and perilipin-2 positively regulate TAG storage/LD accumulation by reducing the access of lipases to the surface of LDs and preventing TAG hydrolysis (Listenberger et al., 2007). Thus, perilipin proteins may protect from lipotoxicity by reducing FFA leakage from LDs therebypreventing FFA-induced cytoxocity. Recently, it was shown that increased expression of perilipin-2 in skeletal muscle enhances storage of FFA into TAG and is paralleled by an improved insulin sensitivity (Bosma et al., 2012). Furthermore, overexpression of muscle perilipin-2 *in vivo* resulted in LD accumulation and prevented high-fat diet-induced abnormalities at the level of oxidative phosphorylation.

Consistent with these findings from skeletal muscle, overexpression of perilipin-1 protected pancreatic β-cells (INS-1 cell line) from lipotoxicity by limiting lipolysis and by promoting storage of FFAs into TAG in LDs (Borg et al., 2009). Moreover, glucose-stimulated insulin secretion (GSIS) was improved in cells overexpressing perilipin-1 when exposed to palmitic acid for an extended period. How perilipin-2 prevents lipotoxicity in islets remains unknown. Future studies are needed to show whether overexpression, knock-down or knock-out of perilipin-2 alters lipotoxicity in islets of T2DM subjects.

In Chapter 5, our studies revealed a striking increase in perilipin-2 expression in pancreatic islets and also in the extra-islet environment of donors with T2DM. We suggest that perilipin-2 in islet cells, particularly in β-cells, serves a protective role against lipotoxicity: perilipin-2 reduces FFA leakage from LDs and thereby prevents or delays β-cell lipotoxicity in T2DM patients. However, as TAG levels continue to increase, perilipin-2 may be unable to cope with the extreme amounts of TAG and in consequence may lose its capacity to reduce lipolysis.

6.4 Conclusions

In the past decade, LDs have emerged as dynamic organelles regulating cellular lipid metabolism, energy homeostasis, and cellular signaling. However, one of the most interesting aspects of LDs is their involvement in inflammation, and in degenerative and metabolic diseases. In this work, we studied LDs during experimentally-induced stressful conditions and in human pathology. We provided further evidence that they are involved in metabolic diseases like T2DM. Our findings reinforce the notion that LDs and their associated proteins are induced by various types of stress, a phenomenon that is evolutionarily conserved among plants, yeast and mammals. Figure 6.2 summarizes the different scenarios of cellular LD content:1) too few LDs in lipodystrophies, during which adipose tissue is severly diminished, 2) normal LD content under physiological conditions and 3) excessive accumulation of LDs in disease states such as T2DM. As mentioned in our manuscripts and in the discussion, this adaptive response to stress may be cytoprotective. In fact, it is suggested that LD formation relieves ER-stress by sequestering toxic lipids and misfolded proteins on their surface. Such recruitment of misfolded proteins may prevent formation of toxic aggregates (Welte, 2007). These proteins recruited to the LD surface may eventually undergo proteasomal degradation in an organized manner.

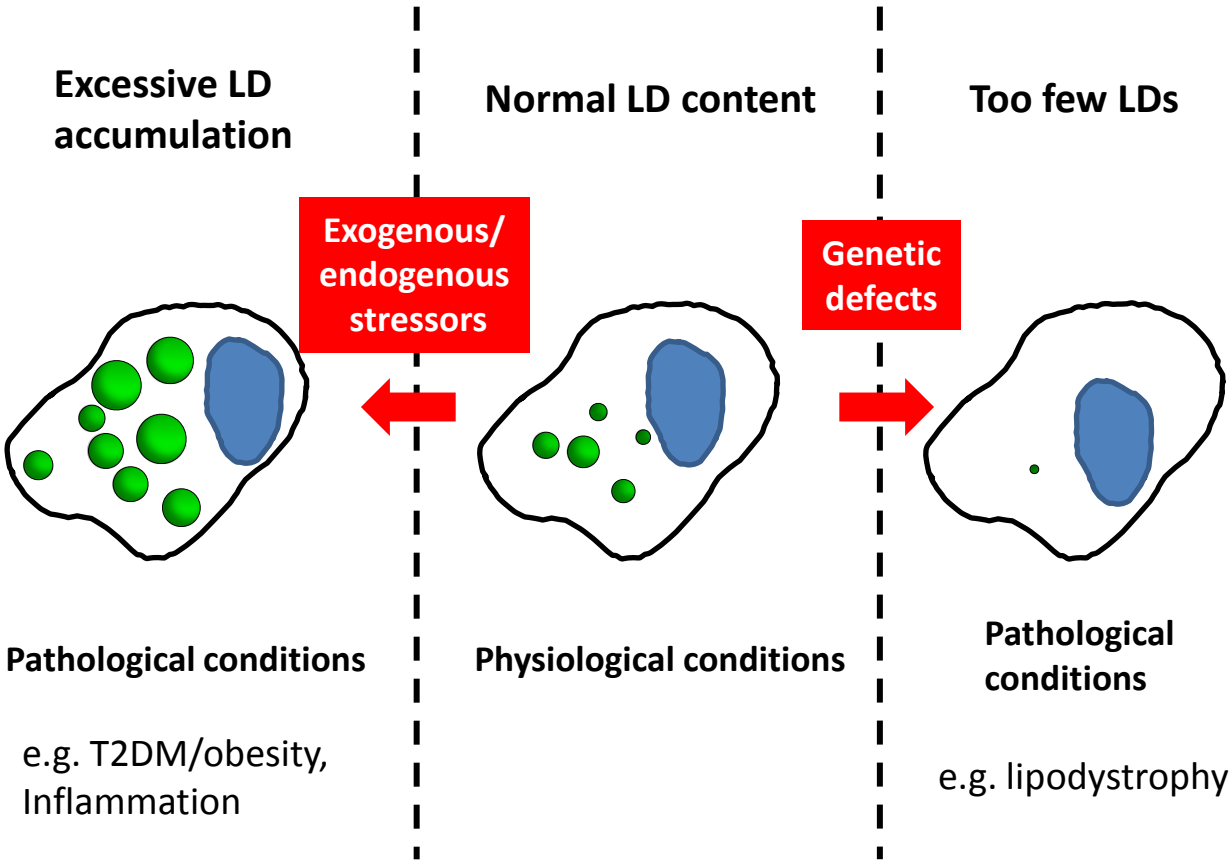

Figure 6.2 Schematic illustration showing cellular LD content under physiological conditions and pathological conditions.

LDs appear to be highly increased in non-adipose tissue during metabolic diseases such as T2DM. On the hand, a marked depletion of LDs in adipose tissue may also occur during lipodystrophy and is undesirable. A normal LD content is ideal for maintaining cellular lipid homeostasis.

It is now recognized that LDs play a critical role in protection from lipotoxicity by serving as a storage site for excess toxic FFA in the form of TAG (Listenberger et al., 2003). A recent study confirmed this idea by showing that LD formation protects against glucotoxicity and lipotoxicity (Nguyen & Nosanchuk, 2011). Of note, the lipotoxicity was strongly associated with saturated, but not unsaturated fatty acids. Importantly, while initial accumulation of LDs may play a protective role, chronically elevated LD formation may eventually be deleterious to cells. Therefore, LD accumulation in tissues as a result of metabolic diseases such as T2DM and obesity could play a protective role against lipotoxicity, at least until the storing capacity of LDs is exceeded. This mechanism would be of major importance in pancreatic islet β-cells, since the failure to store FFAs into TAG/LDs would be deleterious to β-cell function and could even cause cell death. Noteworthy, β-cells are particularly sensitive to oxidative stress due to their low antioxidant capacity and therefore are highly susceptible to lipotoxic and glucotoxic events (Drews et al., 2010)

In this decade, one of the greatest challenges in the field of LDs and metabolic disorders will be to come up with new strategies to prevent obesity-associated lipotoxicity. In 2008, Ducharme and Bickel proposed that one strategy to prevent lipotoxicity in non-adipose tissue could be to trap excess lipids in the adipose tissue by favoring LD expandability in adipocytes. This can be achieved by manipulating levels of specific LD proteins that are involved in stabilizing the LD surface and which can prevent the spillover of FFAs from LDs into the cytosol and subsequently into the circulation. A similar strategy could be applied in non-adipose tissue by altering levels of perililin-2 in such a way as to enhance the stability of LDs. This would considerably reduce the leakage of toxic FFA and prevent related adverse effects, such as insulin resistance.

APPENDICES

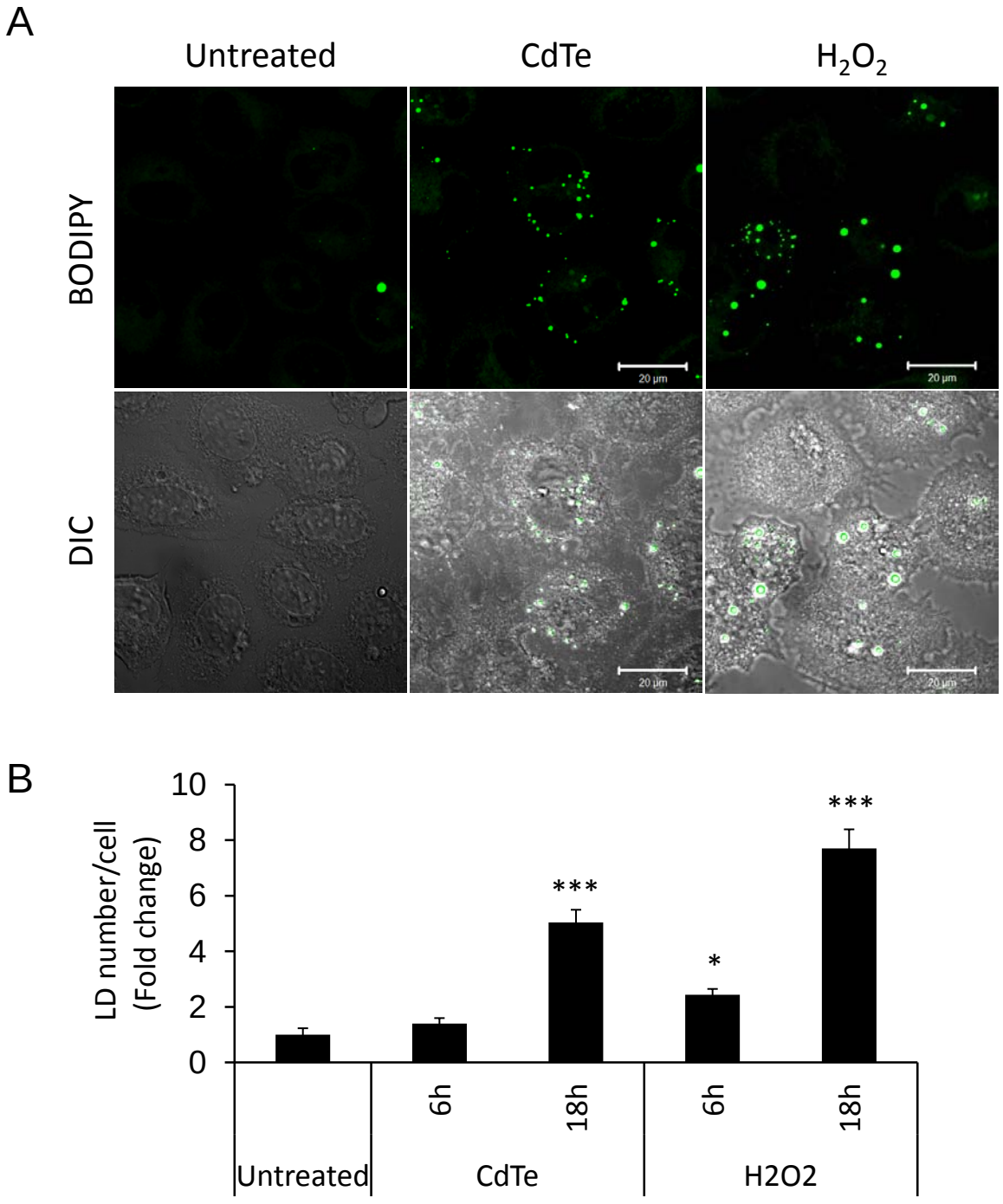
A
Untreated
CdTe
H2O2
BODIPY
DIC
20 µm
B
LD number/cell
(Fold change)
10
8
6
4
2
0
***
*
***
6h
18h
6h
18h
Untreated
CdTe
H2O2

Appendix I

Confocal imaging of LD accumulation in CdTe and H_2O_2-treated PC12 cells

(A) Confocal Z-stack images showing LDs in cells exposed to CdTe (10 µg/ml) or H_2O_2 (50 µM) overnight (18h). LDs were labeled with BODIPY 493/503 (10 µM). Scale bar, 20 µm.

(B) Quantification of number of LDs per cell following CdTe- or H_2O_2- treatment (6 or 18h). Bars show average LD number/cell expressed as fold-increase over untreated group. Statistically significant differences are indicated by *** $p<.005$ or *$p<0.05$.

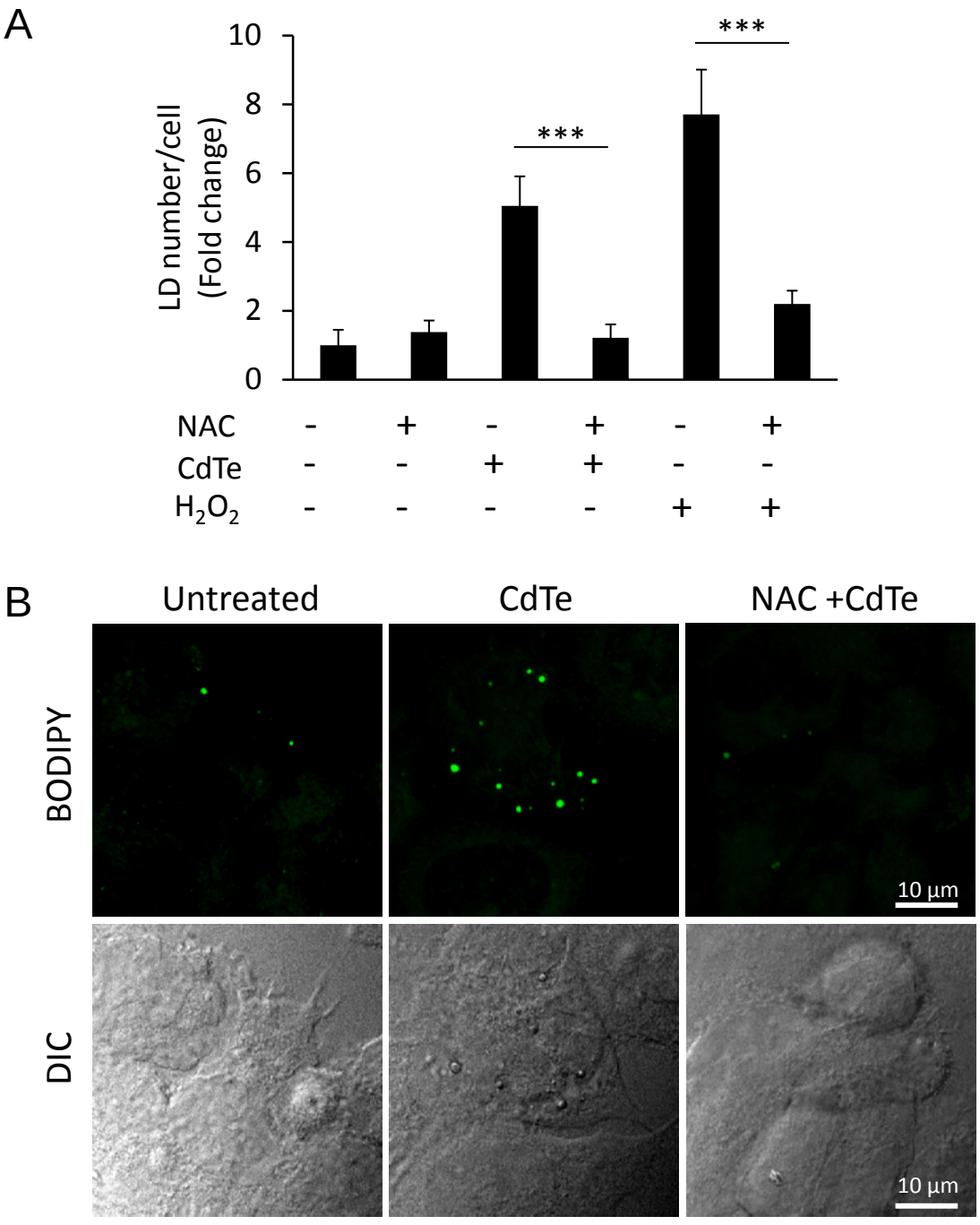
A
LD number/cell
(Fold change)
10
8
6
4
2
0
***
***
NAC - + - + - +
CdTe - - + + - -
H2O2 - - - - + +
B
Untreated
CdTe
NAC +CdTe
BODIPY
DIC
10 µm
10 µm

Appendix II

Antioxidant (NAC) inhibits LD accumulation induced by CdTe and H_2O_2 in PC12 cells.

(A) Assessment of the effect of pre-treatment with NAC on LD number/cell following exposure to CdTe and H_2O_2. Cells were pre-treated with NAC (2 mM, 30 min) and treated with CdTe (10 µg/ml) or H_2O_2 (50 µM) overnight (18h). Bars show average LD number/cell expressed as fold-increase over untreated group. Statistically significant differences are indicated by *** $p<.005$.

(B) Representative confocal Z-stack images showing LDs in cells pre-treated with NAC and exposed to CdTe. Scale bar, 10 µm.

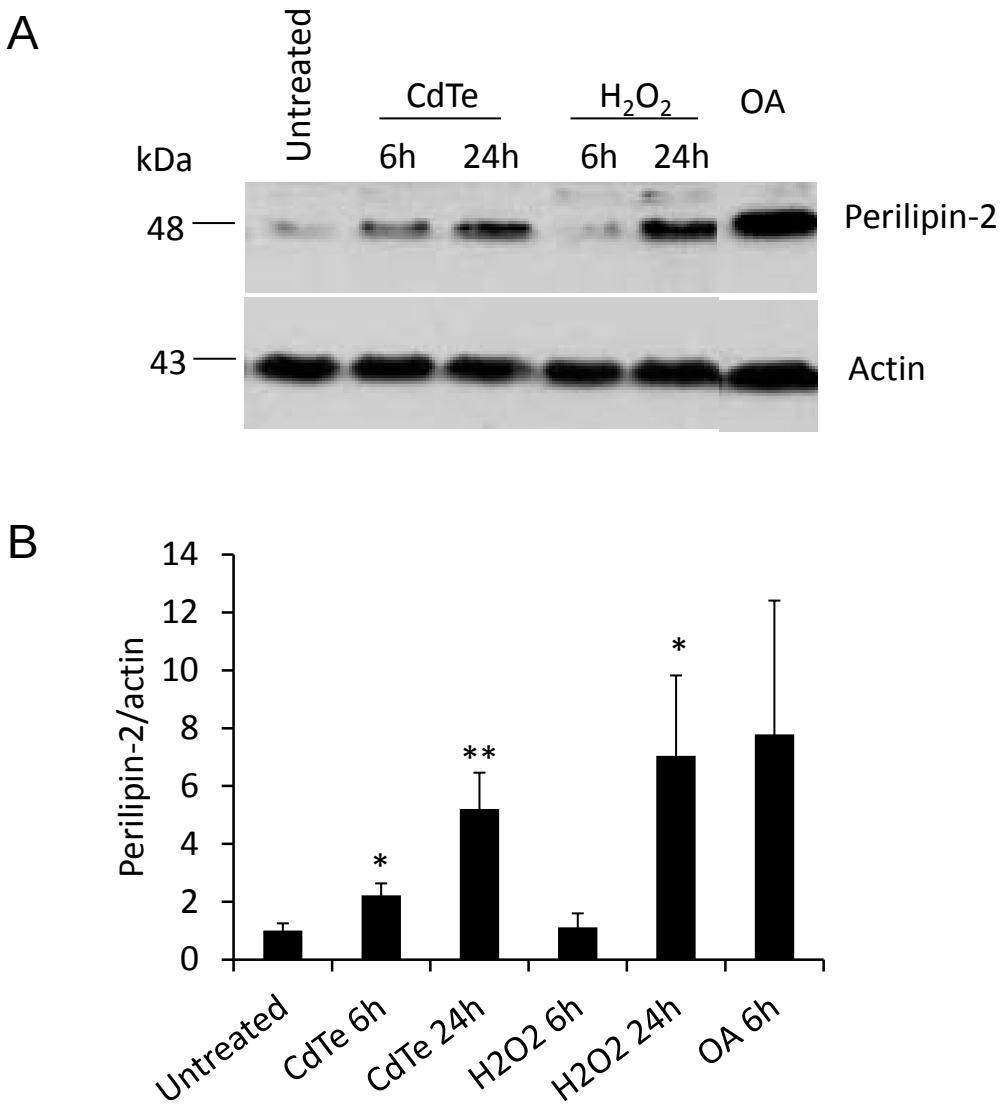
A
Untreated
CdTe
H2O2
OA
kDa
6h
24h
6h
24h
48
Perilipin-2
43
Actin
B
Perilipin-2/actin
14
12
10
8
6
4
2
0
*
**
*
Untreated
CdTe 6h
CdTe 24h
H2O2 6h
H2O2 24h
OA 6h

Appendix III

Oxidative stress increases perilipin-2 expression

(A) PC12 cells were treated with CdTe (10 µg/ml) or H_2O_2 (50 µM) for either 6h or 24h in serum-free media and harvested for western blot analysis. Oleic acid treatment (6h, 50 µM) was used as a control for perilipin-2 induction. Perilipin-2 in whole cell lysates was detected by using a polyclonal antibody to perilipin-2.

(B) Densitometric analysis of perilipin-2 in stressed cells. Perilipin-2 signal was normalized to that of actin and expressed as perilipin-2/actin. Bar graphs show fold increase in perilipin-2 over untreated cells. Statistically significant differences are indicated by *$p<0.05$ and **$p<0.01$.

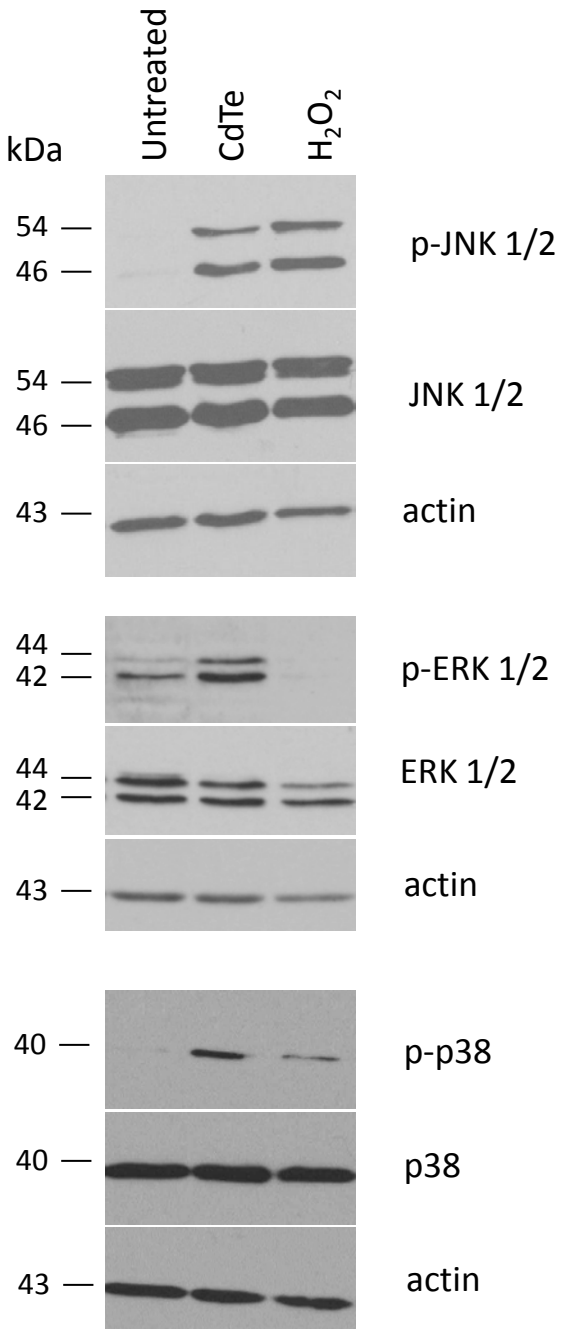
Untreated
CdTe
H_2O_2
kDa
54
46
p-JNK 1/2
54
46
JNK 1/2
43
actin
44
42
p-ERK 1/2
44
42
ERK 1/2
43
actin
40
p-p38
40
p38
43
actin

Appendix IV

Activation of JNK, ERK and p38 MAPK upon treatment with CdTe nanoparticles and H_2O_2.

Serum-starved PC12 cells were treated with CdTe (10 µg/ml) or H_2O_2 (50 µM) for 6h. Cells were harvested and whole cell lysates prepared for western blot analysis. Specific antibodies were used to detect either the phosphorylated or the non-phosphorylated forms of JNK (1, 2), ERK (1, 2) and p38 MAPK. Actin was used as a loading control.

A

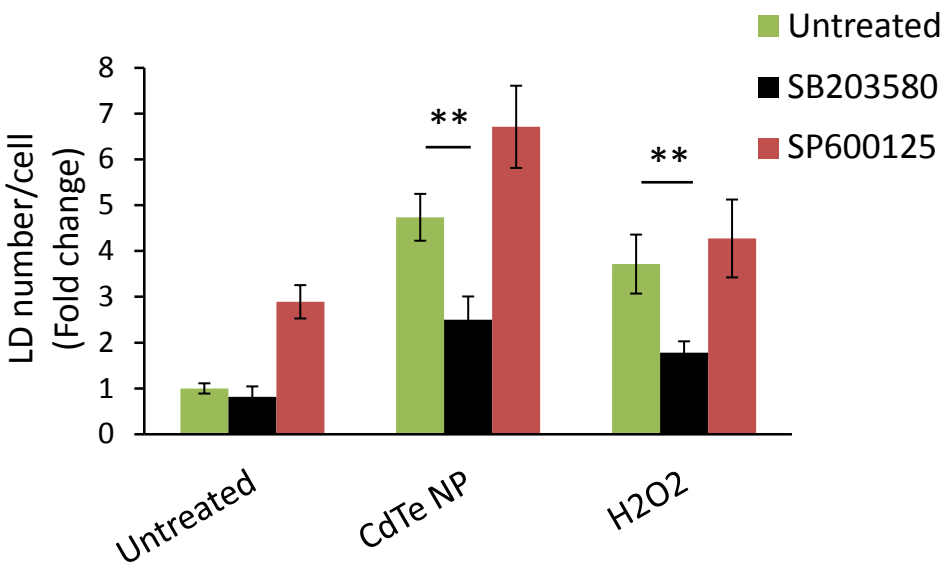
Untreated
SB203580
SP600125
LD number/cell
(Fold change)
8
7
6
5
4
3
2
1
0
**
**
Untreated
CdTe NP
H2O2

B

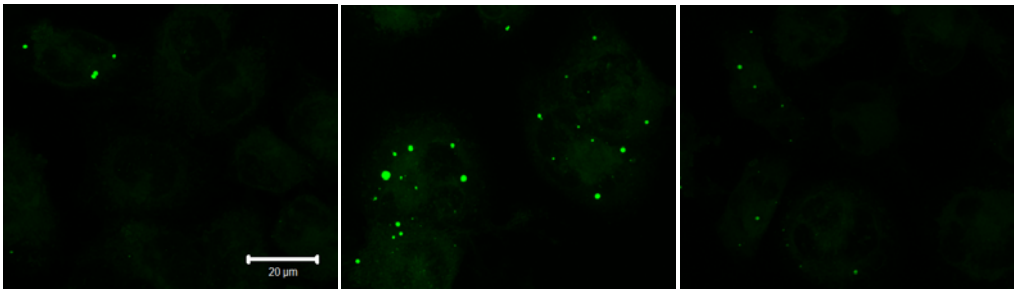
20 µm
Untreated
CdTe
SB+CdTe

Appendix V

Assessment of the effect of p38 and JNK inhibitors on stress-induced LD formation by confocal microscopy.

(A) Assessment of the average number of LDs per cell in the presence or absence of pharmacological inhibitors, SP600125 (JNK) and SB203580 (p38). Cells were pre-treated with the inhibitors (10 μM) for 30 min and then exposed to CdTe (10 μg/ml) or H_2O_2 (50 μM) overnight (18h). Bars show average LD number/cell expressed as fold-increase over untreated group. Statistically significant differences are indicated by **$p<0.01$.

(B) Representative confocal images show LDs in CdTe-treated cells in the absence or presence of SB203580. Scale bar = 20 μm.

References

Aardema, H., Vos, P.L., Lolicato, F., Roelen, B.A., Knijn, H.M., Vaandrager, A.B., Helms, J.B., Gadella, B.M. (2011) Oleic acid prevents detrimental effects of saturated fatty acids on bovine oocyte developmental competence, Biology of reproduction 85:62-69.

Accioly, M.T., Pacheco, P., Maya-Monteiro, C.M., Carrossini, N., Robbs, B.K., Oliveira, S.S., Kaufmann, C., Morgado-Diaz, J.A., Bozza, P.T., Viola, J.P. (2008) Lipid bodies are reservoirs of cyclooxygenase-2 and sites of prostaglandin-E2 synthesis in colon cancer cells, Cancer research 68:1732-1740.

Al-Saffar, N.M., Titley, J.C., Robertson, D., Clarke, P.A., Jackson, L.E., Leach, M.O., Ronen, S.M. (2002) Apoptosis is associated with triacylglycerol accumulation in Jurkat T-cells, British journal of cancer 86:963-970.

Alberti, K.G., Zimmet, P., Shaw, J. (2005) The metabolic syndrome--a new worldwide definition, Lancet 366:1059-1062.

Almahbobi, G., Williams, L.J., Hall, P.F. (1992) Attachment of steroidogenic lipid droplets to intermediate filaments in adrenal cells, Journal of cell science 101 (Pt 2):383-393.

American Diabetes Association (2011) Diagnosis and classification of diabetes mellitus, Diabetes care 34 Suppl 1:S62-69.

Antonietta Ajmone-Cat, M., Lavinia Salvatori, M., De Simone, R., Mancini, M., Biagioni, S., Bernardo, A., Cacci, E., Minghetti, L. (2012) Docosahexaenoic acid modulates inflammatory and antineurogenic functions of activated microglial cells, Journal of neuroscience research 90:575-587.

Artwohl, M., Roden, M., Waldhausl, W., Freudenthaler, A., Baumgartner-Parzer, S.M. (2004) Free fatty acids trigger apoptosis and inhibit cell cycle progression in human vascular endothelial cells, Faseb J 18:146-148.

Astrup, A., Finer, N. (2000) Redefining type 2 diabetes: 'diabesity' or 'obesity dependent diabetes mellitus'?, Obes Rev 1:57-59.

Avogaro, A., Pagnin, E., Calo, L. (2003) Monocyte NADPH oxidase subunit p22(phox) and inducible hemeoxygenase-1 gene expressions are increased in type II diabetic patients: relationship with oxidative stress, The Journal of clinical endocrinology and metabolism 88:1753-1759.

Bakker, S.J., RG, I.J., Teerlink, T., Westerhoff, H.V., Gans, R.O., Heine, R.J. (2000) Cytosolic triglycerides and oxidative stress in central obesity: the missing link between excessive atherosclerosis, endothelial dysfunction, and beta-cell failure?, Atherosclerosis 148:17-21.

Bampton, E.T., Goemans, C.G., Niranjan, D., Mizushima, N., Tolkovsky, A.M. (2005) The dynamics of autophagy visualized in live cells: from autophagosome formation to fusion with endo/lysosomes, Autophagy 1:23-36.

Bandeira-Melo, C., Phoofolo, M., Weller, P.F. (2001) Extranuclear lipid bodies, elicited by CCR3-mediated signaling pathways, are the sites of chemokine-enhanced leukotriene C4 production in eosinophils and basophils, The Journal of biological chemistry 276:22779-22787.

Bao, W., Song, F., Li, X., Rong, S., Yang, W., Zhang, M., Yao, P., Hao, L., Yang, N., Hu, F.B., Liu, L. (2010) Plasma heme oxygenase-1 concentration is elevated in individuals with type 2 diabetes mellitus, PloS one 5:e12371.

Bartels, E.D., Nielsen, J.M., Bisgaard, L.S., Goetze, J.P., Nielsen, L.B. (2010) Decreased expression of natriuretic peptides associated with lipid accumulation in cardiac ventricle of obese mice, Endocrinology 151:5218-5225.

Barton, G.M., Medzhitov, R. (2003) Toll-like receptor signaling pathways, Science (New York, N.Y 300:1524-1525.

Bartz, R., Li, W.H., Venables, B., Zehmer, J.K., Roth, M.R., Welti, R., Anderson, R.G., Liu, P., Chapman, K.D. (2007) Lipidomics reveals that adiposomes store ether lipids and mediate phospholipid traffic, Journal of lipid research 48:837-847.

Bauerfeld, C.P., Rastogi, R., Pirockinaite, G., Lee, I., Huttemann, M., Monks, B., Birnbaum, M.J., Franchi, L., Nunez, G., Samavati, L. (2012) TLR4-mediated AKT activation is MyD88/TRIF dependent and critical for induction of oxidative phosphorylation and mitochondrial transcription factor A in murine macrophages, J Immunol 188:2847-2857.

Bazan, N.G. (2005) Neuroprotectin D1 (NPD1): a DHA-derived mediator that protects brain and retina against cell injury-induced oxidative stress, Brain pathology (Zurich, Switzerland) 15:159-166.

Bell, M., Wang, H., Chen, H., McLenithan, J.C., Gong, D.W., Yang, R.Z., Yu, D., Fried, S.K., Quon, M.J., Londos, C., Sztalryd, C. (2008) Consequences of lipid droplet coat protein downregulation in liver cells: abnormal lipid droplet metabolism and induction of insulin resistance, Diabetes 57:2037-2045.

Beller, M., Riedel, D., Jansch, L., Dieterich, G., Wehland, J., Jackle, H., Kuhnlein, R.P. (2006) Characterization of the Drosophila lipid droplet subproteome, Mol Cell Proteomics 5:1082-1094.

Beltowski, J., Wojcicka, G., Gorny, D., Marciniak, A. (2000) The effect of dietary-induced obesity on lipid peroxidation, antioxidant enzymes and total plasma antioxidant capacity, J Physiol Pharmacol 51:883-896.

Bennett, B.L., Sasaki, D.T., Murray, B.W., O'Leary, E.C., Sakata, S.T., Xu, W., Leisten, J.C., Motiwala, A., Pierce, S., Satoh, Y., Bhagwat, S.S., Manning, A.M., Anderson, D.W. (2001) SP600125, an anthrapyrazolone inhibitor of Jun N-terminal kinase, Proceedings of the National Academy of Sciences of the United States of America 98:13681-13686.

Berson, E.L., Rosner, B., Sandberg, M.A., Weigel-DiFranco, C., Moser, A., Brockhurst, R.J., Hayes, K.C., Johnson, C.A., Anderson, E.J., Gaudio, A.R., Willett, W.C., Schaefer, E.J. (2004) Clinical trial of docosahexaenoic acid in patients with retinitis pigmentosa receiving vitamin A treatment, Archives of ophthalmology 122:1297-1305.

Bickel, P.E., Tansey, J.T., Welte, M.A. (2009) PAT proteins, an ancient family of lipid droplet proteins that regulate cellular lipid stores, Biochimica et biophysica acta 1791:419-440.

Biju, V., Itoh, T., Anas, A., Sujith, A., Ishikawa, M. (2008) Semiconductor quantum dots and metal nanoparticles: syntheses, optical properties, and biological applications, Analytical and bioanalytical chemistry 391:2469-2495.

Bildirici, I., Roh, C.R., Schaiff, W.T., Lewkowski, B.M., Nelson, D.M., Sadovsky, Y. (2003) The lipid droplet-associated protein adipophilin is expressed in human trophoblasts and is regulated by peroxisomal proliferator-activated receptor-gamma/retinoid X receptor, The Journal of clinical endocrinology and metabolism 88:6056-6062.

Binns, D., Januszewski, T., Chen, Y., Hill, J., Markin, V.S., Zhao, Y., Gilpin, C., Chapman, K.D., Anderson, R.G., Goodman, J.M. (2006) An intimate collaboration between peroxisomes and lipid bodies, The Journal of cell biology 173:719-731.

Blair, A.S., Hajduch, E., Litherland, G.J., Hundal, H.S. (1999) Regulation of glucose transport and glycogen synthesis in L6 muscle cells during oxidative stress. Evidence for cross-talk between the insulin and SAPK2/p38 mitogen-activated protein kinase signaling pathways, The Journal of biological chemistry 274:36293-36299.

Blanchette-Mackie, E.J., Dwyer, N.K., Barber, T., Coxey, R.A., Takeda, T., Rondinone, C.M., Theodorakis, J.L., Greenberg, A.S., Londos, C. (1995) Perilipin is located on the

surface layer of intracellular lipid droplets in adipocytes, Journal of lipid research 36:1211-1226.

Bland, E.J., Keshavarz, T., Bucke, C. (2001) Using 2', 7'-dichlorodihydrofluorescein-diacetate to assess polysaccharides as immunomodulating agents, Molecular biotechnology 19:125-131.

Block, M.L., Zecca, L., Hong, J.S. (2007) Microglia-mediated neurotoxicity: uncovering the molecular mechanisms, Nat Rev Neurosci 8:57-69.

Blundell, J.E., Burley, V.J., Cotton, J.R., Lawton, C.L. (1993) Dietary fat and the control of energy intake: evaluating the effects of fat on meal size and postmeal satiety, The American journal of clinical nutrition 57:772S-777S; discussion 777S-778S.

Boden, G. (1997) Role of fatty acids in the pathogenesis of insulin resistance and NIDDM, Diabetes 46:3-10.

Boren, J., Brindle, K.M. (2012) Apoptosis-induced mitochondrial dysfunction causes cytoplasmic lipid droplet formation, Cell death and differentiation 19:1561-1570.

Borg, J., Klint, C., Wierup, N., Strom, K., Larsson, S., Sundler, F., Lupi, R., Marchetti, P., Xu, G., Kimmel, A., Londos, C., Holm, C. (2009) Perilipin is present in islets of Langerhans and protects against lipotoxicity when overexpressed in the beta-cell line INS-1, Endocrinology 150:3049-3057.

Bosma, M., Hesselink, M.K., Sparks, L.M., Timmers, S., Ferraz, M.J., Mattijssen, F., van Beurden, D., Schaart, G., de Baets, M.H., Verheyen, F.K., Kersten, S., Schrauwen, P. (2012) Perilipin 2 Improves Insulin Sensitivity in Skeletal Muscle Despite Elevated Intramuscular Lipid Levels, Diabetes 61:2679-2690.

Bostrom, P., Andersson, L., Rutberg, M., Perman, J., Lidberg, U., Johansson, B.R., Fernandez-Rodriguez, J., Ericson, J., Nilsson, T., Boren, J., Olofsson, S.O. (2007) SNARE proteins mediate fusion between cytosolic lipid droplets and are implicated in insulin sensitivity, Nature cell biology 9:1286-1293.

Bouchoux, J., Beilstein, F., Pauquai, T., Guerrera, I.C., Chateau, D., Ly, N., Alqub, M., Klein, C., Chambaz, J., Rousset, M., Lacorte, J.M., Morel, E., Demignot, S. (2011) The proteome of cytosolic lipid droplets isolated from differentiated Caco-2/TC7 enterocytes reveals cell-specific characteristics, Biology of the cell / under the auspices of the European Cell Biology Organization 103:499-517.

Bourque, S.D., Titorenko, V.I. (2009) A quantitative assessment of the yeast lipidome using electrospray ionization mass spectrometry, J Vis Exp.

Bozza, P.T., Bakker-Abreu, I., Navarro-Xavier, R.A., Bandeira-Melo, C. (2011) Lipid body function in eicosanoid synthesis: an update, Prostaglandins, leukotrienes, and essential fatty acids 85:205-213.

Bozza, P.T., Magalhaes, K.G., Weller, P.F. (2009) Leukocyte lipid bodies - Biogenesis and functions in inflammation, Biochimica et biophysica acta 1791:540-551.

Bozza, P.T., Payne, J.L., Goulet, J.L., Weller, P.F. (1996) Mechanisms of platelet-activating factor-induced lipid body formation: requisite roles for 5-lipoxygenase and de novo protein synthesis in the compartmentalization of neutrophil lipids, The Journal of experimental medicine 183:1515-1525.

Bozza, P.T., Viola, J.P. (2010) Lipid droplets in inflammation and cancer, Prostaglandins, leukotrienes, and essential fatty acids 82:243-250.

Bozza, P.T., Yu, W., Cassara, J., Weller, P.F. (1998) Pathways for eosinophil lipid body induction: differing signal transduction in cells from normal and hypereosinophilic subjects, Journal of leukocyte biology 64:563-569.

Bozza, P.T., Yu, W., Penrose, J.F., Morgan, E.S., Dvorak, A.M., Weller, P.F. (1997) Eosinophil lipid bodies: specific, inducible intracellular sites for enhanced eicosanoid formation, The Journal of experimental medicine 186:909-920.

Brasaemle, D.L., Barber, T., Kimmel, A.R., Londos, C. (1997) Post-translational regulation of perilipin expression. Stabilization by stored intracellular neutral lipids, The Journal of biological chemistry 272:9378-9387.

Brasaemle, D.L., Barber, T., Wolins, N.E., Serrero, G., Blanchette-Mackie, E.J., Londos, C. (1997) Adipose differentiation-related protein is an ubiquitously expressed lipid storage droplet-associated protein, Journal of lipid research 38:2249-2263.

Briaud, I., Harmon, J.S., Kelpe, C.L., Segu, V.B., Poitout, V. (2001) Lipotoxicity of the pancreatic beta-cell is associated with glucose-dependent esterification of fatty acids into neutral lipids, Diabetes 50:315-321.

Bruchez, M., Jr., Moronne, M., Gin, P., Weiss, S., Alivisatos, A.P. (1998) Semiconductor nanocrystals as fluorescent biological labels, Science (New York, N.Y 281:2013-2016.

Buchanan, M.M., Hutchinson, M., Watkins, L.R., Yin, H. (2010) Toll-like receptor 4 in CNS pathologies, Journal of neurochemistry 114:13-27.

Buhman, K.K., Chen, H.C., Farese, R.V., Jr. (2001) The enzymes of neutral lipid synthesis, The Journal of biological chemistry 276:40369-40372.

Bulankina, A.V., Deggerich, A., Wenzel, D., Mutenda, K., Wittmann, J.G., Rudolph, M.G., Burger, K.N., Honing, S. (2009) TIP47 functions in the biogenesis of lipid droplets, The Journal of cell biology 185:641-655.

Burgermeister, E., Tencer, L., Liscovitch, M. (2003) Peroxisome proliferator-activated receptor-gamma upregulates caveolin-1 and caveolin-2 expression in human carcinoma cells, Oncogene 22:3888-3900.

Butler, D., Bahr, B.A. (2006) Oxidative stress and lysosomes: CNS-related consequences and implications for lysosomal enhancement strategies and induction of autophagy, Antioxidants & redox signaling 8:185-196.

Buzea, C., Pacheco, II, Robbie, K. (2007) Nanomaterials and nanoparticles: sources and toxicity, Biointerphases 2:MR17-71.

Callies, R., Sri-Pathmanathan, R.M., Ferguson, D.Y., Brindle, K.M. (1993) The appearance of neutral lipid signals in the 1H NMR spectra of a myeloma cell line correlates with the induced formation of cytoplasmic lipid droplets, Magn Reson Med 29:546-550.

Carbonell, A.L., Boya, J., Calvo, J.L., Marin, J.F. (1991) Ultrastructural study of the neuroglial and macrophagic reaction in Wallerian degeneration of the adult rat optic nerve, Histology and histopathology 6:443-451.

Cardell, R.R., Jr., Badenhausen, S., Porter, K.R. (1967) Intestinal triglyceride absorption in the rat. An electron microscopical study, The Journal of cell biology 34:123-155.

Caroff, M., Karibian, D. (2003) Structure of bacterial lipopolysaccharides, Carbohydrate research 338:2431-2447.

Centers for Disease Control and Prevention (2011) National diabetes fact sheet: national estimates and general information on diabetes and prediabetes in the United States,.

Cermelli, S., Guo, Y., Gross, S.P., Welte, M.A. (2006) The lipid-droplet proteome reveals that droplets are a protein-storage depot, Curr Biol 16:1783-1795.

Chai, W., Liu, Z. (2007) p38 mitogen-activated protein kinase mediates palmitate-induced apoptosis but not inhibitor of nuclear factor-kappaB degradation in human coronary artery endothelial cells, Endocrinology 148:1622-1628.

Chan, W.Y., Kohsaka, S., Rezaie, P. (2007) The origin and cell lineage of microglia: new concepts, Brain research reviews 53:344-354.

Chang, B.H., Chan, L. (2007) Regulation of Triglyceride Metabolism. III. Emerging role of lipid droplet protein ADFP in health and disease, American journal of physiology 292:G1465-1468.

Chang, B.H., Li, L., Paul, A., Taniguchi, S., Nannegari, V., Heird, W.C., Chan, L. (2006) Protection against fatty liver but normal adipogenesis in mice lacking adipose differentiation-related protein, Molecular and cellular biology 26:1063-1076.

Chang, T.Y., Li, B.L., Chang, C.C., Urano, Y. (2009) Acyl-coenzyme A:cholesterol acyltransferases, American journal of physiology 297:E1-9.

Chaturvedi, R.K., Beal, M.F. (2008) Mitochondrial approaches for neuroprotection, Annals of the New York Academy of Sciences 1147:395-412.

Chen, C., Chen, Y.H., Lin, W.W. (1999) Involvement of p38 mitogen-activated protein kinase in lipopolysaccharide-induced iNOS and COX-2 expression in J774 macrophages, Immunology 97:124-129.

Chen, J.S., Greenberg, A.S., Wang, S.M. (2002) Oleic acid-induced PKC isozyme translocation in RAW 264.7 macrophages, Journal of cellular biochemistry 86:784-791.

Chen, Q., Vazquez, E.J., Moghaddas, S., Hoppel, C.L., Lesnefsky, E.J. (2003) Production of reactive oxygen species by mitochondria: central role of complex III, The Journal of biological chemistry 278:36027-36031.

Cheng, H., Guan, S., Han, X. (2006) Abundance of triacylglycerols in ganglia and their depletion in diabetic mice: implications for the role of altered triacylglycerols in diabetic neuropathy, Journal of neurochemistry 97:1288-1300.

Cho, S.J., Maysinger, D., Jain, M., Roder, B., Hackbarth, S., Winnik, F.M. (2007) Long-term exposure to CdTe quantum dots causes functional impairments in live cells, Langmuir 23:1974-1980.

Choi, A.O., Cho, S.J., Desbarats, J., Lovric, J., Maysinger, D. (2007) Quantum dot-induced cell death involves Fas upregulation and lipid peroxidation in human neuroblastoma cells, Journal of nanobiotechnology 5:1.

Choi, S.S., Diehl, A.M. (2008) Hepatic triglyceride synthesis and nonalcoholic fatty liver disease, Current opinion in lipidology 19:295-300.

Cnop, M., Hannaert, J.C., Hoorens, A., Eizirik, D.L., Pipeleers, D.G. (2001) Inverse relationship between cytotoxicity of free fatty acids in pancreatic islet cells and cellular triglyceride accumulation, Diabetes 50:1771-1777.

Cohen, A.W., Razani, B., Schubert, W., Williams, T.M., Wang, X.B., Iyengar, P., Brasaemle, D.L., Scherer, P.E., Lisanti, M.P. (2004) Role of caveolin-1 in the modulation of lipolysis and lipid droplet formation, Diabetes 53:1261-1270.

Colhoun, H.M., Otvos, J.D., Rubens, M.B., Taskinen, M.R., Underwood, S.R., Fuller, J.H. (2002) Lipoprotein subclasses and particle sizes and their relationship with coronary artery calcification in men and women with and without type 1 diabetes, Diabetes 51:1949-1956.

Collins, S.C., Salehi, A., Eliasson, L., Olofsson, C.S., Rorsman, P. (2008) Long-term exposure of mouse pancreatic islets to oleate or palmitate results in reduced glucose-induced somatostatin and oversecretion of glucagon, Diabetologia 51:1689-1693.

Coppack, S.W., Jensen, M.D., Miles, J.M. (1994) In vivo regulation of lipolysis in humans, Journal of lipid research 35:177-193.

Cotton, H.A. (1915) Fatty Degeneration of the Cerebral Cortex in the Psychoses, with Special Reference to Dementia Praecox, The Journal of experimental medicine 22:492-516.

Cutler, R.G., Kelly, J., Storie, K., Pedersen, W.A., Tammara, A., Hatanpaa, K., Troncoso, J.C., Mattson, M.P. (2004) Involvement of oxidative stress-induced abnormalities in ceramide and cholesterol metabolism in brain aging and Alzheimer's disease, Proceedings of the National Academy of Sciences of the United States of America 101:2070-2075.

D'Autreaux, B., Toledano, M.B. (2007) ROS as signalling molecules: mechanisms that generate specificity in ROS homeostasis, Nature reviews 8:813-824.

D'Avila, H., Maya-Monteiro, C.M., Bozza, P.T. (2008) Lipid bodies in innate immune response to bacterial and parasite infections, International immunopharmacology 8:1308-1315.

D'Avila, H., Melo, R.C., Parreira, G.G., Werneck-Barroso, E., Castro-Faria-Neto, H.C., Bozza, P.T. (2006) Mycobacterium bovis bacillus Calmette-Guerin induces TLR2-mediated formation of lipid bodies: intracellular domains for eicosanoid synthesis in vivo, J Immunol 176:3087-3097.

Dalen, K.T., Dahl, T., Holter, E., Arntsen, B., Londos, C., Sztalryd, C., Nebb, H.I. (2007) LSDP5 is a PAT protein specifically expressed in fatty acid oxidizing tissues, Biochimica et biophysica acta 1771:210-227.

Dalen, K.T., Schoonjans, K., Ulven, S.M., Weedon-Fekjaer, M.S., Bentzen, T.G., Koutnikova, H., Auwerx, J., Nebb, H.I. (2004) Adipose tissue expression of the lipid

droplet-associating proteins S3-12 and perilipin is controlled by peroxisome proliferator-activated receptor-gamma, Diabetes 53:1243-1252.

Das, G.D. (1976) Resting and reactive macrophages in the developing cerebellum: an experimental ultrastructural study, Virchows Archiv 20:287-298.

Davies, K.J. (2000) Oxidative stress, antioxidant defenses, and damage removal, repair, and replacement systems, IUBMB life 50:279-289.

de Estable-Puig, R.F., Estable-Puig, J.F. (1973) Intraneuronal lipid droplets in irradiated nervous tissue, Virchows Archiv 14:117-125.

De Smedt-Peyrusse, V., Sargueil, F., Moranis, A., Harizi, H., Mongrand, S., Laye, S. (2008) Docosahexaenoic acid prevents lipopolysaccharide-induced cytokine production in microglial cells by inhibiting lipopolysaccharide receptor presentation but not its membrane subdomain localization, Journal of neurochemistry 105:296-307.

DeFronzo, R.A., Tripathy, D. (2009) Skeletal muscle insulin resistance is the primary defect in type 2 diabetes, Diabetes care 32 Suppl 2:S157-163.

Del Boca, J., Flatt, J.P. (1969) Fatty acid synthesis from glucose and acetate and the control of lipogenesis in adipose tissue, European journal of biochemistry / FEBS 11:127-134.

Delikatny, E.J., Cooper, W.A., Brammah, S., Sathasivam, N., Rideout, D.C. (2002) Nuclear magnetic resonance-visible lipids induced by cationic lipophilic chemotherapeutic agents are accompanied by increased lipid droplet formation and damaged mitochondria, Cancer research 62:1394-1400.

Denes, A., Drake, C., Stordy, J., Chamberlain, J., McColl, B., Gram, G., Crossman, D., Francis, S., Allan, S., Rothwell, N. (2012) Interleukin-1 Mediates Neuroinflammatory Changes Associated With Diet-Induced Atherosclerosis, Journal of the American Heart Association DOI: 10.1161/JAHA.112.002006.

Derfus, A.M., Chan, W.C.W., Bhatia, S.N. (2004) Probing the Cytotoxicity of Semiconductor Quantum Dots, Nano letters 4:11-18.

Diaz, G., Melis, M., Batetta, B., Angius, F., Falchi, A.M. (2008) Hydrophobic characterization of intracellular lipids in situ by Nile Red red/yellow emission ratio, Micron 39:819-824.

Dinarello, C.A. (2010) Anti-inflammatory Agents: Present and Future, Cell 140:935-950.

Drews, G., Krippeit-Drews, P., Dufer, M. (2010) Oxidative stress and beta-cell dysfunction, Pflugers Arch 460:703-718.

Du, L., Hickey, R.W., Bayir, H., Watkins, S.C., Tyurin, V.A., Guo, F., Kochanek, P.M., Jenkins, L.W., Ren, J., Gibson, G., Chu, C.T., Kagan, V.E., Clark, R.S. (2008) Starving neurons show sex difference in autophagy, The Journal of biological chemistry.

Ducharme, N.A., Bickel, P.E. (2008) Lipid droplets in lipogenesis and lipolysis, Endocrinology 149:942-949.

Duval, C., Auge, N., Frisach, M.F., Casteilla, L., Salvayre, R., Negre-Salvayre, A. (2002) Mitochondrial oxidative stress is modulated by oleic acid via an epidermal growth factor receptor-dependent activation of glutathione peroxidase, Biochem J 367:889-894.

Dvorak, A.M., Dvorak, H.F., Peters, S.P., Shulman, E.S., MacGlashan, D.W., Jr., Pyne, K., Harvey, V.S., Galli, S.J., Lichtenstein, L.M. (1983) Lipid bodies: cytoplasmic organelles important to arachidonate metabolism in macrophages and mast cells, J Immunol 131:2965-2976.

Dvorak, A.M., Weller, P.F., Harvey, V.S., Morgan, E.S., Dvorak, H.F. (1993) Ultrastructural localization of prostaglandin endoperoxide synthase (cyclooxygenase) to isolated, purified fractions of guinea pig peritoneal macrophage and line 10 hepatocarcinoma cell lipid bodies, International archives of allergy and immunology 101:136-142.

Dyall, S.C., Michael-Titus, A.T. (2008) Neurological benefits of omega-3 fatty acids, Neuromolecular medicine 10:219-235.

Ebert, S., Weigelt, K., Walczak, Y., Drobnik, W., Mauerer, R., Hume, D.A., Weber, B.H., Langmann, T. (2009) Docosahexaenoic acid attenuates microglial activation and delays early retinal degeneration, Journal of neurochemistry 110:1863-1875.

Edvardsson, U., Ljungberg, A., Linden, D., William-Olsson, L., Peilot-Sjogren, H., Ahnmark, A., Oscarsson, J. (2006) PPARalpha activation increases triglyceride mass and adipose differentiation-related protein in hepatocytes, Journal of lipid research 47:329-340.

Elliott, S.S., Keim, N.L., Stern, J.S., Teff, K., Havel, P.J. (2002) Fructose, weight gain, and the insulin resistance syndrome, The American journal of clinical nutrition 76:911-922.

Emerit, J., Edeas, M., Bricaire, F. (2004) Neurodegenerative diseases and oxidative stress, Biomedicine & pharmacotherapy = Biomedecine & pharmacotherapie 58:39-46.

Exner, M., Minar, E., Wagner, O., Schillinger, M. (2004) The role of heme oxygenase-1 promoter polymorphisms in human disease, Free radical biology & medicine 37:1097-1104.

Falconer, J.S., Ross, J.A., Fearon, K.C., Hawkins, R.A., O'Riordain, M.G., Carter, D.C. (1994) Effect of eicosapentaenoic acid and other fatty acids on the growth in vitro of human pancreatic cancer cell lines, Br J Cancer 69:826-832.

Faleck, D.M., Ali, K., Roat, R., Graham, M.J., Crooke, R.M., Battisti, R., Garcia, E., Ahima, R.S., Imai, Y. (2010) Adipose differentiation-related protein regulates lipids and insulin in pancreatic islets, American journal of physiology 299:E249-257.

Fan, B., Ikuyama, S., Gu, J.Q., Wei, P., Oyama, J., Inoguchi, T., Nishimura, J. (2009) Oleic acid-induced ADRP expression requires both AP-1 and PPAR response elements, and is reduced by Pycnogenol through mRNA degradation in NMuLi liver cells, Am J Physiol Endocrinol Metab 297:E112-123.

Farese, R.V., Jr., Walther, T.C. (2009) Lipid droplets finally get a little R-E-S-P-E-C-T, Cell 139:855-860.

Farooqui, A.A., Horrocks, L.A. (2006) Phospholipase A2-generated lipid mediators in the brain: the good, the bad, and the ugly, Neuroscientist 12:245-260.

Farooqui, A.A., Horrocks, L.A., Farooqui, T. (2007) Modulation of inflammation in brain: a matter of fat, Journal of neurochemistry 101:577-599.

Feingold, K.R., Kazemi, M.R., Magra, A.L., McDonald, C.M., Chui, L.G., Shigenaga, J.K., Patzek, S.M., Chan, Z.W., Londos, C., Grunfeld, C. (2010) ADRP/ADFP and Mal1 expression are increased in macrophages treated with TLR agonists, Atherosclerosis 209:81-88.

Fex, M., Nitert, M.D., Wierup, N., Sundler, F., Ling, C., Mulder, H. (2007) Enhanced mitochondrial metabolism may account for the adaptation to insulin resistance in islets from C57BL/6J mice fed a high-fat diet, Diabetologia 50:74-83.

Fraenkel, M., Weiss, R., Leizerman, I., Anaby, D., Golomb, E., Leibowitz, G., Kaiser, N. (2008) Scanning electron microscopic analysis of intramyocellular lipid droplets in an animal model of type 2 diabetes, Obesity (Silver Spring, Md 16:695-699.

Franson, P. (1985) Quantitative electron microscopic observations on the non-neuronal cells and lipid droplets in the posterior funiculus of the cat after dorsal rhizotomy, The Journal of comparative neurology 231:490-499.

Franson, P. (1988) Quantitative electron microscopic observations on the non-neuronal cells and lipid droplets in the posterior funiculus of the kitten after dorsal rhizotomy, Anatomy and embryology 178:95-105.

Frohnert, B.I., Bernlohr, D.A. (2000) Regulation of fatty acid transporters in mammalian cells, Progress in lipid research 39:83-107.

Fruhbeck, G., Gomez-Ambrosi, J., Muruzabal, F.J., Burrell, M.A. (2001) The adipocyte: a model for integration of endocrine and metabolic signaling in energy metabolism regulation, American journal of physiology 280:E827-847.

Fujimoto, Y., Onoduka, J., Homma, K.J., Yamaguchi, S., Mori, M., Higashi, Y., Makita, M., Kinoshita, T., Noda, J., Itabe, H., Takanoa, T. (2006) Long-chain fatty acids induce lipid droplet formation in a cultured human hepatocyte in a manner dependent of Acyl-CoA synthetase, Biological & pharmaceutical bulletin 29:2174-2180.

Fukumoto, S., Fujimoto, T. (2002) Deformation of lipid droplets in fixed samples, Histochemistry and cell biology 118:423-428.

Funk, J.L., Feingold, K.R., Moser, A.H., Grunfeld, C. (1993) Lipopolysaccharide stimulation of RAW 264.7 macrophages induces lipid accumulation and foam cell formation, Atherosclerosis 98:67-82.

Furukawa, S., Fujita, T., Shimabukuro, M., Iwaki, M., Yamada, Y., Nakajima, Y., Nakayama, O., Makishima, M., Matsuda, M., Shimomura, I. (2004) Increased oxidative stress in obesity and its impact on metabolic syndrome, The Journal of clinical investigation 114:1752-1761.

Galland, L. (2010) Diet and inflammation, Nutr Clin Pract 25:634-640.

Gastaldelli, A., Baldi, S., Pettiti, M., Toschi, E., Camastra, S., Natali, A., Landau, B.R., Ferrannini, E. (2000) Influence of obesity and type 2 diabetes on gluconeogenesis and glucose output in humans: a quantitative study, Diabetes 49:1367-1373.

Goodman, J.M. (2008) The gregarious lipid droplet, The Journal of biological chemistry 283:28005-28009.

Goodrum, J.F., Earnhardt, T.S., Goines, N.D., Bouldin, T.W. (1990) Lipid droplets in Schwann cells during tellurium neuropathy are derived from newly synthesized lipid, Journal of neurochemistry 55:1928-1932.

Goris, R.J., te Boekhorst, T.P., Nuytinck, J.K., Gimbrere, J.S. (1985) Multiple-organ failure. Generalized autodestructive inflammation?, Arch Surg 120:1109-1115.

Graeber, M.B. (2010) Changing face of microglia, Science (New York, N.Y 330:783-788.

Greenberg, A.S., Coleman, R.A., Kraemer, F.B., McManaman, J.L., Obin, M.S., Puri, V., Yan, Q.W., Miyoshi, H., Mashek, D.G. (2011) The role of lipid droplets in metabolic disease in rodents and humans, The Journal of clinical investigation 121:2102-2110.

Greenberg, A.S., Egan, J.J., Wek, S.A., Garty, N.B., Blanchette-Mackie, E.J., Londos, C. (1991) Perilipin, a major hormonally regulated adipocyte-specific phosphoprotein associated with the periphery of lipid storage droplets, The Journal of biological chemistry 266:11341-11346.

Greenspan, P., Mayer, E.P., Fowler, S.D. (1985) Nile red: a selective fluorescent stain for intracellular lipid droplets, The Journal of cell biology 100:965-973.

Griffin, J.L., Lehtimaki, K.K., Valonen, P.K., Grohn, O.H., Kettunen, M.I., Yla-Herttuala, S., Pitkanen, A., Nicholson, J.K., Kauppinen, R.A. (2003) Assignment of 1H nuclear magnetic resonance visible polyunsaturated fatty acids in BT4C gliomas undergoing ganciclovir-thymidine kinase gene therapy-induced programmed cell death, Cancer research 63:3195-3201.

Gronke, S., Beller, M., Fellert, S., Ramakrishnan, H., Jackle, H., Kuhnlein, R.P. (2003) Control of fat storage by a Drosophila PAT domain protein, Curr Biol 13:603-606.

Gu, J.Q., Ikuyama, S., Wei, P., Fan, B., Oyama, J., Inoguchi, T., Nishimura, J. (2008) Pycnogenol, an extract from French maritime pine, suppresses Toll-like receptor 4-mediated expression of adipose differentiation-related protein in macrophages, Am J Physiol Endocrinol Metab 295:E1390-1400.

Gubern, A., Barcelo-Torns, M., Casas, J., Barneda, D., Masgrau, R., Picatoste, F., Balsinde, J., Balboa, M.A., Claro, E. (2009) Lipid droplet biogenesis induced by stress involves triacylglycerol synthesis that depends on group VIA phospholipase A2, The Journal of biological chemistry 284:5697-5708.

Guha, M., Mackman, N. (2001) LPS induction of gene expression in human monocytes, Cellular signalling 13:85-94.

Guillon-Munos, A., van Bemmelen, M.X., Clarke, P.G. (2005) Role of phosphoinositide 3-kinase in the autophagic death of serum-deprived PC12 cells, Apoptosis 10:1031-1041.

Guo, Y., Cordes, K.R., Farese, R.V., Jr., Walther, T.C. (2009) Lipid droplets at a glance, Journal of cell science 122:749-752.

Guo, Y., Walther, T.C., Rao, M., Stuurman, N., Goshima, G., Terayama, K., Wong, J.S., Vale, R.D., Walter, P., Farese, R.V. (2008) Functional genomic screen reveals genes involved in lipid-droplet formation and utilization, Nature 453:657-661.

Hakumaki, J.M., Kauppinen, R.A. (2000) 1H NMR visible lipids in the life and death of cells, Trends in biochemical sciences 25:357-362.

Hakumaki, J.M., Poptani, H., Sandmair, A.M., Yla-Herttuala, S., Kauppinen, R.A. (1999) 1H MRS detects polyunsaturated fatty acid accumulation during gene therapy of glioma: implications for the in vivo detection of apoptosis, Nature medicine 5:1323-1327.

Hanisch, U.K. (2002) Microglia as a source and target of cytokines, Glia 40:140-155.

Hanisch, U.K., Kettenmann, H. (2007) Microglia: active sensor and versatile effector cells in the normal and pathologic brain, Nature neuroscience 10:1387-1394.

Hapala, I., Marza, E., Ferreira, T. (2011) Is fat so bad? Modulation of endoplasmic reticulum stress by lipid droplet formation, Biology of the cell / under the auspices of the European Cell Biology Organization 103:271-285.

Hardman, R. (2006) A toxicologic review of quantum dots: toxicity depends on physicochemical and environmental factors, Environmental health perspectives 114:165-172.

Harmon, J.S., Bogdani, M., Parazzoli, S.D., Mak, S.S., Oseid, E.A., Berghmans, M., Leboeuf, R.C., Robertson, R.P. (2009) beta-Cell-specific overexpression of glutathione peroxidase preserves intranuclear MafA and reverses diabetes in db/db mice, Endocrinology 150:4855-4862.

Hart, C.M., Gupta, M.P., Evanoff, V. (1997) Oleic acid reduces oxidant stress in cultured pulmonary artery endothelial cells, Experimental lung research 23:405-425.

Hashimoto, T., Fujita, T., Usuda, N., Cook, W., Qi, C., Peters, J.M., Gonzalez, F.J., Yeldandi, A.V., Rao, M.S., Reddy, J.K. (1999) Peroxisomal and mitochondrial fatty acid beta-oxidation in mice nullizygous for both peroxisome proliferator-activated receptor alpha and peroxisomal fatty acyl-CoA oxidase. Genotype correlation with fatty liver phenotype, The Journal of biological chemistry 274:19228-19236.

Hauck, T.S., Anderson, R.E., Fischer, H.C., Newbigging, S., Chan, W.C. (2010) In vivo quantum-dot toxicity assessment, Small (Weinheim an der Bergstrasse, Germany) 6:138-144.

Havel, R.J. (1997) Postprandial lipid metabolism: an overview, The Proceedings of the Nutrition Society 56:659-666.

Herman, L., Fitzgerald, P.J. (1962) The degenerative changes in pancreatic acinar cells caused by DL-ethionine, The Journal of cell biology 12:277-296.

Hillier, T. (1867) Poisoning by Phosphorus; Jaundice; death in six days. Fatty Degeneration of Liver and Kidneys, Medico-chirurgical transactions 50:99-101.

Holloway, G.P., Snook, L.A., Harris, R.J., Glatz, J.F., Luiken, J.J., Bonen, A. (2011) In obese Zucker rats, lipids accumulate in the heart despite normal mitochondrial content, morphology and long-chain fatty acid oxidation, The Journal of physiology 589:169-180.

Holthuis, J.C., Levine, T.P. (2005) Lipid traffic: floppy drives and a superhighway, Nat Rev Mol Cell Biol 6:209-220.

Hong, S., Gronert, K., Devchand, P.R., Moussignac, R.L., Serhan, C.N. (2003) Novel docosatrienes and 17S-resolvins generated from docosahexaenoic acid in murine brain, human blood, and glial cells. Autacoids in anti-inflammation, The Journal of biological chemistry 278:14677-14687.

Hu, Q., Li, B., Xu, R., Chen, D., Mu, C., Fei, E., Wang, G. (2012) The Protease Omi Cleaves the Mitogen-Activated Protein Kinase Kinase MEK1 to Inhibit Microglial Activation, Science signaling 5:ra61.

Huang, X., Sun, M., Li, D., Liu, J., Guo, H., Dong, Y., Jiang, L., Pan, Q., Man, Y., Wang, S., Li, J. (2011) Augmented NADPH oxidase activity and p22phox expression in monocytes underlie oxidative stress of patients with type 2 diabetes mellitus, Diabetes research and clinical practice 91:371-380.

Hughes, V. (2012) Microglia: The constant gardeners, Nature 485:570-572.

Igal, R.A., Wang, P., Coleman, R.A. (1997) Triacsin C blocks de novo synthesis of glycerolipids and cholesterol esters but not recycling of fatty acid into phospholipid: evidence for functionally separate pools of acyl-CoA, The Biochemical journal 324 (Pt 2):529-534.

Imamura, M., Inoguchi, T., Ikuyama, S., Taniguchi, S., Kobayashi, K., Nakashima, N., Nawata, H. (2002) ADRP stimulates lipid accumulation and lipid droplet formation in murine fibroblasts, American journal of physiology 283:E775-783.

Innis, S.M. (2007) Dietary (n-3) fatty acids and brain development, The Journal of nutrition 137:855-859.

Iorio, E., Di Vito, M., Spadaro, F., Ramoni, C., Lococo, E., Carnevale, R., Lenti, L., Strom, R., Podo, F. (2003) Triacsin C inhibits the formation of 1H NMR-visible mobile lipids and lipid bodies in HuT 78 apoptotic cells, Biochimica et biophysica acta 1634:1-14.

Iozzo, P., Geisler, F., Oikonen, V., Maki, M., Takala, T., Solin, O., Ferrannini, E., Knuuti, J., Nuutila, P. (2003) Insulin stimulates liver glucose uptake in humans: an 18F-FDG PET Study, J Nucl Med 44:682-689.

Isahara, K., Ohsawa, Y., Kanamori, S., Shibata, M., Waguri, S., Sato, N., Gotow, T., Watanabe, T., Momoi, T., Urase, K., Kominami, E., Uchiyama, Y. (1999) Regulation of a novel pathway for cell death by lysosomal aspartic and cysteine proteinases, Neuroscience 91:233-249.

Jack, C.S., Arbour, N., Manusow, J., Montgrain, V., Blain, M., McCrea, E., Shapiro, A., Antel, J.P. (2005) TLR signaling tailors innate immune responses in human microglia and astrocytes, J Immunol 175:4320-4330.

Jacquier, N., Choudhary, V., Mari, M., Toulmay, A., Reggiori, F., Schneiter, R. (2011) Lipid droplets are functionally connected to the endoplasmic reticulum in Saccharomyces cerevisiae, Journal of cell science 124:2424-2437.

Jagerstrom, S., Polesie, S., Wickstrom, Y., Johansson, B.R., Schroder, H.D., Hojlund, K., Bostrom, P. (2009) Lipid droplets interact with mitochondria using SNAP23, Cell biology international 33:934-940.

Jancso, G. (1978) Selective degeneration of chemosensitive primary sensory neurones induced by capsaicin: glial changes, Cell and tissue research 195:145-152.

Jones, D.P. (2008) Radical-free biology of oxidative stress, Am J Physiol Cell Physiol 295:C849-868.

Jones, D.P. (2006) Redefining oxidative stress, Antioxidants & redox signaling 8:1865-1879.

Kang, J.X., Weylandt, K.H. (2008) Modulation of inflammatory cytokines by omega-3 fatty acids, Sub-cellular biochemistry 49:133-143.

Kersten, S. (2001) Mechanisms of nutritional and hormonal regulation of lipogenesis, EMBO reports 2:282-286.

Kesavulu, M.M., Rao, B.K., Giri, R., Vijaya, J., Subramanyam, G., Apparao, C. (2001) Lipid peroxidation and antioxidant enzyme status in Type 2 diabetics with coronary heart disease, Diabetes research and clinical practice 53:33-39.

Khatchadourian, A., Bourque, S.D., Richard, V.R., Titorenko, V.I., Maysinger, D. (2012) Dynamics and regulation of lipid droplet formation in lipopolysaccharide (LPS)-stimulated microglia, Biochimica et biophysica acta 1821:607-617.

Khatchadourian, A., Maysinger, D. (2009) Lipid droplets: their role in nanoparticle-induced oxidative stress, Molecular pharmaceutics 6:1125-1137.

Kimmel, A.R., Brasaemle, D.L., McAndrews-Hill, M., Sztalryd, C., Londos, C. (2010) Adoption of PERILIPIN as a unifying nomenclature for the mammalian PAT-family of intracellular lipid storage droplet proteins, Journal of lipid research 51:468-471.

Kjorholt, C., Akerfeldt, M.C., Biden, T.J., Laybutt, D.R. (2005) Chronic hyperglycemia, independent of plasma lipid levels, is sufficient for the loss of beta-cell differentiation and secretory function in the db/db mouse model of diabetes, Diabetes 54:2755-2763.

Klein, S. (2004) The case of visceral fat: argument for the defense, The Journal of clinical investigation 113:1530-1532.

Kliewer, S.A., Sundseth, S.S., Jones, S.A., Brown, P.J., Wisely, G.B., Koble, C.S., Devchand, P., Wahli, W., Willson, T.M., Lenhard, J.M., Lehmann, J.M. (1997) Fatty acids and eicosanoids regulate gene expression through direct interactions with peroxisome proliferator-activated receptors alpha and gamma, Proceedings of the National Academy of Sciences of the United States of America 94:4318-4323.

Kobayashi, K., Forte, T.M., Taniguchi, S., Ishida, B.Y., Oka, K., Chan, L. (2000) The db/db mouse, a model for diabetic dyslipidemia: molecular characterization and effects of Western diet feeding, Metabolism: clinical and experimental 49:22-31.

Kong, W., Yen, J.H., Vassiliou, E., Adhikary, S., Toscano, M.G., Ganea, D. (2010) Docosahexaenoic acid prevents dendritic cell maturation and in vitro and in vivo expression of the IL-12 cytokine family, Lipids in health and disease 9:12.

Koopman, R., Schaart, G., Hesselink, M.K. (2001) Optimisation of oil red O staining permits combination with immunofluorescence and automated quantification of lipids, Histochemistry and cell biology 116:63-68.

Kousteni, S. (2012) FoxO1, the transcriptional chief of staff of energy metabolism, Bone 50:437-443.

Krahmer, N., Guo, Y., Wilfling, F., Hilger, M., Lingrell, S., Heger, K., Newman, H.W., Schmidt-Supprian, M., Vance, D.E., Mann, M., Farese, R.V., Jr., Walther, T.C. (2011) Phosphatidylcholine synthesis for lipid droplet expansion is mediated by localized activation of CTP:phosphocholine cytidylyltransferase, Cell metabolism 14:504-515.

Kroemer, G., Jaattela, M. (2005) Lysosomes and autophagy in cell death control, Nat Rev Cancer 5:886-897.

Kruger, A.L., Peterson, S.J., Schwartzman, M.L., Fusco, H., McClung, J.A., Weiss, M., Shenouda, S., Goodman, A.I., Goligorsky, M.S., Kappas, A., Abraham, N.G. (2006) Up-regulation of heme oxygenase provides vascular protection in an animal model of diabetes through its antioxidant and antiapoptotic effects, The Journal of pharmacology and experimental therapeutics 319:1144-1152.

Kuerschner, L., Moessinger, C., Thiele, C. (2008) Imaging of lipid biosynthesis: how a neutral lipid enters lipid droplets, Traffic (Copenhagen, Denmark) 9:338-352.

Kuhnlein, R.P. (2012) Lipid droplet-based storage fat metabolism in Drosophila: Thematic Review Series: Lipid Droplet Synthesis and Metabolism: from Yeast to Man, Journal of lipid research 53:1430-1436.

Kurz, T., Terman, A., Gustafsson, B., Brunk, U.T. (2008) Lysosomes in iron metabolism, ageing and apoptosis, Histochemistry and cell biology 129:389-406.

Lacraz, G., Figeac, F., Movassat, J., Kassis, N., Coulaud, J., Galinier, A., Leloup, C., Bailbe, D., Homo-Delarche, F., Portha, B. (2009) Diabetic beta-cells can achieve self-protection against oxidative stress through an adaptive up-regulation of their antioxidant defenses, PloS one 4:e6500.

Lafontan, M., Berlan, M. (1993) Fat cell adrenergic receptors and the control of white and brown fat cell function, Journal of lipid research 34:1057-1091.

Lalancette-Hebert, M., Moquin, A., Choi, A.O., Kriz, J., Maysinger, D. (2010) Lipopolysaccharide-QD micelles induce marked induction of TLR2 and lipid droplet accumulation in olfactory bulb microglia, Molecular pharmaceutics 7:1183-1194.

Lali, F.V., Hunt, A.E., Turner, S.J., Foxwell, B.M. (2000) The pyridinyl imidazole inhibitor SB203580 blocks phosphoinositide-dependent protein kinase activity, protein kinase B phosphorylation, and retinoblastoma hyperphosphorylation in interleukin-2-stimulated T cells independently of p38 mitogen-activated protein kinase, The Journal of biological chemistry 275:7395-7402.

Lalloyer, F., Vandewalle, B., Percevault, F., Torpier, G., Kerr-Conte, J., Oosterveer, M., Paumelle, R., Fruchart, J.C., Kuipers, F., Pattou, F., Fievet, C., Staels, B. (2006) Peroxisome proliferator-activated receptor alpha improves pancreatic adaptation to insulin resistance in obese mice and reduces lipotoxicity in human islets, Diabetes 55:1605-1613.

Larigauderie, G., Furman, C., Jaye, M., Lasselin, C., Copin, C., Fruchart, J.C., Castro, G., Rouis, M. (2004) Adipophilin enhances lipid accumulation and prevents lipid efflux from THP-1 macrophages: potential role in atherogenesis, Arteriosclerosis, thrombosis, and vascular biology 24:504-510.

Lavie, C.J., Milani, R.V., Ventura, H.O. (2009) Obesity and cardiovascular disease: risk factor, paradox, and impact of weight loss, Journal of the American College of Cardiology 53:1925-1932.

Le Lay, S., Briand, N., Blouin, C.M., Chateau, D., Prado, C., Lasnier, F., Le Liepvre, X., Hajduch, E., Dugail, I. (2010) The lipoatrophic caveolin-1 deficient mouse model reveals autophagy in mature adipocytes, Autophagy 6:754-763.

Le Lay, S., Dugail, I. (2009) Connecting lipid droplet biology and the metabolic syndrome, Progress in lipid research 48:191-195.

Leahy, J.L., Bonner-Weir, S., Weir, G.C. (1992) Beta-cell dysfunction induced by chronic hyperglycemia. Current ideas on mechanism of impaired glucose-induced insulin secretion, Diabetes care 15:442-455.

Lebovitz, H.E., Banerji, M.A. (2005) Point: visceral adiposity is causally related to insulin resistance, Diabetes care 28:2322-2325.

Lee, J.C., Laydon, J.T., McDonnell, P.C., Gallagher, T.F., Kumar, S., Green, D., McNulty, D., Blumenthal, M.J., Heys, J.R., Landvatter, S.W., et al. (1994) A protein kinase involved in the regulation of inflammatory cytokine biosynthesis, Nature 372:739-746.

Lee, J.S., Mendez, R., Heng, H.H., Yang, Z.Q., Zhang, K. (2012) Pharmacological ER stress promotes hepatic lipogenesis and lipid droplet formation, American journal of translational research 4:102-113.

Lee, Y., Hirose, H., Ohneda, M., Johnson, J.H., McGarry, J.D., Unger, R.H. (1994) Beta-cell lipotoxicity in the pathogenesis of non-insulin-dependent diabetes mellitus of obese rats: impairment in adipocyte-beta-cell relationships, Proceedings of the National Academy of Sciences of the United States of America 91:10878-10882.

Lee, Y., Lingvay, I., Szczepaniak, L.S., Ravazzola, M., Orci, L., Unger, R.H. (2010) Pancreatic steatosis: harbinger of type 2 diabetes in obese rodents, International journal of obesity (2005) 34:396-400.

Leventis, P.A., Grinstein, S. (2010) The distribution and function of phosphatidylserine in cellular membranes, Annual review of biophysics 39:407-427.

Levine, B., Yuan, J. (2005) Autophagy in cell death: an innocent convict?, The Journal of clinical investigation 115:2679-2688.

Levine, T. (2004) Short-range intracellular trafficking of small molecules across endoplasmic reticulum junctions, Trends in cell biology 14:483-490.

Lewinski, N., Colvin, V., Drezek, R. (2008) Cytotoxicity of nanoparticles, Small (Weinheim an der Bergstrasse, Germany) 4:26-49.

Li, L.O., Klett, E.L., Coleman, R.A. (2010) Acyl-CoA synthesis, lipid metabolism and lipotoxicity, Biochimica et biophysica acta 1801:246-251.

Li, M., Kim, D.H., Tsenovoy, P.L., Peterson, S.J., Rezzani, R., Rodella, L.F., Aronow, W.S., Ikehara, S., Abraham, N.G. (2008) Treatment of obese diabetic mice with a heme oxygenase inducer reduces visceral and subcutaneous adiposity, increases adiponectin levels, and improves insulin sensitivity and glucose tolerance, Diabetes 57:1526-1535.

Listenberger, L.L., Brown, D.A. (2007) Fluorescent detection of lipid droplets and associated proteins, Current protocols in cell biology / editorial board, Juan S. Bonifacino ... [et al Chapter 24:Unit 24 22.

Listenberger, L.L., Han, X., Lewis, S.E., Cases, S., Farese, R.V., Jr., Ory, D.S., Schaffer, J.E. (2003) Triglyceride accumulation protects against fatty acid-induced lipotoxicity, Proceedings of the National Academy of Sciences of the United States of America 100:3077-3082.

Listenberger, L.L., Ory, D.S., Schaffer, J.E. (2001) Palmitate-induced apoptosis can occur through a ceramide-independent pathway, The Journal of biological chemistry 276:14890-14895.

Listenberger, L.L., Ostermeyer-Fay, A.G., Goldberg, E.B., Brown, W.J., Brown, D.A. (2007) Adipocyte differentiation-related protein reduces the lipid droplet association of adipose triglyceride lipase and slows triacylglycerol turnover, Journal of lipid research 48:2751-2761.

Liu, P., Ying, Y., Zhao, Y., Mundy, D.I., Zhu, M., Anderson, R.G. (2004) Chinese hamster ovary K2 cell lipid droplets appear to be metabolic organelles involved in membrane traffic, The Journal of biological chemistry 279:3787-3792.

Londos, C., Brasaemle, D.L., Gruia-Gray, J., Servetnick, D.A., Schultz, C.J., Levin, D.M., Kimmel, A.R. (1995) Perilipin: unique proteins associated with intracellular neutral lipid droplets in adipocytes and steroidogenic cells, Biochemical Society transactions 23:611-615.

Lopez-Miranda, J., Williams, C., Lairon, D. (2007) Dietary, physiological, genetic and pathological influences on postprandial lipid metabolism, The British journal of nutrition 98:458-473.

Lovric, J., Bazzi, H.S., Cuie, Y., Fortin, G.R., Winnik, F.M., Maysinger, D. (2005) Differences in subcellular distribution and toxicity of green and red emitting CdTe quantum dots, Journal of molecular medicine (Berlin, Germany) 83:377-385.

Lovric, J., Cho, S.J., Winnik, F.M., Maysinger, D. (2005) Unmodified cadmium telluride quantum dots induce reactive oxygen species formation leading to multiple organelle damage and cell death, Chemistry & biology 12:1227-1234.

Maedler, K., Spinas, G.A., Dyntar, D., Moritz, W., Kaiser, N., Donath, M.Y. (2001) Distinct effects of saturated and monounsaturated fatty acids on beta-cell turnover and function, Diabetes 50:69-76.

Magnusson, B., Asp, L., Bostrom, P., Ruiz, M., Stillemark-Billton, P., Linden, D., Boren, J., Olofsson, S.O. (2006) Adipocyte differentiation-related protein promotes fatty acid storage in cytosolic triglycerides and inhibits secretion of very low-density lipoproteins, Arteriosclerosis, thrombosis, and vascular biology 26:1566-1571.

Man, Z.W., Zhu, M., Noma, Y., Toide, K., Sato, T., Asahi, Y., Hirashima, T., Mori, S., Kawano, K., Mizuno, A., Sano, T., Shima, K. (1997) Impaired beta-cell function and deposition of fat droplets in the pancreas as a consequence of hypertriglyceridemia in OLETF rat, a model of spontaneous NIDDM, Diabetes 46:1718-1724.

Marselli, L., Thorne, J., Dahiya, S., Sgroi, D.C., Sharma, A., Bonner-Weir, S., Marchetti, P., Weir, G.C. (2010) Gene expression profiles of Beta-cell enriched tissue obtained by laser capture microdissection from subjects with type 2 diabetes, PloS one 5:e11499.

Martin, P.G., Guillou, H., Lasserre, F., Dejean, S., Lan, A., Pascussi, J.M., Sancristobal, M., Legrand, P., Besse, P., Pineau, T. (2007) Novel aspects of PPARalpha-mediated regulation of lipid and xenobiotic metabolism revealed through a nutrigenomic study, Hepatology (Baltimore, Md 45:767-777.

Martin, S., Parton, R.G. (2006) Lipid droplets: a unified view of a dynamic organelle, Nat Rev Mol Cell Biol 7:373-378.

Mashek, D.G., Li, L.O., Coleman, R.A. (2007) Long-chain acyl-CoA synthetases and fatty acid channeling, Future lipidology 2:465-476.

Masuda, Y., Itabe, H., Odaki, M., Hama, K., Fujimoto, Y., Mori, M., Sasabe, N., Aoki, J., Arai, H., Takano, T. (2006) ADRP/adipophilin is degraded through the proteasome-dependent pathway during regression of lipid-storing cells, Journal of lipid research 47:87-98.

Matsuo, M., Hamasaki, Y., Fujiyama, F., Miyazaki, S. (1995) Eicosanoids are produced by microglia, not by astrocytes, in rat glial cell cultures, Brain research 685:201-204.

Mattos, K.A., D'Avila, H., Rodrigues, L.S., Oliveira, V.G., Sarno, E.N., Atella, G.C., Pereira, G.M., Bozza, P.T., Pessolani, M.C. (2010) Lipid droplet formation in leprosy: Toll-like receptor-regulated organelles involved in eicosanoid formation and Mycobacterium leprae pathogenesis, Journal of leukocyte biology 87:371-384.

Maurel, D.B., Pallu, S., Jaffre, C., Fazzalari, N.L., Boisseau, N., Uzbekov, R., Benhamou, C.L., Rochefort, G.Y. (2012) Osteocyte apoptosis and lipid infiltration as mechanisms of alcohol-induced bone loss, Alcohol and alcoholism (Oxford, Oxfordshire) 47:413-422.

Maysinger, D. (2007) Nanoparticles and cells: good companions and doomed partnerships, Organic & biomolecular chemistry 5:2335-2342.

Maysinger, D., Lovric, J. (2007) Quantum dots and other fluorescent nanoparticles: quo vadis in the cell?, Advances in experimental medicine and biology 620:156-167.

Mazzone, T., Chait, A., Plutzky, J. (2008) Cardiovascular disease risk in type 2 diabetes mellitus: insights from mechanistic studies, Lancet 371:1800-1809.

McCubrey, J.A., Lahair, M.M., Franklin, R.A. (2006) Reactive oxygen species-induced activation of the MAP kinase signaling pathways, Antioxidants & redox signaling 8:1775-1789.

McGarry, J.D., Dobbins, R.L. (1999) Fatty acids, lipotoxicity and insulin secretion, Diabetologia 42:128-138.

McGookey, D.J., Anderson, R.G. (1983) Morphological characterization of the cholesteryl ester cycle in cultured mouse macrophage foam cells, The Journal of cell biology 97:1156-1168.

McKimmie, C.S., Roy, D., Forster, T., Fazakerley, J.K. (2006) Innate immune response gene expression profiles of N9 microglia are pathogen-type specific, Journal of neuroimmunology 175:128-141.

Meadows, J.W., Pitzer, B., Brockman, D.E., Myatt, L. (2005) Expression and localization of adipophilin and perilipin in human fetal membranes: association with lipid bodies and enzymes involved in prostaglandin synthesis, The Journal of clinical endocrinology and metabolism 90:2344-2350.

Medina, J.M., Tabernero, A. (2002) Astrocyte-synthesized oleic acid behaves as a neurotrophic factor for neurons, Journal of physiology, Paris 96:265-271.

Meigs, J.B., Larson, M.G., Fox, C.S., Keaney, J.F., Jr., Vasan, R.S., Benjamin, E.J. (2007) Association of oxidative stress, insulin resistance, and diabetes risk phenotypes: the Framingham Offspring Study, Diabetes care 30:2529-2535.

Melo, R.C., Fabrino, D.L., Dias, F.F., Parreira, G.G. (2006) Lipid bodies: Structural markers of inflammatory macrophages in innate immunity, Inflamm Res 55:342-348.

Michalet, X., Pinaud, F.F., Bentolila, L.A., Tsay, J.M., Doose, S., Li, J.J., Sundaresan, G., Wu, A.M., Gambhir, S.S., Weiss, S. (2005) Quantum dots for live cells, in vivo imaging, and diagnostics, Science (New York, N.Y 307:538-544.

Minnaard, R., Schrauwen, P., Schaart, G., Jorgensen, J.A., Lenaers, E., Mensink, M., Hesselink, M.K. (2009) Adipocyte differentiation-related protein and OXPAT in rat and human skeletal muscle: involvement in lipid accumulation and type 2 diabetes mellitus, The Journal of clinical endocrinology and metabolism 94:4077-4085.

Mishra, R., Emancipator, S.N., Miller, C., Kern, T., Simonson, M.S. (2004) Adipose differentiation-related protein and regulators of lipid homeostasis identified by gene expression profiling in the murine db/db diabetic kidney, Am J Physiol Renal Physiol 286:F913-921.

Miura, S., Gan, J.W., Brzostowski, J., Parisi, M.J., Schultz, C.J., Londos, C., Oliver, B., Kimmel, A.R. (2002) Functional conservation for lipid storage droplet association among Perilipin, ADRP, and TIP47 (PAT)-related proteins in mammals, Drosophila, and Dictyostelium, The Journal of biological chemistry 277:32253-32257.

Moffitt, J.H., Fielding, B.A., Evershed, R., Berstan, R., Currie, J.M., Clark, A. (2005) Adverse physicochemical properties of tripalmitin in beta cells lead to morphological changes and lipotoxicity in vitro, Diabetologia 48:1819-1829.

Moldovan, L., Moldovan, N.I. (2004) Oxygen free radicals and redox biology of organelles, Histochemistry and cell biology 122:395-412.

Moreira, L.S., Piva, B., Gentile, L.B., Mesquita-Santos, F.P., D'Avila, H., Maya-Monteiro, C.M., Bozza, P.T., Bandeira-Melo, C., Diaz, B.L. (2009) Cytosolic phospholipase A2-driven PGE2 synthesis within unsaturated fatty acids-induced lipid bodies of epithelial cells, Biochimica et biophysica acta 1791:156-165.

Moro, C., Bajpeyi, S., Smith, S.R. (2008) Determinants of intramyocellular triglyceride turnover: implications for insulin sensitivity, American journal of physiology 294:E203-213.

Morse, D., Choi, A.M. (2005) Heme oxygenase-1: from bench to bedside, American journal of respiratory and critical care medicine 172:660-670.

Motomura, W., Inoue, M., Ohtake, T., Takahashi, N., Nagamine, M., Tanno, S., Kohgo, Y., Okumura, T. (2006) Up-regulation of ADRP in fatty liver in human and liver steatosis in mice fed with high fat diet, Biochemical and biophysical research communications 340:1111-1118.

Mottagui-Tabar, S., Ryden, M., Lofgren, P., Faulds, G., Hoffstedt, J., Brookes, A.J., Andersson, I., Arner, P. (2003) Evidence for an important role of perilipin in the regulation of human adipocyte lipolysis, Diabetologia 46:789-797.

Moustaid, N., Jones, B.H., Taylor, J.W. (1996) Insulin increases lipogenic enzyme activity in human adipocytes in primary culture, The Journal of nutrition 126:865-870.

Muller, L., Riediker, M., Wick, P., Mohr, M., Gehr, P., Rothen-Rutishauser, B. (2010) Oxidative stress and inflammation response after nanoparticle exposure: differences between human lung cell monocultures and an advanced three-dimensional model of the human epithelial airways, Journal of the Royal Society, Interface / the Royal Society 7 Suppl 1:S27-40.

Murphy, D.J. (2001) The biogenesis and functions of lipid bodies in animals, plants and microorganisms, Progress in lipid research 40:325-438.

Murphy, D.J., Vance, J. (1999) Mechanisms of lipid-body formation, Trends in biochemical sciences 24:109-115.

Murphy, S., Martin, S., Parton, R.G. (2009) Lipid droplet-organelle interactions; sharing the fats, Biochimica et biophysica acta 1791:441-447.

Murphy, S., Martin, S., Parton, R.G. (2008) Lipid droplet-organelle interactions; sharing the fats, Biochimica et biophysica acta.

Murphy, S., Martin, S., Parton, R.G. (2010) Quantitative analysis of lipid droplet fusion: inefficient steady state fusion but rapid stimulation by chemical fusogens, PloS one 5:e15030.

Nakamura, N., Banno, Y., Tamiya-Koizumi, K. (2005) Arf1-dependent PLD1 is localized to oleic acid-induced lipid droplets in NIH3T3 cells, Biochemical and biophysical research communications 335:117-123.

Nakamura, Y., Si, Q.S., Kataoka, K. (1999) Lipopolysaccharide-induced microglial activation in culture: temporal profiles of morphological change and release of cytokines and nitric oxide, Neuroscience research 35:95-100.

Nan, X., Cheng, J.X., Xie, X.S. (2003) Vibrational imaging of lipid droplets in live fibroblast cells with coherent anti-Stokes Raman scattering microscopy, Journal of lipid research 44:2202-2208.

National Center for Health Statistics (NCHS) Data Brief (2012) Prevalence of Obesity in the United States, 2009–2010.

Neff, L.M., Culiner, J., Cunningham-Rundles, S., Seidman, C., Meehan, D., Maturi, J., Wittkowski, K.M., Levine, B., Breslow, J.L. (2011) Algal docosahexaenoic acid affects plasma lipoprotein particle size distribution in overweight and obese adults, The Journal of nutrition 141:207-213.

Nel, A., Xia, T., Madler, L., Li, N. (2006) Toxic potential of materials at the nanolevel, Science (New York, N.Y 311:622-627.

Nguyen, L.N., Nosanchuk, J.D. (2011) Lipid droplet formation protects against gluco/lipotoxicity in Candida parapsilosis: an essential role of fatty acid desaturase Ole1, Cell cycle (Georgetown, Tex 10:3159-3167.

Oh, Y.T., Lee, J.Y., Lee, J., Kim, H., Yoon, K.S., Choe, W., Kang, I. (2009) Oleic acid reduces lipopolysaccharide-induced expression of iNOS and COX-2 in BV2 murine microglial cells: possible involvement of reactive oxygen species, p38 MAPK, and IKK/NF-kappaB signaling pathways, Neuroscience letters 464:93-97.

Ohsaki, Y., Cheng, J., Fujita, A., Tokumoto, T., Fujimoto, T. (2006) Cytoplasmic lipid droplets are sites of convergence of proteasomal and autophagic degradation of apolipoprotein B, Molecular biology of the cell 17:2674-2683.

Ohsaki, Y., Shinohara, Y., Suzuki, M., Fujimoto, T. (2010) A pitfall in using BODIPY dyes to label lipid droplets for fluorescence microscopy, Histochemistry and cell biology 133:477-480.

Ono, K., Kim, S.O., Han, J. (2003) Susceptibility of lysosomes to rupture is a determinant for plasma membrane disruption in tumor necrosis factor alpha-induced cell death, Molecular and cellular biology 23:665-676.

Osman, C., Haag, M., Potting, C., Rodenfels, J., Dip, P.V., Wieland, F.T., Brugger, B., Westermann, B., Langer, T. (2009) The genetic interactome of prohibitins: coordinated control of cardiolipin and phosphatidylethanolamine by conserved regulators in mitochondria, The Journal of cell biology 184:583-596.

Osman, C., Voelker, D.R., Langer, T. (2011) Making heads or tails of phospholipids in mitochondria, The Journal of cell biology 192:7-16.

Ouimet, M., Franklin, V., Mak, E., Liao, X., Tabas, I., Marcel, Y.L. (2011) Autophagy regulates cholesterol efflux from macrophage foam cells via lysosomal acid lipase, Cell metabolism 13:655-667.

Ozeki, S., Cheng, J., Tauchi-Sato, K., Hatano, N., Taniguchi, H., Fujimoto, T. (2005) Rab18 localizes to lipid droplets and induces their close apposition to the endoplasmic reticulum-derived membrane, Journal of cell science 118:2601-2611.

Pacheco, P., Bozza, F.A., Gomes, R.N., Bozza, M., Weller, P.F., Castro-Faria-Neto, H.C., Bozza, P.T. (2002) Lipopolysaccharide-induced leukocyte lipid body formation in vivo: innate immunity elicited intracellular Loci involved in eicosanoid metabolism, J Immunol 169:6498-6506.

Pacheco, P., Vieira-de-Abreu, A., Gomes, R.N., Barbosa-Lima, G., Wermelinger, L.B., Maya-Monteiro, C.M., Silva, A.R., Bozza, M.T., Castro-Faria-Neto, H.C., Bandeira-Melo, C., Bozza, P.T. (2007) Monocyte chemoattractant protein-1/CC chemokine ligand 2 controls microtubule-driven biogenesis and leukotriene B4-synthesizing function of macrophage lipid bodies elicited by innate immune response, J Immunol 179:8500-8508.

Panzram, G. (1987) Mortality and survival in type 2 (non-insulin-dependent) diabetes mellitus, Diabetologia 30:123-131.

Park, K.S., Ciaraldi, T.P., Abrams-Carter, L., Mudaliar, S., Nikoulina, S.E., Henry, R.R. (1997) PPAR-gamma gene expression is elevated in skeletal muscle of obese and type II diabetic subjects, Diabetes 46:1230-1234.

Patel, R.T., Soulages, J.L., Hariharasundaram, B., Arrese, E.L. (2005) Activation of the lipid droplet controls the rate of lipolysis of triglycerides in the insect fat body, The Journal of biological chemistry 280:22624-22631.

Perez-Jimenez, F., Espino, A., Lopez-Segura, F., Blanco, J., Ruiz-Gutierrez, V., Prada, J.L., Lopez-Miranda, J., Jimenez-Pereperez, J., Ordovas, J.M. (1995) Lipoprotein concentrations in normolipidemic males consuming oleic acid-rich diets from two different sources: olive oil and oleic acid-rich sunflower oil, The American journal of clinical nutrition 62:769-775.

Phillips, S.A., Choe, C.C., Ciaraldi, T.P., Greenberg, A.S., Kong, A.P., Baxi, S.C., Christiansen, L., Mudaliar, S.R., Henry, R.R. (2005) Adipocyte differentiation-related protein in human skeletal muscle: relationship to insulin sensitivity, Obesity research 13:1321-1329.

Piga, R., Saito, Y., Yoshida, Y., Niki, E. (2007) Cytotoxic effects of various stressors on PC12 cells: involvement of oxidative stress and effect of antioxidants, Neurotoxicology 28:67-75.

Pinnick, K.E., Collins, S.C., Londos, C., Gauguier, D., Clark, A., Fielding, B.A. (2008) Pancreatic ectopic fat is characterized by adipocyte infiltration and altered lipid composition, Obesity (Silver Spring, Md 16:522-530.

Poitout, V. (2004) Beta-cell lipotoxicity: burning fat into heat?, Endocrinology 145:3563-3565.

Ponugoti, B., Dong, G., Graves, D.T. (2012) Role of forkhead transcription factors in diabetes-induced oxidative stress, Experimental diabetes research 2012:939751.

Porter, S.A., Massaro, J.M., Hoffmann, U., Vasan, R.S., O'Donnel, C.J., Fox, C.S. (2009) Abdominal subcutaneous adipose tissue: a protective fat depot?, Diabetes care 32:1068-1075.

Posokhova, E.N., Khoshchenko, O.M., Chasovskikh, M.I., Pivovarova, E.N., Dushkin, M.I. (2008) Lipid synthesis in macrophages during inflammation in vivo: effect of agonists of peroxisome proliferator activated receptors alpha and gamma and of retinoid X receptors, Biochemistry 73:296-304.

Pu, J., Ha, C.W., Zhang, S., Jung, J.P., Huh, W.K., Liu, P. (2011) Interactomic study on interaction between lipid droplets and mitochondria, Protein & cell 2:487-496.

Public Health Agency of Canada (2011) Diabetes in Canada: Facts and figures from a public health perspective.

Public Health Agency of Canada, Canadian Institute for Health Information, Obesity in Canada: A joint report from the Public Health Agency of Canada and the Canadian Institute for Health Information, 2011.

Puri, V., Czech, M.P. (2008) Lipid droplets: FSP27 knockout enhances their sizzle, The Journal of clinical investigation 118:2693-2696.

Puri, V., Konda, S., Ranjit, S., Aouadi, M., Chawla, A., Chouinard, M., Chakladar, A., Czech, M.P. (2007) Fat-specific protein 27, a novel lipid droplet protein that enhances triglyceride storage, The Journal of biological chemistry 282:34213-34218.

Qi, H.Y., Shelhamer, J.H. (2005) Toll-like receptor 4 signaling regulates cytosolic phospholipase A2 activation and lipid generation in lipopolysaccharide-stimulated macrophages, The Journal of biological chemistry 280:38969-38975.

Quehenberger, O., Armando, A.M., Brown, A.H., Milne, S.B., Myers, D.S., Merrill, A.H., Bandyopadhyay, S., Jones, K.N., Kelly, S., Shaner, R.L., Sullards, C.M., Wang, E., Murphy, R.C., Barkley, R.M., Leiker, T.J., Raetz, C.R., Guan, Z., Laird, G.M., Six, D.A., Russell, D.W., McDonald, J.G., Subramaniam, S., Fahy, E., Dennis, E.A. (2010) Lipidomics reveals a remarkable diversity of lipids in human plasma, Journal of lipid research 51:3299-3305.

Quinn, J.F., Raman, R., Thomas, R.G., Yurko-Mauro, K., Nelson, E.B., Van Dyck, C., Galvin, J.E., Emond, J., Jack, C.R., Jr., Weiner, M., Shinto, L., Aisen, P.S. (2010) Docosahexaenoic acid supplementation and cognitive decline in Alzheimer disease: a randomized trial, Jama 304:1903-1911.

Raclot, T., Groscolas, R. (1995) Selective mobilization of adipose tissue fatty acids during energy depletion in the rat, Journal of lipid research 36:2164-2173.

Raederstorff, D., Pantze, M., Bachmann, H., Moser, U. (1996) Anti-inflammatory properties of docosahexaenoic and eicosapentaenoic acids in phorbol-ester-induced mouse ear inflammation, International archives of allergy and immunology 111:284-290.

Reye, R.D., Morgan, G., Baral, J. (1963) Encephalopathy and Fatty Degeneration of the Viscera. a Disease Entity in Childhood, Lancet 2:749-752.

Rinia, H.A., Burger, K.N., Bonn, M., Muller, M. (2008) Quantitative label-free imaging of lipid composition and packing of individual cellular lipid droplets using multiplex CARS microscopy, Biophysical journal 95:4908-4914.

Rivest, S. (2009) Regulation of innate immune responses in the brain, Nat Rev Immunol 9:429-439.

Robenek, H., Lorkowski, S., Schnoor, M., Troyer, D. (2005) Spatial integration of TIP47 and adipophilin in macrophage lipid bodies, The Journal of biological chemistry 280:5789-5794.

Robertson, R.P. (2004) Chronic oxidative stress as a central mechanism for glucose toxicity in pancreatic islet beta cells in diabetes, The Journal of biological chemistry 279:42351-42354.

Robson-Doucette, C.A., Sultan, S., Allister, E.M., Wikstrom, J.D., Koshkin, V., Bhattacharjee, A., Prentice, K.J., Sereda, S.B., Shirihai, O.S., Wheeler, M.B. Beta-cell uncoupling protein 2 regulates reactive oxygen species production, which influences both insulin and glucagon secretion, Diabetes 60:2710-2719.

Rock, R.B., Gekker, G., Hu, S., Sheng, W.S., Cheeran, M., Lokensgard, J.R., Peterson, P.K. (2004) Role of microglia in central nervous system infections, Clinical microbiology reviews 17:942-964.

Ross, R. (1995) Cell biology of atherosclerosis, Annual review of physiology 57:791-804.

Rubinsztein, D.C., Gestwicki, J.E., Murphy, L.O., Klionsky, D.J. (2007) Potential therapeutic applications of autophagy, Nat Rev Drug Discov 6:304-312.

Sacks, F.M., Campos, H. (2003) Clinical review 163: Cardiovascular endocrinology: Low-density lipoprotein size and cardiovascular disease: a reappraisal, The Journal of clinical endocrinology and metabolism 88:4525-4532.

Salata, O. (2004) Applications of nanoparticles in biology and medicine, Journal of nanobiotechnology 2:3.

Saleh, J., Sniderman, A.D., Cianflone, K. (1999) Regulation of Plasma fatty acid metabolism, Clinica chimica acta; international journal of clinical chemistry 286:163-180.

Sanchez-Tillo, E., Comalada, M., Xaus, J., Farrera, C., Valledor, A.F., Caelles, C., Lloberas, J., Celada, A. (2007) JNK1 Is required for the induction of Mkp1 expression in macrophages during proliferation and lipopolysaccharide-dependent activation, The Journal of biological chemistry 282:12566-12573.

Saponaro, C., Cianciulli, A., Calvello, R., Dragone, T., Iacobazzi, F., Panaro, M.A. (2012) The PI3K/Akt pathway is required for LPS activation of microglial cells, Immunopharmacology and immunotoxicology.

Satoh, T., Enokido, Y., Aoshima, H., Uchiyama, Y., Hatanaka, H. (1997) Changes in mitochondrial membrane potential during oxidative stress-induced apoptosis in PC12 cells, Journal of neuroscience research 50:413-420.

Schadinger, S.E., Bucher, N.L., Schreiber, B.M., Farmer, S.R. (2005) PPARgamma2 regulates lipogenesis and lipid accumulation in steatotic hepatocytes, American journal of physiology 288:E1195-1205.

Schaffer, J.E. (2003) Lipotoxicity: when tissues overeat, Current opinion in lipidology 14:281-287.

Schmitz, G., Grandl, M. (2008) Endolysosomal phospholipidosis and cytosolic lipid droplet storage and release in macrophages, Biochimica et biophysica acta.

Schmitz, J.E., Kettunen, M.I., Hu, D.E., Brindle, K.M. (2005) 1H MRS-visible lipids accumulate during apoptosis of lymphoma cells in vitro and in vivo, Magn Reson Med 54:43-50.

Sekiya, M., Hiraishi, A., Touyama, M., Sakamoto, K. (2008) Oxidative stress induced lipid accumulation via SREBP1c activation in HepG2 cells, Biochemical and biophysical research communications 375:602-607.

Seleverstov, O., Zabirnyk, O., Zscharnack, M., Bulavina, L., Nowicki, M., Heinrich, J.M., Yezhelyev, M., Emmrich, F., O'Regan, R., Bader, A. (2006) Quantum dots for human mesenchymal stem cells labeling. A size-dependent autophagy activation, Nano letters 6:2826-2832.

Shacka, J.J., Roth, K.A., Zhang, J. (2008) The autophagy-lysosomal degradation pathway: role in neurodegenerative disease and therapy, Front Biosci 13:718-736.

Shanik, M.H., Xu, Y., Skrha, J., Dankner, R., Zick, Y., Roth, J. (2008) Insulin resistance and hyperinsulinemia: is hyperinsulinemia the cart or the horse?, Diabetes care 31 Suppl 2:S262-268.

Shibata, M., Kanamori, S., Isahara, K., Ohsawa, Y., Konishi, A., Kametaka, S., Watanabe, T., Ebisu, S., Ishido, K., Kominami, E., Uchiyama, Y. (1998) Participation of cathepsins B and D in apoptosis of PC12 cells following serum deprivation, Biochemical and biophysical research communications 251:199-203.

Silva, A.R., Pacheco, P., Vieira-de-Abreu, A., Maya-Monteiro, C.M., D'Alegria, B., Magalhaes, K.G., de Assis, E.F., Bandeira-Melo, C., Castro-Faria-Neto, H.C., Bozza, P.T. (2009) Lipid bodies in oxidized LDL-induced foam cells are leukotriene-

synthesizing organelles: a MCP-1/CCL2 regulated phenomenon, Biochimica et biophysica acta 1791:1066-1075.

Singh, R., Kaushik, S., Wang, Y., Xiang, Y., Novak, I., Komatsu, M., Tanaka, K., Cuervo, A.M., Czaja, M.J. (2009) Autophagy regulates lipid metabolism, Nature 458:1131-1135.

Smirnova, E., Goldberg, E.B., Makarova, K.S., Lin, L., Brown, W.J., Jackson, C.L. (2006) ATGL has a key role in lipid droplet/adiposome degradation in mammalian cells, EMBO reports 7:106-113.

Smith, C.L. (2001) Basic confocal microscopy, Current protocols in cell biology / editorial board, Juan S. Bonifacino ... [et al Chapter 4:Unit 4 5.

Sobaniec-Lotowska, M.E. (2005) A transmission electron microscopic study of microglia/macrophages in the hippocampal cortex and neocortex following chronic exposure to valproate, International journal of experimental pathology 86:91-96.

Spitz, D.R., Kinter, M.T., Kehrer, J.P., Roberts, R.J. (1992) The effect of monosaturated and polyunsaturated fatty acids on oxygen toxicity in cultured cells, Pediatric research 32:366-372.

Starke, A.A., Erhardt, G., Berger, M., Zimmermann, H. (1984) Elevated pancreatic glucagon in obesity, Diabetes 33:277-280.

Stern, S.T., Zolnik, B.S., McLeland, C.B., Clogston, J., Zheng, J., McNeil, S.E. (2008) Induction of Autophagy in Porcine Kidney Cells by Quantum Dots: A Common Cellular Response to Nanomaterials?, Toxicol Sci.

Storlien, L.H., Jenkins, A.B., Chisholm, D.J., Pascoe, W.S., Khouri, S., Kraegen, E.W. (1991) Influence of dietary fat composition on development of insulin resistance in rats. Relationship to muscle triglyceride and omega-3 fatty acids in muscle phospholipid, Diabetes 40:280-289.

Stratton, I.M., Adler, A.I., Neil, H.A., Matthews, D.R., Manley, S.E., Cull, C.A., Hadden, D., Turner, R.C., Holman, R.R. (2000) Association of glycaemia with macrovascular and microvascular complications of type 2 diabetes (UKPDS 35): prospective observational study, BMJ (Clinical research ed 321:405-412.

Straub, B.K., Stoeffel, P., Heid, H., Zimbelmann, R., Schirmacher, P. (2008) Differential pattern of lipid droplet-associated proteins and de novo perilipin expression in hepatocyte steatogenesis, Hepatology (Baltimore, Md 47:1936-1946.

Strohmaier, A.R., Porwol, T., Acker, H., Spiess, E. (1997) Tomography of cells by confocal laser scanning microscopy and computer-assisted three-dimensional image reconstruction: localization of cathepsin B in tumor cells penetrating collagen gels in vitro, J Histochem Cytochem 45:975-983.

Sturmey, R.G., O'Toole, P.J., Leese, H.J. (2006) Fluorescence resonance energy transfer analysis of mitochondrial:lipid association in the porcine oocyte, Reproduction (Cambridge, England) 132:829-837.

Sturrock, R.R. (1984) Microglia in the human embryonic optic nerve, Journal of anatomy 139 (Pt 1):81-91.

Sun, G.Y., Xu, J., Jensen, M.D., Simonyi, A. (2004) Phospholipase A2 in the central nervous system: implications for neurodegenerative diseases, Journal of lipid research 45:205-213.

Suzuki, K., Takahashi, K., Nishimaki-Mogami, T., Kagechika, H., Yamamoto, M., Itabe, H. (2009) Docosahexaenoic acid induces adipose differentiation-related protein through activation of retinoid x receptor in human choriocarcinoma BeWo cells, Biological & pharmaceutical bulletin 32:1177-1182.

Suzuki, M., Shinohara, Y., Ohsaki, Y., Fujimoto, T. (2011) Lipid droplets: size matters, Journal of electron microscopy 60 Suppl 1:S101-116.

Swinburn, B.A., Sacks, G., Hall, K.D., McPherson, K., Finegood, D.T., Moodie, M.L., Gortmaker, S.L. (2011) The global obesity pandemic: shaped by global drivers and local environments, Lancet 378:804-814.

Taegtmeyer, H., Harmancey, R. (2008) Virchow's metamorphosis revealed triglycerides in the heart, Journal of the American College of Cardiology 52:1013-1014.

Takeuchi, K., Reue, K. (2009) Biochemistry, physiology, and genetics of GPAT, AGPAT, and lipin enzymes in triglyceride synthesis, American journal of physiology 296:E1195-1209.

Targett-Adams, P., McElwee, M.J., Ehrenborg, E., Gustafsson, M.C., Palmer, C.N., McLauchlan, J. (2005) A PPAR response element regulates transcription of the gene for human adipose differentiation-related protein, Biochimica et biophysica acta 1728:95-104.

Tassoni, D., Kaur, G., Weisinger, R.S., Sinclair, A.J. (2008) The role of eicosanoids in the brain, Asia Pacific journal of clinical nutrition 17 Suppl 1:220-228.

Tauchi-Sato, K., Ozeki, S., Houjou, T., Taguchi, R., Fujimoto, T. (2002) The surface of lipid droplets is a phospholipid monolayer with a unique Fatty Acid composition, The Journal of biological chemistry 277:44507-44512.

Tavian, D., Colombo, R. (2007) Improved cytochemical method for detecting Jordans' bodies in neutral lipid storage diseases, J Clin Pathol 60:956-958.

Thannickal, V.J., Fanburg, B.L. (2000) Reactive oxygen species in cell signaling, Am J Physiol Lung Cell Mol Physiol 279:L1005-1028.

Thiberge, S., Nechushtan, A., Sprinzak, D., Gileadi, O., Behar, V., Zik, O., Chowers, Y., Michaeli, S., Schlessinger, J., Moses, E. (2004) Scanning electron microscopy of cells and tissues under fully hydrated conditions, Proceedings of the National Academy of Sciences of the United States of America 101:3346-3351.

Tobin, K.A., Harsem, N.K., Dalen, K.T., Staff, A.C., Nebb, H.I., Duttaroy, A.K. (2006) Regulation of ADRP expression by long-chain polyunsaturated fatty acids in BeWo cells, a human placental choriocarcinoma cell line, Journal of lipid research 47:815-823.

Tontonoz, P., Nagy, L., Alvarez, J.G., Thomazy, V.A., Evans, R.M. (1998) PPARgamma promotes monocyte/macrophage differentiation and uptake of oxidized LDL, Cell 93:241-252.

Triggiani, M., Oriente, A., Seeds, M.C., Bass, D.A., Marone, G., Chilton, F.H. (1995) Migration of human inflammatory cells into the lung results in the remodeling of arachidonic acid into a triglyceride pool, The Journal of experimental medicine 182:1181-1190.

Tso, P., Balint, J.A. (1986) Formation and transport of chylomicrons by enterocytes to the lymphatics, The American journal of physiology 250:G715-726.

Tzen, J., Cao, Y., Laurent, P., Ratnayake, C., Huang, A. (1993) Lipids, Proteins, and Structure of Seed Oil Bodies from Diverse Species, Plant physiology 101:267-276.

Uchiyama, Y. (2001) Autophagic cell death and its execution by lysosomal cathepsins, Archives of histology and cytology 64:233-246.

Valetti, C., Wetzel, D.M., Schrader, M., Hasbani, M.J., Gill, S.R., Kreis, T.E., Schroer, T.A. (1999) Role of dynactin in endocytic traffic: effects of dynamitin overexpression and colocalization with CLIP-170, Molecular biology of the cell 10:4107-4120.

Valko, M., Rhodes, C.J., Moncol, J., Izakovic, M., Mazur, M. (2006) Free radicals, metals and antioxidants in oxidative stress-induced cancer, Chemico-biological interactions 160:1-40.

van Herpen, N.A., Schrauwen-Hinderling, V.B. (2008) Lipid accumulation in non-adipose tissue and lipotoxicity, Physiology & behavior 94:231-241.

van Meer, G., Voelker, D.R., Feigenson, G.W. (2008) Membrane lipids: where they are and how they behave, Nat Rev Mol Cell Biol 9:112-124.

Vandesompele, J., De Preter, K., Pattyn, F., Poppe, B., Van Roy, N., De Paepe, A., Speleman, F. (2002) Accurate normalization of real-time quantitative RT-PCR data by geometric averaging of multiple internal control genes, Genome biology 3:RESEARCH0034.

Varela, G.M., Antwi, D.A., Dhir, R., Yin, X., Singhal, N.S., Graham, M.J., Crooke, R.M., Ahima, R.S. (2008) Inhibition of ADRP prevents diet-induced insulin resistance, American journal of physiology 295:G621-628.

Vereshchagina, N., Wilson, C. (2006) Cytoplasmic activated protein kinase Akt regulates lipid-droplet accumulation in Drosophila nurse cells, Development (Cambridge, England) 133:4731-4735.

Verma, A., Uzun, O., Hu, Y., Hu, Y., Han, H.S., Watson, N., Chen, S., Irvine, D.J., Stellacci, F. (2008) Surface-structure-regulated cell-membrane penetration by monolayer-protected nanoparticles, Nature materials 7:588-595.

Vickers, A.E., Bentley, P., Fisher, R.L. (2006) Consequences of mitochondrial injury induced by pharmaceutical fatty acid oxidation inhibitors is characterized in human and rat liver slices, Toxicol In Vitro 20:1173-1182.

Viola, H.M., Arthur, P.G., Hool, L.C. (2007) Transient exposure to hydrogen peroxide causes an increase in mitochondria-derived superoxide as a result of sustained alteration in L-type Ca2+ channel function in the absence of apoptosis in ventricular myocytes, Circulation research 100:1036-1044.

Voelker, D.R. (2005) Bridging gaps in phospholipid transport, Trends in biochemical sciences 30:396-404.

Voelker, D.R. (2003) New perspectives on the regulation of intermembrane glycerophospholipid traffic, Journal of lipid research 44:441-449.

Waetzig, V., Czeloth, K., Hidding, U., Mielke, K., Kanzow, M., Brecht, S., Goetz, M., Lucius, R., Herdegen, T., Hanisch, U.K. (2005) c-Jun N-terminal kinases (JNKs) mediate pro-inflammatory actions of microglia, Glia 50:235-246.

Wagner, E.F., Nebreda, A.R. (2009) Signal integration by JNK and p38 MAPK pathways in cancer development, Nature reviews 9:537-549.

Wan, H.C., Melo, R.C., Jin, Z., Dvorak, A.M., Weller, P.F. (2007) Roles and origins of leukocyte lipid bodies: proteomic and ultrastructural studies, Faseb J 21:167-178.

Wang, H., Gilham, D., Lehner, R. (2007) Proteomic and lipid characterization of apolipoprotein B-free luminal lipid droplets from mouse liver microsomes: implications for very low density lipoprotein assembly, The Journal of biological chemistry 282:33218-33226.

Wang, S., Soni, K.G., Semache, M., Casavant, S., Fortier, M., Pan, L., Mitchell, G.A. (2008) Lipolysis and the integrated physiology of lipid energy metabolism, Molecular genetics and metabolism 95:117-126.

Wang, Y., Sullivan, S., Trujillo, M., Lee, M.J., Schneider, S.H., Brolin, R.E., Kang, Y.H., Werber, Y., Greenberg, A.S., Fried, S.K. (2003) Perilipin expression in human adipose tissues: effects of severe obesity, gender, and depot, Obesity research 11:930-936.

Wei, P., Taniguchi, S., Sakai, Y., Imamura, M., Inoguchi, T., Nawata, H., Oda, S., Nakabeppu, Y., Nishimura, J., Ikuyama, S. (2005) Expression of adipose differentiation-related protein (ADRP) is conjointly regulated by PU.1 and AP-1 in macrophages, Journal of biochemistry 138:399-412.

Weinstein, J. (1980) Synovial fluid leukocytosis associated with intracellular lipid inclusions, Archives of internal medicine 140:560-561.

Weller, P.F., Dvorak, A.M. (1994) Lipid bodies: intracellular sites for eicosanoid formation, The Journal of allergy and clinical immunology 94:1151-1156.

Wells, H.G. (1910) The Relation of Fatty Degeneration to the Oxidation of Purines by Liver Cells, The Journal of experimental medicine 12:607-615.

Wells, J.C., Siervo, M. (2011) Obesity and energy balance: is the tail wagging the dog?, European journal of clinical nutrition 65:1173-1189.

Welte, M.A. (2007) Proteins under new management: lipid droplets deliver, Trends in cell biology 17:363-369.

Weylandt, K.H., Chiu, C.Y., Gomolka, B., Waechter, S.F., Wiedenmann, B. (2012) Omega-3 fatty acids and their lipid mediators: towards an understanding of resolvin and protectin formation, Prostaglandins & other lipid mediators 97:73-82.

Winborn, W.B. (1963) Light and Electron Microscopy of the Islets of Langerhans of the Saimiri Monkey Pancreas, The Anatomical record 147:65-93.

Winzell, M.S., Wulff, E.M., Olsen, G.S., Sauerberg, P., Gotfredsen, C.F., Ahren, B. (2010) Improved insulin sensitivity and islet function after PPARdelta activation in diabetic db/db mice, European journal of pharmacology 626:297-305.

Witt, S.N., Flower, T.R. (2006) alpha-Synuclein, oxidative stress and apoptosis from the perspective of a yeast model of Parkinson's disease, FEMS Yeast Res 6:1107-1116.

Wolins, N.E., Brasaemle, D.L., Bickel, P.E. (2006) A proposed model of fat packaging by exchangeable lipid droplet proteins, FEBS letters 580:5484-5491.

Wolins, N.E., Quaynor, B.K., Skinner, J.R., Schoenfish, M.J., Tzekov, A., Bickel, P.E. (2005) S3-12, Adipophilin, and TIP47 package lipid in adipocytes, The Journal of biological chemistry 280:19146-19155.

Wolins, N.E., Rubin, B., Brasaemle, D.L. (2001) TIP47 associates with lipid droplets, The Journal of biological chemistry 276:5101-5108.

Wolins, N.E., Skinner, J.R., Schoenfish, M.J., Tzekov, A., Bensch, K.G., Bickel, P.E. (2003) Adipocyte protein S3-12 coats nascent lipid droplets, The Journal of biological chemistry 278:37713-37721.

Wood, R.J., Volek, J.S., Liu, Y., Shachter, N.S., Contois, J.H., Fernandez, M.L. (2006) Carbohydrate restriction alters lipoprotein metabolism by modifying VLDL, LDL, and HDL subfraction distribution and size in overweight men, The Journal of nutrition 136:384-389.

World Health Organization (WHO) (2012) Obesity and overweight, Fact Sheet No 311.

Xia, Y. (2008) Nanomaterials at work in biomedical research, Nature materials 7:758-760.

Xu, G., Sztalryd, C., Lu, X., Tansey, J.T., Gan, J., Dorward, H., Kimmel, A.R., Londos, C. (2005) Post-translational regulation of adipose differentiation-related protein by the ubiquitin/proteasome pathway, The Journal of biological chemistry 280:42841-42847.

Xu, Q.M., Cheng, J.S., Ge, Z.Q., Yuan, Y.J. (2005) Antioxidant responses to oleic acid in two-liquid-phase suspension cultures of Taxus cuspidata, Applied biochemistry and biotechnology 125:11-26.

Xue, H., Wan, M., Song, D., Li, Y., Li, J. (2006) Eicosapentaenoic acid and docosahexaenoic acid modulate mitogen-activated protein kinase activity in endothelium, Vascular pharmacology 44:434-439.

Yamaguchi, T., Matsushita, S., Motojima, K., Hirose, F., Osumi, T. (2006) MLDP, a novel PAT family protein localized to lipid droplets and enriched in the heart, is regulated by peroxisome proliferator-activated receptor alpha, The Journal of biological chemistry 281:14232-14240.

Yang, L., Ding, Y., Chen, Y., Zhang, S., Huo, C., Wang, Y., Yu, J., Zhang, P., Na, H., Zhang, H., Ma, Y., Liu, P. (2012) The proteomics of lipid droplets: structure, dynamics, and functions of the organelle conserved from bacteria to humans, Journal of lipid research 53:1245-1253.

Ye, J., Li, J.Z., Liu, Y., Li, X., Yang, T., Ma, X., Li, Q., Yao, Z., Li, P. (2009) Cideb, an ER- and lipid droplet-associated protein, mediates VLDL lipidation and maturation by interacting with apolipoprotein B, Cell metabolism 9:177-190.

Yen, C.L., Stone, S.J., Koliwad, S., Harris, C., Farese, R.V., Jr. (2008) Thematic review series: glycerolipids. DGAT enzymes and triacylglycerol biosynthesis, Journal of lipid research 49:2283-2301.

Yeste-Velasco, M., Folch, J., Casadesus, G., Smith, M.A., Pallas, M., Camins, A. (2009) Neuroprotection by c-Jun NH2-terminal kinase inhibitor SP600125 against potassium deprivation-induced apoptosis involves the Akt pathway and inhibition of cell cycle reentry, Neuroscience 159:1135-1147.

Yonezawa, T., Yonekura, S., Kobayashi, Y., Hagino, A., Katoh, K., Obara, Y. (2004) Effects of long-chain fatty acids on cytosolic triacylglycerol accumulation and lipid droplet formation in primary cultured bovine mammary epithelial cells, Journal of dairy science 87:2527-2534.

Yu, W., Bozza, P.T., Tzizik, D.M., Gray, J.P., Cassara, J., Dvorak, A.M., Weller, P.F. (1998) Co-compartmentalization of MAP kinases and cytosolic phospholipase A2 at cytoplasmic arachidonate-rich lipid bodies, The American journal of pathology 152:759-769.

Yu, W., Cassara, J., Weller, P.F. (2000) Phosphatidylinositide 3-kinase localizes to cytoplasmic lipid bodies in human polymorphonuclear leukocytes and other myeloid-derived cells, Blood 95:1078-1085.

Yu, W.W., Qu, L., Guo, W., Peng, X. (2003) Experimental Determination of Extinction Coefficient of CdTe, CdSe, and CdS Nanocrystals, Chemistry of Materials 15:2854-2860.

Zabirnyk, O., Yezhelyev, M., Seleverstov, O. (2007) Nanoparticles as a novel class of autophagy activators, Autophagy 3:278-281.

Zechner, R., Zimmermann, R., Eichmann, T.O., Kohlwein, S.D., Haemmerle, G., Lass, A., Madeo, F. (2012) FAT SIGNALS--lipases and lipolysis in lipid metabolism and signaling, Cell metabolism 15:279-291.

Zehmer, J.K., Huang, Y., Peng, G., Pu, J., Anderson, R.G., Liu, P. (2009) A role for lipid droplets in inter-membrane lipid traffic, Proteomics 9:914-921.

Zhou, H., Lapointe, B.M., Clark, S.R., Zbytnuik, L., Kubes, P. (2006) A requirement for microglial TLR4 in leukocyte recruitment into brain in response to lipopolysaccharide, J Immunol 177:8103-8110.

Zimmet, P., Alberti, K.G., Shaw, J. (2001) Global and societal implications of the diabetes epidemic, Nature 414:782-787.

Zoula, S., Rijken, P.F., Peters, J.P., Farion, R., Van der Sanden, B.P., Van der Kogel, A.J., Decorps, M., Remy, C. (2003) Pimonidazole binding in C6 rat brain glioma: relation with lipid droplet detection, Br J Cancer 88:1439-1444.